

Polimery w Medycynie

Polymers in Medicine

BIANNUAL ISSN: 0370-0747 e-ISSN: 2451-2699

polimery.umw.edu.pl

2023, Vol. 53, No. 1 (January–June)

Ministry of Science and Higher Education – 70 pts.
Index Copernicus (ICV) – 120.65 pts.



WROCLAW
MEDICAL UNIVERSITY

Polimery w Medycynie
Polymers in Medicine



Polimery w Medycynie

Polymers in Medicine

ISSN 0370-0747 (PRINT)

ISSN 2451-2699 (ONLINE)

polimery.umw.edu.pl

BIANNUAL
2023, Vol. 53, No. 1
(January–June)

“Polymers in Medicine” is an independent, multidisciplinary forum to exchange scientific and clinical information, which publishes original papers (technical, analytical, experimental, clinical), preliminary reports and reviews regarding the use of polymers (natural and synthetic) and biomaterials in different specialties of medicine (biochemistry, clinical medicine, pharmacology, dentistry, implantology), biotechnology and veterinary science.

Address of Editorial Office

Marcinkowskiego 2–6
50-368 Wrocław, Poland
Tel.: +48 71 784 11 33
E-mail: redakcja@umw.edu.pl

Publisher

Wrocław Medical University
Wybrzeże L. Pasteura 1
50-367 Wrocław, Poland

Online edition is the original version of the journal

Editor-in-Chief

Prof. Witold Musiał

Deputy Editor

Dr. Konrad Szustakiewicz, DSc., Eng.

Statistical Editors

Wojciech Bombała, MSc

Anna Kopszak, MSc

Dr. Krzysztof Kujawa

Scientific Committee

Prof. Mirosława El-Fray

Prof. Franciszek Główka

Prof. Jörg Kreßler

Dr. Anna Krupa

Prof. Maciej Małecki

Prof. Bożena B. Michniak-Kohn

Prof. Wojciech Miltik

Prof. Masami Okamoto

Prof. Elżbieta Pamuła

Prof. Wiesław Sawicki

Prof. Szczepan Zapotoczny

Section Editors

Dr. Tomasz Urbaniak

(synthesis, evaluation, medical use of polymers, sensitive to environmental factors, applied in controlled and targeted drug delivery)

Dr. Monika Gasztych

(preparation, assessment and application of polymers in pharmaceutical technology and medical devices)

Dr. BEng., Agnieszka Gadomska-Gajadur

(synthesis and characterization of polymers having biomedical potential, composites for regenerative medicine)

Manuscript editing

Marek Misiak, Jolanta Krzyżak

Editorial Policy

During the review process, the Editorial Board conforms to the “Uniform Requirements for Manuscripts Submitted to Biomedical Journals: Writing and Editing for Biomedical Publication” approved by the International Committee of Medical Journal Editors (<http://www.icmje.org/>). Experimental studies must include a statement that the experimental protocol and informed consent procedure were in compliance with the Helsinki Convention and were approved by the ethics committee.

For more information visit the following page: <https://polimery.umw.edu.pl>

Polimery w Medycynie – Polymers in Medicine has received financial support from the resources of Ministry of Science and Higher Education within the “Social Responsibility of Science – Support for Academic Publishing” project based on agreement No. RCN/SP/0504/2021.



Ministry of Education and Science
Republic of Poland

Czasopismo Polimery w Medycynie – Polymers in Medicine korzysta ze wsparcia finansowego ze środków Ministerstwa Edukacji i Nauki w ramach programu „Społeczna Odpowiedzialność Nauki – Rozwój Czasopism Naukowych” na podstawie umowy nr RCN/SP/0504/2021.



Ministerstwo
Edukacji i Nauki

Indexed in: OCLC, WorldCat, PBL, EBSCO, MEDLINE, Index Copernicus

Typographic design: Monika Kołęda, Piotr Gil

Cover: Monika Kołęda

DTP: Wrocław Medical University Press

Printing and binding: Drukarnia I-BIS Bieronscy Sp.k.

Circulation: 11 copies

Contents

5 Preface

Original papers

- 7 Mohd Imran, Sahaya Mercy Jaqueline Robert, Manju Sharma, Vidhu Aeri
Evaluation of *Sida cordifolia* and *Sida rhombifolia* extracts in a rat model of streptozotocin-induced diabetic nephropathy
- 19 Clóvis Lamartine de Moraes Melo Neto, Bruno Simão Bernardi, Stefan Fiuza de Carvalho Dekon, Daniela Micheline dos Santos, Marcelo Coelho Goiato
Influence of thermal cycles and disinfection on the roughness, microhardness and color of PETG/TPU and PMMA
- 25 Andrzej Ślęzak, Sławomir Marek Grzegorzczyn, Anna Pilis, Izabella Ślęzak-Prochazka
A method for evaluating the transport and energy conversion properties of polymer biomembranes using the Kedem–Katchalsky–Peusner equations
- 37 Marcelo Coelho Goiato, Agda Marobo Andreotti, Fernanda Pereira de Caxias, Emily Vivianne Freitas da Silva, Letícia de Oliveira Gonçalves, Sandra Helena Penha de Oliveira, Victor Gustavo Balera Brito, Clóvis Lamartine de Moraes Melo Neto, Daniela Micheline dos Santos
Cytotoxicity of cleaning agents for ocular prostheses

Reviews

- 47 Sylwia Stiler-Wyszyńska, Sylwia Golba, Justyna Jurek-Suliga, Sławomir Kuczkowski
Review of the latest solutions in the use of contact lenses as controlled release systems for ophthalmic drugs
- 59 Sajal Jain, Simrandeep Kaur, Ritu Rathi, Upendra Nagaich, Inderbir Singh
Application of co-processed excipients for developing fast disintegrating tablets: A review
- 69 Mohd Imran, Haya Majid, Tasha Riaz, Shayan Maqsood
Identification of botanicals using molecular biotechnology
- 81 Akram Choudhary, Mohammad Noman, Uzma Bano, Jamal Akhtar, Yahya Shaikh, Mohammad Shahar Yar
Global uses of traditional herbs for hepatic diseases and other pharmacological actions: A comprehensive review

PREFACE

Dear Readers, Authors, Reviewers,
Members of the Scientific Committee and Section Editors,



The past six months brought further developments in the field of medicinal chemistry, focused on new molecules with a potentially beneficial effect on the human body. Also, the latest achievements in the field of physiology and pharmacology give hope for better treatment, e.g. diseases of the central nervous system and cancer. Extensive research is conducted on the risk factors associated with the occurrence of a number of civilization diseases, including diabetes.

Scientists from Denmark and the USA have reported the discovery of a thin protective membrane of the meningeal layer in the structure of the brain. Cell bioengineers in Taiwan and the USA have reported the development of non-replicating bacterial “cyborg cells”. The whole of June 2023 brought a number of very important reports: at the University of Edinburgh, machine learning made it possible to recognize the senolytic activity of ginkgetin, periplocin and oleandrin, while the authors from *The Lancet* predict that by 2050 the number of adults with diabetes will increase from 529 million to over 1.3 billion.

Against this background, in this issue of *Polimery w Medycynie – Polymers in Medicine* we present four original articles and four review articles, carefully selected by our editors to represent the interesting accomplishments of original research currently conducted in the whole world. The article opening the current issue is devoted to the detailed study of plant extracts intended for the control or prevention of diabetes in animal models. Studies presented by authors from India confirm the effect of these extracts on the natural protein polymer, i.e. alpha-amylase, associated with the pathophysiology of diabetes. The article from Brazil concerns the significant influence of temperature changes and disinfectants on the properties of thermoplastic polymer mixtures derived from polyethylene glycol and polyurethane used in dentistry. One of the extremely important issues of scientific pharmacy, which is currently widely researched, is the transport of medicinal substances through natural and artificial membranes in the human body and in modern drug delivery systems. A team of authors from the universities in Upper Silesia and Częstochowa proposed an interesting method for assessing the transport properties of polymer biomembranes based on the Kedem–Katchalsky–Peusner equations. The care of ocular prostheses requires the use of appropriate disinfectants, which, unfortunately, may have cytotoxic properties. Scientists from São Paulo have prepared an experimental work in which they explained the potential impact of selected substances suitable for disinfecting eye prostheses based on acrylic resins.

In the second part of our issue, we present review papers that may be useful not only to scientists, but also to practitioners who use polymers in their professional work on a daily basis. This applies especially to specialists developing new forms of drugs intended for application to the surface of the eyeball – an excellent article about contact lenses as carriers of medicinal substances and pharmaceutical technologists – an extensive presentation of polymers used as initiators of rapid tablet disintegration. The summary of the issue are two articles on substances of natural origin with potential use in medicine and pharmacy.

As you can see from the content sent to our magazine and articles selected by the editors, we present the latest achievements and research, which are a significant contribution to the global discourse on the use of polymers in modern medicine and pharmacy.

Editor-in-Chief
Witold Musiał, Prof., PhD, DSc

Evaluation of *Sida cordifolia* and *Sida rhombifolia* extracts in a rat model of streptozotocin-induced diabetic nephropathy

Mohd Imran^{1,A–D}, Sahaya Mercy Jaqueline Robert^{1,E}, Manju Sharma^{2,C,F}, Vidhu Aeri^{1,A–F}

¹ Department of Pharmacognosy and Phytochemistry, School of Pharmaceutical Education and Research, Jamia Hamdard University, New Delhi, India

² Department of Pharmacology, School of Pharmaceutical Education and Research, Jamia Hamdard University, New Delhi, India

A – research concept and design; B – collection and/or assembly of data; C – data analysis and interpretation;

D – writing the article; E – critical revision of the article; F – final approval of the article

Polymers in Medicine, ISSN 0370-0747 (print), ISSN 2451-2699 (online)

Polim Med. 2023;53(1):7–18

Address for correspondence

Vidhu Aeri

E-mail: vidhuaeri@yahoo.com

Funding sources

The study was funded by Hamdard National Foundation [grant No. HNF 28.09.21].

Conflict of interest

None declared

Acknowledgements

The authors would like to thank the Department of Pharmacognosy and Phytochemistry, School of Pharmaceutical Education and Research (Jamia Hamdard University, New Delhi, India) for letting us conduct the experiments.

Received on October 5, 2022

Reviewed on October 23, 2022

Accepted on November 23, 2022

Published online on March 28, 2023

Cite as

Imran M, Jaqueline RSM, Sharma M, Aeri V. Evaluation of *Sida cordifolia* and *Sida rhombifolia* extracts in a rat model of streptozotocin-induced diabetic nephropathy. *Polim Med.* 2023;53(1):7–18. doi:10.17219/pim/156847

DOI

10.17219/pim/156847

Copyright

Copyright by Author(s)

This is an article distributed under the terms of the Creative Commons Attribution 3.0 Unported (CC BY 3.0) (<https://creativecommons.org/licenses/by/3.0/>)

Abstract

Background. *Sida cordifolia* and *Sida rhombifolia* are regarded as useful herbs as they have been shown to be effective, inexpensive and harmless in the prevention of diabetes, and are recognized as valuable therapeutic substances.

Objectives. The purpose of this study was to assess the effect of *S. cordifolia* and *S. rhombifolia* in the treatment of diabetic nephropathy using a rat model.

Materials and methods. Extracts of *S. cordifolia* and *S. rhombifolia* were obtained using the Soxhlet method. The hydroalcoholic extract solvent was used in the following proportions: 70:30, 50:50 and 80:20. The 80:20 hydroalcoholic extract was observed to be the most potent. The inhibitory effects of the extract were determined using the α -amylase assay. The most potent extract also underwent total flavonoid, phenolic and free radical scavenging tests, and was incorporated into an animal study. Diabetes was induced in rats by administering nicotinamide (NAD; 230 mg/kg) and streptozotocin (STZ; 65 mg/kg) intraperitoneally. In addition to a standard control of pioglitazone, the rats received extract dosages of 100 mg/kg/day or 200 mg/kg/day. Body weight, blood glucose, glycated hemoglobin (HbA1c), blood urea nitrogen (BUN), serum albumin, serum creatinine, homeostatic model assessment of insulin resistance (HOMA-IR), and oral glucose tolerance were assessed at various time points. The animals also underwent histopathological examination to observe alterations induced by the treatment.

Results. *Sida cordifolia* was the most successful in lowering blood glucose and HbA1c levels. Renal function indices and antioxidant enzyme levels were regained in a dose-dependent manner. Furthermore, *S. cordifolia* (200 mg/kg/day) extract, similar to pioglitazone, inhibited the production of advanced glycation byproducts by the kidney.

Conclusions. The effects of various *S. cordifolia* and *S. rhombifolia* extracts on rats with diabetic nephropathy were observed. *Sida cordifolia* may be further explored for the treatment of diabetic nephropathy and, due to its diverse nature, may be utilized for the treatment of a wide range of diseases, as it provided more significant findings.

Key words: *Sida cordifolia*, *Sida rhombifolia*, diabetic nephropathy, extraction, blood glucose, HbA1c

Background

The International Diabetes Federation (IDF) has reported the incidence of diabetes mellitus to be 8.8% among adults. Diabetes mellitus has impacted roughly 400,000,000 individuals, and the number is expected to rise to 550,000,000 individuals in the next decade.^{1,2} One of the serious consequences of diabetes mellitus is diabetic nephropathy, also known as diabetic kidney disease. If not addressed, the disease causes from 20% to 40% of individuals to develop renal failure or blatant nephropathy due to untreated microalbuminuria within 2 decades. This condition is usually distinguished through early symptoms of renal cell death or failure, oxidative stress, expansion of interstitial fibrosis and mesangial matrices, bulking of basement membranes, and inflammatory responses.³ The activation of many biochemical and metabolic processes, including fluxes of glucose from polyol and hexosamine routes, along with the excessive or unnecessary activity of isoforms of protein kinase C and buildup of end products of advanced glycation, is caused by hyperglycemia. These pathways and routes are the primary cause of nephropathy and are therefore therapeutic targets in managing the disease.⁴

Herbs are considered valuable therapeutic substances, as they have been shown to be inexpensive, harmless and effective in the prevention of diabetes. Furthermore, using therapeutics derived from herbal plants is critical in underdeveloped nations due to the financial restraints related to conventional drugs. Therefore, there is an increased need to develop medicines that are cheap and efficacious.

Sida rhombifolia is a 1.5-meter tall upright shrub that is grown perennially or yearly and has stellate bristles and coarse stems. It belongs to the Malvaceae family, is also known as Atibala or Bala, and is among the 200 varieties of *Sida*. The plant has various therapeutic uses and pharmacological effects on cardiac, diabetic, rheumatic, and migraine-like issues, and is distinguished by its green diamond-structured leaf that has prickly stipules and grey hair-like features on the underside.⁵ Hypoglycemic and hypolipidemic effects of this herb have been observed in pre-clinical research on mice affected with diabetes. The effects of the plant are associated with its free radical scavenging activity, which has proven useful in indicating new roles for the herb.⁶

Similarly, *Sida cordifolia*, another potentially useful herb of the Malvaceae family, has proven to be an asset in traditional medicine. The herb is native to America and tends to grow in tropical areas in other parts of the globe, as it propagates fast in soils spoilt by grazing, heat and rain. Different parts of the herb are being used in day-to-day medicine for ailments related to respiratory and central nervous system, as well as inflammatory, tonic, diuretic, and various other disorders.⁷ Structurally, the herb is perennially upright and has a layer of white-colored hair that gives rise to its common name, “flannel weed”.⁸ In previous studies conducted on diabetic rats, reductions in blood

glucose levels, triglycerides, plasma urea and creatinine, low-density lipids, and cholesterol were observed. Also, an increase in superoxide dismutase and catalase enzymes that are required for antioxidant synthesis was reported.⁹ It has also been observed that *S. cordifolia* has nephro-protective effects, which may be due to its antioxidant properties.¹⁰

Both plants have shown the potential to exhibit hypoglycemic effects that may help to reduce the damage caused by diabetic nephropathy. In the present study, extracts of *S. cordifolia* and *S. rhombifolia* were individually evaluated and compared in rats with induced diabetic nephropathy, through the observation of changes and protective effects.

Materials and methods

Experimental model

The study used adult male Wistar rats weighing 250–300 g. The rats were given a conventional rodent diet along with water, and were housed at a temperature of $23 \pm 2^\circ\text{C}$ with a 12-hour day-night cycle.

Plant material collection

The aerial part of 2 species of the plant, *S. cordifolia* and *S. rhombifolia*, were obtained from Varuni Exports (Chennai, India).

Extraction

The aerial parts of *S. cordifolia* and *S. rhombifolia* were dried, crushed into powder form and kept in air-tight bags at approx. -80°C . The extraction was performed using the Soxhlet method, which employs water/ethanol (80:20) and distilled water as the solvent solutions. Constituents with antidiabetic effects were derived and added separately into solvents in hydroalcoholic solution. The procedure for extraction was repeated until the mixture showed no color, and the mixture was then distilled. Then, the mixture was later concentrated and freeze-dried under low pressure. Further extractions were conducted using hydroalcohol in varying ratios, including 70:30 and 50:50, to find the most potent extract. Such extract was observed during the procedure that used a ratio of 80:20.

α -amylase assay

Porcine pancreatic α -amylase (0.5 mg/mL) was prepared in an aqueous solution containing 1% starch and 20 mM sodium phosphate buffer. Stock solution A was prepared by adding 1 M sodium phosphate monobasic monohydrate ($\text{NaH}_2\text{PO}_4 \cdot \text{H}_2\text{O}$, molecular weight: 138) and 2.76 g of $\text{NaH}_2\text{PO}_4 \cdot \text{H}_2\text{O}$ (monobasic) to a final volume of 1 L of water. Stock solution B was prepared by adding 1 M

sodium phosphate dibasic (Na_2HPO_4 , molecular weight: 142) and 2.84 g of Na_2HPO_4 (dibasic) to a final volume of 1 L of water. Stock solution A (450 mL) and 0.3504 mg sodium chloride (NaCl) were added to stock solution B (550 mL). The 2nd reagent, dinitrosalicylic acid (DNS) (molecular weight: 228.12), was prepared by warming and constantly stirring 20 mL of deionized water with 96 mM DNS, without boiling. The final reagent was prepared by dissolving 2 M sodium hydroxide (NaOH , molecular weight: 0.7999) in 8 mL of 5.31 M sodium potassium tartrate, and 10 mL of 2 M NaOH in water. This solution was warmed and stirred on a heating/stirring plate without boiling. Throughout the stirring, reagent A was gradually added to reagent B and diluted to 40 mL with deionized water. The colored reagent solution was then stored in an amber container at ambient temperature for up to 6 months.

Assay procedure

Multiple extract preparations were produced in a broad range of concentrations (0.1–1000 $\mu\text{g}/\text{mL}$). Extracts (100 μL) were then mixed with 100 μL of a 1% starch solution prepared in 20 mM trisodium phosphate (Na_3PO_4) buffer. This solution was transferred to microtubes and maintained at 25°C for 10 min, after which 100 μL of porcine α -amylase (0.5 mg/mL) was added to each tube. The preparations were then incubated for 10 min at 25°C. Next, 200 μL of DNS reagent was added to each tube. The tubes were incubated at 100°C for 5 min. This was performed to keep the samples cool. Each tube had 50 μL of material removed and transferred to 96-well microplates. To dissolve the solution in each well, water was added (200 μL). The absorbance of each well was read at 540 nm. In addition, blank measurements were recorded from wells that did not contain the enzyme, and the results were compared to the control, acarbose. Conventional procedures were used to assess α -amylase assay activity, as follows (Equation 1):

$$\text{percentage of activity} = \frac{\text{extract absorbance}}{\text{control absorbance}} \times 100. \quad (1)$$

Chemicals

The chemicals used in the study were of analytical grade. Nicotinamide (NAD) and streptozotocin (STZ) were acquired from Sigma-Aldrich (St. Louis, USA). The kits for diagnosing biochemical estimations were purchased from Krishgen BioSystems (Mumbai, India).

Phytochemical screening

Using previously established methods with some modifications, chemical compounds including amino acids, alkaloids, flavonoids, tannins, carbohydrates, fats, terpenoids, oils, phenols, saponins, glycosides, and proteins were measured in both plant extracts.¹¹

Estimation of total flavonoid composition

Total flavonoid content was determined using an aluminum chloride colorimetric test. Reference solutions of quercetin at concentrations of 30, 40, 50, 60, 70, 80, 90, and 100 g/mL were prepared in 96% ethanol. Also, 150 mL of 10% aluminum chloride was combined with 10 mL of reference solution in 96% ethanol. A 10 mL volume of 1 M sodium acetate was then combined with the mixture in a 96-well plate. Ethanol was used as a blank reagent in 96% of the cases. The reagents were subsequently kept at room temperature for 40 min, sheltered from light. The VersaMax Microplate Reader (Merck Millipore, Burlington, USA) was used to measure the absorbance at 415 nm. The obtained composition was presented as milligrams of quercetin.

Estimation of total phenolic composition

The Folin–Ciocalteu technique was used to measure total phenolic content. Throughout a flat-bottom 96-well microplate, 25 mL of extracts diluted from each part of *S. cordifolia* and *S. rhombifolia* were mixed with 100 mL of 1:4-diluted Folin–Ciocalteu reagent and stirred for 1 min. After 240 s, a 75-mL solution of sodium carbonate (Na_2CO_3 ; 100 g/L) was combined and spun at a reasonable pace for 1 min. After 240 s, a 75-mL concentration of Na_2CO_3 (100 g/L) was combined and spun at a reasonable pace for 1 min. The VersaMax Microplate Reader (was used to measure the absorbance at 765 nm over 2 h at room temperature. The absorbance activity was calculated from ethanol absorbance activities. Calibration was performed using dilutions of a gallic acid standard ($\text{C}_7\text{H}_6\text{O}_5$; 10–200 mg/L). Gallic acid equivalents (GAE) from the plant were used to determine the total phenolic content in milligrams per gram of extracts.

Antioxidant activity

The antioxidant activity of extracts was determined by measuring their scavenging capacity using 2,2-diphenyl-1-picrylhydrazyl (DPPH). Tests were carried out on 96-well plates, using a 20-L solution of extract stock in each well. The quantities used were 2000, 1500, 1000, 500, and 100 ppm in 180 L of DPPH solution. The absorbance was measured 30 min after incubation using a VersaMax Microplate Reader. Measurements were recorded in a dimly lit chamber at 517 nm. Methanol was used as a procedural control, while ascorbic acid was used as a positive control. All tests were performed 3 times. The sample concentration required to inhibit DPPH by 50% was calculated (IC₅₀ value). The percentage of scavenging capability was calculated using the following equation (Equation 2):

$$\% \text{ inhibition} = \frac{\text{absorbance of standard} - \text{absorbance of crude extract}}{\text{absorbance of standard}} \times 100. \quad (2)$$

Animals and design of experiment

To induce diabetic nephropathy, animals were injected intraperitoneally with NAD (230 mg/kg). After 15 min, STZ was dissolved in citrate buffer (pH: 4.5) and immediately injected intraperitoneally at a dosage of 65 mg/kg. Fasting blood glucose levels were measured 72 h after STZ injection to confirm diabetes. Only rats with fasting blood glucose levels ≥ 250 mg/dL were used in the study. After a literature search on acute toxicity studies, 2 dosages of extracts were chosen, 100 mg/kg and 200 mg/kg. All animal experiments were conducted following national guidelines and relevant national laws on the protection of animals. The experimental protocol (No. 1834) was approved by the Ethics Committee of Jamia Hamdard University (New Delhi, India; approval No. 1834).

Body weight and estimation of blood glucose

Before STZ induction, body weight of each animal was measured and rats of comparable weight were housed together. Each group's body weight was calculated and monitored regularly until the completion of the study. To confirm diabetes, glucose levels were measured 72 h after NAD/STZ injection. The fasting blood glucose level was measured at 15-day intervals using commercially available enzymatic kits (Krishgen BioSystems).

Enzyme-linked immunosorbent assay for the assessment of blood parameters

A standard curve was constructed using buffer diluents covering a broad range of concentrations between 0 pg/mL to 3 times the highest predicted concentration of the antigen. The capture antibody was diluted to 15 μ g/mL to a volume of 100 μ L/well and incubated at 37°C for 2 h in a 96-well polystyrene plate, along with 100 μ L of each standard. The solution from all of the individual wells was removed and replaced with a wash buffer (200 μ L/well). The plate was then shaken for 5 min, and 200 μ L of blocking buffer was added to each well. Next, the plate was covered and incubated at 37°C for 1 h. The wash buffer was removed, and the samples and standards were placed in separate wells and incubated at 37°C for 1 h. The 96-well plate was washed again. Detection antibodies were added to each well of the 96-well plate and incubated for 1 h before being washed again. The enzyme-conjugated secondary antibody (100 μ L) was added to each well and the plate was incubated at 37°C for 1 h. The 96-well plate was washed again, twice, to minimize nonspecific binding. Horseradish peroxidase (HRP) substrate solution was added to each well (100 μ L) and the plate was incubated at 37°C for 10 min until the color changed to blue. To turn the solution to yellow, 100 μ L

of stop buffer was added to each well, and the absorbance was measured at 450 nm using a plate reader (ELX800MS ELISA Reader; Shimadzu, Tokyo, Japan).

Tests for renal function

Samples of blood were analyzed using enzymatic kits (Krishgen BioSystems) to assess the control of diabetic nephropathy in rats that were treated for 0, 7, 14, or 21 days. This included estimates of blood urea nitrogen (BUN), serum albumin and serum creatinine.

Histopathology

Tissues were harvested from the pancreas and kidneys of euthanized animals and then dehydrated in ethanol, fixed in neutral buffered formalin solution (10%) and embedded in paraffin. To conduct a microscopic examination, 5-millimeter thick sections of tissue were collected using a rotary microtome LMIUK histopathology microscope (Sigma Histology, Center; New Delhi, India) and stained using hematoxylin and eosin (H&E).

Statistical analyses

GraphPad Prism v. 6 (GraphPad Software, San Diego, USA) was utilized for the analysis of data. The values from statistical analysis are presented as mean \pm standard error of the mean ($M \pm SEM$). Data were analyzed using one-way analysis of variance (ANOVA), followed by Tukey's post hoc test for multiple comparisons. The value of $p \leq 0.05$ was considered statistically significant.

Results

α -amylase assay

Extracts with effective α -amylase inhibition were discovered. The hydroalcoholic extract with an IC₅₀ concentration of 70.82 \pm 0.28 mg/mL was determined to be the most effective for further examination. Table 1 summarizes the extraction profile used to find the most effective fraction.

Total flavonoid composition

The potency of the hydroalcoholic extracts derived from the extraction tests was assessed. The total flavonoid content was expressed in terms of the milligram of quercetin equivalent per gram of the dry mass (mg QE/gm). The quercetin standard calibration curve for total flavonoid concentration in both plant extracts is reported in Table 2 as $Y = 0.0613x + 0.0004$, $R^2 = 0.9872$. *Sida rhombifolia* had a greater total flavonoid concentration, 35.12 \pm 0.49 mg QE/gm, than the other plant extract.

Table 1. IC50 values for alpha amylase inhibitory potential of alcoholic, hydroalcoholic and aqueous extracts of aerial parts of *Sida cordifolia* and *Sida rhombifolia*

Serial number	Name	IC50 [$\mu\text{g}/\text{mL}$]
1	<i>Sida cordifolia</i> aqueous extract	95.81 \pm 0.58
2	<i>Sida cordifolia</i> alcoholic extract	87.21 \pm 1.25
3	<i>Sida cordifolia</i> hydroalcoholic extract	
	50:50	103 \pm 1.5
	70:30	73.49 \pm 0.70
	80:20	70.82 \pm 0.28
4	<i>Sida rhombifolia</i> aqueous extract	109 \pm 0.44
5	<i>Sida rhombifolia</i> alcoholic extract	96.85 \pm 1.31
6	<i>Sida rhombifolia</i> hydroalcoholic extract	
	50:50	102 \pm 1.47
	70:30	71.98 \pm 0.91
	80:20	71.05 \pm 0.83
7	standard acarbose	57 \pm 0.51

IC50 – sample concentration required to inhibit 2,2-diphenyl-1-picrylhydrazyl (DPPH) by 50%.

Total phenolic composition

The experiments yielded potent hydroalcoholic extracts. Table 2 shows the total phenolic content of the aerial parts of both plants, together with a calibration curve ($Y = 0.0371x + 0.0234$, $R^2 = 0.9930$). *Sida rhombifolia* produced a greater total phenolic content than the other plant, with 5.395 ± 0.81 mg GAE/gm.

Antioxidant scavenging activity

The potent hydroalcoholic extract was used to evaluate the antioxidant scavenging activity. Table 2 shows the antioxidant scavenging activity of aerial sections of both plants, with *S. rhombifolia* exhibiting a greater scavenging activity than the other plant, with 92.13 ± 2.4 IC50 $\mu\text{g}/\text{mL}$ of free radicals.

The extracts were used on the animals and the parameters described in the following sections were analyzed.

Effects of *Sida cordifolia* and *Sida rhombifolia* extracts on body weight

Substantial weight loss was observed in the experimental animals. The doses of extracts administered were 100 mg/kg and 200 mg/kg, with body weight reductions occurring in a dose-dependent manner. Pioglitazone also decreased the body weight of rats affected by diabetic nephropathy. The results of the body weight tests conducted are presented in Fig. 1 and Table 3.

Effects of *Sida cordifolia* and *Sida rhombifolia* extracts on blood glucose

Various extract dosages were administered to rats and maintained for up to 21 days. Tests for the detection of blood glucose were conducted on days 0, 7, 14, and 21. During the 21 days, the fasting blood glucose levels varied from 92.1 mg/dL to 96.3 mg/dL in the control rats. At the same time, glucose levels observed in rats affected by diabetes were elevated to 431.8–477.4 mg/dL. Dosages of both extracts (100 mg/kg and 200 mg/kg) were administered for 21 days and resulted in a considerable modulation of blood glucose levels. The 200 mg/kg dosage of *S. cordifolia* caused

Table 2. Total flavonoid, total phenolic and antioxidant content in different extracts of the plants

Serial number	Different solvent extract (aerial part)	Total flavonoid composition in different extracts [mg QE/gm]	Total phenolic content in different extracts [mg GAE/gm]	Half-minimum inhibitory concentration in different extracts [IC50 $\mu\text{g}/\text{mL}$]
1	<i>Sida rhombifolia</i> hydroalcoholic (SRHA)	35.12 \pm 0.49	5.395 \pm 0.81	92.13 \pm 2.4
2	<i>Sida cordifolia</i> hydroalcoholic (SCHA)	25.93 \pm 0.27	4.21 \pm 0.23	86.14 \pm 5

Table 3. Body weight

Serial number	Body weight [g]	Day 0 [g]	Day 7 [g]	Day 14 [g]	Day 21 [g]
1	normal control	400.12 \pm 8.32	399 \pm 8.71	401.32 \pm 7.31	402.17 \pm 8.28
2	diabetic control (toxic)	218.63 \pm 16.83	201.12 \pm 7.21	189 \pm 9.31	184 \pm 6.27
3	standard drug 10 mg/kg (pioglitazone)	232.66 \pm 10.67	202 \pm 6.31	215 \pm 7.21	221.1 \pm 8.92
4	<i>Sida cordifolia</i> 100 mg/kg	249.21 \pm 10.63	221 \pm 8.67	201 \pm 9.23	228.1 \pm 9.18
5	<i>Sida cordifolia</i> 200 mg/kg	253.17 \pm 9.45	245.13 \pm 9.36	247 \pm 10.37	251.12 \pm 8.21
6	<i>Sida rhombifolia</i> 100 mg/kg	239.18 \pm 10.45	228.27 \pm 10.11	232 \pm 16.32	241.1 \pm 11.2
7	<i>Sida rhombifolia</i> 200 mg/kg	251.10 \pm 11.47	239.12 \pm 13.21	239.18 \pm 14.2	249.13 \pm 10.2

Table 4. Blood glucose and glycated hemoglobin (HbA1c) levels

Serial number	Animal groups	Blood glucose [mg/dL]				HbA1C [mmol/mol]			
		day 0 [mg/dL]	day 7 [mg/dL]	day 14 [mg/dL]	day 21 [mg/dL]	day 0 [mmol/mol]	day 7 [mmol/mol]	day 14 [mmol/mol]	day 21 [mmol/mol]
1	normal control	92.1 ±5.58	95.5 ±4.14	94.7 ±5.4	96.3 ±5.58	6.07 ±0.06	6.10 ±0.05	6.20 ±0.05	6.21 ±0.05
2	diabetic control (toxic)	447.5 ±55.44	457.2 ±57.6	477.4 ±27	431.8 ±24.48	5.03 ±0.05	4.31 ±0.05	4.21 ±0.03	3.20 ±0.02
3	standard drug 10 mg/kg (pioglitazone)	432 ±48.06	413.9 ±68.76	339.84 ±63.36	396.3 ±62.64	7.03 ±0.21	7.71 ±0.28	7.89 ±0.27	8.71 ±0.29
4	<i>Sida cordifolia</i> 100 mg/kg	447.8 ±72.36	439.7 ±25.38	458.8 ±30.6	421 ±45.18	5.40 ±0.24	6.89 ±0.04	6.94 ±0.07	7.01 ±0.71
5	<i>Sida cordifolia</i> 200 mg/kg	444.6 ±45.9	375.84 ±74.7	287.3 ±20.7	325.26 ±32.4	6.21 ±0.03	6.59 ±0.28	6.85 ±0.05	7.1 ±0.29
6	<i>Sida rhombifolia</i> 100 mg/kg	482.2 ±90.18	458.5 ±27	459.9 ±36	439.9 ±54.18	6.31 ±0.27	6.49 ±0.06	6.78 ±0.25	6.91 ±0.26
7	<i>Sida rhombifolia</i> 200 mg/kg	485.1 ±54.18	424.8 ±72.18	358.2 ±63.9	443.7 ±71.82	7.73 ±0.12	7.79 ±0.03	7.91 ±0.13	7.99 ±0.29

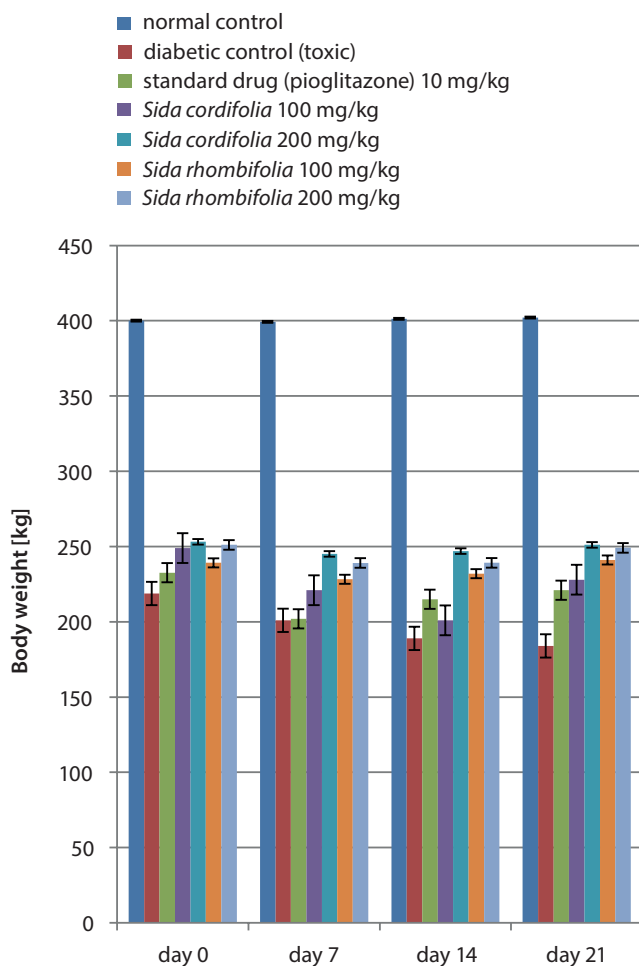


Fig. 1. Results of the body weight tests

the greatest attenuation (287.3 mg/dL) when compared to the rats affected by diabetes. Pioglitazone therapy also led to a considerable reduction in the levels of blood glucose (339.84 mg/dL). The results of the blood glucose level tests are presented in Fig. 2A and Table 4.

Effects of *Sida cordifolia* and *Sida rhombifolia* extracts on glycated hemoglobin

The assessment of glycated hemoglobin (HbA1c) levels was performed on days 0, 7, 14, and 21 of the experiment. A significant reduction in HbA1c levels was observed within the nephropathy control group (3.20 ±0.02 mmol/mol) when compared to the rats in the normal control group (6.21 ±0.05 mmol/mol) at the end of the study. The dosages of 100 mg/kg and 200 mg/kg of both extracts resulted in substantial reductions in HbA1c levels. For the *S. cordifolia* 100 mg/kg group, a value of 5.40 mmol/mol was recorded on day 0, while the highest value (7.99 mmol/mol) was observed in the *S. rhombifolia*-treated group (concentration: 200 mg/kg) on day 21. It was observed that 200 mg/kg of *S. cordifolia* caused a consistent rise from day 0 to day 21. The results of the HbA1c level tests are presented in Fig. 2B and Table 4.

Effects of *Sida cordifolia* and *Sida rhombifolia* extracts on the homeostatic model assessment of insulin resistance

A dose-dependent increase was observed in the results of the homeostatic model assessment of insulin resistance (HOMA-IR) for all extracts and pioglitazone in the diabetic control group compared to the normal control group. The results of the HOMA-IR tests are presented in Fig. 3 and Table 5.

Oral glucose tolerance test

After conducting the oral glucose tolerance tests (OGTT) on day 7, we observed a similar reduction of glucose levels in the *S. cordifolia* (200 mg/kg) administered group along with the pioglitazone administered group at different time points of 30 min, 60 min and 120 min. Similarly, the group treated with *S. cordifolia* (200 mg/kg) had significantly decreased levels of glucose in the same timeframe. Other

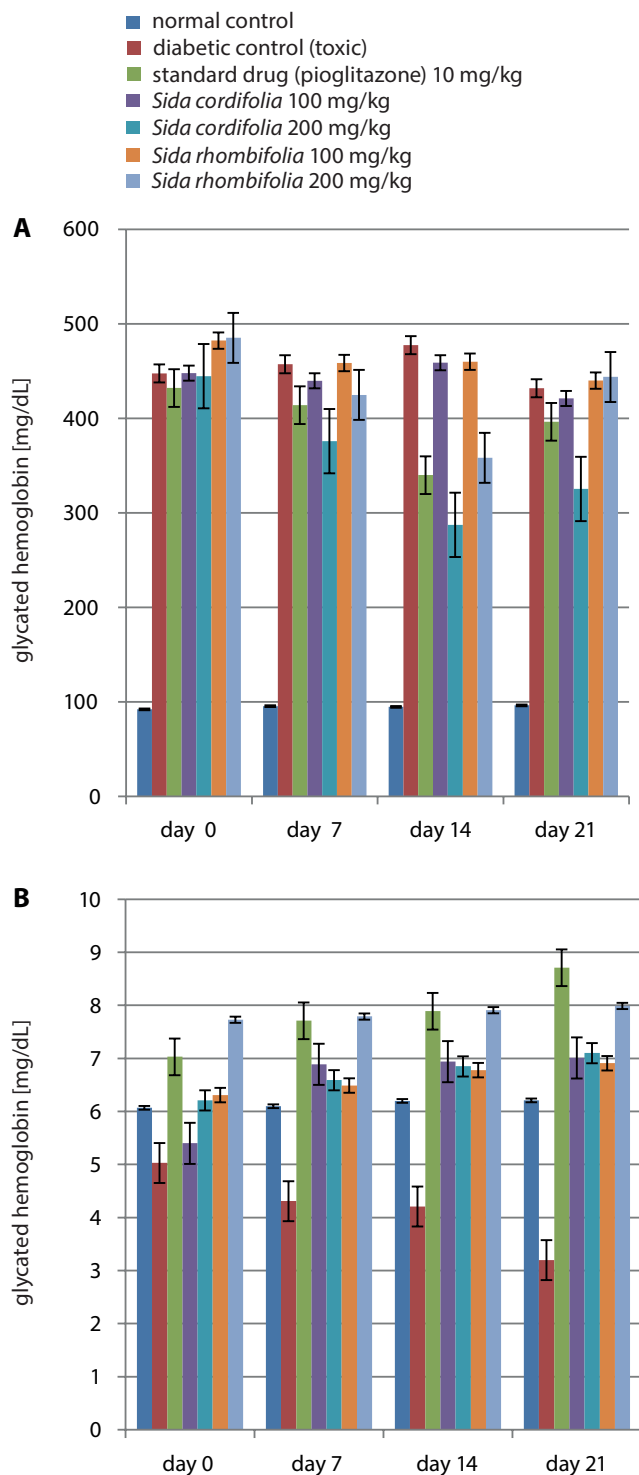


Fig. 2. Results of the blood glucose (A) and glycated hemoglobin (HbA1c) (B) level tests

extracts caused increased oral glucose tolerance at a dosage of 200 mg/kg, except for *S. rhombifolia*, which considerably reduced the oral glucose tolerance in rats.

On day 14, it was observed that oral glucose tolerance had significantly decreased within 120 min in the normal and *S. cordifolia* 200 mg/kg groups. On day 21, it was observed that *S. cordifolia* (200 mg/kg) caused the lowest value for the OGTT at 60 min, which then rose by 120 min. The other

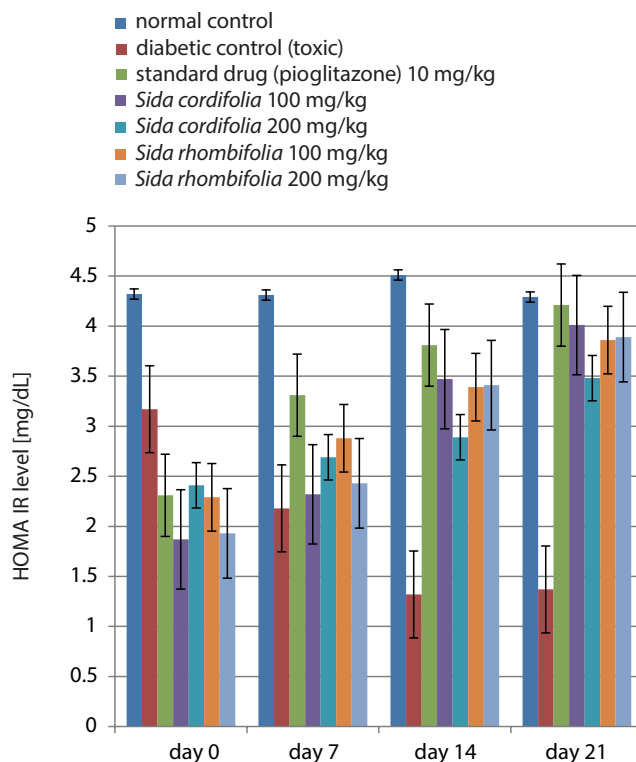


Fig. 3. Results of the homeostatic model assessment of insulin resistance (HOMA-IR) tests

doses of extracts caused a similar decrease and rise from 60 min to 120 min, while pioglitazone caused a considerable decrease throughout the discussed timeframe. The results of the OGTT tests are presented in Fig. 4 and Table 6.

Effects of *Sida cordifolia* and *Sida rhombifolia* extracts on renal function

The study measured levels of BUN, serum albumin and serum creatinine.

Effects of *Sida cordifolia* and *Sida rhombifolia* extracts on blood urea nitrogen

During the 21 days of treatment, the BUN level of the normal control group was in a range of 16.01–17.9 mg/dL, while the diabetic control group had very high levels of BUN (40.01 mg/dL). Pioglitazone caused a considerable increase in BUN levels, while the extracts caused higher values of BUN. The results of the BUN level tests are presented in Fig. 5 and Table 7.

Effects of *Sida cordifolia* and *Sida rhombifolia* extracts on serum albumin

During the 21-day treatment period, the normal control group had the highest serum albumin levels on day 14 (7.21 g/dL). *Sida cordifolia* (100 mg/kg) caused significantly decreased levels of serum albumin (2.24 ± 0.45 g/dL), similar

Table 5. Homeostatic model assessment of insulin resistance (HOMA-IR)

Serial number	HOMA-IR [mg/dL]	Day 0 [mg/dL]	Day 7 [mg/dL]	Day 14 [mg/dL]	Day 21 [mg/dL]
1	normal control	4.32 ±0.65	4.31 ±0.71	4.51 ±1.79	4.29 ±1.89
2	diabetic control (toxic)	3.17 ±0.81	2.18 ±1.21	1.32 ±0.59	1.37 ±0.63
3	standard drug 10 mg/kg (pioglitazone)	2.31 ±0.67	3.31 ±1.61	3.81 ±1.71	4.21 ±1.82
4	<i>Sida cordifolia</i> 100 mg/kg	1.87 ±0.61	2.32 ±1.87	3.47 ±1.58	4.01 ±1.91
5	<i>Sida cordifolia</i> 200 mg/kg	2.41 ±0.37	2.69 ±1.03	2.89 ±1.31	3.48 ±1.93
6	<i>Sida rhombifolia</i> 100 mg/kg	2.29 ±0.61	2.88 ±1.32	3.39 ±1.71	3.86 ±1.51
7	<i>Sida rhombifolia</i> 200 mg/kg	1.93 ±0.51	2.43 ±1.80	341 ±1.51	389 ±1.79

Table 6. Oral glucose tolerance tests (OGTT) on day 7, 14 and 21

Serial number	Animal groups	OGTT – day 7 [mg/dL]			OGTT – day 14 [mg/dL]			OGTT – day 21 [mg/dL]		
		30 min [mg/dL]	60 min [mg/dL]	120 min [mg/dL]	30 min [mg/dL]	60 min [mg/dL]	120 min [mg/dL]	30 min [mg/dL]	60 min [mg/dL]	120 min [mg/dL]
1	normal control	137 ±1.21	125 ±2.38	119 ±2.29	140 ±1.27	136 ±1.93	87 ±1.29	144 ±1.27	117 ±1.37	93 ±0.65
2	diabetic control (toxic)	284 ±2.27	427 ±3.21	321 ±1.97	580 ±2.32	547 ±1.48	566 ±1.02	599 ±2.93	536 ±1.28	452 ±2.17
3	standard drug 10 mg/kg (pioglitazone)	372 ±1.71	418 ±1.93	433 ±1.83	263 ±2.89	176 ±1.78	151 ±1.07	145 ±1.73	142 ±1.72	117 ±1.38
4	<i>Sida cordifolia</i> 100 mg/kg	361 ±1.89	570 ±2.27	205 ±1.95	223 ±1.72	109 ±1.05	90 ±0.15	223 ±1.28	90 ±1.31	109 ±1.19
5	<i>Sida cordifolia</i> 200 mg/kg	181 ±1.27	192 ±1.73	129 ±1.29	165 ±1.23	119 ±1.09	56 ±0.59	165 ±1.34	35 ±0.05	119 ±1.02
6	<i>Sida rhombifolia</i> 100 mg/kg	559 ±1.29	540 ±1.82	209 ±1.27	239 ±1.38	465 ±1.29	328 ±1.51	147 ±1.39	103 ±1.02	85 ±0.59
7	<i>Sida rhombifolia</i> 200 mg/kg	540 ±1.72	486 ±1.29	166 ±1.97	232 ±1.72	224 ±1.33	409 ±1.23	185 ±1.51	65 ±0.29	85 ±0.67

Table 7. Blood urea nitrogen

Serial number	Blood urea nitrogen [mg/dL]	Day 0 [mg/dL]	Day 7 [mg/dL]	Day 14 [mg/dL]	Day 21 [mg/dL]
1	normal control	16.01 ±3.20	16.5 ±3.01	17.01 ±2.99	17.9 ±3.07
2	diabetic control (toxic)	32.81 ±2.19	35.82 ±2.45	40.01 ±3.02	30.5 ±2.7
3	standard drug 10 mg/kg (pioglitazone)	20.00 ±1.25	18.21 ±1.20	17.56 ±1.75	19.6 ±1.8
4	<i>Sida cordifolia</i> 100 mg/kg	23.99 ±0.30	24.25 ±0.36	26.21 ±0.42	22.05 ±0.31
5	<i>Sida cordifolia</i> 200 mg/kg	22.82 ±1.00	22.55 ±1.06	23.07 ±1.19	24.00 ±1.8
6	<i>Sida rhombifolia</i> 100 mg/kg	24.20 ±0.35	25.44 ±0.39	24.95 ±0.41	25.05 ±0.5
7	<i>Sida rhombifolia</i> 200 mg/kg	23.85 ±1.05	25.02 ±1.72	25.9 ±2.01	24.56 ±1.9

to those found in the diabetic control (2.49 ± 0.19 g/dL) and *S. rhombifolia*-treated (100 mg/kg) animals (2.29 ± 0.51 g/dL). *Sida cordifolia* (200 mg/kg), along with pioglitazone, caused a consistent change throughout the treatment period. The results of the serum albumin level tests are presented in Fig. 6A and Table 8.

Effects of *Sida cordifolia* and *Sida rhombifolia* extracts on serum creatinine

Treatment with both extract dosages (100 mg/kg and 200 mg/kg) did not result in a considerable change in the levels of serum creatinine, although pioglitazone

and *S. cordifolia* (200 mg/kg) had similar effects on this parameter. The results of the serum creatinine level tests are presented in Fig. 6B and Table 8.

Histopathology of kidney tissues from different groups

The rats in the normal control group exhibited normal Bowman's capsules and parenchyma, with renal glomeruli enclosed by the distal and proximal tubules. The rats with STZ-induced diabetic nephropathy had severe congestion and hemorrhage of glomerular tufts, cloudy and swollen renal tubules, lymphocytic cell infiltration around

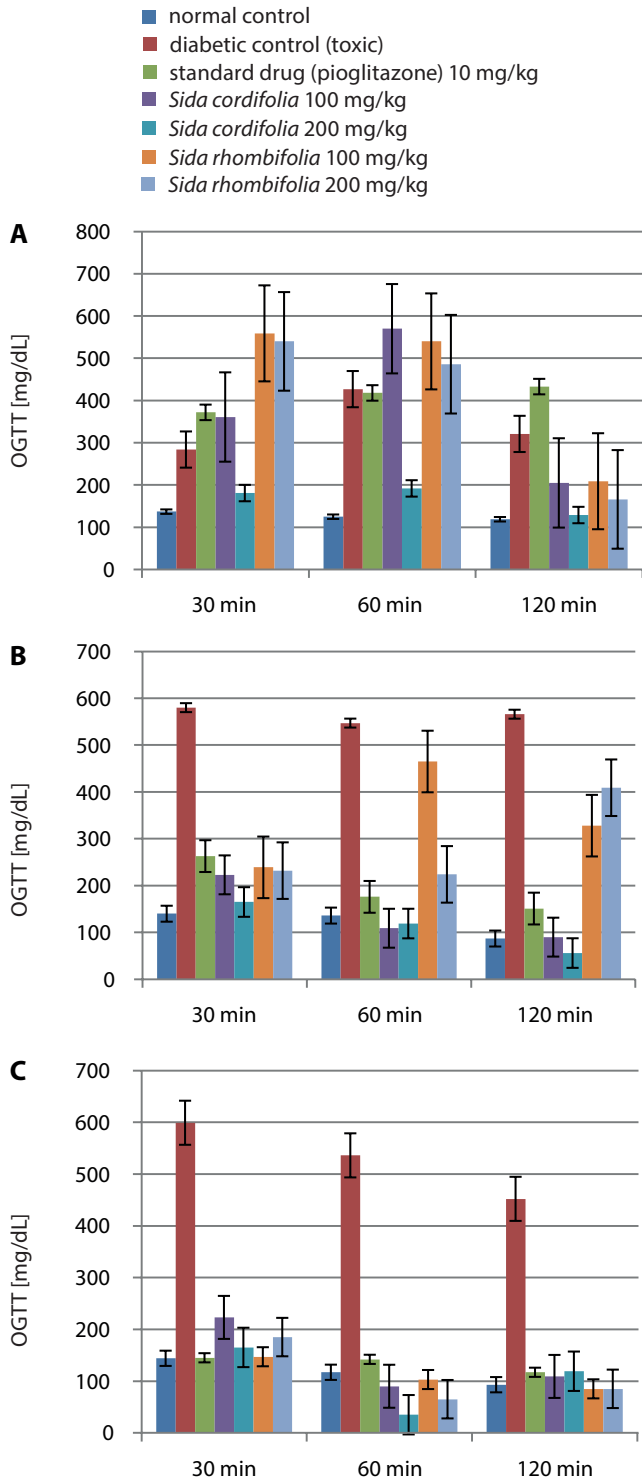


Fig. 4. Oral glucose tolerance tests (OGTT). A. Day 7; B. Day 14; C. Day 21

glomeruli, and renal tubules with edema in the interstitial tissue. The pioglitazone-treated group had almost normal glomeruli and renal tubules. *Sida cordifolia*- (100 mg/kg and 200 mg/kg) and *S. rhombifolia*- (100 mg/kg and 200 mg/kg) treated animals showed less congestion and hemorrhage of glomerular tufts and some mildly swollen tubules. The *S. cordifolia*-treated group (200 mg/kg) also demonstrated protection against diabetic nephropathy,

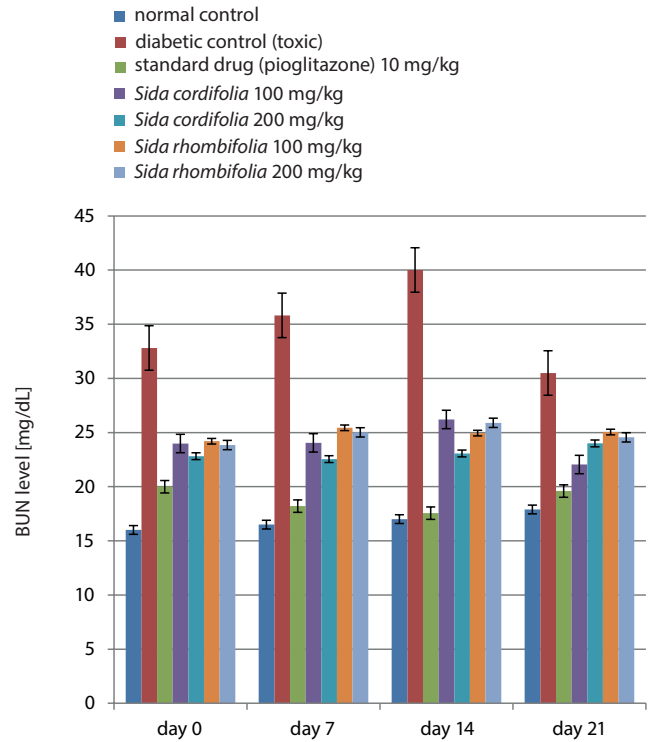


Fig. 5. Results of the blood urea nitrogen (BUN) level tests

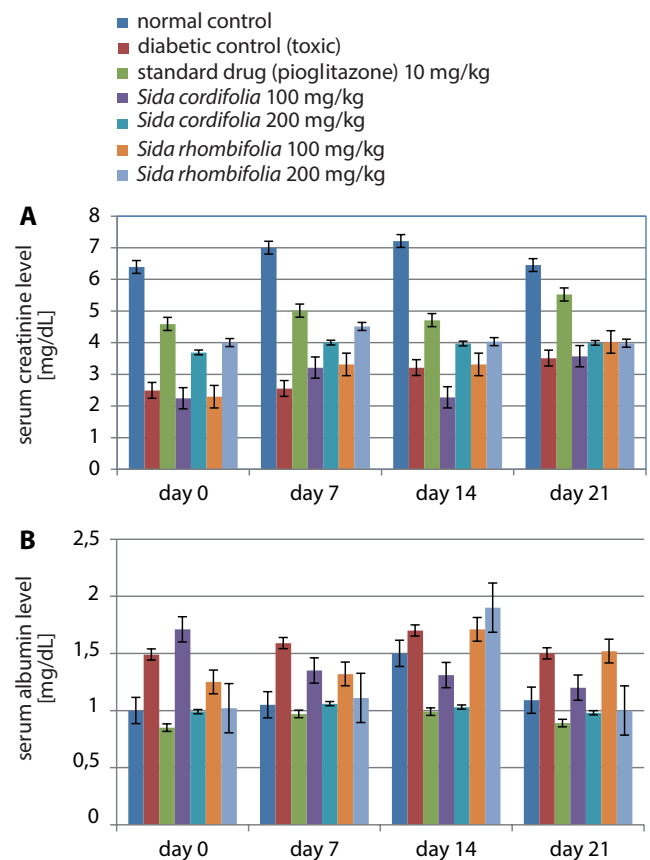


Fig. 6. Results of the serum albumin (A) and serum creatinine (B) level tests

which was indicated by a decrease in atrophy, thickness of membranes and mesangial enlargements. Before the onset of microalbuminuria, oxidative stress in combination

Table 8. Serum albumin and serum creatinine levels

Serial number	Group	Serum albumin [gm %]				Serum creatinine [mg/dL]			
		day 0 [gm %]	day 7 [gm %]	day 14 [gm %]	day 21 [gm %]	day 0 [mg/dL]	day 7 [mg/dL]	day 14 [mg/dL]	day 21 [mg/dL]
1	normal control	6.39 ± 0.03	7.00 ± 0.07	7.21 ± 0.09	6.45 ± 0.08	1.00 ± 0.15	1.05 ± 0.20	1.5 ± 0.26	1.09 ± 0.18
2	diabetic control (toxic)	2.49 ± 0.19	2.55 ± 1.01	3.21 ± 1.05	3.51 ± 1.11	1.49 ± 0.04	1.59 ± 0.09	1.7 ± 0.10	1.50 ± 0.01
3	standard drug 10 mg/kg (pioglitazone)	4.59 ± 0.40	5.01 ± 0.60	4.71 ± 0.51	5.52 ± 0.71	0.85 ± 0.01	0.97 ± 0.15	0.99 ± 0.14	0.88 ± 0.10
4	<i>Sida cordifolia</i> 100 mg/kg	2.24 ± 0.45	3.21 ± 0.62	2.27 ± 0.79	3.57 ± 0.91	1.20 ± 0.20	1.31 ± 0.27	1.35 ± 0.32	1.71 ± 0.30
5	<i>Sida cordifolia</i> 200 mg/kg	3.69 ± 0.65	4.00 ± 0.81	3.97 ± 0.68	3.99 ± 0.89	0.99 ± 0.09	1.06 ± 0.16	1.03 ± 0.19	0.98 ± 0.12
6	<i>Sida rhombifolia</i> 100 mg/kg	2.29 ± 0.51	3.31 ± 0.55	3.31 ± 0.55	4.02 ± 0.75	1.25 ± 0.29	1.32 ± 0.35	1.71 ± 0.25	1.52 ± 0.31
7	<i>Sida rhombifolia</i> 200 mg/kg	4.00 ± 0.70	4.51 ± 0.75	4.03 ± 0.81	3.98 ± 0.85	1.02 ± 0.11	1.11 ± 0.20	1.9 ± 0.37	1.00 ± 0.10

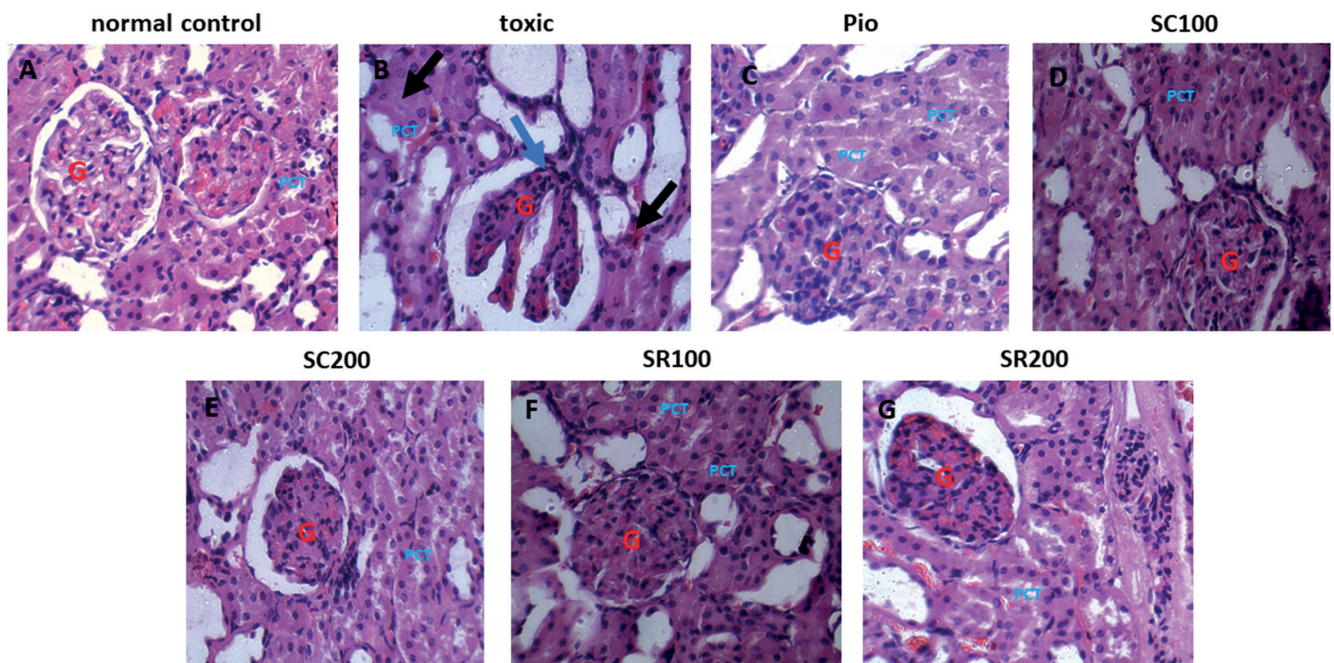


Fig. 7. Histopathology staining of kidney in different groups. A. Normal control: showing normal histological architecture; B. Toxic: showing severe congestion and hemorrhage of glomerular tuft (blue arrows), cloudy and swollen renal tubules (black arrow), lymphocytic cell infiltration around glomeruli and renal tubules with edema in the interstitial tissue; C–F. SC100 & SC200 and SR100 & SR200: showing lesser congestion and hemorrhage of glomerular tuft, with some mild swollen tubules; G. Pioglitazone: showing nearly normal glomeruli and renal tubules

SC – *Sida cordifolia*; SR – *Sida rhombifolia*.

with persistent hyperglycemia may play an essential role in the etiology of tubular, glomerular, structural, and functional anomalies. Figure 7 depicts the histopathological changes observed in the kidneys of different groups.

Histopathology of the pancreatic tissue of control and treated animals

The normal control group was vehicle-treated and had a normal histological structure. The diabetic control group revealed atrophy in the islet of Langerhans, as well

as degeneration and necrosis of islet cells. The group treated with pioglitazone (10 mg/kg/day) and *S. cordifolia* (200 mg/kg/day) had normal structures. The group treated with *S. cordifolia* (100 mg/kg/day) displayed atrophy, degeneration and necrosis in the islet of Langerhans. *Sida rhombifolia* treatment (100 mg/kg/day) resulted in a very mild atrophy in the islet Langerhans, along with the degeneration of islet cells and a little necrosis. *Sida rhombifolia*-treated rats (200 mg/kg/day) had a normal histological structure, although degeneration in islet cells and a little necrosis were observed.

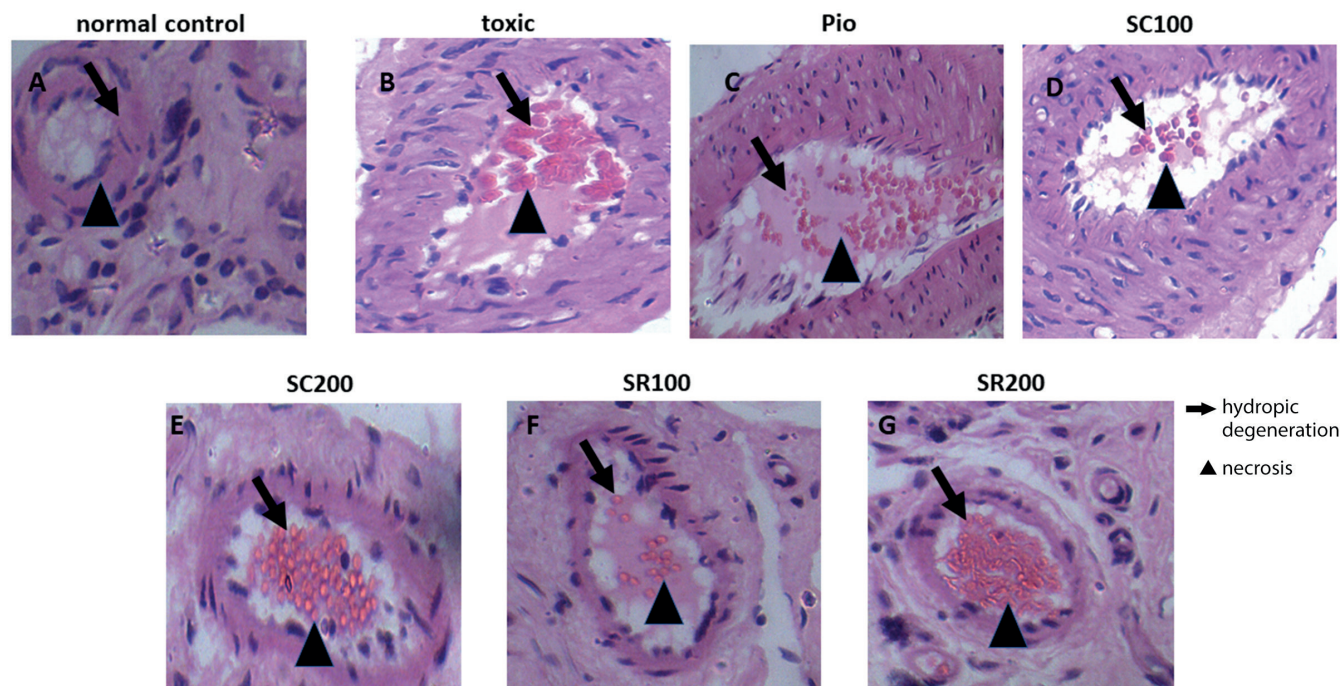


Fig. 8. Histopathology of the pancreatic tissue of control and treatment groups. A. Control (vehicle-treated): normal histological structure; B. Diabetic control: atrophy in the islet of Langerhans, degeneration and necrosis in islet cells; C. Pioglitazone 10 mg/kg/day: normal histological structure; D. SC 100 mg/kg/day: atrophy in the islet of Langerhans, degeneration and necrosis in islet cells; E. SC 200 mg/kg/day: normal histological structure; F. SR 100 mg/kg/day: very mild atrophy in the islet of Langerhans, degeneration in islet cells and a small extent of necrosis; G. SR 200 mg/kg/day: normal histological structure, degeneration in islet cells and a small extent of necrosis. Hematoxylin and eosin (H&E) staining, bar: 20 μ m

SC – *Sida cordifolia*; SR – *Sida rhombifolia*.

Figure 8 depicts the histopathological changes observed in the pancreatic tissue of the control and treatment groups.

Discussion

This study was conducted to examine the pharmacological activity of pioglitazone and extracts of *S. cordifolia* and *S. rhombifolia* in the treatment of rats with STZ-induced nephropathy. Blood glucose levels of the animals with STZ-induced nephropathy increased over the course of the experiment, which was significantly improved by a range of treatment dosages. Parameters, namely BUN, serum albumin and serum creatinine, were used to assess renal function and to diagnose nephropathy in diabetic rats. It was observed that among all of the extracts, *S. cordifolia* (200 mg/kg/day) improved kidney parameters and antioxidant levels. The antioxidant utilized in this study was NAD, which protects from the cytotoxic effects of STZ by eliminating free radicals. It achieves this while causing only modest harm to the β -cells of the pancreas. A similar situation occurs in type II diabetes. Nicotinamide, along with STZ, provides an excellent model for the study of pathophysiology of diabetes and is comparable to the human condition.¹²

The formation of chronic microalbuminuria is the initial clinical sign of emerging nephropathy in diabetes.

If patients suffering from diabetes do not receive therapy or medication, around 20–40% of them will advance to extreme albuminuria, and another 20% will develop end-stage renal disease (ESRD) within the following 20 years. The pathogenesis of microalbuminuria is heavily influenced by oxidative stress and dysfunctional endothelial cells.¹³ In a previous study on type II diabetes conducted for over a decade, 38% of participants developed microalbuminuria that was indicative of nephropathy.¹⁴ In the current study, microalbuminuria was prevalent in the group of untreated diabetic rats, which was changed through the administration of plant extracts. High concentrations of metabolic waste products such as BUN, serum creatinine and serum albumin compromise the function of the renal system. The administration of different dosages of extracts led to considerable reduction in these parameters, and it was observed that the administration of *S. cordifolia* (200 mg/kg/day) resulted in the most effective response.

The HbA1c is an effective indicator for the management of hyperglycemia, as it represents the true levels of glucose in the blood, does not disintegrate quickly and is generated gradually. Furthermore, HbA1c levels have been reported to rise in diabetic individuals.^{15,16} The administration of either *S. cordifolia* or *S. rhombifolia* decreased HbA1c levels in the blood and alleviated the hyperglycemic effects. The body weight of the treated animals was also lower. The most effective results, in comparison to pioglitazone, were achieved with *S. cordifolia* at 200 mg/kg/day.



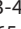
Kidneys play a major role in eliminating and metabolizing serum, which increases during chronic insufficiency of the renal system. The STZ-induced rats had observable changes in renal functioning, similar to those seen in the nephropathy of diabetic humans. This included activation of nuclear factor kappa-B (NF- κ B), expansion of mesangial matrices, overexpression of connective tissue growth factor (CTGF), hypertrophy of glomeruli, and thickening of glomeruli basement membranes.¹⁷ The histopathology reports for the group treated with *S. cordifolia* (200 mg/kg/day) were similar to the results obtained after pioglitazone treatment, and proved to be significant. These results can be utilized for the treatment of diabetic nephropathy and can stimulate further research into the use of the herb. However, it was observed that other doses of *S. rhombifolia* extract caused abnormalities in the kidneys and pancreas, making them unsuitable for further analysis.

Previous research findings suggest that *S. cordifolia* has the potential to exhibit nephroprotective properties. This could be due to the reduction of glucose pathways or through antioxidant activity.^{9,18,19} The plant is considered to be safe, with its median lethal dose (LD50) being greater than 3 g/kg. It may be of benefit in therapeutic practice as its toxicity potential is low.²⁰ Our results suggest that further research is warranted on *S. cordifolia* (200 mg/kg/day) for the assessment and treatment of diabetic nephropathy.

Conclusions

In this study, the effects of *S. cordifolia* and *S. rhombifolia* extracts on rats affected by diabetic nephropathy were observed. The study highlighted and provided evidence that *S. cordifolia* (200 mg/kg/day) produced the most vital results by reducing HbA1c and blood glucose levels, along with having a significant impact on the results of the OGTT. Of the 2 plants, given their varied nature in the treatment of different ailments, *S. cordifolia* can be further studied and incorporated into the treatment of diabetic nephropathy.

ORCID iDs

Mohd Imran  <https://orcid.org/0000-0001-7349-3019>
 Sahaya Mercy Jaqueline Robert  <https://orcid.org/0000-0002-6626-1153>
 Manju Sharma  <https://orcid.org/0000-0003-4013-6626>
 Vidhu Aeri  <https://orcid.org/0000-0002-7465-4619>

References

- Ogurtsova K, da Rocha Fernandes JD, Huang Y, et al. IDF Diabetes Atlas: Global estimates for the prevalence of diabetes for 2015 and 2040. *Diabetes Res Clin Pract.* 2017;128:40–50. doi:10.1016/j.diabres.2017.03.024
- Andersen AR, Christiansen JS, Andersen JK, Kreiner S, Deckert T. Diabetic nephropathy in type 1 (insulin-dependent) diabetes: An epidemiological study. *Diabetologia.* 1983;25(6):496–501. doi:10.1007/BF00284458
- Evans WC, Evans D. The scope and practice of pharmacognosy. In: Evans WC, *Trease and Evans' Pharmacognosy.* 16th ed. St. Louis, USA: Elsevier Health Sciences; 2009:5–7. doi:10.1016/B978-0-7020-2933-2.00002-2
- Edwards JL, Vincent AM, Cheng HT, Feldman EL. Diabetic neuropathy: Mechanisms to management. *Pharmacol Ther.* 2008;120(1):1–34. doi:10.1016/j.pharmthera.2008.05.005
- Dinda B, Das N, Dinda S, Dinda M, SilSarma I. The genus *Sida* L.: A traditional medicine. Its ethnopharmacological, phytochemical and pharmacological data for commercial exploitation in herbal drugs industry. *J Ethnopharmacol.* 2015;176:135–176. doi:10.1016/j.jep.2015.10.027
- Chaturvedi P, Kwape TE. Attenuation of diabetic conditions by *Sida rhombifolia* in moderately diabetic rats and inability to produce similar effects in severely diabetic rats. *J Pharmacopuncture.* 2015;18(4):12–19. doi:10.3831/KPI.2015.18.032
- Galal A, Raman V, A. Khan I. *Sida cordifolia*, a traditional herb in modern perspective: A review. *Curr Trad Med.* 2015;1(1):5–17. doi:10.2174/2215083801666141226215639
- Berbudi A, Rahmadika N, Tjahjadi AI, Ruslami R. Type 2 diabetes and its impact on the immune system. *Curr Diabetes Rev.* 2020;16(5):442–449. doi:10.2174/1573399815666191024085838
- Ahmad M, Prawez S, Sultana M, et al. Anti-hyperglycemic, anti-hyperlipidemic and antioxidant potential of alcoholic-extract of *Sida cordifolia* (areal part) in streptozotocin-induced-diabetes in Wistar rats. *Proc Natl Acad Sci India Sect B Biol Sci.* 2014;84(2):397–405. doi:10.1007/s40011-013-0218-2
- Srinivasan N, Murali R, Sivakrishnan S. *Sida cordifolia*: An update on its traditional use, phytochemistry, and pharmacological importance. *Int J Pharm Res Allied Sci.* 2022;11(1):74–86. doi:10.51847/Q1trGLYB0E
- Harborne AJ. Methods of plant analysis. In: Harborne AJ, *Phytochemical Methods. A Guide to Modern Techniques of Plant Analysis.* Dordrecht, the Netherlands: Springer Netherlands; 1984:1–36. doi:10.1007/978-94-009-5570-7
- Nagella P. Chemical constituents, larvicidal effects and antioxidant activity of petroleum ether extract from seeds of *Coriandrum sativum* L. *J Med Plants Res.* 2012;6(15):2948–2954. doi:10.5897/JMPR11.992
- Srinivasan K, Ramarao P. Animal models in type 2 diabetes research: An overview. *Indian J Med Res.* 2007;125(3):451–472. PMID:17496368.
- Singh VP, Bali A, Singh N, Jaggi AS. Advanced glycation end products and diabetic complications. *Korean J Physiol Pharmacol.* 2014;18(1):1–14. doi:10.4196/kjpp.2014.18.1.1
- Baskaran K, Ahamath BK, Shanmugasundaram KR, Shanmugasundaram ERB. Antidiabetic effect of a leaf extract from *Gymnema sylvestre* in non-insulin-dependent diabetes mellitus patients. *J Ethnopharmacol.* 1990;30(3):295–305. doi:10.1016/0378-8741(90)90108-6
- Kumar A, Pathak M, Chaudhary R, Verma V, Singh L. Pharmacognostical studies and quality control parameters of *Sida rhombifolia*. *Int J Biol Pharm Allied Sci.* 2022;11(2):662–672. doi:10.31032/IJBPAS/2022/11.2.5884
- Sarwar Alam M, Kaur G, Jabbar Z, Javed K, Athar M. Eruca sativa seeds possess antioxidant activity and exert a protective effect on mercuric chloride induced renal toxicity. *Food Chem Toxicol.* 2007;45(6):910–920. doi:10.1016/j.fct.2006.11.013
- Ahmed H, Juraimi AS, Swamy MK, et al. Botany, chemistry, and pharmaceutical significance of *Sida cordifolia*: A traditional medicinal plant. In: Akhtar MS, Swamy MK, eds. *Anticancer Plants: Properties and Application.* Singapore: Springer Singapore; 2018:517–537. doi:10.1007/978-981-10-8548-2_22
- Momin MAM, Bellah SF, Rahman SMR, Rahman AA, Murshid GMM, Emran TB. Phytopharmacological evaluation of ethanol extract of *Sida cordifolia* L. roots. *Asian Pac J Trop Biomed.* 2014;4(1):18–24. doi:10.1016/S2221-1691(14)60202-1
- Konaté K, Bassolé IHN, Hilou A, et al. Toxicity assessment and analgesic activity investigation of aqueous acetone extracts of *Sida acuta* Burn f. and *Sida cordifolia* L. (Malvaceae), medicinal plants of Burkina Faso. *BMC Complement Altern Med.* 2012;12(1):120. doi:10.1186/1472-6882-12-120

Influence of thermal cycles and disinfection on the roughness, microhardness and color of PETG/TPU and PMMA

Clóvis Lamartine de Moraes Melo Neto^{A,C,D}, Bruno Simão Bernardi^{A,B}, Stefan Fiuza de Carvalho Dekon^{A,B,D}, Daniela Micheline dos Santos^{E,F}, Marcelo Coelho Goiato^{A,C,E,F}

Department of Dental Materials and Prosthodontics, School of Dentistry, São Paulo State University (UNESP), Araçatuba, Brazil

A – research concept and design; B – collection and/or assembly of data; C – data analysis and interpretation; D – writing the article; E – critical revision of the article; F – final approval of the article

Polymers in Medicine, ISSN 0370-0747 (print), ISSN 2451-2699 (online)

Polim Med. 2023;53(1):19–24

Address for correspondence

Marcelo Coelho Goiato
E-mail: m.goiato@unesp.br

Funding sources

None declared

Conflict of interest

None declared

Received on November 24, 2022

Reviewed on January 4, 2023

Accepted on January 16, 2023

Published online on March 16, 2023

Abstract

Background. Occlusal splints can protect teeth during bruxism, preventing tooth wear, as well as during sports activities, shielding them from impacts.

Objectives. To verify the influence of thermal cycles and disinfection on the roughness, microhardness and color of polyethylene terephthalate glycol/thermoplastic polyurethane (PETG/TPU) and poly(methyl methacrylate) (PMMA).

Materials and methods. Thirty-six PETG/TPU samples and 36 PMMA samples were prepared ($\varnothing 10 \text{ mm} \times 3 \text{ mm}$). Six groups were created according to the material and the disinfection method used ($n = 12$ each): PETG/TPU (glistler), PETG/TPU (hypochlorite), PETG/TPU (soap), PMMA (glistler), PMMA (hypochlorite), and PMMA (soap). Roughness, Knoop microhardness and color evaluations were performed before the experiments (T1), after thermocycling (T2) and after disinfection (T3). Three-way repeated measures analysis of variance (ANOVA) and Tukey's test were used for statistical evaluations.

Results. For roughness and color, ANOVA showed statistical significance based on the interaction between thermal cycling, material and disinfectant factors. In terms of Knoop microhardness, ANOVA showed statistical significance based on the interaction between thermal cycling and material factors.

Conclusions. Roughness results were clinically acceptable in all groups at all time points, except the PETG/TPU and PMMA groups disinfected with hypochlorite. Microhardness significantly increased for both materials after thermal cycling, and at all time points, the microhardness of PMMA was significantly higher than that of PETG/TPU. After thermal cycling, the color changes were clinically unacceptable in all groups.

Key words: polymers, polyurethane, occlusal splints, polymethyl methacrylate, polyethylene terephthalate glycol

Cite as

de Moraes Melo Neto CL, Bernardi BS, Dekon SFC, dos Santos DM, Goiato MC. Influence of thermal cycles and disinfection on the roughness, microhardness and color of PETG/TPU and PMMA. *Polim Med.* 2023;53(1):19–24. doi:10.17219/pim/159350

DOI

10.17219/pim/159350

Copyright

Copyright by Author(s)

This is an article distributed under the terms of the Creative Commons Attribution 3.0 Unported (CC BY 3.0) (<https://creativecommons.org/licenses/by/3.0/>)

Background

Most occlusal splints are based on acrylic resin (poly(methyl methacrylate) (PMMA) – a thermoplastic polymer).¹ Such splints can protect teeth during bruxism, preventing tooth wear, as well as during sports activities, shielding them from impacts.^{1–4} Additionally, the splints can be used after orthodontic movement to prevent teeth from returning to their pre-treatment positions,⁵ and for orthognathic treatment for the repositioning of skeletal structures.^{6–8}

In recent years, a new material has been used to manufacture splints.² This material combines polyethylene terephthalate glycol (PETG – a thermoplastic polymer) with thermoplastic polyurethane (TPU). The PETG/TPU splint has a hard outer part, which comes into contact with opposing teeth during bruxism, and a soft inner part, which fits over the teeth.² The PETG is a rigid polymer with excellent conformability, optical quality, resistance to mechanical stress, and dimensional stability. The TPU is a ductile elastomer that helps absorb impacts due to its elasticity, providing patient comfort.² It is worth mentioning that the PETG/TPU occlusal splint (Erkodent) can only be manufactured in a thermoplasticizer from the same company, due to the precise temperature control of this device, which is necessary to manipulate the PETG/TPU without damaging it.

Roughness, microhardness and color are important clinical factors for polymers used in dentistry (e.g., PMMA or PETG/TPU occlusal splints). The roughness of a material is related to the accumulation of microbes on its surface.⁹ Thus, the greater the roughness of an occlusal splint, the greater the accumulation of microbes on its surface.⁹ The microhardness of a material is related to its wear resistance.⁹ Therefore, the greater the microhardness of a material, the greater its longevity.⁹ The color of a material is one of the most important factors in dentistry. A change in the color of an occlusal splint over time can cause discomfort to its user, especially if people are around while the splint is in use.

This study, evaluating the physical and mechanical properties of PETG/TPU, is justified for several reasons. First, there is only 1 recent study (2021) evaluating the effects of thermal cycles and different disinfection methods on the physical and mechanical properties of PETG/TPU, and comparing them with those of PETG.² Second, no published study has compared the physical and mechanical properties of PETG/TPU with those of PMMA. Third, the manufacturing cost of a PETG/TPU splint is higher compared with the manufacturing cost of a PMMA splint. Thus, it is important for dentists to learn more about this new material (PETG/TPU) before recommending it to their patients.

The objective of the current study is to examine the impact of thermal cycles and disinfection on the roughness, microhardness and color of PETG/TPU and PMMA.

Materials and methods

Groups

Thirty-six PETG/TPU samples and 36 PMMA samples were fabricated. Next, 6 groups were created according to the material and disinfection method used ($n = 12$ each): PETG/TPU (glistler), PETG/TPU (hypochlorite), PETG/TPU (soap), PMMA (glistler), PMMA (hypochlorite), and PMMA (soap). All manufactured samples (colorless and translucent) had the same dimensions ($\varnothing 10 \text{ mm} \times 3 \text{ mm}$).^{2,10}

Evaluation times

Assessments were performed at 3 time points (T1, T2 and T3):

- T1 (initial): roughness, microhardness and color change tests were performed in all groups;
- T2 (after thermal cycling): all groups underwent thermal cycling and, subsequently, all tests performed at T1 were repeated;
- T3 (after disinfection): each group was exposed to its respective disinfectant, and the tests performed at T1 were subsequently repeated (note: disinfection was performed on specimens that had already been subjected to thermal cycling).

All tests were performed by the same operator.

Sample manufacturing

In this study, samples of PMMA (Clássico, São Paulo, Brazil) and PETG/TPU (Erkoloc-Pro Clear; Erkodent, Pflzgrafenweiler, Germany) were fabricated.

Thermopolymerizable PMMA samples with dimensions of $\varnothing 10 \text{ mm} \times 3 \text{ mm}$ ^{2,10} were prepared according to a study by Goiato et al.,^{11,12} using the conventional resin polymerization method.¹³ After manufacturing, the samples were submitted to finishing with Maxi-Cut burs to remove excess acrylic resin. Next, the samples were polished using a sequence of abrasive papers in a universal automatic polisher (APL-4; Arotec SA Indústria e Comércio Ltda., Cotia, Brazil).¹¹ The abrasive papers were used in ascending order (600-, 800- and 1200-grit) for 1 min each, at a speed of 300 rpm and under constant irrigation.¹¹ After finishing and polishing, the samples were stored in distilled water inside an incubator (CIENLAB, Campinas, Brazil) at a temperature of 37°C for 24 h to hydrate them while residual monomers were eliminated.¹¹ Each group was stored separately.

The thermoplastic PETG/TPU samples were manufactured from sheets of material measuring $\varnothing 120 \times 3 \text{ mm}$.² Before cutting the samples, the PETG/TPU sheets were thermoprocessed using the Erkoform 3D Motion (Erkodent), according to the manufacturer's recommendations.² After this process, metallic cylinders were used to cut the heated PETG/TPU sheets.² The PETG/TPU groups were stored in the same way as the PMMA groups.

All PETG/TPU and PMMA samples were prepared by the same operator.

Roughness

The roughness of all samples was determined using a profilometer (Dektak 150; Veeco, Plainview, USA). The samples were placed on a support and the profilometer tip was used on their surface.¹⁰ The roughness average (Ra) values were measured using a cutoff of 500 μm in a 12-second time constant.¹⁰ Three readings were taken on each sample and the average value was calculated.¹⁰ The roughness was measured in micrometers [μm].¹⁰ For the PETG/TPU samples, this evaluation was performed only on the PETG part.²

Knoop microhardness

The Knoop microhardness test was performed with a load of 25 g for 10 s (HMV/2T; Shimadzu, Kyoto, Japan).² Three readings were taken on each sample.² The distance between penetrations, and between penetrations and the edges of the sample was 500 μm .² Values were recorded as Knoop hardness numbers (KHN). An average of the 3 readings was taken.² For the PETG/TPU samples, this evaluation was performed only on the PETG part.²

Color change

The color change (ΔE^*) was calculated using the Commission Internationale de l'Éclairage (CIE) $L^*a^*b^*$ system (UV/2450; Shimadzu).² The formula used was: $\Delta E^* = [(\Delta L^*)^2 + (\Delta a^*)^2 + (\Delta b^*)^2]^{1/2}$. The L^* variable represents luminosity and varies from 0 (black) to 100 (white).² The a^* variable represents the amount of red (positive values) or green (negative values), while the b^* variable represents the amount of yellow (positive values) or blue (negative values).²

For the PETG/TPU samples, this evaluation was performed only on the PETG part, as this is the part that is visible when the patient is using an occlusal splint.²

Thermal cycles

The samples were submitted to 2000 cycles of immersion in alternating baths of distilled water at 5°C and 55°C for 60 s (MSCT/3; Convel, São Paulo, Brazil).²

Disinfection

Each group was disinfected with one of the following: Glistier™ Concentrated Multi-Action Oral Rinse (Amway, São Paulo, Brazil), 1% hypochlorite⁹ and liquid soap² (liquid soap with glycerin, physiologic pH, Johnson's Baby; Johnson & Johnson, São Paulo, Brazil).²

The liquid soap was not diluted with any substance. The Glistier™ oral rinse was diluted with water according to the manufacturer's recommendations (5 jets were applied inside the product dosing cup and then the cup was filled up to the 1-ounce-line with water).

Disinfection was performed for 60 days, 3 times a week.⁹ During disinfection, each group remained immersed in its respective disinfectant for 15 min at 37°C. After each disinfection, the samples were washed in running water for 30 s.⁹

Statistical analyses

Three-way repeated measures analysis of variance (ANOVA) and Tukey's test were used for statistical evaluations ($p < 0.05$; Jamovi, v. 2.2.5.0; Jamovi Project, Sydney, Australia).

Results

Roughness

For roughness, ANOVA showed statistical significance based on the interaction between thermal cycling, material and disinfectant factors ($p < 0.001$; Table 1). At T1 (Table 2), the PMMA (hypochlorite) group showed a significantly higher roughness value than the other groups. At T2, the PMMA (hypochlorite) and PMMA (soap) groups showed significantly higher roughness values than the other groups. At T3, the PETG/TPU (hypochlorite) group showed a significantly higher roughness value than the other groups, and the PETG/TPU (glistier) and PMMA (hypochlorite) groups showed significantly higher roughness values than the PETG/TPU (soap), PMMA (glistier) and PMMA (soap) groups.

When measurements taken at different time points were compared (Table 2), the PMMA (hypochlorite) group showed a significant increase in roughness at T2 (T2 compared with

Table 1. Three-way repeated measures analysis of variance (ANOVA) for the roughness test

Factors	Sum of squares	df	Mean square	F	p-value
Thermal cycling	0.1011	2	0.05053	116.64	<0.001*
Thermal cycling × material	0.0146	2	0.00731	16.87	<0.001*
Thermal cycling × disinfectant	0.0178	4	0.00444	10.24	<0.001*
Thermal cycling × material × disinfectant	0.0145	4	0.00363	8.37	<0.001*
Residue	0.0572	132	4.33e-4	–	–

* interaction between the factors was statistically significant or the analyzed factor was statistically significant; df – degrees of freedom.

Table 2. Mean (standard deviation) of the roughness values (μm) of the evaluated groups

Groups	Initial (T1)	After thermal cycling (T2)	After disinfection (T3)
PETG/TPU (glister)	0.173 (0.0172) Aa	0.195 (0.0291) Aa	0.248 (0.0219) Ab
PETG/TPU (hypochlorite)	0.186 (0.0309) Aa	0.194 (0.0274) Aa	0.288 (0.0350) Bb
PETG/TPU (soap)	0.185 (0.0216) Aa	0.193 (0.0199) Aa	0.200 (0.0179) Ca
PMMA (glister)	0.163 (0.0208) Aa	0.193 (0.0214) Aa	0.200 (0.0224) Ca
PMMA (hypochlorite)	0.207 (0.0289) Ba	0.233 (0.0384) Bb	0.251 (0.0355) Ab
PMMA (soap)	0.173 (0.0381) Ab	0.210 (0.0260) Bb	0.217 (0.0262) Cb

Different lowercase letters horizontally represent a statistically significant difference. Different capital letters vertically represent a statistically significant difference (Tukey's test, $p < 0.05$). PETG – polyethylene terephthalate glycol; TPU – thermoplastic polyurethane; PMMA – poly(methyl methacrylate).

T1). The PETG/TPU (glister) and PETG/TPU (hypochlorite) groups showed a significant increase in roughness at T3 (T3 compared with T2).

Knoop microhardness

For microhardness, ANOVA showed statistical significance based on the interaction between thermal cycling and material factors ($p < 0.001$; Table 3). There was a significant increase in microhardness after thermal cycling (T2 compared with T1) for PETG/TPU and PMMA (Table 4). At all time points (T1, T2 and T3), the microhardness of PMMA was significantly higher than that of PETG/TPU (Table 4).

Color change

For color change, ANOVA showed statistical significance based on the interaction between thermal cycling, material and disinfectant factors ($p < 0.001$; Table 5). Based on $\Delta E1$, there were no significant differences between groups (Table 6). Based on $\Delta E2$, the PETG/TPU (hypochlorite) group showed a significantly greater color change compared with the other groups (Table 6).

From $\Delta E1$ to $\Delta E2$, there was a significant reduction in color change values in all groups, except for PMMA (glister) ($p > 0.05$) and PETG/TPU (hypochlorite – this group showed a significant increase in color value from $\Delta E1$ to $\Delta E2$; Table 6).

Table 3. Three-way repeated measures analysis of variance (ANOVA) for the microhardness test

Factors	Sum of squares	df	Mean square	F	p-value
Thermal cycling	239.08	2	119.538	102.573	<0.001*
Thermal cycling \times material	53.21	2	26.607	22.831	<0.001*
Thermal cycling \times disinfectant	1.80	4	0.451	0.387	0.818
Thermal cycling \times material \times disinfectant	2.87	4	0.718	0.661	0.652
Residue	153.83	132	1.165	–	–

* interaction between the factors was statistically significant or the analyzed factor was statistically significant; df – degrees of freedom.

Table 4. Mean (standard deviation) of the Knoop hardness numbers (KHN) of the evaluated materials

Material	Initial (T1)	After thermal cycling (T2)	After disinfection (T3)
PETG/TPU	11.5 (1.17) Aa	12.5 (0.91) Ab	12.8 (0.90) Ab
PMMA	18.7 (1.47) Ba	21.7 (1.43) Bb	22.2 (1.42) Bb

Different lowercase letters horizontally represent a statistically significant difference. Different capital letters vertically represent a statistically significant difference (Tukey's test, $p < 0.05$). PETG – polyethylene terephthalate glycol; TPU – thermoplastic polyurethane; PMMA – poly(methyl methacrylate).

Table 5. Three-way repeated measures analysis of variance (ANOVA) for the color change test

Factors	Sum of squares	df	Mean square	F	p-value
Thermal cycling	89.4	1	89.39	24.70	<0.001*
Thermal cycling \times material	14.2	1	14.17	3.92	0.052
Thermal cycling \times disinfectant	93.8	2	46.92	12.97	<0.001*
Thermal cycling \times material \times disinfectant	201.6	2	100.78	27.85	<0.001*
Residue	238.8	66	3.62	–	–

* interaction between the factors was statistically significant or the analyzed factor was statistically significant; df – degrees of freedom.

Table 6. Mean (standard deviation) of the color values (ΔE) of the evaluated groups

Groups	$\Delta E1$	$\Delta E2$
PETG/TPU (glister)	6.35 (1.60) Aa	3.67 (2.62) Ab
PETG/TPU (hypochlorite)	4.23 (1.94) Aa	8.46 (1.75) Bb
PETG/TPU (soap)	6.90 (2.58) Aa	2.51 (2.20) Ab
PMMA (glister)	4.22 (1.69) Aa	4.23 (2.41) Aa
PMMA (hypochlorite)	5.65 (2.00) Aa	1.96 (0.84) Ab
PMMA (soap)	4.72 (2.15) Aa	1.79 (1.30) Ab

Different lowercase letters horizontally represent a statistically significant difference. Different capital letters vertically represent a statistically significant difference (Tukey's test, $p < 0.05$). PETG – polyethylene terephthalate glycol; TPU – thermoplastic polyurethane; PMMA – poly(methyl methacrylate).

Discussion

The purpose of thermal cycling was to simulate the extreme temperature changes that occur during the clinical use of an occlusal splint. In this study, 2000 thermal cycles were performed, which represents 2 years of clinical use of an occlusal splint.² This procedure can promote successive expansions and contractions of the material causing microcracks.² The literature shows that temperature variations combined with high humidity, as well as the use of disinfection methods over time, are extrinsic degradation factors for a polymer.^{2,9,11,14} It is noteworthy that the intrinsic degradation factor for a polymer is represented by a change in its matrix over time.^{2,9,11,14}

When comparing the groups at T1 (Table 2), there was no significant difference between the PETG/TPU groups, while the PMMA groups showed significant differences between them. Furthermore, the roughness of the PMMA (hypochlorite) group samples was significantly higher than those of the PETG/TPU groups (T1; Table 2). These results may suggest that the industrial polishing of PETG/TPU was more standardized than the manual polishing of PMMA. Based on the statistical analysis, comparing the groups at T2, it is possible to verify that in most cases, the roughness values of PMMA were significantly higher than those of PETG/TPU (Table 2). Thus, this may suggest that, clinically, PETG/TPU accumulates less bacterial plaque on its surface over time.

Table 2 shows that from T1 to T2, only 1 group (PMMA (hypochlorite)) showed a significant increase in the roughness value. This result can be explained by a degradation of this type of material. The degradation of a polymer, due to extrinsic and intrinsic factors, is represented, for example, by a significant change in its roughness, microhardness and color values.^{2,9,11,14} Despite this, as previously reported, the increase in roughness occurred in 1 group only (Table 2), which shows the excellent quality of both types of materials.

At T3 (Table 2), the following information on roughness values can be observed: 1) comparing the PETG/TPU

groups: soap < glister < hypochlorite ($p < 0.05$); and 2) comparing the PMMA groups: soap = glister < hypochlorite ($p < 0.05$). Thus, hypochlorite was the disinfectant that most increased the roughness of these materials. Furthermore, still based on the T3 time point (Table 2), the glister and the hypochlorite generated a significantly greater roughness on the PETG/TPU surface than on the PMMA surface. Thus, PMMA is likely to be less negatively influenced by these disinfectants than PETG/TPU. It is noteworthy that, based on another analysis of Table 2 (i.e., from T2 to T3), PMMA roughness was not influenced by any disinfectant, unlike PETG/TPU roughness, which increased significantly after disinfection with hypochlorite and glister.

The level of roughness that prevents the accumulation of microbes on the surface of a material is $\leq 0.2 \mu\text{m}$ (clinically acceptable value).^{15,16,17} A greater roughness than this promotes bacterial adhesion to the surface of the material, which may result in gingival inflammation and caries.^{16,17} In this study, values $< 0.25 \mu\text{m}$ were considered clinically acceptable. Thus, despite the statistically significant differences in Table 2, all results were clinically acceptable, with the exception of 2 groups (T3 – PMMA (hypochlorite) and T3 – PETG/TPU (hypochlorite)). Therefore, hypochlorite was the most aggressive disinfectant for the materials used.

For PETG/TPU or PMMA, there was a significant increase in microhardness at T2 when compared with T1 (Table 4). This shows that, at T2, both materials showed degradation based on microhardness. It should be noted that, at all time points, the microhardness values of PMMA were significantly higher than those of PETG/TPU. Therefore, clinically, PMMA is more resistant to wear than PETG/TPU, contributing to the greater longevity of PMMA splints (Table 4). Based on this result, it is possible to recommend PMMA splints for severe cases of bruxism and PETG/TPU splints for milder cases of bruxism.

Specification number 12 of the American Dental Association (ADA) indicates that the microhardness of acrylic resins for denture bases should not be lower than 15 KHN.¹⁸ Based on this recommendation, all PMMA microhardness values (T1, T2 and T3) were clinically acceptable (Table 4).¹⁸

Based on $\Delta E1$ (Table 6), there were no significant differences between PETG/TPU or PMMA groups; and between PETG/TPU and PMMA groups. This demonstrates that thermal cycling generated similar effects in all evaluated groups ($\Delta E1$), and that occlusal splints made of PMMA or PETG/TPU may show similar color changes over time. Based on $\Delta E2$ (Table 6), the PETG/TPU (hypochlorite) group showed a significantly higher color change value than the other groups, and from $\Delta E1$ to $\Delta E2$, the PETG/TPU (hypochlorite) group was the only group that showed a significant increase in color change. Thus, the chronic use of this disinfectant can clinically change the color of a PETG/TPU splint.

The $\Delta E < 3.7$ is considered clinically acceptable for a material.^{19,20} Thus, based on $\Delta E1$ (Table 6), all observed

values were clinically unacceptable, demonstrating that a large color change can be expected for both materials over time. Based on ΔE_2 (Table 6), in most situations, disinfectants acceptably changed the color of the materials used (PETG/TPU (glistler), PETG/TPU (soap), PMMA (hypochlorite), and PMMA (soap)). However, this only shows that, in most situations, disinfectants acceptably changed the color of materials that have already undergone a clinically unacceptable color change.


A limitation of this study is that only 3 disinfectants were used. Thus, more studies are needed using other disinfectants.

Conclusions

Roughness results were clinically acceptable in all groups at all time points, except for the PETG/TPU and PMMA groups disinfected with hypochlorite. The microhardness was increased for both materials after thermal cycling, and, at all time points, the microhardness of PMMA was significantly higher than that of PETG/TPU. The color change was clinically unacceptable after thermal cycling in all groups.

ORCID iDs

Clóvis Lamartine de Moraes Melo Neto

 <https://orcid.org/0000-0003-1477-2055>

Bruno Simão Bernardi  <https://orcid.org/0000-0003-1228-1789>

Stefan Fiuza de Carvalho Dekon

 <https://orcid.org/0000-0001-7858-2256>

Daniela Micheline dos Santos

 <https://orcid.org/0000-0001-6297-6154>

Marcelo Coelho Goiato  <https://orcid.org/0000-0002-3800-3050>

References

1. Reyes-Sevilla M, Kuijs RH, Werner A, Kleverlaan CJ, Lobbezoo F. Comparison of wear between occlusal splint materials and resin composite materials. *J Oral Rehabil.* 2018;45(7):539–544. doi:10.1111/joor.12636
2. de Almeida Salles C, de Moraes Melo Neto CL, de Carvalho Dekon SF, et al. Influence of thermocycling and disinfection on the color stability and hardness of thermoplastic sheets used for occlusal splint fabrication. *Gen Dent.* 2021;69(3):42–45. PMID:33908877.
3. Cesanelli L, Cesaretti G, Ylaitè B, Iovane A, Bianco A, Messina G. Occlusal splints and exercise performance: A systematic review of current evidence. *Int J Environ Res Public Health.* 2021;18(19):10338. doi:10.3390/ijerph181910338
4. Kalman L, Dal Piva AM de O, de Queiroz TS, Tribst JPM. Biomechanical behavior evaluation of a novel hybrid occlusal splint-mouthguard for contact sports: 3D-FEA. *Dent J.* 2021;10(1):3. doi:10.3390/dj10010003
5. Mai W, He J, Meng H, et al. Comparison of vacuum-formed and Hawley retainers: A systematic review. *Am J Orthod Dentofacial Orthop.* 2014;145(6):720–727. doi:10.1016/j.ajodo.2014.01.019
6. Vale F, Scherzberg J, Cavaleiro J, et al. 3D virtual planning in orthognathic surgery and CAD/CAM surgical splints generation in one patient with craniofacial microsomia: A case report. *Dental Press J Orthod.* 2016;21(1):89–100. doi:10.1590/2177-6709.21.1.089-100.oar
7. Ng JH, Chen YA, Hsieh YJ, Yao CF, Liao YF, Chen YR. One-splint versus two-splint technique in orthognathic surgery for class III asymmetry: Comparison of patient-centred outcomes. *Clin Oral Invest.* 2021; 25(12):6799–6811. doi:10.1007/s00784-021-03967-9
8. Chen H, Bi R, Hu Z, et al. Comparison of three different types of splints and templates for maxilla repositioning in bimaxillary orthognathic surgery: A randomized controlled trial. *Int J Oral Maxillofac Surg.* 2021; 50(5):635–642. doi:10.1016/j.ijom.2020.09.023
9. Moreno A, Goiato MC, dos Santos DM, Haddad MF, Pesqueira AA, Bannwart LC. Effect of different disinfectants on the microhardness and roughness of acrylic resins for ocular prosthesis. *Gerodontology.* 2013;30(1):32–39. doi:10.1111/j.1741-2358.2012.00642.x
10. Andreotti AM, Sousa CAD, Goiato MC, et al. In vitro evaluation of microbial adhesion on the different surface roughness of acrylic resin specific for ocular prosthesis. *Eur J Dent.* 2018;12(2):176–183. doi:10.4103/ejd.ejd_50_18
11. Goiato MC, dos Santos DM, Baptista GT, et al. Effect of thermal cycling and disinfection on colour stability of denture base acrylic resin. *Gerodontology.* 2013;30(4):276–282. doi:10.1111/j.1741-2358.2012.00676.x
12. Goiato MC, dos Santos DM, Baptista GT, Moreno A, Andreotti AM, Dekon SF de C. Effect of thermal cycling and disinfection on microhardness of acrylic resin denture base. *J Med Eng Technol.* 2013;37(3): 203–207. doi:10.3109/03091902.2013.774444
13. Berteretche MV, Frot A, Woda A, Pereira B, Hennequin M. Different types of antagonists modify the outcome of complete denture renewal. *Int J Prosthodont.* 2016;28(3):270–278. doi:10.11607/ijp.3916
14. dos Santos DM, Borgui Paulini M, Silva Faria TG, et al. Analysis of color and hardness of a medical silicone with extrinsic pigmentation after accelerated aging. *Eur J Dent.* 2020;14(4):634–638. doi:10.1055/s-0040-1715782
15. Happe A, Röling N, Schäfer A, Rothamel D. Effects of different polishing protocols on the surface roughness of Y-TZP surfaces used for custom-made implant abutments: A controlled morphologic SEM and profilometric pilot study. *J Prosthet Dent.* 2015;113(5):440–447. doi:10.1016/j.prosdent.2014.12.005
16. Onwubu SC, Vahed A, Singh S, Kanny KM. Reducing the surface roughness of dental acrylic resins by using an eggshell abrasive material. *J Prosthet Dent.* 2017;117(2):310–314. doi:10.1016/j.prosdent.2016.06.024
17. Bollenl CML, Lambrechts P, Quirynen M. Comparison of surface roughness of oral hard materials to the threshold surface roughness for bacterial plaque retention: A review of the literature. *Dent Mater.* 1997;13(4):258–269. doi:10.1016/S0109-5641(97)80038-3
18. de Moraes Melo Neto CL, Sábio S, Santin GC, et al. Effects of 50- and 70-Gy radiation doses on polymethyl methacrylate denture bases. *Gen Dent.* 2020;68(6):56–59. PMID:33136047.
19. Sayed M, Jain S, Jain M, et al. Effect of cigarette smoke on color stability and surface roughness of different soft denture lining materials: An in vitro study. *Am J Dent.* 2021;34(3):132–136. PMID:34143582.
20. Paravina RD, Kimura M, Powers JM. Evaluation of polymerization-dependent changes in color and translucency of resin composites using two formulae. *Odontology.* 2005;93(1):46–51. doi:10.1007/s10266-005-0048-7

A method for evaluating the transport and energy conversion properties of polymer biomembranes using the Kedem–Katchalsky–Peusner equations

Metoda oceny właściwości transportowych i konwersji energii w biomembranach polimerowych z wykorzystaniem równań Kedem–Katchalskiego–Peusnera

Andrzej Ślęzak^{1,A,C–F}, Sławomir Marek Grzegorzczyn^{2,C–F}, Anna Pilis^{1,B}, Izabella Ślęzak-Prochazka^{3,4,E,F}

¹ Faculty of Medicine and Health Science, Jan Długosz University, Częstochowa, Poland

² Department of Biophysics, Faculty of Medical Sciences in Zabrze, Medical University of Silesia, Poland

³ Department of Systems Biology and Engineering, Silesian University of Technology, Gliwice, Poland

⁴ Biotechnology Center, Silesian University of Technology, Gliwice, Poland

A – research concept and design; B – collection and/or assembly of data; C – data analysis and interpretation; D – writing the article; E – critical revision of the article; F – final approval of the article

Polymers in Medicine, ISSN 0370-0747 (print), ISSN 2451-2699 (online)

Polim Med. 2023;53(1):25–36

Address for correspondence

Sławomir Marek Grzegorzczyn
E-mail: grzegorzczyn@sum.edu.pl

Funding sources

None declared

Conflict of interest

None declared

Received on November 29, 2022

Reviewed on February 16, 2023

Accepted on February 28, 2023

Published online on May 16, 2023

Cite as

Ślęzak A, Grzegorzczyn SM, Pilis A, Ślęzak-Prochazka I. A method for evaluating the transport and energy conversion properties of polymer biomembranes using the Kedem–Katchalsky–Peusner equations. *Polim Med.* 2023;53(1):25–36. doi:10.17219/pim/161743

DOI

10.17219/pim/161743

Copyright

Copyright by Author(s)

This is an article distributed under the terms of the Creative Commons Attribution 3.0 Unported (CC BY 3.0) (<https://creativecommons.org/licenses/by/3.0/>)

Abstract

Background. A basic parameter in non-equilibrium thermodynamics is the production of entropy (S -entropy), which is a consequence of the irreversible processes of mass, charge, energy, and momentum transport in various systems. The product of S -entropy production and absolute temperature (T) is called the dissipation function and is a measure of energy dissipation in non-equilibrium processes.

Objectives. This study aimed to estimate energy conversion in membrane transport processes of homogeneous non-electrolyte solutions. The stimulus version of the R , L , H , and P equations for the intensity of the entropy source achieved this purpose.

Materials and methods. The transport parameters for aqueous glucose solutions through Nephrophan® and Ultra-Flo 145 dialyser® synthetic polymer biomembranes were experimentally determined. Kedem–Katchalsky–Peusner (KKP) formalism was used for binary solutions of non-electrolytes, with Peusner coefficients introduced.

Results. The R , L , H , and P versions of the equations for the S -energy dissipation were derived for the membrane systems based on the linear non-equilibrium Onsager and Peusner network thermodynamics. Using the equations for the S -energy and the energy conversion efficiency factor, equations for F -energy and U -energy were derived. The S -energy, F -energy and U -energy were calculated as functions of osmotic pressure difference using the equations obtained and presented as suitable graphs.

Conclusions. The R , L , H , and P versions of the equations describing the dissipation function had the form of second-degree equations. Meanwhile, the S -energy characteristics had the form of second-degree curves located in the 1st and 2nd quadrants of the coordinate system. These findings indicate that the R , L , H , and P versions of S -energy, F -energy and U -energy are not equivalent for the Nephrophan® and Ultra-Flo 145 dialyser® membranes.

Keywords: membrane transport, Kedem–Katchalsky–Peusner equations, polymer biomembrane, transport coefficients, S -entropy production

Streszczenie

Wprowadzenie. Podstawowym parametrem termodynamiki nierównowagowej jest produkcja S -entropii, która jest konsekwencją nieodwracalnych procesów transportu masy, ładunku, energii i pędu w różnych typach układów. Iloczyn produkcji S -entropii i temperatury bezwzględnej T nazywany jest funkcją rozpraszania i jest miarą rozpraszania energii w procesach nierównowagowych.

Cel pracy. Celem pracy było oszacowanie konwersji energii w procesach transportu membranowego jednorodnych roztworów nieelektrolitów. W tym celu wykorzystano bodźcową wersję równań R, L, H i P dla natężenia źródła entropii.

Materiał i metody. Przedmiotem badań były syntetyczne biomembrany polimerowe (Nephrophan® i Ultra-Flo 145 dialyser®) o eksperymentalnie wyznaczonych parametrach transportu dla wodnych roztworów glukozy. Jako metodę badawczą zastosowano formalizm Kedem–Katchalsky'ego–Peusnera dla binarnych roztworów nieelektrolitów, z wprowadzonymi współczynnikami Peusnera.

Wyniki. Wersje R, L, H i P równań dyssypacji S -energii zostały wyprowadzone dla układu membranowego na podstawie liniowej nierównowagowej termodynamiki sieciowej Onsagera i Peusnera. Korzystając z równania na S -energię i równania na współczynnik sprawności konwersji energii, wyprowadzono równania na F -energię i U -energię. Na podstawie otrzymanych równań obliczono S -energię, F -energię i U -energię jako funkcje różnicy ciśnień osmotycznych i przedstawiono je w postaci odpowiednich wykresów.

Wnioski. Wersje R, L, H i P równań opisujących funkcję dyssypacji mają postać równań drugiego stopnia. Charakterystyki S -energii mają postać krzywych drugiego stopnia znajdujących się w pierwszej i drugiej ćwiartce układu współrzędnych. Artykuł pokazuje, że wersje R, L, H i P S -energii, F -energii i U -energii nie są równoważne zarówno dla membran Nephrophan®, jak i Ultra-Flo 145 dialyser®.

Słowa kluczowe: transport membranowy, biomembrana polimerowa, współczynniki transportu, produkcja S -entropii, równania Kedem–Katchalsky'ego–Peusnera

Background

Thermodynamic entropy (S -entropy) is the only physical parameter that indicates the irreversible one-way time course of biological processes.¹ An increase in S -entropy results from the transition from a more to a less ordered state that is less precisely understood than the initial state. For this reason, the applicability of the concept of S -entropy is limited to linear irreversible processes in states close to equilibrium.² Nevertheless, it plays an important role in the study of non-equilibrium processes by quantitatively characterizing the degree of irreversibility of physicochemical processes, including biological ones, that fulfill the second law of thermodynamics expressed as the law of increase of entropy.^{3–6}

One of the basic parameters in non-equilibrium thermodynamics is the production of S -entropy, which is a consequence of irreversible processes of mass, charge, energy, and momentum transport in various systems, including membrane systems.^{7,8} Membrane transport processes are important in many areas of human cognitive and utilitarian activity, including science, technology and medicine.⁹ Research methods and tools developed using non-equilibrium thermodynamics and network thermodynamics describe such membrane transport,^{5,10} including the Kedem–Katchalsky⁵ and Kedem–Katchalsky–Peusner^{10–16} formalisms. Several papers^{5,7,8,13,17} focused on estimating the entropy source in membrane systems used equations derived from the Kedem–Katchalsky formalism, while others presented entropy calculations for bacterial nanocellulose and Textus Bioactive biomembranes used as active dressings.^{18–20} The product of S -entropy production and absolute temperature (T)

is termed the dissipation function and is a measure of energy dissipation in non-equilibrium processes.

The present work aimed to evaluate the energy conversion in membrane systems using the formalism developed within the framework of Peusner network thermodynamics. The introduction presents the equations for S -energy dissipation in the Kedem and Katchalsky versions, the R , L , H , and P versions of the Kedem–Katchalsky–Peusner (KKP) equations for membrane transport of homogeneous non-electrolyte solutions, the equations representing the R , L , H , and P versions of the Q coupling parameter, and the energy conversion efficiency ratio. This part also contains the mathematical equations for $\phi(S)_{Y(Y=R,L,H \text{ or } P)}$, derived from the KKP formalism describing the energy dissipation function as a function of thermodynamic forces. Based on the obtained equations $R_{ij} = f(\Delta\pi)_{\Delta P=0}$, $L_{ij} = f(\Delta\pi)_{\Delta P=0}$, $H_{ij} = f(\Delta\pi)_{\Delta P=0}$, and $P_{ij} = f(\Delta\pi)_{\Delta\pi=0}$ ($i, j \in \{1, 2\}$), the characteristics of $\phi(S)_{Y(Y=R,L,H \text{ or } P)} = f(\Delta\pi)_{\Delta\pi=0}$ were calculated for Ultra-Flo 145 dialyser® and Nephrophan® synthetic membranes. To evaluate the conversion of chemical energy, the value of the coupling parameter and the energy conversion efficiency was calculated.

Materials and methods

Membrane system

The system used to study membrane transport is illustrated schematically in Fig. 1. This system consists of a membrane located in the horizontal plane that separates 2 aqueous solutions of glucose with initial concentrations

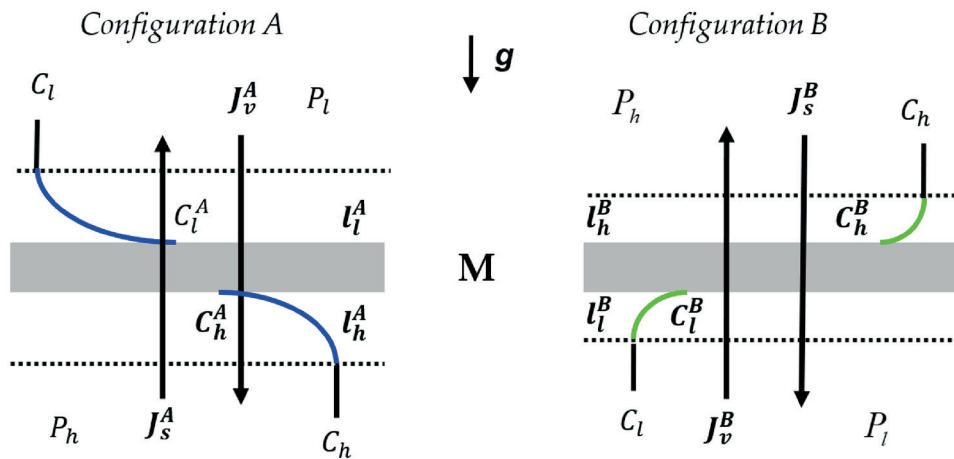


Fig. 1. Model of a single-membrane system

M – membrane; g – gravitational acceleration; l_l^A and l_h^A – concentration boundary layers (CBLs) in configuration A; l_h^B and l_l^B – CBLs in configuration B; P_h and P_l – mechanical pressures; C_h and C_l – total solution concentrations ($C_h > C_l$); C_l^A , C_h^A , C_l^B and C_h^B – local (at boundaries between membrane and CBLs) solution concentrations; J_v^A – solute and volume fluxes in configuration A; J_s^B – solute and volume fluxes in configuration B.

of C_h and $C_l = \text{const.}$ ($C_h \geq C_l$). The density of solutions with concentrations of C_h and C_l fulfilled the condition $\rho_h \geq \rho_l$ ($\rho_l = \text{const.}$). In configuration A, the compartment above the membrane contains a solution with concentration C_l , and the compartment below the membrane has a solution with the concentration C_h . In configuration B, the solutions with the concentration of C_l and C_h were reversed.

Water and dissolved substances transported through the membrane cause membrane concentration polarization (CP) since they form concentration boundary layers (CBLs), l_h^r and l_l^r , on both sides of the membrane. The thickness of the CBL (l_h^r) is δ_h^r , and the thickness of CBL (l_l^r) is δ_l^r . As a consequence of the CBL formation, the concentration difference through the membrane decreases from $C_h - C_l$ to $C_h^r - C_l^r$, where $C_h^r > C_l^r$, $C_h > C_h^r$, and $C_l^r > C_l$, and the density difference increases from $\rho_h - \rho_l$ to $\rho_h^r - \rho_l^r$, where $\rho_h^r > \rho_l^r$, $\rho_h > \rho_h^r$, and $\rho_l^r > \rho_l$. When a lower-density solution is located in the compartment below the membrane, and a higher-density solution is in the compartment above the membrane, the complex $l_h^r/M/l_l^r$, can lose hydrodynamic stability.

Hydrodynamic instability is manifested by natural convection in near-membrane areas.^{21–23} When the concentration Rayleigh number (R_C), which provides information about the process of the appearance of gravitational convection, exceeds its critical value, hydrodynamic instabilities appear in the near membrane areas.^{13,22,24–26} Over time, the destructive effect of gravitational convection limits the growth of δ_h^r and δ_l^r , and accelerates the diffusion of substances beyond the layers, which extends the convection to the entire volume of the solution. Self-organization of the liquid may occur under certain conditions, which is manifested in the “plum structure.”²⁷

Equations for S-energy dissipation in the Kedem–Katchalsky version

The measure of S-energy dissipation is the so-called dissipation function $\phi(S)$, which is equal to the product of T and entropy production ($d_i S/dt$). Mathematical expressions for

S-energy dissipation in a system in which a membrane separates 2 homogeneous non-electrolytic solutions of different concentrations will be obtained using the procedure described in previous papers.^{3,5} The S-energy dissipation function can be described by the expression (Eq. 1):

$$\phi(S) = T \frac{d_i S}{dt} = \sum_{i=1}^n J_i X_i = \sum_{i=1}^n L_{ii} X_i^2 + \sum_{i,j(i \neq j)=1}^n (L_{ij} + L_{ji}) X_i X_j \geq 0 \quad (1)$$

This equation shows that $\phi(S)$ is a bilinear form and is the sum of the products of the generalized thermodynamic fluxes (J_i) and the thermodynamic forces (X_i) of the same tensor order. In this equation, L_{ij} are phenomenological coefficients coupling J_i with X_j .⁵ Diagonal (L_{ii}) and non-diagonal (L_{ij} , L_{ji}) coefficients satisfy the following Onsager relations:

$$L_{ij} \neq L_{ji}, L_{ii} \geq 0, L_{jj} \geq 0, L_{ii} L_{jj} \geq L_{ij}^2 \quad (i, j \in \{1, 2\})^{3,5}$$

For stationary membrane transport of homogeneous non-electrolytic solutions containing 1 solute (s) and solvent (w), caused by thermodynamic forces, $\Delta\pi$ (osmotic pressure difference) and ΔP (hydrostatic pressure difference), the Equation (1) can be written in the form (Eq. 2)⁵:

$$\phi(S)_{Y=(R,L,H,\text{or } P)} = J_w \bar{V}_w (\Delta P - \Delta\pi) + J_s \left(\bar{V}_s \Delta P + \frac{\Delta\pi}{\bar{C}_s} \right) \quad (2)$$

where \bar{V}_s and \bar{V}_w denote the partial molar volumes of the s -th and w -th component of the solution, J_s and J_w are the fluxes of s and w , respectively, $\bar{C}_s = (C_h - C_l) \ln(C_h C_l^{-1})^{-1}$, C_h and C_l ($C_h > C_l$) are solute concentrations, $\Delta\pi = RT(C_h - C_l)$ is the osmotic pressure difference, and RT is the product of the gas constant and absolute temperature. \bar{C}_s can also be expressed as $\bar{C}_s = \Delta\pi [RT \ln(C_h C_l^{-1})]^{-1}$.

Taking into consideration the expressions $J_s \bar{V}_s + J_w \bar{V}_w \equiv J_v$ and $J_s \bar{C}_s^{-1} - J_w \bar{V}_w \equiv J_D$ (J_v – volume flux, J_D – diffusive flux), we can write Equation (2) in the form (Eq. 3)^{3,5}:

$$\phi(S)_{Y=(R,L,H,\text{or } P)} = J_v (\Delta P - \Delta\pi) + J_s \left(\frac{1}{\bar{C}_s} + \bar{V}_s \right) \Delta\pi \quad (3)$$

Assuming glucose concentration $C_h = 201 \text{ mol m}^{-3}$ and $C_l = 1 \text{ mol m}^{-3}$, we get $\bar{C}_s = 37.71 \text{ mol m}^{-3}$ and $1/\bar{C}_s = 2.65 \times 10^{-2} \text{ m}^3 \text{ mol}^{-1}$. On the other hand, $\bar{V}_s = 1.2 \times 10^{-4} \text{ m}^3 \text{ mol}^{-1}$.

This means that $1/\bar{C}_s \gg \bar{V}_s$, and Equation (3) can be written in the form (Eq. 4):

$$\phi(S)_{Y(Y=R,L,H, \text{ or } P)} = J_v(\Delta P - \Delta\pi) + J_s \frac{\Delta\pi}{\bar{C}_s} \quad (4)$$

The expression obtained is a practical form of the S -energy dissipation function for the osmotic-diffusion transport of homogeneous solutions. The $\phi(S)_{Y(Y=R,L,H \text{ or } P)}$ of Equation (3) can then be written using the R , L , H , and P versions of the KKP equations.

R , L , H , and P versions of the Kedem–Katchalsky–Peusner equations

The R , L , H , and P versions of the KKP equations are obtained through an appropriate transformation of the classical Kedem–Katchalsky equations (Eq. 5),⁵

$$J_v = L_p \Delta P - L_p \sigma \Delta\pi \quad (5)$$

$$J_s = \omega \Delta\pi + \bar{C}_s (1 - \sigma) J_v \quad (6)$$

where L_p , σ , and ω are coefficients of hydraulic permeability and reflection and diffusion permeability, respectively, J_v is volume flux, J_s is solute flux, ΔP is the hydrostatic pressure difference, $\Delta\pi = RT\Delta C$ is the osmotic pressure difference, RT is the product of the gas constant and absolute temperature, $\Delta C = C_h - C_l$ ($C_h > C_l$) is the difference of concentrations on the membrane, and $\bar{C}_s = (C_h + C_l)/2$ [$\ln(C_h C_l^{-1})^{-1} = \Delta\pi [RT \ln(C_h C_l^{-1})]^{-1}$] is the average concentration of the solution in the membrane.

By appropriate transformations of Equations (5) and (6), it is possible to obtain the R , L , H , and P versions of the KKP equations.^{10,14} The R , L , H , and P versions of the KKP equations obtained as a result of the transformation of Equations (5) and (6) are summarized in Table 1. The R , L , H , and P versions of the KKP equations contain

$$\phi(S)_R = \frac{1}{(R_{11}R_{22} - R_{12}R_{21})} \left[R_{22}(\Delta P - \Delta\pi)^2 - (R_{12} + R_{21})(\Delta P - \Delta\pi) \frac{\Delta\pi}{\bar{C}_s} + R_{11} \left(\frac{\Delta\pi}{\bar{C}_s} \right)^2 \right] \quad (10)$$

$$\phi(S)_L = L_{11}(\Delta P - \Delta\pi)^2 + (L_{12} + L_{21})(\Delta P - \Delta\pi) \frac{\Delta\pi}{\bar{C}_s} + L_{22} \left(\frac{\Delta\pi}{\bar{C}_s} \right)^2 \quad (11)$$

$$\phi(S)_H = \frac{1}{H_{11}} \left[(\Delta P - \Delta\pi)^2 + (H_{21} - H_{12})(\Delta P - \Delta\pi) \frac{\Delta\pi}{\bar{C}_s} + (H_{11}H_{22} - H_{12}H_{21}) \left(\frac{\Delta\pi}{\bar{C}_s} \right)^2 \right] \quad (12)$$

$$\phi(S)_P = \frac{1}{P_{22}} \left[(P_{11}P_{22} - P_{12}P_{21})(\Delta P - \Delta\pi)^2 + (P_{12} - P_{21})(\Delta P - \Delta\pi) \frac{\Delta\pi}{\bar{C}_s} + \left(\frac{\Delta\pi}{\bar{C}_s} \right)^2 \right] \quad (13)$$

These equations do not contain J_v and J_s fluxes, but do contain the thermodynamic forces ΔP and $\Delta\pi$. Therefore, these equations determine the thermodynamic forces of the equations for $\phi(S)_{Y(Y=R,L,H \text{ or } P)}$. From Equations (10–13), it follows that in order to calculate $\phi(S)_{Y(Y=R,L,H \text{ or } P)}$, the characteristics $R_{ij} = f(\Delta\pi)_{\Delta P=0}$, $L_{ij} = f(\Delta\pi)_{\Delta P=0}$, $H_{ij} = f(\Delta\pi)_{\Delta P=0}$, and $P_{ij} = f(\Delta\pi)_{\Delta P=0}$ must first be calculated and included in Equations (7–9).

Peusner coefficients, R_{ij} , L_{ij} , H_{ij} and P_{ij} , where $i, j \in \{1, 2\}$, respectively.

R , L , H , and P versions of the Q coupling parameter and energy conversion ratio e_{max}

Using the definition of the Q coupling parameter and the energy conversion efficiency, $(e_{max})_{Y(Y=R,L,H \text{ or } P)}$, presented by Peusner,¹⁰ expressions for the R , L , H , and P versions of the Q coupling parameter and $(e_{max})_{Y(Y=R,L,H \text{ or } P)}$ coefficients can be written. These expressions are listed in the 2nd and 3rd columns of Table 2.

Taking into account the equations listed in the 2nd, 3rd and 4th columns of Table 2, and the expressions listed in the 3rd column of Table 1, we get (Eq. 7–9):

$$r_{12} = l_{12} = \frac{L_p(1 - \sigma)^2 \Delta\pi}{\omega RT \ln \frac{C_h}{C_l} + L_p(1 - \sigma)^2 \Delta\pi} = r_{21} = l_{21} \quad (7)$$

$$h_{12} = p_{12} = \frac{L_p(1 - \sigma)^2 \Delta\pi}{\omega RT \ln \frac{C_h}{C_l}} = -h_{21} = -p_{21} \quad (8)$$

$$Q_R = Q_L = \frac{L_p(1 - \sigma)^2 \Delta\pi}{\omega RT \ln \frac{C_h}{C_l} + L_p(1 - \sigma)^2 \Delta\pi} = -Q_H = -Q_P \quad (9)$$

R , L , H , and P versions of the equation for energy dissipation

Taking into account the R , L , H , and P versions of the KKP equations in Equation (3), we obtain the R , L , H , and P versions of the S -energy dissipation equations for the thermodynamic force version denoted by $\phi(S)_R$, $\phi(S)_L$, $\phi(S)_H$, and $\phi(S)_P$ (Eq. 10–13):

Evaluation of internal energy conversion

The internal energy conversion process is governed by the principle of conservation of energy. According to this principle, the fluxes of the U -energy ($\phi(U)_{Y(Y=R,L,H \text{ or } P)}$), F -energy ($\phi(F)_{Y(Y=R,L,H \text{ or } P)}$) and S -energy ($\phi(S)_{Y(Y=R,L,H \text{ or } P)}$) satisfy the equation (Eq. 14)²⁸:

$$\phi(U)_{Y(Y=R,L,H, \text{ or } P)} = \phi(F)_{Y(Y=R,L,H, \text{ or } P)} = \phi(S)_{Y(Y=R,L,H, \text{ or } P)} \quad (14)$$

Table 1. Comparison of the *R*, *L*, *H*, and *P* versions of the Kedem–Katchalsky–Peusner (KKP) equations

KKP version	Form of the equations	Peusner's coefficients
R	$\Delta P - \Delta \pi = R_{11}J_v + R_{12}J_s$ $\frac{\Delta \pi}{\bar{C}_s} = R_{11}J_v + R_{12}J_s$	$R_{11} = \frac{\omega RT \ln \frac{C_h}{C_l} + \Delta \pi (1 - \sigma)^2 L_p}{L_p \omega RT \ln \frac{C_h}{C_l}}$ $R_{12} = -\frac{1 - \sigma}{\omega} = R_{21}$ $R_{22} = \frac{RT \ln \frac{C_h}{C_l}}{\omega \Delta \pi}$
L	$J_v = L_{11}(\Delta P - \Delta \pi) + L_{12} \frac{\Delta \pi}{\bar{C}_s}$ $J_s = L_{21}(\Delta P - \Delta \pi) + L_{22} \frac{\Delta \pi}{\bar{C}_s}$	$L_{11} = L_p$ $L_{12} = -\frac{\Delta \pi}{RT \ln \frac{C_h}{C_l}} (1 - \sigma) L_p = L_{21}$ $L_{22} = \frac{\Delta \pi}{RT \ln \frac{C_h}{C_l}} \left(\omega + \frac{\Delta \pi (1 - \sigma)^2 L_p}{RT \ln \frac{C_h}{C_l}} \right)$
H	$\Delta P - \Delta \pi = H_{11}J_v + L_{12} \frac{\Delta \pi}{\bar{C}_s}$ $J_s = H_{21}J_v + H_{22} \frac{\Delta \pi}{\bar{C}_s}$	$H_{11} = \frac{1}{L_p}$ $H_{12} = -\frac{\Delta \pi}{RT \ln \frac{C_h}{C_l}} (1 - \sigma) = -H_{21}$ $H_{22} = \frac{\omega \Delta \pi}{RT \ln \frac{C_h}{C_l}}$
P	$J_v = P_{11}(\Delta P - \Delta \pi) + P_{12}J_s$ $\frac{\Delta \pi}{\bar{C}_s} = P_{21}(\Delta P - \Delta \pi) + P_{22}J_s$	$P_{11} = \frac{L_p \omega RT \ln \frac{C_h}{C_l}}{\omega RT \ln \frac{C_h}{C_l} + \Delta \pi (1 - \sigma)^2 L_p}$ $P_{12} = \frac{(1 - \sigma) L_p \omega RT \ln \frac{C_h}{C_l}}{\omega RT \ln \frac{C_h}{C_l} + \Delta \pi (1 - \sigma)^2 L_p} = -P_{21}$ $P_{22} = \frac{\left(\omega RT \ln \frac{C_h}{C_l} \right)^2}{\left(\omega RT \ln \frac{C_h}{C_l} + \Delta \pi (1 - \sigma)^2 L_p \right) \Delta \pi}$

Here, $\phi(U)_Y = A^{-1}dU_Y/dt$ is the *U*-energy flux (W m⁻²), $\phi(F)_Y = A^{-1}dF_Y/dt$ the *F*-energy flux (W m⁻²), and $\phi(S)_Y = TA^{-1}d_iS_Y/dt$ is the *S*-energy flux (W m⁻²).

An explicit form of the coefficients R_{ij} , L_{ij} , H_{ij} , and P_{ij} for $i, j \in \{1, 2\}$, appearing in the above equation is given in Equations (10–13). To obtain *S*-energy for the conditions of homogeneity of solutions ($\phi(S)_{Y(Y=R,L,H \text{ or } P)}$) in Equations (10–13), the free energy flux $\phi(F)_{Y(Y=R,L,H \text{ or } P)}$ can be calculated using the definition of the energy conversion efficiency coefficient (Eq. 15):

$$(e_{\max})_{Y(Y=R,L,H, \text{ or } P)} = \frac{\phi(F)_{Y(Y=R,L,H, \text{ or } P)}}{\phi(U)_{Y(Y=R,L,H, \text{ or } P)}} = \frac{\phi(F)_{Y(Y=R,L,H, \text{ or } P)}}{\phi(U)_{Y(Y=R,L,H, \text{ or } P)} + \phi(U)_{Y(Y=R,L,H, \text{ or } P)}} \quad (15)$$

By transforming Equation (15), we get (Eq. 16,17)

$$\phi(F)_{Y(Y=R,L,H, \text{ or } P)} = \frac{(e_{\max})_{Y(Y=R,L,H, \text{ or } P)}}{1 - (e_{\max})_{Y(Y=R,L,H, \text{ or } P)}} \phi(S)_{Y(Y=R,L,H, \text{ or } P)} \quad (16)$$

$$\phi(U)_{Y(Y=R,L,H, \text{ or } P)} = \frac{1}{1 - (e_{\max})_{Y(Y=R,L,H, \text{ or } P)}} \phi(S)_{Y(Y=R,L,H, \text{ or } P)} \quad (17)$$

From a formal point of view, the cases of $\phi(F)_{Y(Y=R,L,H \text{ or } P)} = 0$ and $\phi(U)_{Y(Y=R,L,H \text{ or } P)} = 0$ are excluded, because in order for the denominator of Equations (16) and (17) to be different from 0, the condition $(e_{\max})_{Y(Y=R,L,H \text{ or } P)} \neq 1$ must be satisfied.

The maximum energy conversion efficiency expressed by the Kedem–Caplan–Peusner coefficients^{10,28,29} in Equations (16) and (17) can be written as (Eq. 18–21):

Table 2. $R, L, H,$ and P versions of coupling coefficient l , coupling parameter Q and energy conversion coefficient $(e_{max})_Y$ ($Y=R, L, H$ or P)

Version	Caplan coupling parameter	Peusner coupling parameter	Energy conversion coefficient
R	$r_{12} = \frac{-R_{12}}{\sqrt{R_{11}R_{22}}}$	$Q_R = \frac{2 R_{21}R_{12} }{4R_{11}R_{22} - 2R_{21}R_{12}}$	$(e_{max})_R = \frac{\frac{R_{21}}{R_{12}}Q_R}{1 + \sqrt{1-Q_R^2}}$
L	$l_{12} = \frac{L_{12}}{\sqrt{L_{11}L_{22}}}$	$Q_L = \frac{2 L_{21}L_{12} }{4L_{11}L_{22} - 2L_{21}L_{12}}$	$(e_{max})_L = \frac{\frac{L_{21}}{L_{12}}Q_L}{1 + \sqrt{1-Q_L^2}}$
H	$h_{12} = \frac{H_{12}}{\sqrt{H_{11}H_{22}}}$	$Q_H = \frac{2 H_{21}H_{12} }{4H_{11}H_{22} - 2H_{21}H_{12}}$	$(e_{max})_H = \frac{\frac{H_{21}}{H_{12}}Q_H}{1 + \sqrt{1-Q_H^2}}$
P	$p_{12} = \frac{-P_{12}}{\sqrt{P_{11}P_{22}}}$	$Q_P = \frac{2 P_{21}P_{12} }{4P_{11}P_{22} - 2P_{21}P_{12}}$	$(e_{max})_P = \frac{\frac{P_{21}}{P_{12}}Q_P}{1 + \sqrt{1-Q_P^2}}$

$$(e_{max})_R = (e_{max})_r = \frac{R_{12}R_{21}}{R_{11}R_{22} \left(1 + \sqrt{1 - \frac{R_{12}R_{21}}{R_{11}R_{22}}}\right)^2} = \frac{r_{12}r_{21}}{\left(1 + \sqrt{1 - r_{12}r_{21}}\right)^2} \quad (18)$$

$$(e_{max})_L = (e_{max})_l = \frac{L_{12}L_{21}}{L_{11}L_{22} \left(1 + \sqrt{1 - \frac{L_{12}L_{21}}{L_{11}L_{22}}}\right)^2} = \frac{l_{12}l_{21}}{\left(1 + \sqrt{1 - l_{12}l_{21}}\right)^2} \quad (19)$$

$$(e_{max})_H = (e_{max})_h = \frac{H_{12}H_{21}}{H_{11}H_{22} \left(1 + \sqrt{1 - \frac{H_{12}H_{21}}{H_{11}H_{22}}}\right)^2} = \frac{h_{12}h_{21}}{\left(1 + \sqrt{1 - h_{12}h_{21}}\right)^2} \quad (20)$$

$$(e_{max})_P = (e_{max})_p = \frac{P_{12}P_{21}}{P_{11}P_{22} \left(1 + \sqrt{1 - \frac{P_{12}P_{21}}{P_{11}P_{22}}}\right)^2} = \frac{p_{12}p_{21}}{\left(1 + \sqrt{1 - p_{12}p_{21}}\right)^2} \quad (21)$$

The values of the $(e_{max})_Y$ ($Y=R, L, H$ or P) coefficient are limited by the relations $0 \leq (e_{max})_Y$ ($Y=R, L, H$ or P) ≤ 1 and $(e_{max})_Y$ ($Y=R, L, H$ or P) = 0, when $R_{12}R_{21} = L_{12}L_{21} = H_{12}H_{21} = P_{12}P_{21} = 0$, when $r_{12}r_{21} = l_{12}l_{21} = h_{12}h_{21} = p_{12}p_{21} = 0$ and $(e_{max})_Y$ ($Y=R, L, H$ or P) = 1, when $R_{12}R_{21} = R_{11}R_{22}$, $L_{12}L_{21} = L_{11}L_{22}$, $H_{12}H_{21} = H_{11}H_{22}$, or when $P_{12}P_{21} = P_{11}P_{22}$ and $r_{12}r_{21} = 1$, $l_{12}l_{21} = 1$, $h_{12}h_{21} = 1$ or $p_{12}p_{21} = 1$.

Biomembrane characteristics

Nephrophan® biomembrane (ORWO VEB Filmfabrik, Wolfen, Germany) is a microporous, highly hydrophilic, electroneutral, and compact-structure membrane made from regenerated cellulose.³⁰ The membrane is used in urology in ganglion hemodialyzers, due to their high-pressure strength, and for controlled release of drugs in ophthalmology and laryngology.³¹

The Ultra-Flo 145 dialyser® (Artificial Organs Division, Travenol Laboratories, Brussels, Belgium) is an ultrafiltration, microporous, hydrophilic, and electroneutral regenerated cellulose biomembrane used in urology.³²

Images of Nephrophan® and Ultra-Flo 145 dialyser® membranes obtained with a Zeiss Supra 35 scanning electron microscope (SEM; Carl Zeiss AG, Jena, Germany) are shown in Fig. 2A,B. The image in Fig. 2A shows the solid structure of the Nephrophan® membrane, and the image in Fig. 2B presents the microfiber structure of the Ultra-Flo 145 dialyser® membrane.

Results

The calculations of $(\phi(S))_Y$ ($Y=R, L, H$ or P) performed for Nephrophan® and Ultra-Flo 145 dialyser® membranes have been used in nephrology and ophthalmology.¹⁷ Each of the biomembranes (monolayer, symmetric, isotropic, and electrically neutral) separated 2 homogeneous aqueous glucose solutions with concentrations C_h and C_l ($C_h > C_l$) and the same temperature ($T = 295$ K). The transport properties of these biomembranes were determined by hydraulic permeability (L_p), reflection (σ) and diffusion permeability (ω). The dry thickness of the membranes

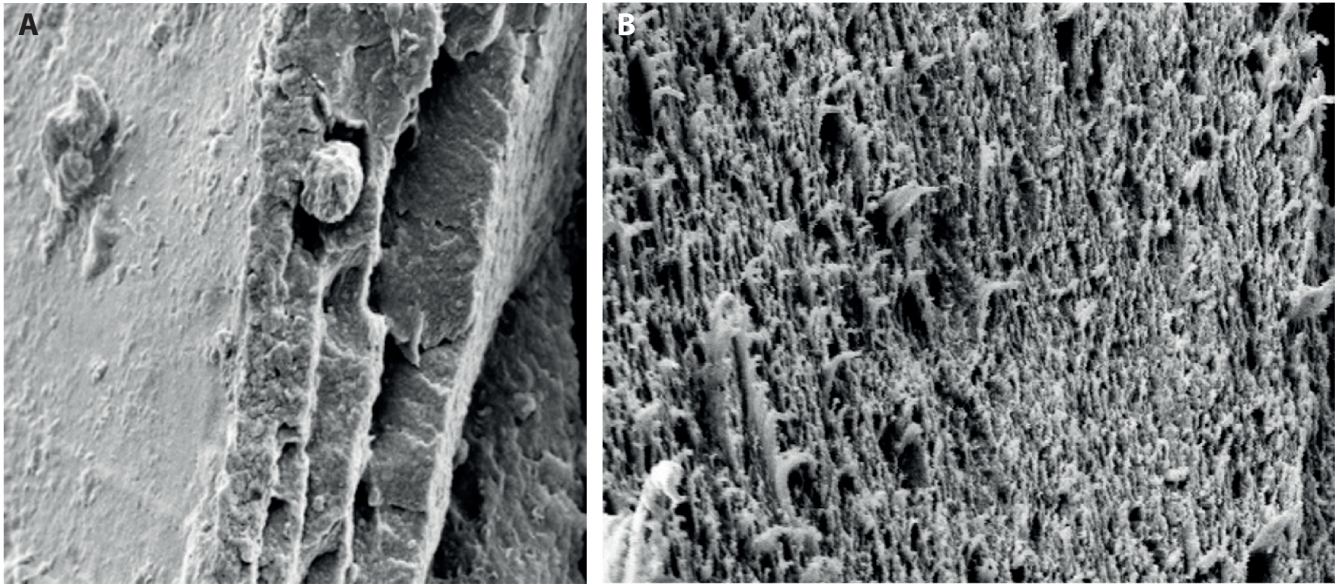


Fig. 2. Images of membrane surfaces obtained from scanning electron microscopy (SEM). A. Surface and cross-section of the Nephrophan® membrane (×15,000 magnification)²⁴; B. Cross-section of the Ultra-Flo 145 dialyser® membrane (×10,500 magnification)

Table 3. Values of the parameters (L_p , σ , ω , and d) for Nephrophan® and Ultra-Flo 145 dialyser® membranes, and for aqueous glucose solutions

Parameters	Biomembrane	
	Nephrophan®	Ultra-Flo 145 dialyser®
$L_p \times 10^{12} [\text{m}^3 \text{N}^{-1} \text{s}^{-1}]$	4.9	0.85
σ	0.068	0.112
$\omega \times 10^9 [\text{mol N}^{-1} \text{s}^{-1}]$	0.8	0.1
$d [\mu\text{m}]$	200	800

is denoted by d . The values of these coefficients are summarized in Table 3.

Table 3 shows that both Nephrophan® and Ultra-Flo 145 dialyser® biomembranes are selective for glucose because $0 < \sigma < 1$. The following data was used for the calculations: $R = 8.31 \text{ J mol}^{-1} \text{K}^{-1}$ and $\Delta\pi$, which ranged from -12.16 kPa to -502.54 kPa or from $+12.16 \text{ kPa}$ to $+502.54 \text{ kPa}$, $C_l = 1 \text{ mol m}^{-3}$ and C_h ranged from 6 mol m^{-3} to 206 mol m^{-3} . To calculate the dependencies $R_{ij} = f(\Delta\pi)_{\Delta P=0}$, $L_{ij} = f(\Delta\pi)_{\Delta P=0}$, $H_{ij} = f(\Delta\pi)_{\Delta P=0}$, and $P_{ij} = f(\Delta\pi)_{\Delta P=0}$ ($i, j \in \{1, 2\}$), the equations listed in the 3rd column of Table 1 were used. All calculations assumed the condition $\Delta P = 0$. The results of the calculations are presented in Fig. 3A–D, Fig. 4A–D and Fig. 5A. The results of calculations show that the values of the coefficients $R_{12} = R_{21}$, L_{11} , and H_{11} are independent of $\Delta\pi$. Therefore, their values are constant and amount to: $R_{12} = R_{21} = -1.165 \times 10^9 \text{ N s mol}^{-1}$, $L_{11} = 4.9 \times 10^{-12} \text{ m}^3 \text{N}^{-1} \text{s}^{-1}$ and $H_{11} = 2.0 \times 10^{11} \text{ Ns m}^{-3}$ for the Nephrophan® membrane, and $R_{12} = R_{21} = -8.88 \times 10^9 \text{ N s mol}^{-1}$, $L_{11} = 0.85 \times 10^{-12} \text{ m}^3 \text{N}^{-1} \text{s}^{-1}$ and $H_{11} = 11.76 \times 10^{11} \text{ Ns m}^{-3}$ for the Ultra-Flo 145 dialyser® membrane.

Increases in the absolute values of glucose osmotic pressure ($\Delta\pi$) cause a nonlinear increase of L_{12} , L_{21} , L_{22} , and R_{11} coefficients in all configurations of the system, while R_{22}

decreases with increased absolute values of $\Delta\pi$. Greater changes of all the coefficients occurred for the Nephrophan® membrane than the Ultra-Flo 145 dialyser® membrane for the same changes in $\Delta\pi$. The smaller changes in coefficients for the Ultra-Flo 145 dialyser® membrane are related to its more porous structure, which makes it easier for solutes and water to permeate the membrane. Therefore, an increase in absolute values of $\Delta\pi$ causes greater coupling between suitable fluxes and forces, when the direct relationship between thermodynamic force and flux of glucose is excluded.

The values of coefficients R_{11} , R_{22} , L_{12} , L_{22} , H_{12} , H_{21} , H_{22} , P_{11} , P_{12} , and P_{22} depend on $\Delta\pi$ for both biomembranes, as is illustrated in Fig. 3A–D and Fig. 4A–D. Figure 3A,C,D and Fig. 4B show that the values of R_{11} , L_{12} , L_{22} , and H_{22} are positive and increase with increasing absolute $\Delta\pi$. Meanwhile, Fig. 3B and Fig. 4D,E demonstrate positive values of R_{22} , P_{11} , P_{12} , and P_{22} , which decrease with increasing absolute $\Delta\pi$. In turn, H_{12} and P_{21} are negative, and H_{12} decreases, while the values of P_{21} increase with increasing absolute $\Delta\pi$. Furthermore, Fig. 3A–D and Fig. 4A–E show greater R_{11} , R_{22} , P_{12} , and P_{22} coefficients for the Ultra-Flo 145 dialyser® than for the Nephrophan® membrane. On the other hand, the coefficients L_{12} , L_{22} , H_{21} , H_{12} , H_{22} , P_{11} , and P_{21} are greater for the Nephrophan® membrane than for the Ultra-Flo 145 dialyser®.

Taking into account the results of calculations for dependencies $R_{ij} = f(\Delta\pi)_{\Delta P=0}$, $L_{ij} = f(\Delta\pi)_{\Delta P=0}$, $H_{ij} = f(\Delta\pi)_{\Delta P=0}$, and $P_{ij} = f(\Delta\pi)_{\Delta P=0}$ ($i, j \in \{1, 2\}$) (Fig. 3A–D and Fig. 4A–E, and the equations listed in the 2nd column of Table 2), the dependencies ($Q_{Y(Y=R,L,H \text{ or } P)} = f(\Delta\pi)_{\Delta P=0}$) were calculated. The results of calculations are presented in Fig. 5A,B.

The curves presented in Fig. 5 show greater values of the coefficients Q_R , Q_L , Q_H , and Q_P for the Nephrophan® membrane than for the Ultra-Flo 145 dialyser®. Furthermore, the values of coefficients Q_R and Q_L are positive, while

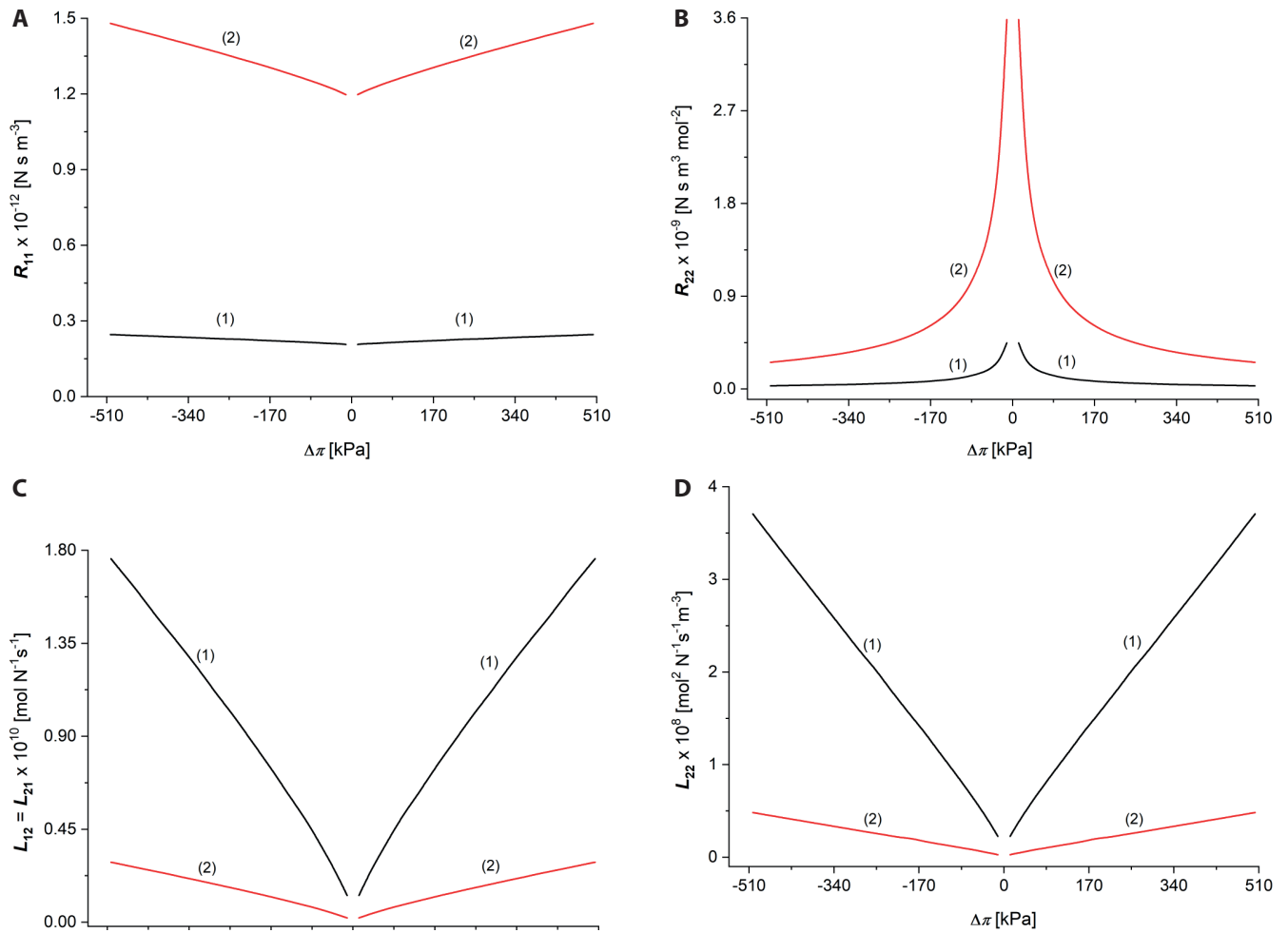


Fig. 3. Illustration of dependencies $R_{ij} = f(\Delta\pi)_{\Delta P=0}$ and $L_{ij} = f(\Delta\pi)_{\Delta P=0}$ ($ij \in \{1, 2\}$) for aqueous glucose solutions. A. $R_{11} = f(\Delta\pi)_{\Delta P=0}$; B. $R_{22} = f(\Delta\pi)_{\Delta P=0}$; C. $L_{12} = L_{21} = f(\Delta\pi)_{\Delta P=0}$; D. $L_{22} = f(\Delta\pi)_{\Delta P=0}$. Plots marked with (1) were obtained for the Nephrophan® membrane and plots marked with (2) were obtained for the Ultra-Flo 145 dialyser® membrane

Q_H and Q_P are negative. The Nephrophan® membrane fulfilled the relations $Q_R > Q_L$ and $Q_H = Q_P$, while $Q_R = Q_L$ and $Q_H > Q_P$ were fulfilled for the Ultra-Flo 145 dialyser®.

Using the results obtained for dependencies $R_{ij} = f(\Delta\pi)_{\Delta P=0}$, $L_{ij} = f(\Delta\pi)_{\Delta P=0}$, $H_{ij} = f(\Delta\pi)_{\Delta P=0}$, and $P_{ij} = f(\Delta\pi)_{\Delta P=0}$ ($ij \in \{1, 2\}$) shown in Fig. 3A–D and Fig. 4A–E, as well as $(Q_{Y(Y=R,L,H \text{ or } P)}) = f(\Delta\pi)_{\Delta P=0}$, shown in Fig. 5A,B, and the equations listed in the 4th column of Table 2, the dependencies $(e_{max})_{Y(Y=R,L,H \text{ or } P)}$ were calculated. The results of calculations are presented in Fig. 5C,D. The curves in these figures show greater values of the coefficients $(e_{max})_{Y(Y=R,L,H \text{ or } P)}$ for the Nephrophan® membrane than for the Ultra-Flo 145 dialyser® membrane. Also, the coefficients $(e_{max})_{Y(Y=R,L,H \text{ or } P)}$ are positive. For the Nephrophan® membrane, the relations $(e_{max})_R > (e_{max})_L$ and $(e_{max})_H = (e_{max})_P$ are fulfilled. In turn, for the Ultra-Flo 145 dialyser® membrane, $(e_{max})_R = (e_{max})_L = (e_{max})_H < (e_{max})_P$.

Accounting for the results obtained for $R_{ij} = f(\Delta\pi)_{\Delta P=0}$, $L_{ij} = f(\Delta\pi)_{\Delta P=0}$, $H_{ij} = f(\Delta\pi)_{\Delta P=0}$, and $P_{ij} = f(\Delta\pi)_{\Delta P=0}$ ($ij \in \{1, 2\}$), shown in Fig. 3A–D, Fig. 4A–D and Fig. 5A–C, as well as Equations (10–13), the dependencies $\phi(S)_{Y(Y=R,L,H \text{ or } P)} = f(\Delta\pi)_{\Delta P=0}$, were calculated. The results of calculations are presented in Fig. 6A,B.

The curves presented in Fig. 6A,B show greater values of the coefficients $\phi(S)_{Y(Y=R,L,H \text{ or } P)}$ for Nephrophan® than for the Ultra-Flo 145 dialyser® membrane. These findings indicate that the dissipation of energy is greater in the Nephrophan® membrane than in the Ultra-Flo 145 dialyser® membrane under similar transport conditions. Furthermore, the values of coefficients $\phi(S)_{Y(Y=R,L,H \text{ or } P)}$ are positive, and the relationship $\phi(S)_R > \phi(S)_L > \phi(S)_H > \phi(S)_P$ is true for both the Nephrophan® and Ultra-Flo 145 dialyser® membranes.

Using the results obtained for the dependencies $(e_{max})_{Y(Y=R,L,H \text{ or } P)}$ and $\phi(S)_{Y(Y=R,L,H \text{ or } P)} = f(\Delta\pi)_{\Delta P=0}$, shown in Fig. 5C,D and Fig. 6A,B, respectively, and in Equation (16), the dependencies $\phi(F)_{Y(Y=R,L,H \text{ or } P)} = f(\Delta\pi)_{\Delta P=0}$, were calculated.

The results of the calculations presented in Fig. 6C,D show greater values of the coefficients $\phi(F)_{Y(Y=R,L,H \text{ or } P)}$ for Nephrophan® in comparison to the Ultra-Flo 145 dialyser® membrane. They also show positive values for the coefficients $\phi(F)_{Y(Y=R,L,H \text{ or } P)}$. The relations $\phi(F)_R > \phi(F)_L > \phi(F)_H > \phi(F)_P$ are fulfilled for both the Nephrophan® and Ultra-Flo 145 dialyser® membranes.

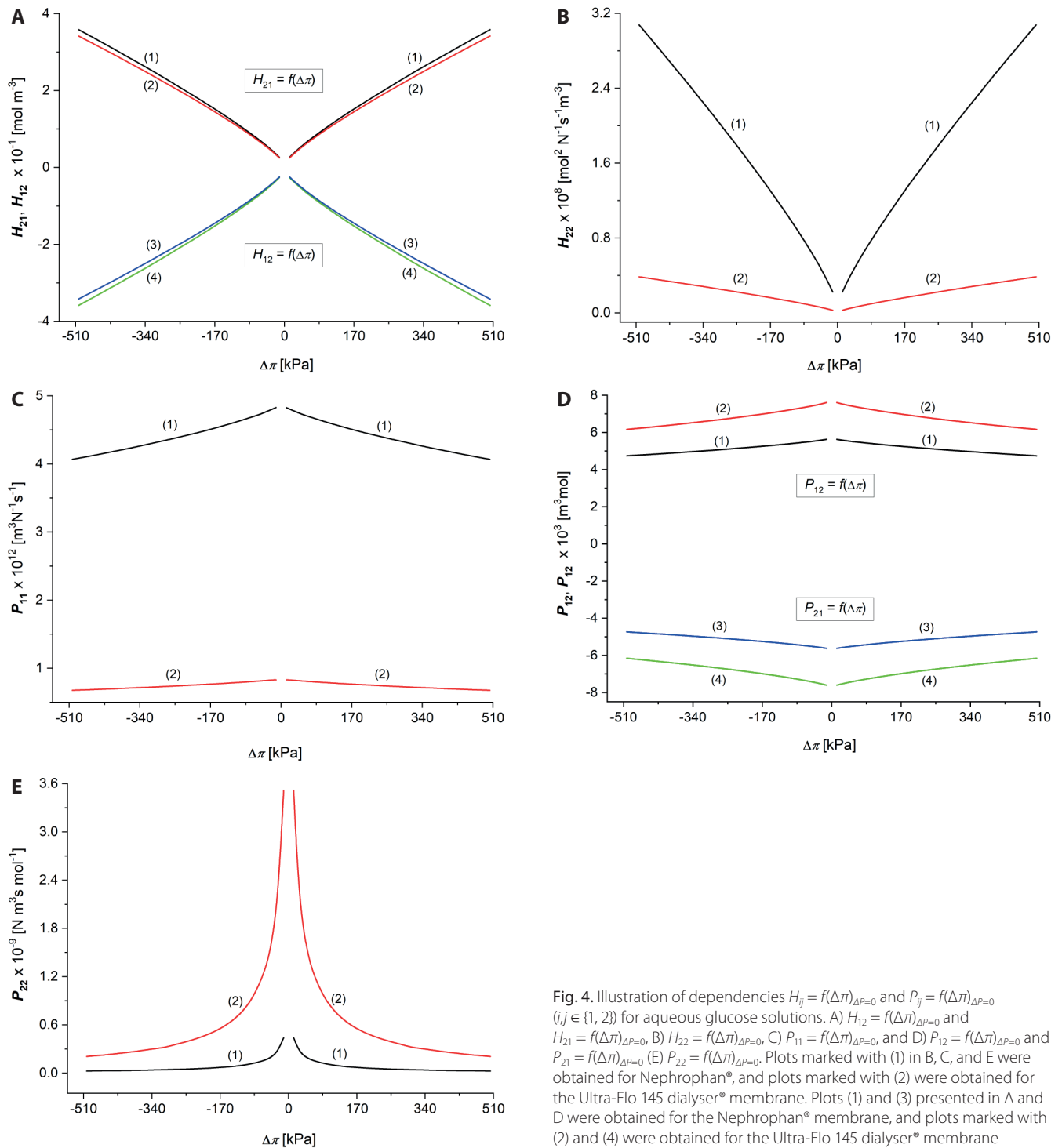


Fig. 4. Illustration of dependencies $H_{ij} = f(\Delta\pi)_{\Delta P=0}$ and $P_{ij} = f(\Delta\pi)_{\Delta P=0}$ ($i, j \in \{1, 2\}$) for aqueous glucose solutions. A) $H_{12} = f(\Delta\pi)_{\Delta P=0}$ and $H_{21} = f(\Delta\pi)_{\Delta P=0}$, B) $H_{22} = f(\Delta\pi)_{\Delta P=0}$, C) $P_{11} = f(\Delta\pi)_{\Delta P=0}$, and D) $P_{12} = f(\Delta\pi)_{\Delta P=0}$ and $P_{21} = f(\Delta\pi)_{\Delta P=0}$ (E) $P_{22} = f(\Delta\pi)_{\Delta P=0}$. Plots marked with (1) in B, C, and E were obtained for Nephrophan®, and plots marked with (2) were obtained for the Ultra-Flo 145 dialyser® membrane. Plots (1) and (3) presented in A and D were obtained for the Nephrophan® membrane, and plots marked with (2) and (4) were obtained for the Ultra-Flo 145 dialyser® membrane

Considering the results obtained for dependences $(e_{max})_{Y(Y=R,L,H \text{ or } P)} = f(\Delta\pi)_{\Delta P=0}$ and $\phi(S)_{Y(Y=R,L,H \text{ or } P)} = f(\Delta\pi)_{\Delta P=0}$, shown in Fig. 5C,D and Fig. 6A,B, respectively, and in Equation (17), the dependences $\phi(U)_{Y(Y=R,L,H \text{ or } P)} = f(\Delta\pi)_{\Delta P=0}$ were calculated and are shown in Fig. 6E,F.

The curves presented in Fig. 6A–F show greater values of $\phi(U)_{Y(Y=R,L,H \text{ or } P)}$ for the Nephrophan® membrane than the Ultra-Flo 145 dialyser® membrane. Furthermore, $\phi(U)_{Y(Y=R,L,H \text{ or } P)}$ are positive, and the relations $\phi(U)_R > \phi(U)_L > \phi(U)_H > \phi(U)_P$ are fulfilled for both membranes.

Discussion

Using Peusner’s lattice thermodynamics formalism, the R , L , H , and P versions of the KKP equations are obtained by transforming the classical Kedem–Katchalsky equations.⁵ Meanwhile, the equations listed in Table 1 should be considered in order to obtain the R , L , H , and P versions of the equations for energy dissipation (S -energy).

The characteristics of $\phi(S)_{Y(Y=R,L,H \text{ or } P)} = f(\Delta\pi, \Delta P)$ should have different types of curved surfaces. Indeed, this was

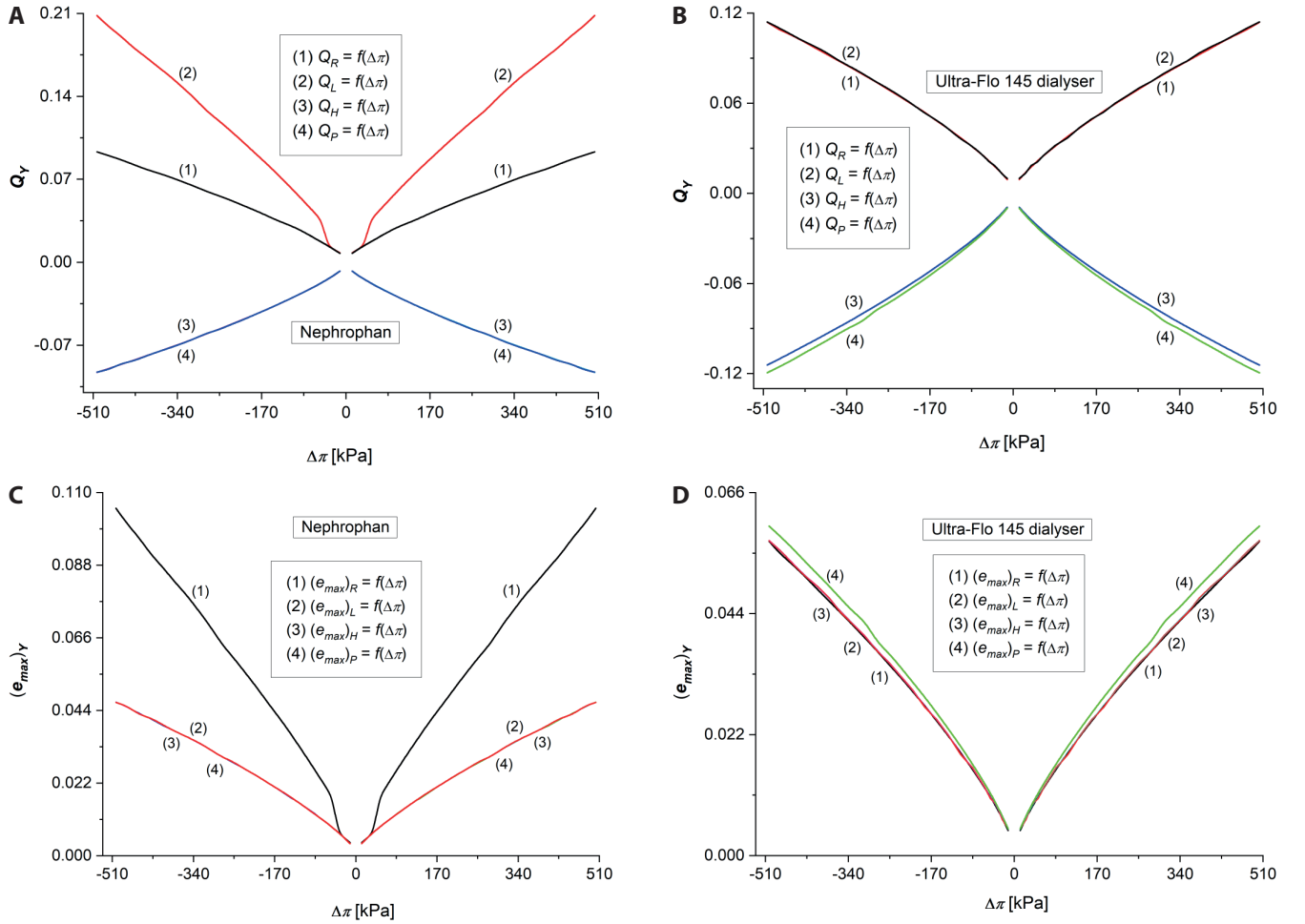


Fig. 5. Illustration of dependencies $Q_{Y(Y=R,L,H \text{ or } P)} = f(\Delta\pi)_{\Delta P=0}$ and $(e_{max})_{Y(Y=R,L,H \text{ or } P)} = f(\Delta\pi)_{\Delta P=0}$ for aqueous glucose solutions. Plots 1, 2, 3, and 4 shown in A and C were obtained for the Nephrophan® membrane, and plots 1, 2, 3, and 4 in B and D represent the Ultra-Flo 145 dialyser® membrane

previously confirmed by the characteristics of $\phi(S)_L = f(\Delta\pi, \Delta P)$ for a bacterial nanocellulose membrane (Biofill).⁸ Similarly, the characteristics of $\phi(S)_{Y(Y=R,L,H \text{ or } P)} = f(\Delta P, \Delta\pi/\bar{C}_s)$ should have different types of curved surfaces, and the characteristics of $\phi(S)_L = f(\Delta P, \Delta\pi/\bar{C}_s)$ presented in past work confirm this hypothesis.⁷

As previously mentioned, Equations (6–9) do not contain fluxes J_v and J_s , but contain thermodynamic forces ΔP and $\Delta\pi$. Therefore, these equations constitute the thermodynamic force version of equations for $\phi(S)_{Y(Y=R,L,H \text{ or } P)}$. As such, a flux version of the equations for $\phi(S)_{Y(Y=R,L,H \text{ or } P)}$ can also be obtained. For this purpose, thermodynamic forces, $\Delta P - \Delta\pi$ and $\Delta\pi/\bar{C}_s$, should be eliminated from Equation (3) using the equations listed in Table 1. Equations for flux versions of $\phi(S)_{Y(Y=R,L,H \text{ or } P)}$ have the form (Eq. 22–25):

$$\phi(S)_R = [R_{11}J_v^2 + (R_{12} + R_{21})J_vJ_s + R_{22}J_s^2] \quad (22)$$

$$\phi(S)_L = \frac{1}{(L_{11}L_{22} - L_{12}L_{21})} [L_{22}J_v^2 - (L_{12} + L_{21})J_vJ_s + L_{11}J_s^2] \quad (23)$$

$$\phi(S)_H = \frac{1}{H_{22}} [(H_{11}H_{22} - H_{12}H_{21})J_v^2 + (H_{12} - H_{21})J_vJ_s + J_s^2] \quad (24)$$

$$\phi(S)_P = \frac{1}{P_{11}} [J_v^2 + (P_{21} - P_{12})J_vJ_s + P_{12}J_s^2] \quad (25)$$

Explicit forms of Peusner coefficients R_{ij} , L_{ij} , H_{ij} , and P_{ij} ($i, j \in \{1, 2\}$) appearing in the above equations is presented in Table 1. The Equations (10–13) are the flux form of the equations for the intensity of the entropy source. Meanwhile, Equations (6–9) will be useful for numerical calculations of the S -energy, and Equations (22–24) can be used for calculations based on experimentally determined J_v and J_s .

Conclusions

Equations describing $\phi(S)_{Y(Y=R,L,H \text{ or } P)}$ versions of S -energy are the sum of the quadratic equations of the ΔP and $\Delta\pi$ variables. The characteristics of $\phi(S)_{Y(Y=R,L,H \text{ or } P)} = f(\Delta\pi)_{\Delta P=0}$ are the second-degree curves located in the 1st and 2nd quadrants of the coordinate system.

Characteristics of $\phi(S)_{Y(Y=R,L,H \text{ or } P)} = f(\Delta\pi)_{\Delta P=0}$, illustrated by curves 1, 2, 3 and 4, for both Nephrophan® and Ultra-Flo 145 dialyser® membranes, have different forms. For the same $\Delta\pi$ values in the Nephrophan® membrane, curves 1, 2, 3, and 4 for the dependencies

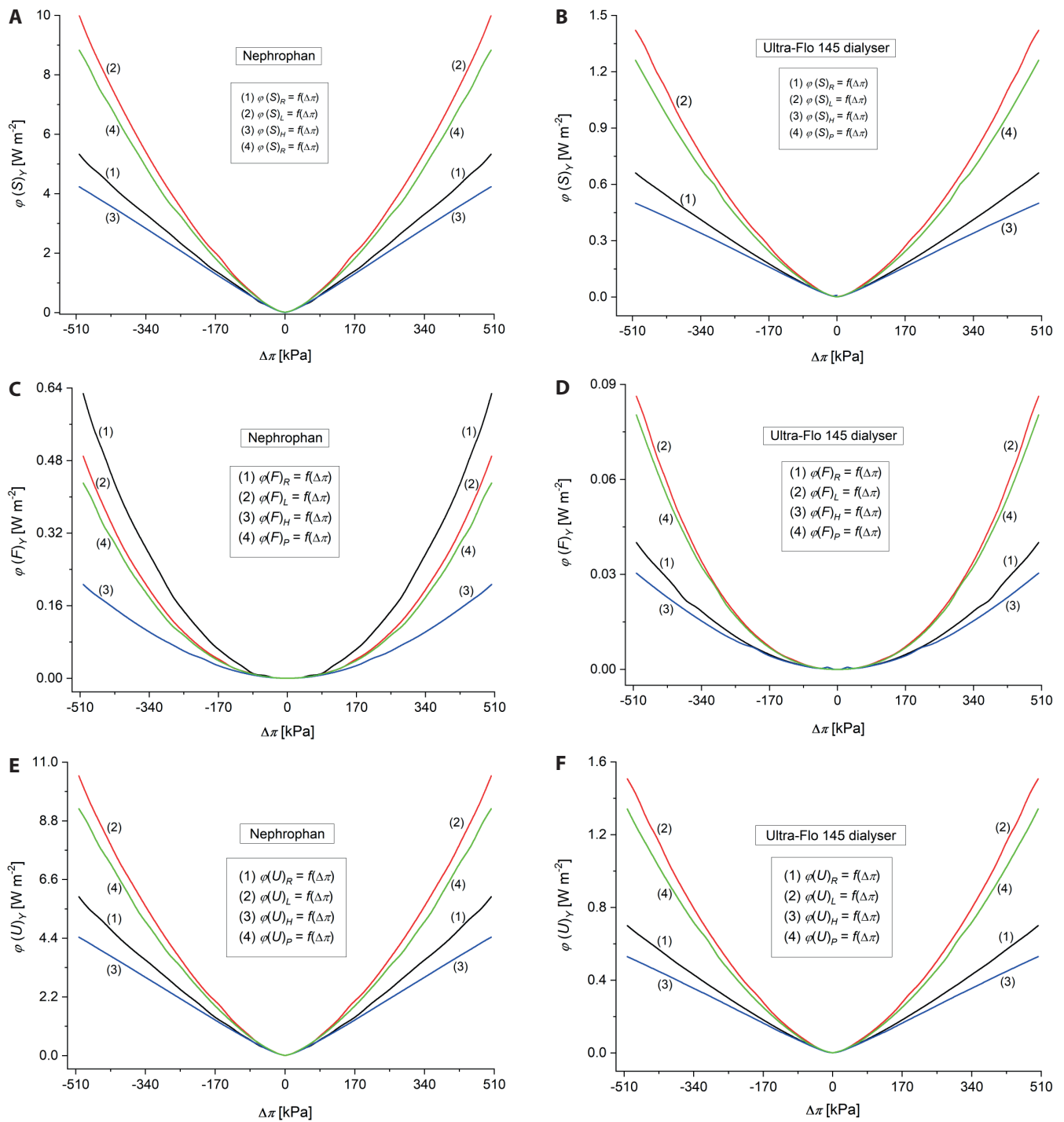


Fig. 6. Illustration of dependencies $\phi(S)_{Y(Y=R,L,H \text{ or } P)} = f(\Delta\pi)_{\Delta P=0}$, $\phi(F)_{Y(Y=R,L,H \text{ or } P)} = f(\Delta\pi)_{\Delta P=0}$, and $\phi(U)_{Y(Y=R,L,H \text{ or } P)} = f(\Delta\pi)_{\Delta P=0}$ for aqueous glucose solutions. Plots 1–4 in A, B, and E were obtained for the Nephrophan membrane, and plots 1–4 in B, D, and F represent the Ultra-Flo 145 dialyzer® membrane

$\phi(S)_{Y(Y=R,L,H \text{ or } P)} = f(\Delta\pi)_{\Delta P=0}$, $\phi(F)_{Y(Y=R,L,H \text{ or } P)} = f(\Delta\pi)_{\Delta P=0}$, and $\phi(U)_{Y(Y=R,L,H \text{ or } P)} = f(\Delta\pi)_{\Delta P=0}$, satisfy the following relations: $\phi(S)_L > \phi(S)_P > \phi(S)_R > \phi(S)_H$, $\phi(F)_R > \phi(F)_L > \phi(F)_P > \phi(F)_H$ and $\phi(U)_L > \phi(U)_P > \phi(U)_R > \phi(U)_H$. In contrast, the same $\Delta\pi$ values for the Ultra-Flo 145 dialyzer® membrane, curves 1, 2, 3, and 4 for the dependencies $\phi(S)_{Y(Y=R,L,H \text{ or } P)} = f(\Delta\pi)_{\Delta P=0}$, $\phi(F)_{Y(Y=R,L,H \text{ or } P)} = f(\Delta\pi)_{\Delta P=0}$, and $\phi(U)_{Y(Y=R,L,H \text{ or } P)} = f(\Delta\pi)_{\Delta P=0}$, satisfy the following relations, $\phi(S)_L > \phi(S)_P > \phi(S)_R > \phi(S)_H$, $\phi(F)_L > \phi(F)_P > \phi(F)_R > \phi(F)_H$ and $\phi(U)_L > \phi(U)_P > \phi(U)_R > \phi(U)_H$.

ORCID iDs

Andrzej Ślęzak <https://orcid.org/0000-0001-6818-2099>
 Sławomir Marek Grzegorzczyn <https://orcid.org/0000-0002-5248-3505>
 Anna Pilis <https://orcid.org/0000-0002-5022-6820>
 Izabella Ślęzak-Prochazka <https://orcid.org/0000-0002-0707-2213>

References

- Coveney P, Highfield R. *The Arrow of Time: The Quest to Solve Time's Greatest Mystery*. London, UK: HarperCollins Publishers; 1991. ISBN:978-0-00-654462-3.
- Kondepudi D. *Introduction to Modern Thermodynamics*. Chichester, UK: Wiley & Sons; 2008. ISBN:978-0-470-98649-3.

3. Demirel Y, Sandler SI. Thermodynamics and bioenergetics. *Biophys Chem.* 2002;97(2–3):87–111. doi:10.1016/S0301-4622(02)00069-8
4. Delmotte M, Chanu J. Non-equilibrium thermodynamics and membrane potential measurement in biology. In: Millazzo G, ed. *Topics in Bioelectrochemistry and Bioenergetics*. Vol. 3. Chichester, UK: Wiley & Sons; 1980:307–359. ISBN:978-0-674-49411-4.
5. Katchalsky A, Curran PF. *Nonequilibrium Thermodynamics in Biophysics*. Harvard, USA: Harvard University Press; 1965. doi:10.4159/harvard.9780674494121
6. Klimek R. Biology of cancer: Thermodynamic answers to some questions. *Neuro Endocrinol Lett.* 2001;22(6):413–416. PMID:11781537.
7. Batko KM, Ślęzak-Prochazka I, Ślęzak A, Bajdur WM, Włodarczyk-Makuła M. Management of energy conversion processes in membrane systems. *Energies.* 2022;15(5):1661. doi:10.3390/en15051661
8. Ślęzak A, Ślęzak-Prochazka I, Grzegorzczyn S, Jasik-Ślęzak J. Evaluation of S-entropy production in a single-membrane system in concentration polarization conditions. *Transp Porous Med.* 2017;116(2):941–957. doi:10.1007/s11242-016-0807-7
9. Baker RW. *Membrane Technology and Applications*. 3rd ed. Chichester, UK–Hoboken, USA: John Wiley & Sons; 2012. ISBN:978-1-118-35971-6.
10. Peusner L. *Studies in Network Thermodynamics*. Amsterdam, the Netherlands–New York, USA: Elsevier; 1986. ISBN:978-0-444-42580-5.
11. Batko KM, Slezak-Prochazka I, Grzegorzczyn S, Slezak A. Membrane transport in concentration polarization conditions: Network thermodynamics model equations. *J Por Media.* 2014;17(7):573–586. doi:10.1615/JPorMedia.v17.i7.20
12. Batko KM, Ślęzak-Prochazka I, Ślęzak A. Network hybrid form of the Kedem–Katchalsky equations for non-homogenous binary non-electrolyte solutions: Evaluation of P_{ij}^* Peusner's tensor coefficients. *Transp Porous Med.* 2015;106(1):1–20. doi:10.1007/s11242-014-0352-1
13. Batko KM, Ślęzak A. Evaluation of the global S-entropy production in membrane transport of aqueous solutions of hydrochloric acid and ammonia. *Entropy.* 2020;22(9):1021. doi:10.3390/e22091021
14. Peusner L. Hierarchies of irreversible energy conversion systems. II. Network derivation of linear transport equations. *J Ther Biol.* 1985; 115(3):319–335. doi:10.1016/S0022-5193(85)80195-8
15. Ślęzak-Prochazka I, Batko KM, Wąsik S, Ślęzak A. H* Peusner's form of the Kedem–Katchalsky equations for non-homogenous non-electrolyte binary solutions. *Transp Porous Med.* 2016;111(2):457–477. doi:10.1007/s11242-015-0604-8
16. Ślęzak A, Grzegorzczyn S, Batko KM. Resistance coefficients of polymer membrane with concentration polarization. *Transp Porous Med.* 2012;95(1):151–170. doi:10.1007/s11242-012-0038-5
17. Batko KM, Ślęzak A, Pilis W. Evaluation of transport properties of biomembranes by means of Peusner network thermodynamics. *Acta Bioeng Biomech.* 2021;23(2):63–72. doi:10.37190/ABB-01774-2020-04
18. Anton-Sales I, D'Antin JC, Fernández-Engroba J, et al. Bacterial nanocellulose as a corneal bandage material: A comparison with amniotic membrane. *Biomater Sci.* 2020;8(10):2921–2930. doi:10.1039/D0BM00083C
19. Batko K, Ślęzak-Prochazka I, Grzegorzczyn S, Pilis A, Dolibog P, Ślęzak A. Energy conversion in Textus Bioactiv Ag membrane dressings using Peusner's network thermodynamic descriptions. *Polim Med.* 2022;52(2):57–66. doi:10.17219/pim/153522
20. Harma B, Gül M, Demircan M. The efficacy of five different wound dressings on some histological parameters in children with partial-thickness burns. *J Burn Care Res.* 2020;41(6):1179–1187. doi:10.1093/jbcr/iraa063
21. Ślęzak A. Irreversible thermodynamic model equations of the transport across a horizontally mounted membrane. *Biophys Chem.* 1989; 34(2):91–102. doi:10.1016/0301-4622(89)80047-X
22. Dworecki K, Slezak A, Ornal-Wasik B, Wasik S. Effect of hydrodynamic instabilities on solute transport in a membrane system. *J Membrane Sci.* 2005;265(1–2):94–100. doi:10.1016/j.memsci.2005.04.041
23. Ślęzak A. A model equation for the gravelectric effect in electrochemical cells. *Biophys Chem.* 1990;38(3):189–199. doi:10.1016/0301-4622(90)87001-2
24. Ślęzak A, Grzegorzczyn S, Jasik-Ślęzak J, Michalska-Małecka K. Natural convection as an asymmetrical factor of the transport through porous membrane. *Transp Porous Med.* 2010;84(3):685–698. doi:10.1007/s11242-010-9534-7
25. Slezak A, Dworecki K, Anderson JE. Gravitational effects on transmembrane flux: The Rayleigh–Taylor convective instability. *J Membrane Sci.* 1985;23(1):71–81. doi:10.1016/S0376-7388(00)83135-X
26. Ślęzak A, Dworecki K, Jasik-Ślęzak J, Wąsik J. Method to determine the critical concentration Rayleigh number in isothermal passive membrane transport processes. *Desalination.* 2004;168:397–412. doi:10.1016/j.desal.2004.07.027
27. Jasik-Ślęzak J, Ślęzak-Prochazka I, Ślęzak A. Evaluation of the Peusner's coefficients matrix for polymeric membrane and ternary non-electrolyte solutions [in Polish]. *Polim Med.* 2014;44(3):167–178. PMID:25696941.
28. Kedem O, Caplan SR. Degree of coupling and its relation to efficiency of energy conversion. *Trans Faraday Soc.* 1965;61:1897. doi:10.1039/tf9656101897
29. Caplan SR. Nonequilibrium thermodynamics and its application to bioenergetics. In: Sanadi RD, ed. *Current Topics in Bioenergetics*. Vol. 4. Elsevier; 1971:1–79. doi:10.1016/B978-0-12-152504-0.50008-3
30. Klinkman H, Holtz M, Willgerodt W, Wilke G, Schoenfelder D. Nephrophon: Eine neue Dialysemembrane. *Zeits Urolog Nephrol.* 1969;4: 285–292.
31. Richter T, Keipert S. In vitro permeation studies comparing bovine nasal mucosa, porcine cornea and artificial membrane: Androstenedione in microemulsions and their components. *Eur J Pharm Biopharm.* 2004;58(1):137–143. doi:10.1016/j.ejpb.2004.03.010
32. Twardowski ZJ. History of hemodialyzers' designs. *Hemodialysis Int.* 2008;12(2):173–210. doi:10.1111/j.1542-4758.2008.00253.x

Cytotoxicity of cleaning agents for ocular prostheses

Marcelo Coelho Goiato^{1,E,F}, Agda Marobo Andreotti^{1,B,D}, Fernanda Pereira de Caxias^{1,D,F}, Emily Vivianne Freitas da Silva^{1,C,E}, Letícia de Oliveira Gonçalves^{1,B}, Sandra Helena Penha de Oliveira^{2,B,E}, Victor Gustavo Balera Brito^{2,B,E}, Clóvis Lamartine de Moraes Melo Neto^{1,D,E}, Daniela Micheline dos Santos^{1,A,E,F}

¹ Department of Dental Materials and Prosthodontics, School of Dentistry, São Paulo State University (UNESP), Araçatuba, Brazil

² Department of Basic Sciences, Immunopharmacology Laboratory, São Paulo State University (UNESP), School of Dentistry, Araçatuba, Brazil

A – research concept and design; B – collection and/or assembly of data; C – data analysis and interpretation;

D – writing the article; E – critical revision of the article; F – final approval of the article

Polymers in Medicine, ISSN 0370-0747 (print), ISSN 2451-2699 (online)

Polim Med. 2023;53(1):37–46

Address for correspondence

Marcelo Coelho Goiato
E-mail: m.goiato@unesp.br

Funding sources

This study was funded by the National Council for Scientific and Technological Development/CNPQ (grant No. #304462/2016-0); CAPES (Coordination for the Improvement of Higher Education Personnel) and FAPESP (São Paulo Research Foundation) (grants No. #2015/04695-9 and No. #2014/25714-9).

Conflict of interest

None declared

Received on January 27, 2023

Reviewed on April 6, 2023

Accepted on April 7, 2023

Published online on June 1, 2023

Abstract

Background. Polymethylmethacrylate (PMMA) is the most used material for the manufacturing of eye prostheses.

Objectives. To investigate the cytotoxicity of different cleaning agents for ocular prostheses on human conjunctival cells.

Materials and methods. Six groups of specimens were created (saline, soap, 4% chlorhexidine, hydrogen peroxide, 1% triclosan, and citronella oil). Three specimens were made for each disinfectant at each disinfection period (1, 7, 15, 30, 60, and 90 days), totaling 108 specimens. Thus, the specimens were disinfected, with different disinfectants, for different periods of time. After each disinfection process, the specimens were washed with sterile distilled water. A human conjunctival cell line was grown on the acrylic resin specimens and then cytotoxicity tests (MTT and Neutral Red (NR)) were performed. A negative control (untreated cell cultures) and positive control (Tween 20) were created. Two-way analysis of variance (ANOVA) and Bonferroni test were performed ($p < 0.05$).

Results. For the MTT and NR tests, when there was a significant difference between the disinfectant and negative control, the disinfectant generated a significant reduction in cell proliferation most of the time.

Conclusions. All reductions in cell proliferation caused by the disinfectants were clinically acceptable. All disinfectants tested in this study were found to be non-cytotoxic to human conjunctival cells.

Key words: artificial eye, acrylic resins, cytotoxicity, materials testing, conjunctiva, PMMA

Cite as

Goiato MC, Andreotti AM, de Caxias FP, da Silva EVF, de Oliveira Gonçalves L, de Oliveira SHP, Balera Brito VG, de Moraes Melo Neto CL, dos Santos DM. Cytotoxicity of cleaning agents for ocular prostheses.

Polim Med. 2023;53(1):37–46.

doi:10.17219/pim/163118

DOI

10.17219/pim/163118

Copyright

Copyright by Author(s)

This is an article distributed under the terms of the Creative Commons Attribution 3.0 Unported (CC BY 3.0) (<https://creativecommons.org/licenses/by/3.0/>)

Background

Ocular prosthetics are important in the rehabilitation of patients who have suffered ocular loss.^{1–6} They can restore facial aesthetics, prevent eyelid deformation, direct and prevent the deposition of tear fluid in the anophthalmic site, protect the mucosa, and help the lacrimal glands partially recover their original position.^{1,3,4,6} Furthermore, these prostheses can help to increase the self-esteem of anophthalmic individuals.^{1,4}

Polymethylmethacrylate (PMMA), also known as acrylic resin, is the most used material for the manufacture of eye prostheses, as it makes them more versatile, resistant and comfortable to use.⁹ Currently, N1 acrylic resin (white color) is among the most used materials for making ocular prostheses due to its similarity to the color of the human ocular sclera, durability, ease of hygiene, and retention in the anophthalmic site.^{3,4}

Soap, chlorhexidine gluconate, hydrogen peroxide, citronella oil, and triclosan are cleaning agents used to disinfect eye prostheses.⁵ Although the disinfection of ocular prostheses is essential, the patient, after using the disinfectant, may not adequately rinse their prosthesis before replacing it in the anophthalmic socket. Thus, chemical components can be released into this cavity, potentially causing damage to the mucosa.⁷

In 2023, a search on PubMed using the terms “conjunctival”, “ocular prosthesis” and “cytotoxicity” showed that there are no articles evaluating the cytotoxicity of disinfectants used to clean ocular prostheses on human conjunctival cells. Thus, this study aimed to evaluate the cytotoxicity of disinfectants (soap, chlorhexidine gluconate, hydrogen peroxide, triclosan, and citronella oil) used for cleaning eye prostheses on human conjunctival cells.

Materials and methods

Manufacturing of acrylic resin specimens

The preparation of the specimens was carried out according to the procedure described by Andreotti et al.⁵ The thermopolymerizable acrylic resin used was N1 (white color, VIPI STG; VIPI Indústria, Pirassununga, Brazil).⁴ Polymerization was carried out using microwaves.⁵ All specimens were circular and had the same dimensions (10 × 3 mm).^{1,3–5}

The specimens were polished with abrasive papers of different granulations (280, 320, 600, and 1200; Norton, São Paulo, Brazil; APL-4; Arotec, Cotia, Brazil) under constant irrigation for 3 min (sum of times used for each sandpaper) and, later, with felt and 1- μ m diamond solution for 1 min. Next, the specimens were cleaned with distilled water in ultrasound for 20 min. This procedure aimed to remove debris from the surface of the material. Then, the specimens remained on a bench to allow their natural drying.

Groups

The specimens were divided into the following groups:

1) saline group (0.9% NaCl; Apothicario Manipulation Pharmacy, Araçatuba, Brazil) – immersion in 1 mL of saline for 10 min⁵;

2) neutral soap group (Johnson & Johnson, São José dos Campos, Brazil) – neutral soap has not been diluted with water. Cleaning with this product was associated with rubbing the samples with gauze for 30 s⁵;

3) 4% chlorhexidine group (Apothicario Manipulation Pharmacy) – immersion in 1 mL of chlorhexidine for 10 min⁵;

4) Efferdent group (effervescent tablets; Efferdent Original Denture Cleanser; Pfizer Consumer Health, Morris Plains, USA) – immersion in the hydrogen peroxide solution (250 mL of sterile H₂O and 1 effervescent tablet = 0.17% H₂O₂) for 15 min^{5,6};

5) 1% triclosan group (Apothicario Manipulation Pharmacy) – immersion in 1 mL of 1% triclosan for 10 min^{5,9};

6) citronella oil group (Apothicario Manipulation Pharmacy) – immersion in 1 mL of citronella oil for 10 min⁵.

Three specimens were made for each disinfectant at each disinfection period (1, 7, 15, 30, 60, and 90 days), totaling 108 specimens. Thus, the specimens were submitted to the processes described above for different time periods (1, 7, 15, 30, 60, and 90 days). Next, the specimens were washed with sterile distilled water for 30 s to simulate a clinical situation.

After disinfecting and rinsing the specimens, the groups were subjected to cytotoxicity testing at each time point.

Cytotoxicity of disinfectants

Specimens from each group were added to a tube with 6 mL of culture medium 199 (Gibco, New York, USA) supplemented with a 5% concentration of fetal bovine serum (FBS), previously determined in a pilot study, and incubated in a bacteriological oven at 37°C for 24 h. Subsequently, Millex filters (0.2 μ m; Merck Millipore, Darmstadt, Germany) were used to filter the eluates.^{1,3,4}

For the culture and maintenance of cells, the human conjunctival cell line (Wong Kilbourne derivative of Chang conjunctival cell line; clone 1-5c-4), obtained from the American Type Culture Collection (ATCC; CCL-20.2; Manassas, USA), was used and expanded in culture medium supplemented with 10% FBS. Cells were incubated at 37°C in a 5% CO₂ environment^{1,3,4} until they reached confluence. Then, 1 mL of cell suspensions of 1 × 10⁵ cells/mL was pipetted into each well of a plate containing 24 wells.^{1,3,4} After 24 h, the culture medium was discarded, and 500 μ L of each previously obtained eluate containing 5% FBS was added to each well (n = 3/group). After incubation, MTT (3-[4,5-dimethylthiazol-2-yl]-2,5-diphenyl tetrazolium bromide)^{1,3,4} and Neutral Red (NR)¹⁰ assays were performed.

The MTT is a colorimetric analysis used to measure mitochondrial metabolic activity.^{1,3,4} After 24 h, eluates were replaced with a FBS-free medium containing 0.5 mg/mL of MTT, and incubated at 37°C for 2 h.^{1,3,4} After incubation, the medium was aspirated and 500 µL of isopropyl alcohol was added to each well.^{1,3,4} Absorbances were measured in triplicate at a 570-nm wavelength using a UV-visible spectrophotometer (SpectraMax 190; Molecular Devices, San Jose, USA).^{1,3,4} The NR assay measures lysosomal activity in a culture. After 24 h, eluates were replaced with 0.5 mL of NR dye, and the plates were incubated at 37°C for 2 h. Then, the NR and medium were replaced with 500 µL of 1% formic acid for washing. The formic acid was removed and 1 mL of 1% acetic acid was added to each well. After extracting the dye from the cells, cell viability was assessed in triplicate using the optical density of the resulting solution at 540 nm with a UV-visible spectrophotometer.

For MTT and NR assays, the negative control were cell cultures without any treatment. They consisted of 1 mL of culture medium with 5% FBS. The positive control consisted of medium with Tween 20 (Sigma-Aldrich, Saint Louis, USA), which is a non-ionic detergent responsible for cell lysis in cytotoxicity assays.^{1,3,4} Both were subjected to the same conditions of incubation and temperature used to obtain the eluates (n = 3/group).

Real-time reverse transcription quantitative polymerase chain reaction (RT-qPCR) was performed to quantitatively assess gene expression levels for type IV collagen (COL IV, COL4A3BP: Hs00178621_m1), transforming growth factor β (TGF-β, TGFB1: Hs0099133_m1), matrix metalloproteinase 9 (MMP9, MMMP9: Hs00234579_m1),^{1,3,4} and markers related to apoptosis and cell death that included myeloid cell leukemia sequence 1 (MCL-1, MCL1: Hs01050896_m1) and caspases 3 (CASP-3, CASP3: Hs0023487_m1) and 9 (CASP-9, CASP9: Hs00609647_m1).^{1,11,12}

The StepOnePlus Real-Time PCR System (Applied Biosystems, Life Technologies, Foster City, USA) was used.^{1,3,4} The β-actin (ACTB: Hs030223880_g1) was utilized as an endogenous control.^{1,3,4} The results were analyzed with the cycle threshold.^{1,3,4}

Cytotoxicity analyses were carried out respecting the norms of the ISO 10993-5 standard for in vitro toxicity analysis.¹³ Cell proliferation percentages of the controls represented 100% and cell viability (%) was calculated for all groups.^{1,3,4}

Statistical analyses

Two-way analysis of variance (ANOVA) and Bonferroni test were used (p < 0.05). The variation factors were disinfectants (saline, soap, chlorhexidine, hydrogen peroxide, triclosan, and citronella oil) and time points (1, 7, 15, 30, 60, and 90 days).

Results

The two-way ANOVA showed a significant relationship between the variation factors (cleaning agents and times) and the results of cytotoxicity assays (MTT, NR and RT-qPCR; p < 0.001 for all factors).

MTT (disinfectant compared to control)

After 7 and 15 days, there was a significant reduction in cell proliferation in the saline group, while in the neutral soap group, such reduction was observed after 1, 7, 15, 60, and 90 days. After 1 day, there was a significant increase in cell proliferation in the chlorhexidine group, followed by a significant reduction after 60 and 90 days. After 1 and 60 days, there was a significant reduction in cell proliferation in the effervescent group, and a significant increase after 30 days. In the triclosan group, after 7 and 30 days, there was a significant reduction in cell proliferation. After 1 day, there was a significant reduction in cell proliferation in the citronella group, followed by a significant increase after 30, 60, and 90 days.

These results are presented in Fig. 1.

NR (disinfectant compared to control)

After 90 days, there was a significant reduction in cell proliferation in the saline group. In the neutral soap group, there was a significant reduction in cell proliferation after 7 and 90 days. After 60 days, there was a significant increase in cell proliferation in the chlorhexidine group, followed by a significant reduction in cell proliferation after 90 days. In the effervescent group, there was a significant reduction in cell proliferation after 15 and 90 days, and a significant increase after 60 days. After 30 days, there was a significant reduction in cell proliferation in the triclosan group. There was a significant increase in cell proliferation in the citronella group after 1 day, followed by a significant decrease after 7 and 15 days.

These results are presented in Fig. 2.

COL IV

Due to the large number of comparisons, only the most important are reported below. After 7 days, the triclosan group showed a significantly higher COL IV gene expression level compared to the other groups. After 15 days, the triclosan group showed a significantly higher COL IV gene expression level than the other groups. After 30 days, the saline, triclosan and citronella groups showed significantly higher COL IV gene expression levels compared to the other groups. After 60 days, the neutral soap group showed a significantly higher COL IV gene expression level compared to the other groups.

These results are presented in Fig. 3.

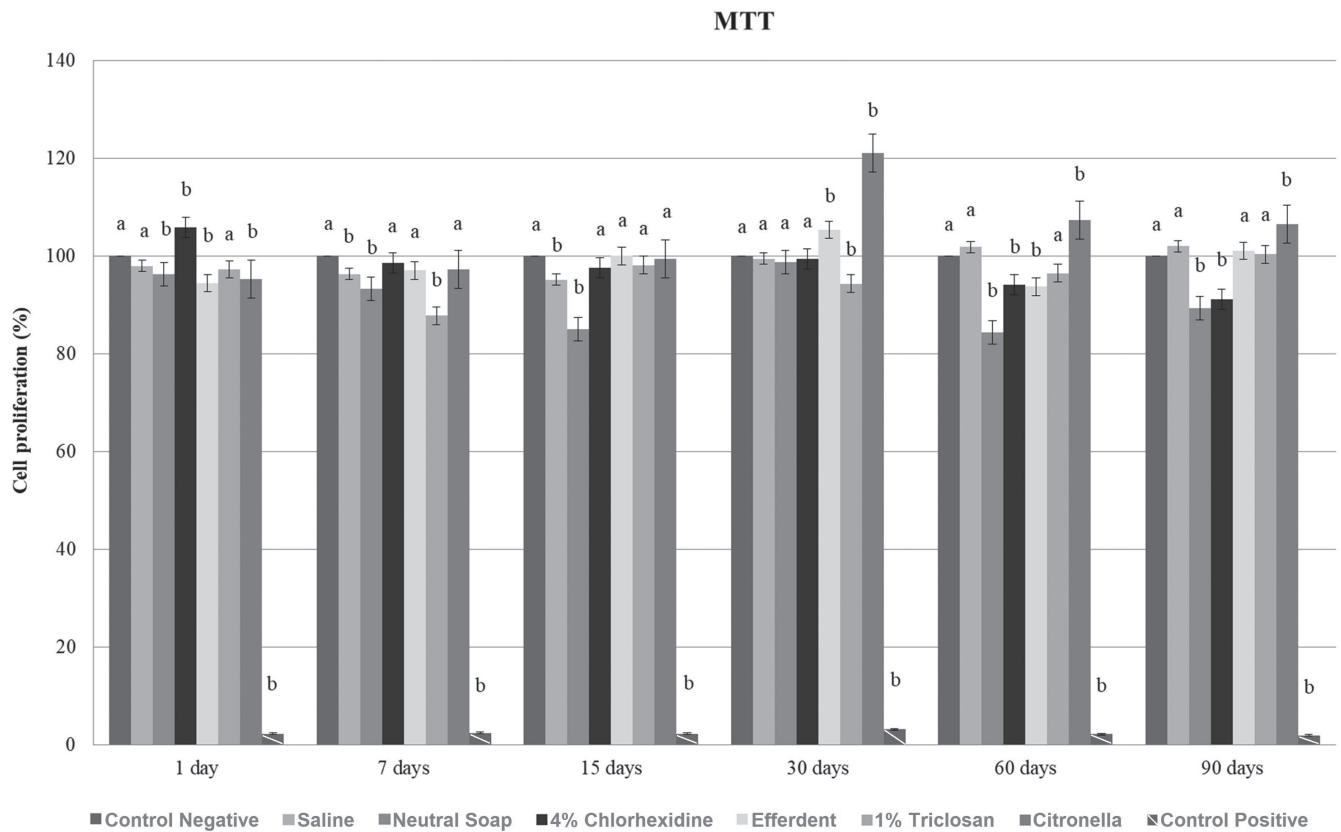


Fig. 1. Mean of cell proliferation percentages obtained using MTT analysis. Different letters at each time indicate a significant difference between each tested group and the negative control group (Bonferroni test)

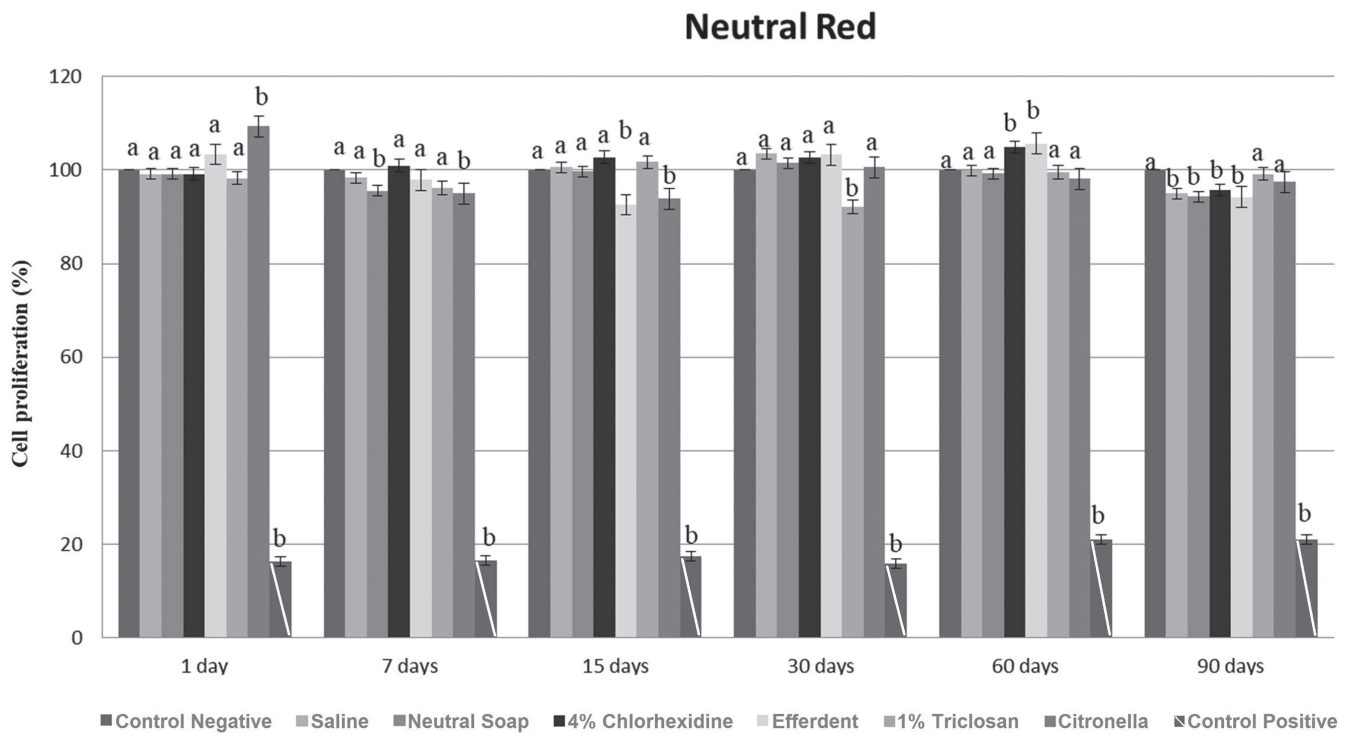


Fig. 2. Mean percentages of cell proliferation obtained using Neutral Red (NR) analysis. Different letters at each time indicate a significant difference between each tested group and the negative control group (Bonferroni test)

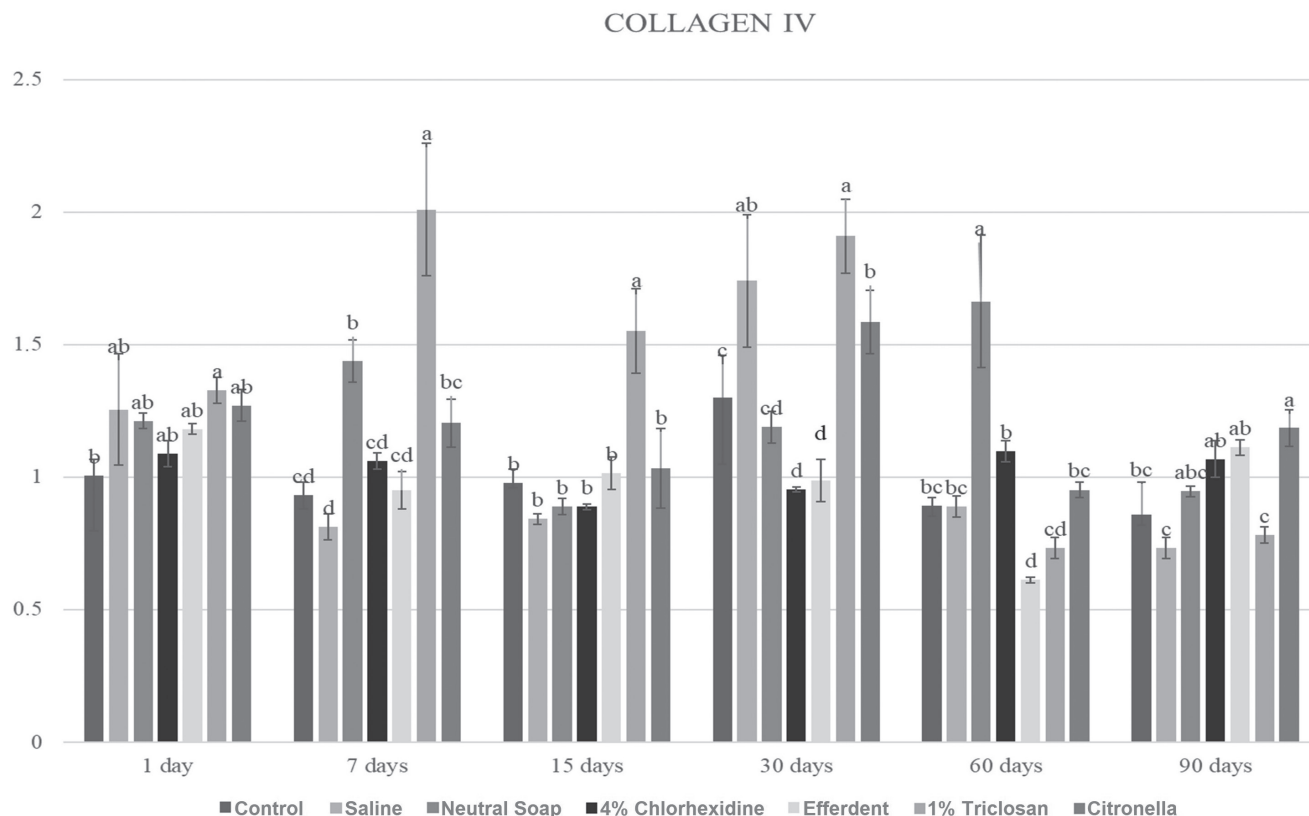


Fig. 3. Type IV collagen (COL IV) expression. Different letters at each time point indicate a significant difference between groups (Bonferroni test)

TGF- β

Due to the large number of comparisons, only the most important are reported below. After 1 day, the triclosan group showed a significantly higher TGF- β gene expression level compared to the other groups. After 7 days, the neutral soap group showed a significantly higher TGF- β gene expression level compared to the other groups. After 15 days, the triclosan group showed a significantly higher TGF- β gene expression level compared to the other groups. After 30 days, the control and saline groups showed significantly higher TGF- β gene expression levels compared to the other groups. After 60 days, the neutral soap group showed a significantly higher TGF- β gene expression level compared to the other groups. After 90 days, the neutral soap and citronella groups showed significantly higher TGF- β gene expression levels compared to the other groups.

These results are presented in Fig. 4.

MCL-1

Due to the large number of comparisons, only the most important are reported below. After 1 day, the control group showed a significantly higher MCL-1 gene expression level compared to the other groups. After 7 days, the triclosan group showed a significantly higher MCL-1 gene expression level compared to the other groups. After

15 days, the citronella group showed a significantly higher Myeloid cell leukemia sequence 1 (MCL-1) gene expression level compared to the other groups, except when compared to the triclosan group. After 30 days, the saline and triclosan groups showed significantly higher MCL-1 gene expression levels compared to the other groups. After 60 days, the neutral soap group showed a significantly higher MCL-1 gene expression level compared to the other groups. After 90 days, the chlorhexidine and citronella groups showed significantly higher MCL-1 gene expression levels compared to the other groups.

These results are presented in Fig. 5.

MMP-9

Due to the large number of comparisons, only the most important are reported below. After 1 day, the citronella group showed a significantly higher MMP-9 gene expression level compared to the other groups. After 7 days, the triclosan group showed a significantly higher MMP-9 gene expression level compared to the other groups. After 30 days, the triclosan group showed a significantly higher MMP-9 gene expression level compared to the other groups. After 60 days, the control and Efferdent groups showed significantly higher MMP-9 gene expression levels compared to the other groups, except when compared to the saline group.

These results are presented in Fig. 6.

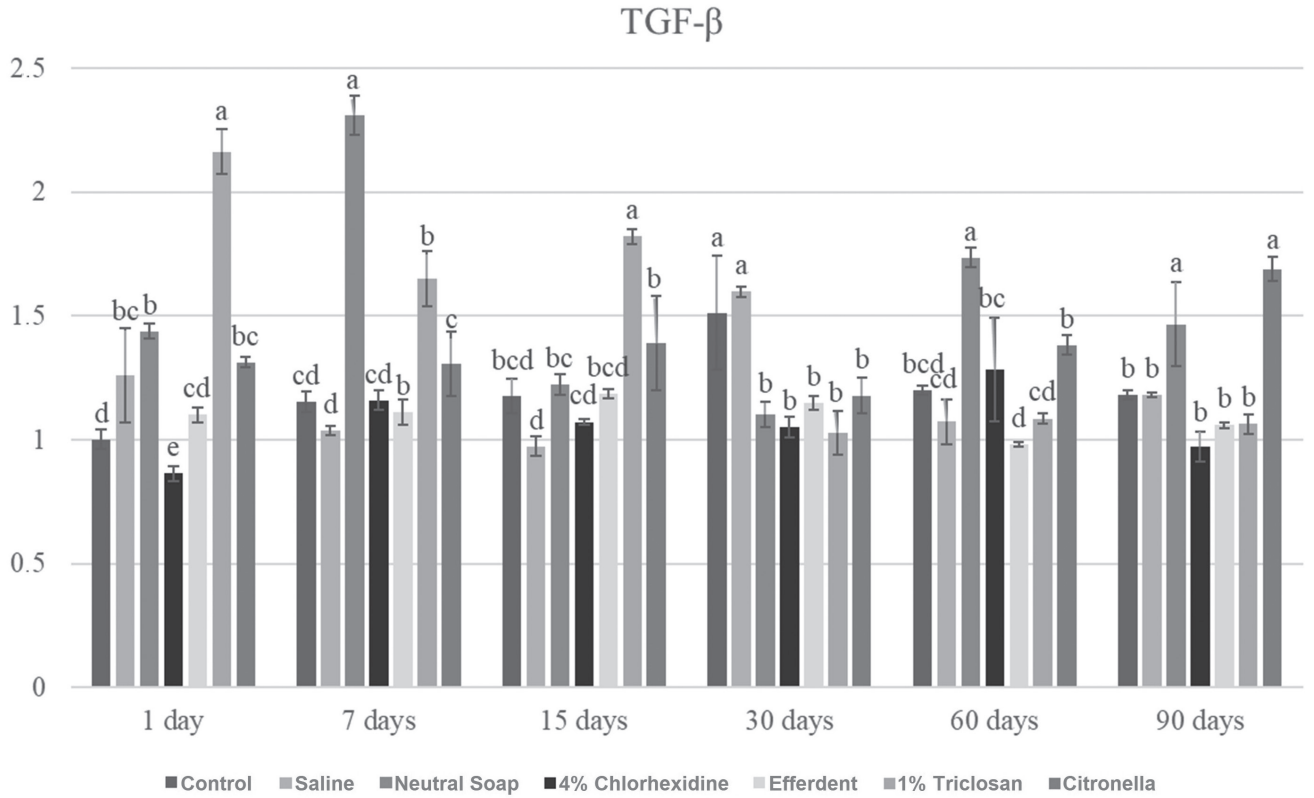


Fig. 4. Transforming growth factor β (TGF-β) expression. Different letters at each time point indicate a significant difference between groups (Bonferroni test)

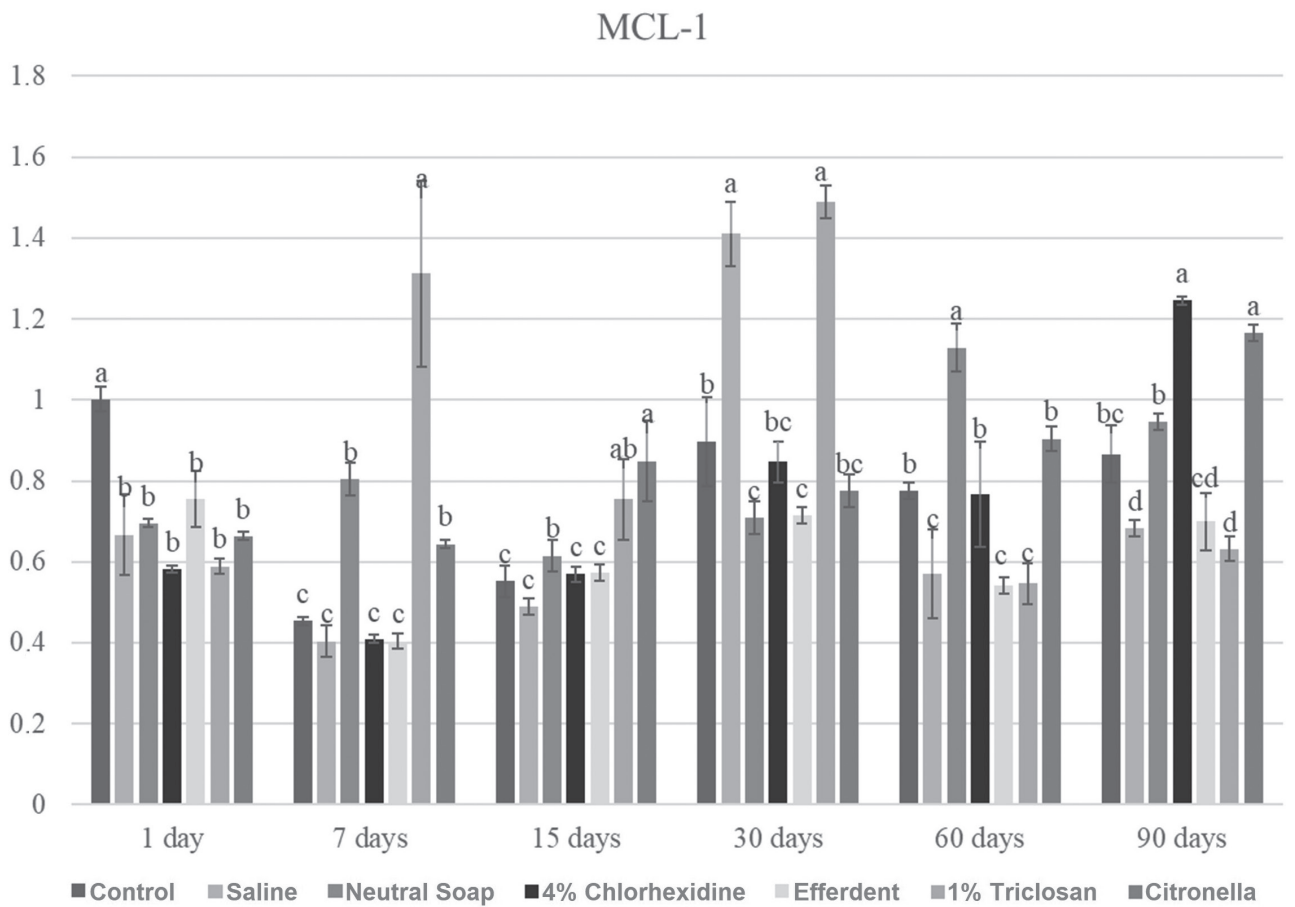


Fig. 5. MCL-1 expression. Different letters at each time point indicate a significant difference between groups (Bonferroni test)

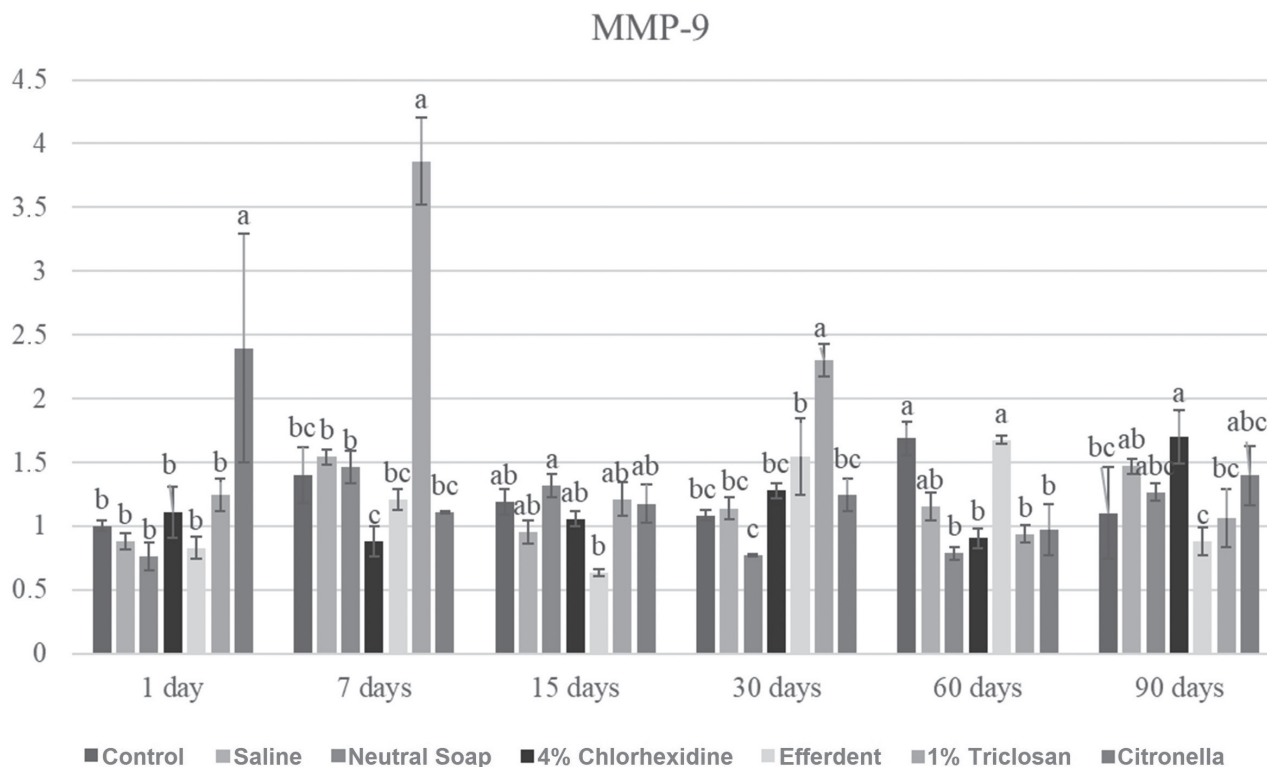


Fig. 6. Matrix metalloproteinase 9 (MMP9) expression. Different letters at each time point indicate a significant difference between groups (Bonferroni test)

CASP-3

Due to the large number of comparisons, only the most important are reported below. After 1 day, the triclosan group showed a significantly higher CASP-3 gene expression level compared to the other groups. After 7 days, the triclosan group showed a significantly higher CASP-3 gene expression level compared to the other groups. After 15 days, the citronella group showed a significantly higher CASP-3 gene expression level compared to the other groups, except when compared to the triclosan group. After 30 days, the triclosan group showed a significantly higher CASP-3 gene expression level compared to the other groups. After 60 days, the chlorhexidine group showed a significantly higher CASP-3 gene expression level compared to the other groups, except when compared to the citronella group. After 90 days, the citronella group showed a significantly higher CASP-3 gene expression level compared to the other groups, except when compared to the chlorhexidine group.

These results are presented in Fig. 7.

CASP-9

Due to the large number of comparisons, only the most important are reported below. After 1 day, the triclosan group showed a significantly higher CASP-9 gene expression level compared to the other groups. After 7 days, the neutral soap and citronella groups showed significantly higher CASP-9 gene expression levels compared

to the other groups. After 15 days, the triclosan group showed a significantly higher CASP-9 gene expression level compared to the other groups. After 60 days, the neutral soap group showed a significantly higher CASP-9 gene expression level compared to the other groups, except when compared to the citronella group. After 90 days, the citronella group showed a significantly higher CASP-9 gene expression level compared to the other groups.

These results are presented in Fig. 8.

Discussion

Based on the MTT and NR tests (Fig. 1,2), although statistically significant differences were observed at each time point between the cleaning agents and the control group, all values were greater than 84%. Based on ISO 10993-5, a substance evaluated (in vitro) can be classified as non-cytotoxic (cell proliferation greater than 75%), slightly cytotoxic (cell proliferation between 50 and 75%), moderately cytotoxic (cell proliferation between 25 and 50%), and highly cytotoxic (cell proliferation less than 25%).¹³ Thus, all cleaning agents were classified as non-cytotoxic, regardless of the evaluated disinfection period.

Based on the statistical evaluation (Fig. 1,2), in most cases, when there was a significant difference between the disinfectant and the control group, there was a significant reduction in cell proliferation generated by the disinfectant. This was probably due to liquid sorption processes and the solubility of PMMA.⁷ Thus, this material

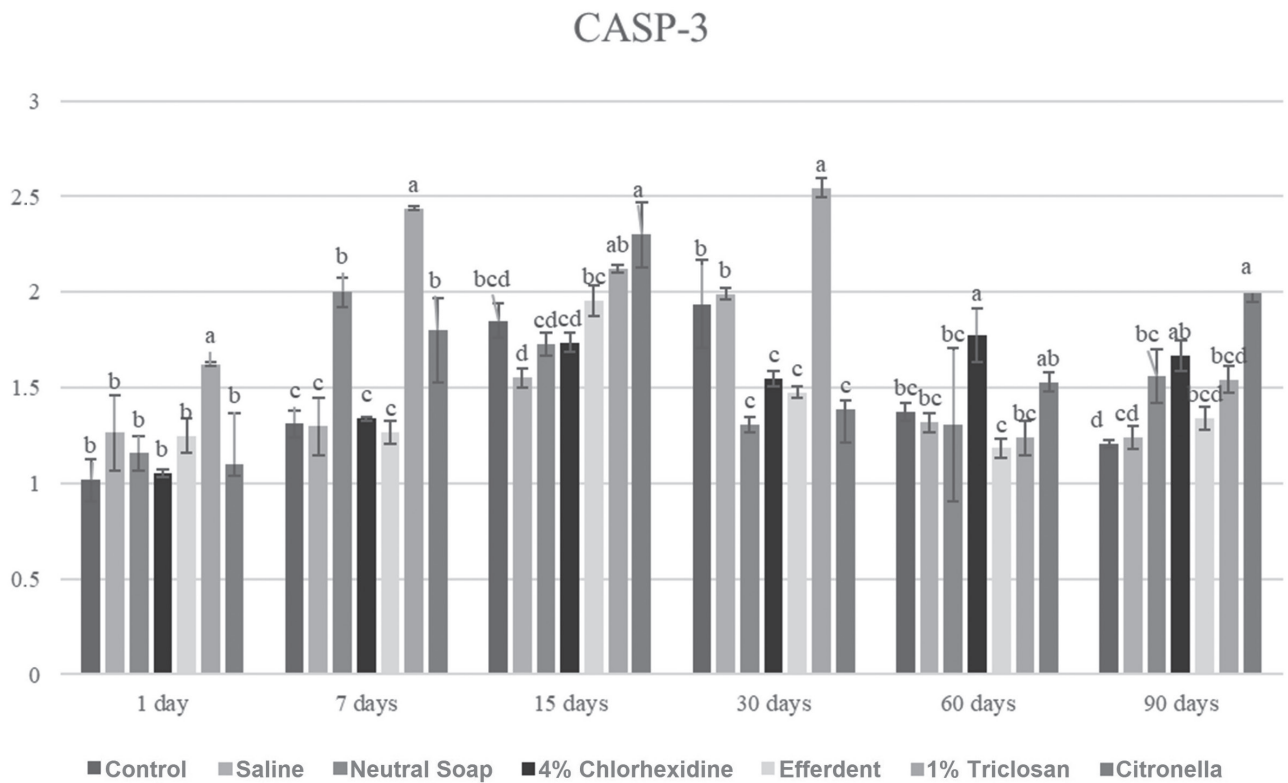


Fig. 7. Caspase 3 (CASP-3) expression. Different letters at each time point indicate a significant difference between groups (Bonferroni test)

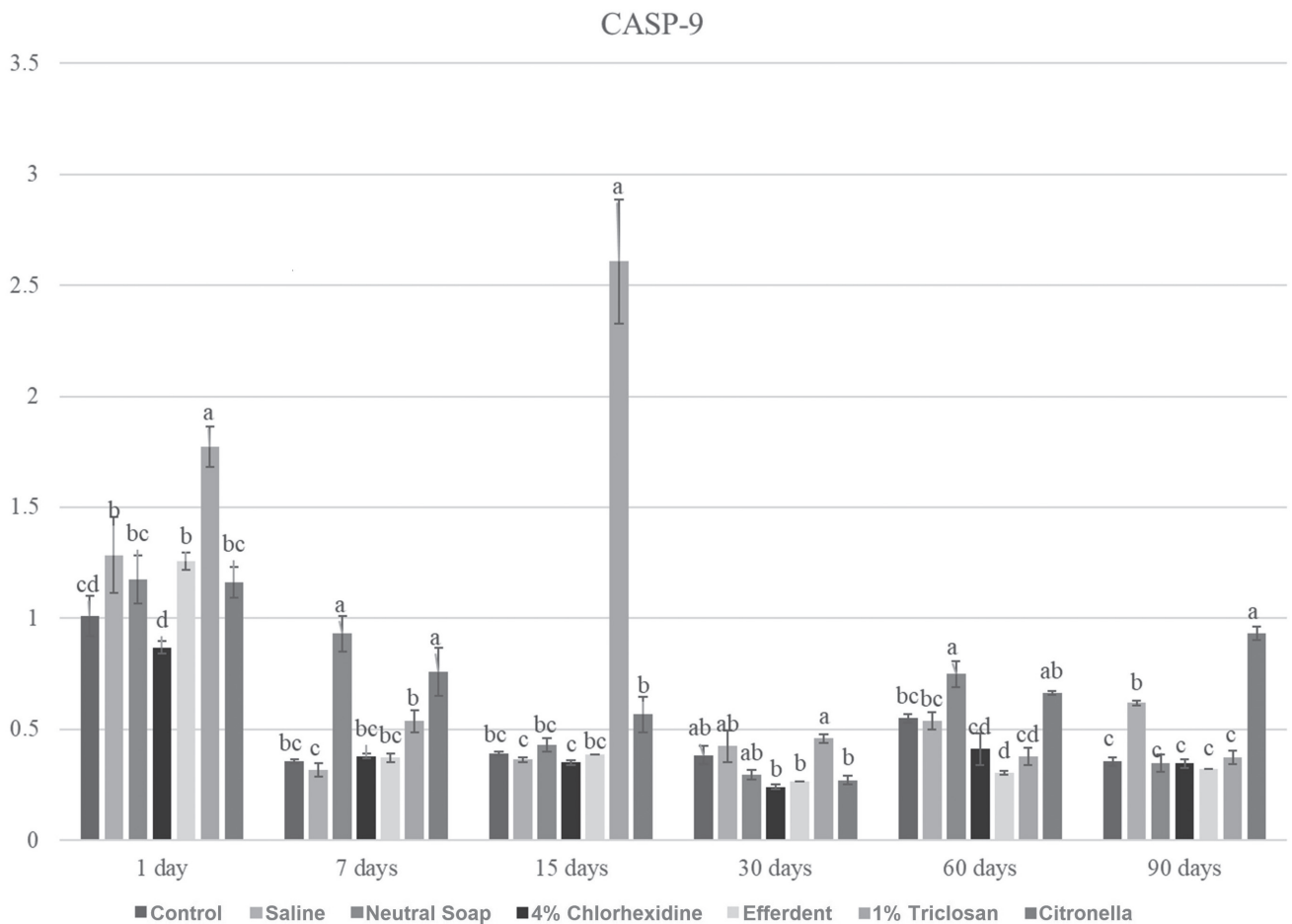


Fig. 8. Caspase 9 (CASP-9) expression. Different letters at each time point indicate a significant difference between groups (Bonferroni test)

may have absorbed chemical agents from the disinfectant used, which remained inside, making it impossible to remove these absorbed substances by rinsing. Later, probably during cell proliferation, due to the solubility process, these chemical substances were released on the surface of the specimen, resulting in decreased cell proliferation. However, these significant reductions in cell proliferation can be considered clinically acceptable based on previously reported ISO 10993-5 criteria.¹³ Furthermore, the significant increase in cell proliferation after disinfectant use can be explained by the failure of PMMA to absorb the disinfectant, causing the rinse to completely remove it from the surface of the material (Fig. 1,2). Thus, cell proliferation was not negatively influenced by the disinfectant and increased.

Andreotti et al. observed that 4% chlorhexidine, 1% triclosan and Efferdent significantly reduced the amount of microorganism colonies (*Staphylococcus aureus* and *Staphylococcus epidermidis*) compared to citronella oil and neutral soap.⁵ They also found no significant differences between the 4% chlorhexidine, 1% triclosan and Efferdent groups based on microbial reduction of *Staphylococcus aureus* and *Staphylococcus epidermidis*.⁵ Also in the study by Andreotti et al., it is noteworthy that neutral soap was significantly more effective in reducing *Staphylococcus aureus* than citronella oil, and had the same effect against *Staphylococcus epidermidis* as citronella oil.⁵ Thus, as all disinfectants tested in this study were classified as non-cytotoxic – 4% chlorhexidine, 1% triclosan and Efferdent are the disinfectants indicated for cleaning ocular prostheses, as they combine high antimicrobial efficiency and absence of cytotoxicity against human conjunctival cells.

Regarding the expression of COL-IV, TGF- β , MCL-1, MMP-9, CASP-3, and CASP-9, the triclosan group was the one that stood out the most among the groups (Fig. 3–8). This group presented, on several occasions, significantly higher values than the other groups (Fig. 3–8), which were very expressive. Higher levels of TGF- β expression stimulate the synthesis of COL IV. On the other hand, the MMP-9 expression acts to degrade COL IV.^{14,15} Therefore, a balance between the synthesis (related to TGF- β) and breakage of collagen (related to MMP-9) is clinically important.^{1,3,4} If a greater expression of TGF- β is not compensated by a greater expression of MMP-9, a fibrous reaction during the tissue repair process may occur, compromising the use of the ocular prosthesis. On the other hand, if there is an increase in the expression of MMP-9, not compensated by the increase in the expression of TGF- β , severe tissue damage may occur, also affecting the patient's rehabilitation.¹⁶ It is noteworthy that COL IV, produced by epithelial cells, is essential in the composition of their basement membrane extracellular matrix.⁴ In turn, MCL-1 (anti-apoptotic protein) promotes cell survival,^{1,12} while CASP-3 and -9 are proteases involved in apoptosis,^{1,11} and their activation (CASP-3 and -9) induces an increase in reactive oxygen species

(ROS).^{1,17} The balance of these markers is also important for the health of the anophthalmic socket tissue. Thus, the ocular prosthesis and its cleaning agent must maintain tissue health, preventing the formation of fibrosis, unbalanced cell death and inflammatory reactions. New studies should be carried out using the disinfectants described in this study in different concentrations, in addition to other disinfectants for cleaning ocular prostheses.

Conclusions

All reductions in cell proliferation generated by the disinfectants were clinically acceptable. All disinfectants tested in this study were found to be non-cytotoxic to human conjunctival cells.

ORCID iDs

Marcelo Coelho Goiato  <https://orcid.org/0000-0002-3800-3050>
 Agda Marobo Andreotti  <https://orcid.org/0000-0003-3259-0482>
 Fernanda Pereira de Caxias  <https://orcid.org/0000-0001-5493-4069>
 Emily Vivianne Freitas da Silva  <https://orcid.org/0000-0002-0164-1788>
 Leticia de Oliveira Gonçalves  <https://orcid.org/0000-0001-8242-3530>
 Sandra Helena Penha de Oliveira  <https://orcid.org/0000-0003-0805-1120>
 Victor Gustavo Balera Brito  <https://orcid.org/0000-0001-5508-3825>
 Clóvis Lamartine de Moraes Melo Neto  <https://orcid.org/0000-0003-1477-2055>
 Daniela Micheline dos Santos  <https://orcid.org/0000-0001-6297-6154>

References

- Da Silva EVF, Goiato MC, Bitencourt SB, et al. Effect of processing methods on the cytotoxicity of methyl methacrylate-based ocular prostheses: An in vitro study. *Toxicol In Vitro*. 2021;76:105211. doi:10.1016/j.tiv.2021.105211
- De Caxias FP, Sa Teles KL, Dos Santos DM, et al. Effect of rehabilitation with a new ocular prosthesis on electromyography of the occipitofrontalis, temporal, masseter, and sternocleidomastoid. *Eur J Dent*. 2022;16(2):346–350. doi:10.1055/s-0041-1735795
- Da Silva EVF, Goiato MC, Dos Santos DM, Bonatto LDR, Brito VGB, De Oliveira SHP. Effect of different methods of polymerizing ocular prosthesis acrylic resin on a human conjunctival cell line. *J Prosthet Dent*. 2016;116(5):818–823. doi:10.1016/j.prosdent.2016.06.001
- da Silva EVF, dos Santos DM, da Rocha Bonatto L, Balera Brito VG, de Oliveira SHP, Goiato MC. Influence of preparation and exposure periods of eluates from ocular prosthesis acrylic resin in human conjunctival cell line. *Iran Biomed J*. 2019;23(1):78–86. doi:10.29252/23.1.78
- Andreotti AM, Pereira de Caxias F, Alves de Sousa C. Antibiofilm effect of cleaning agents for ocular prostheses. *Clin Ter*. 2023;174(1):23–27. doi:10.7417/CT.2023.2492
- Moreno A, Dos Santos DM, Lamartine De Moraes Melo Neto C, Luiz De Melo Moreno A, De Magalhães Bertoz AP, Goiato MC. In vitro evaluation of the effect of different disinfectants on the biofilm of *Staphylococcus epidermidis* and *Staphylococcus aureus* formed on acrylic ocular prostheses. *PLoS One*. 2020;15(10):e0240116. doi:10.1371/journal.pone.0240116
- Zafar MS. Prosthodontic applications of polymethyl methacrylate (PMMA): An update. *Polymers (Basel)*. 2020;12(10):2299. doi:10.3390/polym12102299
- Goiato MC, Dos Santos DM, Baptista GT, Moreno A, Andreotti AM, Dekon SFDC. Effect of thermal cycling and disinfection on microhardness of acrylic resin denture base. *J Med Eng Technol*. 2013;37(3):203–207. doi:10.3109/03091902.2013.774444
- Ortega KL, Rech BO, El Haje GLC, Gallo CB, Pérez-Sayáns M, Braz-Silva PH. Do hydrogen peroxide mouthwashes have a virucidal effect? A systematic review. *J Hosp Infect*. 2020;106(4):657–662. doi:10.1016/j.jhin.2020.10.003

10. Repetto G, Del Peso A, Zurita JL. Neutral red uptake assay for the estimation of cell viability/cytotoxicity. *Nat Protoc.* 2008;3(7):1125–1131. doi:10.1038/nprot.2008.75
11. Yan S, Li YZ, Zhu XW, Liu CL, Wang P, Liu YL. HuGE systematic review and meta-analysis demonstrate association of CASP-3 and CASP-7 genetic polymorphisms with cancer risk. *Genet Mol Res.* 2013;12(2):1561–1573. doi:10.4238/2013.May.13.10
12. Wei AH, Roberts AW, Spencer A, et al. Targeting MCL-1 in hematologic malignancies: Rationale and progress. *Blood Rev.* 2020;44:100672. doi:10.1016/j.blre.2020.100672
13. International Organization for Standardization. ISO 10993-5: 2009 – Biological evaluation of medical devices. Part 5: Tests for in vitro cytotoxicity. Geneva, Switzerland: International Organization for Standardization; 2009. <https://www.iso.org/standard/36406.html>. Accessed May 16, 2023.
14. Simon RH, Scott MJ, Reza MM, Killen PD. Type IV collagen production by rat pulmonary alveolar epithelial cells. *Am J Respir Cell Mol Biol.* 1993;8(6):640–646. doi:10.1165/ajrcmb/8.6.640
15. Tirado-Rodriguez B, Ortega E, Segura-Medina P, Huerta-Yepez S. TGF- β : An important mediator of allergic disease and a molecule with dual activity in cancer development. *J Immunol Res.* 2014;2014:318481. doi:10.1155/2014/318481
16. Yang K, Palm J, König J, et al. Matrix-metallo-proteinases and their tissue inhibitors in radiation-induced lung injury. *Int J Radiat Biol.* 2007;83(10):665–676. doi:10.1080/09553000701558977
17. Wang CY, Yang TT, Chen CL, Lin WC, Lin CF. Reactive oxygen species-regulated glycogen synthase kinase-3 β activation contributes to all-trans retinoic acid-induced apoptosis in granulocyte-differentiated HL60 cells. *Biochem Pharmacol.* 2014;88(1):86–94. doi:10.1016/j.bcp.2013.12.021

Review of the latest solutions in the use of contact lenses as controlled release systems for ophthalmic drugs

Przegląd najnowszych rozwiązań w zastosowaniu soczewek kontaktowych jako systemów do kontrolowanego uwalniania leków okulistycznych

Sylwia Stiler-Wyszyńska^{1,A–D}, Sylwia Golba^{1,E,F}, Justyna Jurek-Suliga^{1,E,F}, Sławomir Kuczkowski^{2,E,F}

¹ Faculty of Science and Technology, University of Silesia, Chorzów, Poland

² Department of Ophthalmology, University Center of Ophthalmology and Oncology University Hospital, Medical University of Silesia, Katowice, Poland

A – research concept and design; B – collection and/or assembly of data; C – data analysis and interpretation; D – writing the article; E – critical revision of the article; F – final approval of the article

Polymers in Medicine, ISSN 0370-0747 (print), ISSN 2451-2699 (online)

Polim Med. 2023;53(1):47–58

Address for correspondence

Sylwia Stiler-Wyszyńska
E-mail: sstiler@us.edu.pl

Funding sources

None declared

Conflict of interest

None declared

Received on July 22, 2022

Reviewed on October 26, 2022

Accepted on November 7, 2022

Published online on January 13, 2023

Abstract

In recent years, there has been a great interest in the potential use of contact lenses as eye drug delivery systems. Static (individual layers of the cornea, sclera and retina) as well as dynamic barriers (blood flow) pose a serious challenge to the effective delivery of the drug substance to the eyeball. The current ophthalmic systems are not optimal for patients, especially in the form of eye drops, where almost 95% of the drug contained in them is lost through the process of absorption through the conjunctiva or tear drainage. This article describes in vitro experiments that examined the use of contact lenses in the context of drug treatment in infectious, inflammatory, allergic, and glaucomatous diseases. Various techniques used to modify the materials as well as their impact on drug release kinetics were discussed. It has also been demonstrated that these methods can be used in practice during in vivo research, both in animal models as well as in sick and healthy people. The advantages of using controlled-release drug systems in the form of contact lenses are the drug dosing regimen, bioavailability and the prolonged residence time of drugs in the eyeball.

Key words: biopolymers, contact lenses, α -tocopherol, polymeric materials, ophthalmic drug release

Cite as

Stiler-Wyszyńska S, Golba S, Jurek-Suliga J, Kuczkowski S.
Review of the latest solutions in the use of contact lenses as controlled release systems for ophthalmic drugs.
Polim Med. 2023;53(1):47–58. doi:10.17219/pim/156348

DOI

10.17219/pim/156348

Copyright

Copyright by Author(s)

This is an article distributed under the terms of the Creative Commons Attribution 3.0 Unported (CC BY 3.0) (<https://creativecommons.org/licenses/by/3.0/>)

Streszczenie

W ostatnich latach widoczne jest duże zainteresowanie potencjalnym zastosowaniem soczewek kontaktowych jako systemów dostarczania leków do gałki ocznej. Bariery statyczne (poszczególne warstwy rogówki, twardówki i siatkówki) oraz dynamiczne (przepływ krwi) stanowią poważne wyzwanie dla skutecznego dostarczenia substancji leczniczej do gałki ocznej. Stosowane obecnie systemy okulistyczne nie są optymalne dla pacjentów, zwłaszcza w postaci kropli do oczu, gdzie prawie 95% zawartego w nich leku jest tracone poprzez proces wchłaniania przez spojówkę lub drenaż łzowy. W artykule opisano eksperymenty *in vitro*, w których badano zastosowanie soczewek kontaktowych w kontekście farmakoterapii w chorobach zakaźnych, zapalnych, alergicznych i jaskrowych. Omówiono techniki zastosowane do modyfikacji materiału oraz ich wpływ na kinetykę uwalniania leków. Wykazano również, że metody te mogą być stosowane w praktyce podczas badań *in vivo*, zarówno na modelach zwierzęcych, jak i u osób chorych i zdrowych. Zalety stosowania systemów leków o kontrolowanym uwalnianiu w postaci soczewek kontaktowych to reżim dawkowania leku, biodostępność, a tym samym wydłużony czas przebywania leków w gałce ocznej.

Słowa kluczowe: soczewki kontaktowe, biopolimery, α -tokoferol, materiały polimerowe, uwalnianie leków okulistycznych

Introduction

In recent years, there has been a significant development and interest in contact lenses as an alternative way of delivering pharmaceuticals to the eyeball. Commercially available contact lenses are unmodified and release medicinal substances in an uncontrolled manner. Incorporating surface-bound particles, such as liposomes, nanoparticles or deposited diffusion barriers from vitamin E, influences drug release kinetics. Obtaining customized materials for patients may be possible by incorporating functional monomers capable of specific interaction with drug molecules, which result in decreased diffusion rate and molecular printing, modification of the ionic charge of the material, or creation of poly(lactic-co-glycolic acid) (PLGA) drug reservoirs. It is an ever-evolving field, and scientists are developing new methods for assessing drug release and improving existing ones, which gives great hope for future applications.

Publications cover various aspects of the use of contact lenses as drug carriers, such as controlled drug release systems and their clinical use in eye diseases. Holgado et al. discussed the subject of design requirements of lenses, various strategies for their production, and concentrations of drug required to obtain the appropriate release

of the drug substance.¹ Peral et al. reviewed different techniques of treating glaucoma with the use of lenses with applied drugs.² Franco and De Marco performed a comprehensive review of several methods employing contact lenses as controlled drug release systems.³ Thanks to this approach, it was possible to obtain information on most of the techniques in the context of many diseases.

Contact lenses are an example of a commonly used polymer biomaterial. They are divided into different groups based on several main criteria: material, size, geometrical features, indications, and methods of use (Fig. 1). From the material point of view, the most commonly used soft contact lenses are divided into 2 basic groups: hydrogel (Hy) and silicone hydrogel (Sil-Hy). They differ regarding the chemical structure of the used materials and their properties. Hydrogels, due to the prefix “hydro”, are identified as water gels, but they should be called synthetic material that swells in water or biological fluids. The Hy is spatially cross-linked and consists of hydrophilic natural polymers such as chitosan and sodium alginate, which can absorb large amounts of water while maintaining their three-dimensional structure. In the Hy, the transport medium for the diffusion of substances is water, while the degree of cross-linking of the matrix affects the possibility of their transport through the material.^{4,5} Silicone hydrogel lenses

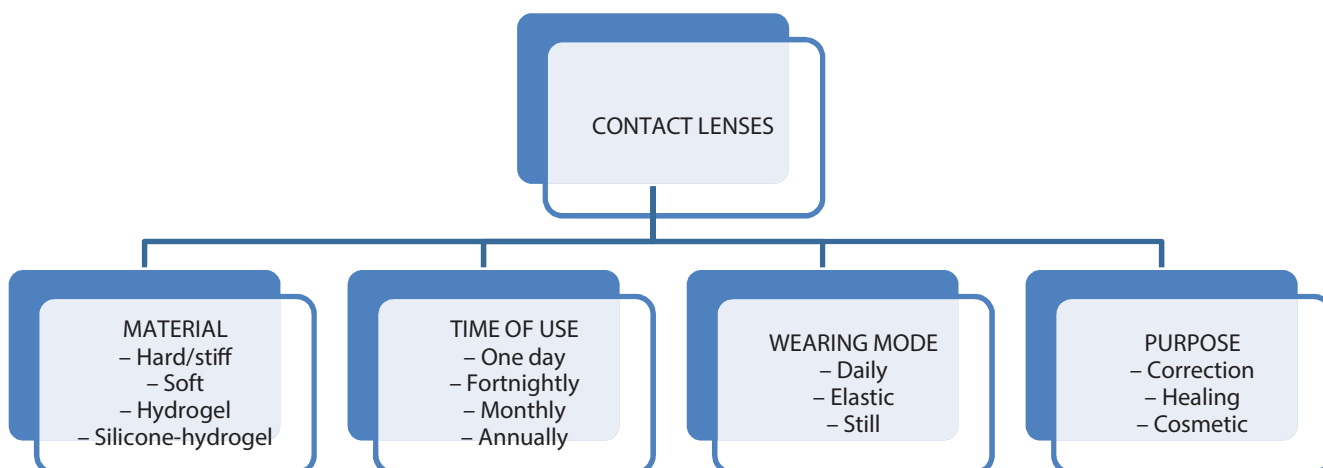


Fig. 1. Division of contact lenses

Table 1. The experimentally determined coefficients of drugs diffusion through the lens material

Drug	CL matrix	D [cm ² /h]	Reference
HPMC	HEMA lenses polymerized with either VP or NIPAAm	PHEMA (100 vol%) 2.48·10 ⁻⁶ (pH = 5.80), PHEMA-VP (20 vol%), 1.68·10 ⁻⁶ (pH = 5.80), PHEMA-NIPAAm (20 vol%), 1.79·10 ⁻⁵	[19]
Epalrestat	silicone hydrogels based on HEMA and bis(hydroxypropyl terminated poly(dimethylsiloxane)) methacryloxypropylmethylsilane hydroxypropyl terminated (MCS-MC12)	(8.57–50.76)·10 ⁻⁶ for non-imprinted hydrogel (5.72–31.72)·10 ⁻⁵ for imprinted hydrogels	[20]
Diclofenac sodium	Etafilcon A (1-Day Acuvue® Moist)	(4.50–8.50)·10 ⁻⁵	[21]
Chlorhexidine levofloxacin	PHEMA/PVP	chlorhexidine 1.80·10 ⁻⁵ , levofloxacin 2.70·10 ⁻⁵	[22]
TM-loaded-loaded ethyl cellulose nanoparticle-laden ring	Methafilcon contact lenses	2.03·10 ⁻⁶	[23]
Flurbiprofen	Hilafilcon B (Soflens)	(0.80–1.56)·10 ⁻⁵ for SFE (0.66–1.24)·10 ⁻⁵ for water extraction	[24]
Ketotifen fumarate	HEMA (92 mol% of the backbone functional monomer) and the balance 3 mol% as combinations of other functional monomers – AA, AM, NVP, PEG200DMA	2.01·10 ⁻⁶ (MIP CL) 1.81·10 ⁻⁵ (nonMIP CL)	[25]
Levofloxacin	Acuvue® Oasys™, 1-Day True Eye	7.5·10 ⁻⁶ (pure), 0.75·10 ⁻⁷ (0.2 vol% of vitamin E)	[26]
Chlorhexidine	Acuvue® Oasys™, 1-Day True Eye	1.3·10 ⁻⁶ (pure), 7.5·10 ⁻⁷ (for 0.1 vol% of vitamin E)	
Levofloxacin	Acuvue® Oasys™, 1-Day True Eye™	1.0·10 ⁻⁶ (pure), 7.5·10 ⁻⁷ (for 0.2 vol% of vitamin E)	
Chlorhexidine	Acuvue® Oasys™, 1-Day True Eye™	5.0·10 ⁻⁷ (pure), 2.0·10 ⁻⁷ (for 0.1 vol% of vitamin E)	
Cysteamine	Acuvue® Oasys™, 1-Day True Eye™ (with 10.22% VE; 22.24% VE) Acuvue® Oasys™ (with 19.14% VE)	5.04·10 ⁻⁵ 1.04·10 ⁻⁵ 6.96·10 ⁻⁶	[27]

VE – vitamin E; MIP CL – molecular imprinting-chemiluminescence; HPMC – hydroxypropyl methylcellulose; TM – timolol maleate; HEMA – 2-hydroxyethyl methacrylate; VP – vinylpyrrolidone; NIPAAm – N-isopropylacrylamide; PHEMA – poly(2-hydroxyethyl methacrylate); PVP – poly(vinylpyrrolidone); AA – acrylic acid; AM – acrylamide; NVP – N-vinyl 2-pyrrolidone; PEG200DMA – poly(ethylene glycol 200 dimethacrylate); SFE – supercritical fluid extraction.

are different from the other groups of materials used to make contact lenses. Combining hydrophobic monomers based on silane units with hydrophilic monomers, such as 2-hydroxyethyl methacrylate (HEMA), was a challenge for researchers due to the phase separation of the individual components and the disturbance of optical focusing, which resulted in blurry vision. Various synthetic methods have been developed, leading to 3 generations of Sil-Hy contact lenses. In generation I, the first approved Sil-Hy materials for contact lenses were lotrafilcon A and balafilcon A, which used phase separation to completely separate the hydrophilic and silicone phases. Lotrafilcon A, belonging to the US Food and Drug Administration (FDA) group, is a mixture of fluoroether macromer and tris hydroxymethyl aminomethane (TRIS), which forms a low-hydrated and non-ionic material with a Dk (oxygen permeability through the lens) coefficient 140. Balafilcon A is the only FDA group III Sil-Hy lens. The material of this lens is manufactured primarily with the use of technologies based on modified TRIS structures. It is a hydrated ionic lens with a Dk of 99. Lenses from generation II consisted of a combination of hydrophilic monomers and made use of macromeric technologies. These materials, galyfilcon

A and senofilcon A, combine various monomers and macromers with an internal wetting agent (polyvinylpyrrolidone (PVP)). Galyfilcon A has a Dk of 60, while senofilcon A has a Dk of 103. In generation III, the newest filcon 3 material was created, which was not based on TRIS or PVP, and the only source of silicon were the macromers. This lens has a Dk of 128, which is higher than that of similar lenses (Table 1).⁶

Witcherle and Lim (German patent DE1084920B) first proposed the use of soft contact lenses as drug delivery systems to the eyes, and taking into account the 1960s patent for Hys applied to the eyeball as contact lenses.⁷ Currently, the European patent databases contain 1052 patents for contact lenses and 1073 patents for drug release systems. The interest in using drug release systems with contact lenses grew along with the development of the field of biomaterials and bioengineering.⁷ Such interest is fully justified, as contact lenses are probably the most popular commercially used biomaterial. This is evidenced by high biocompatibility of contact lenses, as well as willingness to use them among patients.^{8,9} The goals of drug therapy to achieve therapeutic drug levels are also clear.¹⁰ Eye drops and ointments, which are the most commonly

used forms of eye treatment today, do not provide patients with the necessary pharmacological limit. They are limited by their bioavailability and the number of active ingredients reaching the site of action, which results from the corneal absorption barrier, as well as unproductive absorption by the conjunctiva and dilution of the preparation with tears.¹¹ The challenge for researchers is the compatibility of the lens material with the drug, especially in the treatment of chronic diseases such as glaucoma. It is estimated that the treatment of glaucoma with eye drops is effective in only 50% of patients. This effectiveness decreases with the frequency of using the drops and the duration of their application.¹² Proper lens design can provide effective dosing over the expected lifetime, which will eliminate frequent drug dosing and carrier replacement. Many methods of determining and modifying characteristics of drug release from contact lenses have been investigated.¹³ This paper will review the methods used to properly modify the lens for the controlled release of drugs, as well as the possibility of their use in the delivery of drugs to the eye in diseases such as eye infection and inflammation, allergy, and glaucoma.

Commercial contact lenses as drug delivery matrices

The use of commercially available, unmodified contact lenses for testing gives the opportunity to obtain results for a material with a specific chemical composition. The test follows immediately after their application to the simulated eyeball and allows one to assess their surface during the simulation of the local treatment in a patient. An additional advantage of these lenses is that their use

to model the possibilities and kinetics of drug release allows for consistent results due to their large-scale availability and repeatability of the tested product. The factors affecting the release of drugs in many studies conducted on commercially available contact lenses, which use various medicinal products such as dexamethasone³ or ciprofloxacin,¹⁴ are the material of the skeleton of the lens (the relationship between Hy and silicone), the equilibrium water content in the lens, and the contact surface with the eyeball. The topic of commercially available contact lenses as systems for the controlled release of ophthalmic drugs has been discussed in recent years. Search in the Scopus database for the phrase “contact lenses” AND “drug delivery” resulted in 642 documents in the period from 1971 to 2020, with intense growth in the number of works since 2003. At the same time, search in the Science Direct database for the same joined phrase resulted in 11,608 documents released until 2020 (Fig. 2). Contact materials can absorb and release a significant amount of drug substance in a direct soaking process, but the release kinetics are fast and uncontrolled, and therefore, unsuitable for a long-term drug delivery.^{3,12,13,15}

Modifications of commercially available contact lenses: diffusion barriers using vitamin E

Taking into account the aforementioned pharmacokinetic limitations of commercial contact lenses, attempts have been made to modify these materials in order to obtain the desired properties – in particular to decrease the drug release rate.¹⁶ It is assumed that the drug release

Documents by year

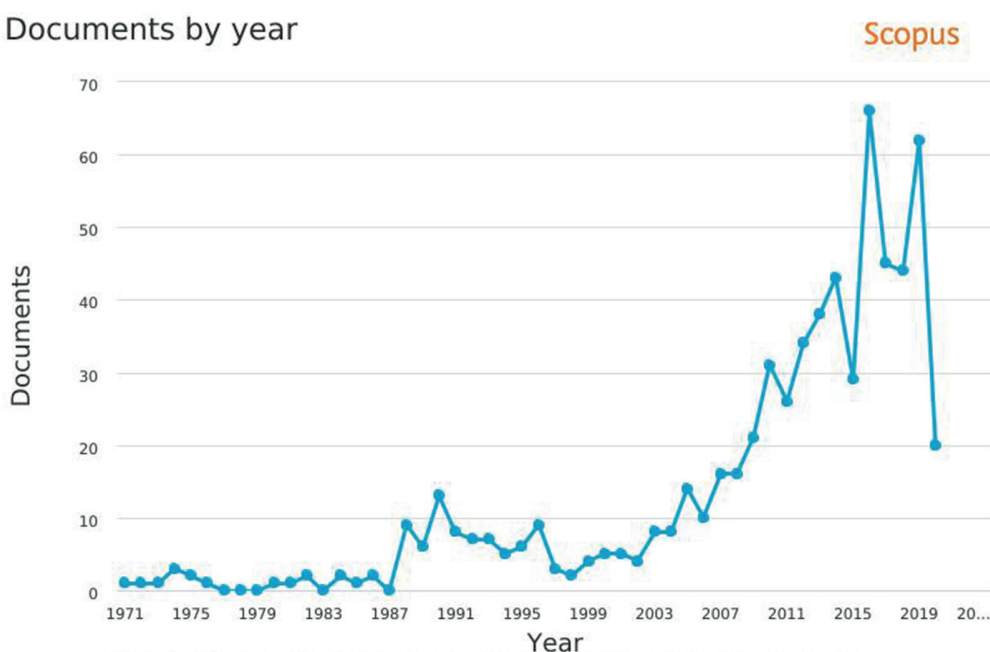


Fig. 2. Number of the documents found in the Scopus database for the conjugated “contact lenses” AND “drug delivery” phrase

from the lens is a diffusion-controlled process. According to Fick's laws (Equation 1,2), the speed is influenced by both the ability of a given drug to diffuse through the material and the length of the path that must be followed. Diffusivity is a constant value, especially when bonding a lens to a drug, therefore the change in drug release time can be modified by increasing the thickness of the material.¹⁷

$$j = -D \frac{\delta c}{\delta x} \quad (1)$$

$$\frac{\delta c}{\delta t} = \frac{\delta}{\delta x} \left(D \frac{\delta c}{\delta x} \right) \quad (2)$$

where:

j – flux of the diffusing component in the x direction [$\text{g}/\text{cm}^2 \cdot \text{s}$], c – concentration of the component in the flow plane [g/cm^3], $\delta c/\delta x$ – concentration gradient of the diffusing component perpendicular to the flow plane, and D – diffusion coefficient [cm^2/s].

Fick's law (Equation 1) describes the relationship between the flow of the diffusing substance (i.e., the amount of flowing substance in a unit of time through a unitary surface perpendicular to this stream) and the concentration gradient. Fick's second law (Equation 2) describes the relationship between the local rate of change in the concentration of the diffusing substance and its concentration gradient. The experimentally determined coefficients of drug diffusion through the lens layer are presented in Table 1.

One way to reduce the rate of drug release is to use a hydrophobic liquid that was incorporated as a component of the contact lenses. One of them is α -tocopherol (α -TOC – vitamin E), which has a low water solubility and is biocompatible with the eye surface.¹⁸ The α -TOC (Fig. 3) has antioxidant properties, and exerts a positive effect on the eyeball by ensuring the tightness of its cell membranes and the inhibition of cataract development.¹⁹ Placing contact lenses in the α -TOC solution after the sorption

of the drug leads to the formation of a hydrophobic diffusion barrier on them. This allows for a stable release of the therapeutic dose for a longer time than in the case of traditional dipping.²⁰ The usage of α -TOC causes a slight decrease in oxygen absorption but to an acceptable level that does not affect the wettability of the lens surface. Moreover, the use of lenses with a hydrophobic diffusion barrier facilitates the treatment of bacterial keratitis.²¹

Both Sil-Hys and pure Hys are commercially available in the form of contact lenses. Attempts have been made to modify them by creating a vitamin diffusion barrier on their surface.²² This led to a significant extension of the drug release time, from several hours for unmodified lenses to several weeks after modification. With the appropriate drug–lens combination, a Sil-Hy lens release time of 3 h was achieved due to drug release time of 10 min for unmodified lenses.²³ Barrier formation was achieved by soaking the lenses in a vitamin E solution with ethanol; the composition of the barrier may vary depending on the desired amount of vitamin E in the final product. The advantage of this method is the biocompatibility of both components, acceptable optical properties after modification, and a certain degree of protection against ultraviolet radiation provided by the coating obtained. However, the durability of vitamin barriers and the long-term use of such lenses is unknown. Thus, there is no information as to whether the function of such a barrier is preserved or destroyed during the cleaning of long-term lenses.^{24,25}

In patients with bacterial and fungal keratitis, the standard treatment consists of administering antibiotics to the conjunctival sac. The frequency of administration (every 30–60 min) is very bothersome. Paradiso et al. combined an in vitro experiment with a mathematical model to develop soft contact lenses for treating keratitis through a prolonged release of appropriate drugs. The focus was on extending the release time of levofloxacin (LVF) and chlorhexidine from 1-Day Acuvue® TrueEye™ and Acuvue® Oasys™ lenses by introducing a vitamin E diffusion barrier. The weight of drugs loaded into the lenses can be controlled to achieve comparable daily release with commonly recommended eye drop therapy. Vitamin E lenses have retained all key properties for in vivo use. Paradiso et al. soaked Sil-Hy lenses in a solution of vitamin E dissolved in ethanol (42 mg/mL) for 3 h. They obtained 32 h of the release of the antibiotic LVF in lenses without vitamin E content, which was extended to 100 h after storage of the lenses in α -TOC solution. This effect has been attributed to the presence of vitamin E nanoaggregates formed in the lenses that have a barrier effect on the release of the drug. The injection of vitamin E into commercial silicone contact lenses did not cause changes in transparency, wettability and ion permeability.²⁶

Hsu et al. developed contact lenses for sustained simultaneous release of timolol and dorzolamide. Co-administration of timolol and dorzolamide increased the release time of both drugs. In addition, the process of releasing

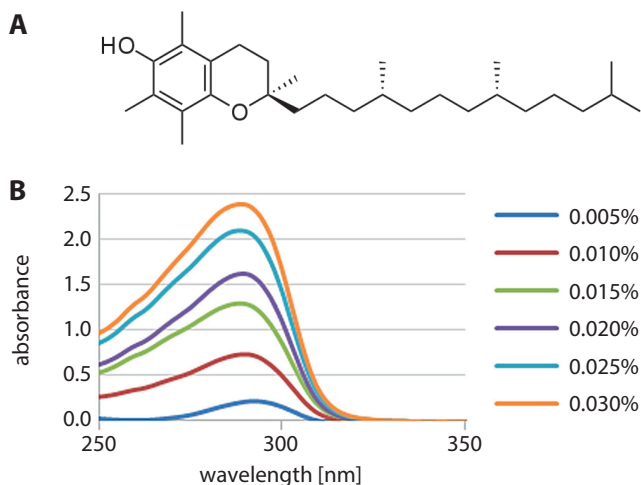


Fig. 3. A. Structural formula of α -tocopherol (own study); B. UV-VIS spectra of α -tocopherol in ethanol depending on concentration (own study)

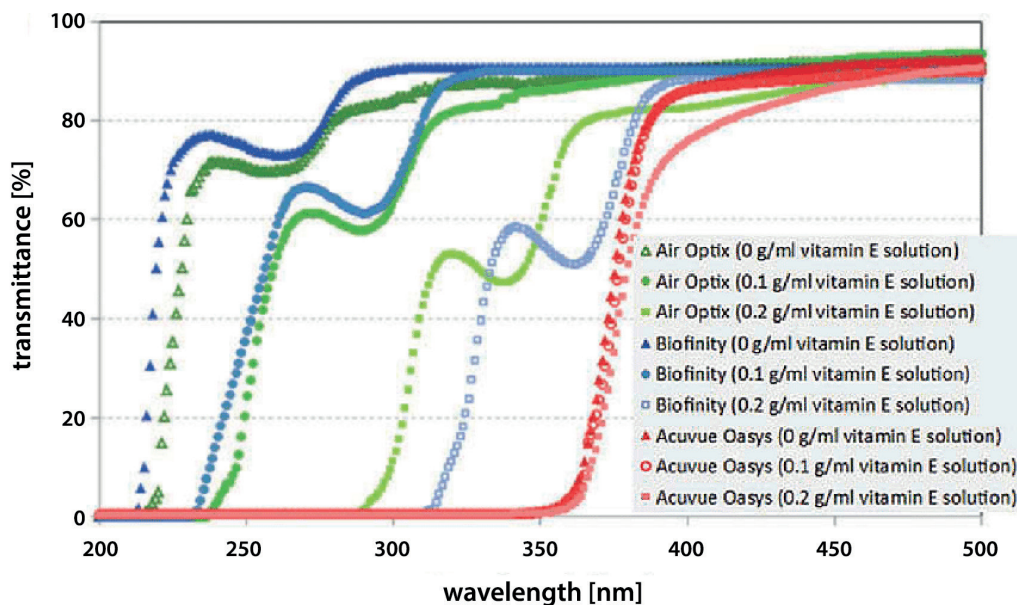


Fig. 4. UV-VIS transmittance spectrum for set of contact lenses (CL) before and after vitamin E loading (0.1 g/mL or 0.2 g/mL vitamin E soaking solutions)³⁰

both drugs was extended to about 2 days due to the formation of a diffusion barrier from vitamin E. This procedure is very effective in providing a combination therapy involving the combination of drugs with vitamin E.²⁷

Another group synthesized contact materials by following the production procedures of one of the companies. The resulting Hys were dried at room temperature. The finished material was immersed in 1.5 mL of the vitamin and ethanol solution for 24 h, while the vitamin concentration was maintained in a range of 0.00–0.28 M. After conditioning, the lenses were washed with ethanol and deionized water to remove excess vitamin from their surface. For sorption of the drug with the vitamin inside the lenses, they were immersed for 24 h in 1.5 mL of a solution that contained 0.5 mg of the drug, ethanol and vitamin. Timolol and brimonidine release tests from contact lenses without a diffusion barrier and with a barrier were performed. The concentration was monitored by measuring absorbance at the wavelength of absorption characteristic for the respective drug ($\lambda^{\max} = 294$ nm for timolol, $\lambda^{\max} = 249$ nm for brimonidine). Contact lenses loaded with vitamin E significantly increased the total amount of released timolol and brimonidine by 19.1% and 18.7%, respectively, compared to the lens without a barrier. These results also suggest that the simultaneous use of vitamin E increases the number of absorbed drugs.²⁸

The results presented by Cheng Chun et al. clearly show that the use of vitamin E in commercial silicone lenses can significantly increase the release time of hydrophilic drugs without affecting the transparency of the matrix. At the same time, a significant reduction in ionic permeability (50%) and a slight reduction in oxygen permeability (45%) were noted, but these reductions were not sufficient to exclude the use of vitamin E in commercial lenses. The mechanism of prolonging the release time of the drug

is due to the barrier effect of vitamin E. It is reasonably assumed that the effect is caused by the presence of vitamin E molecules; however, it is also possible that vitamin E does not form macroscopic aggregates and is simply adsorbed on a polymer gel. Surface adsorption may impede the surface diffusion of the drug over the lens surface, leading to a reduction in diffusion rate. Differences between the effects of vitamin E on ion transport and oxygen suggest that vitamin E aggregates can only form in the hydrophilic Sil-Hy lens channels.²⁹

The work of Rad and Mohajeri showed the capability of modified contact lenses to prevent ultraviolet (UV) radiation exposure. Soaking the lenses in vitamin E solution (0.1 g/mL or 0.2 g/mL) shifted UV transmission edge of the spectra to the longer wavelengths in corresponding contact lenses Air Optix and Biofinity (Fig. 4). It was shown that UV radiation could be blocked by using such a barrier on the surface of the lenses. Moreover, the data proved that vitamin E loading did not influence the visible light transmittance (400–700 nm) in the studied series, hence the transparency of lenses was still acceptable.³⁰

Drug delivery using novel techniques: molecular printing

Molecular printing is one of the most widely studied methods in which lens materials are designed specifically for the sustained and controlled release of drugs into the eyeball.³¹ This method is a type of forced ordering on the surface of a polymer that generates areas complementary to the shape and functional groups of the molecule that is to be originally absorbed (acting as a template) and then released from the matrix. This is achieved by incorporating functional monomers into the matrix

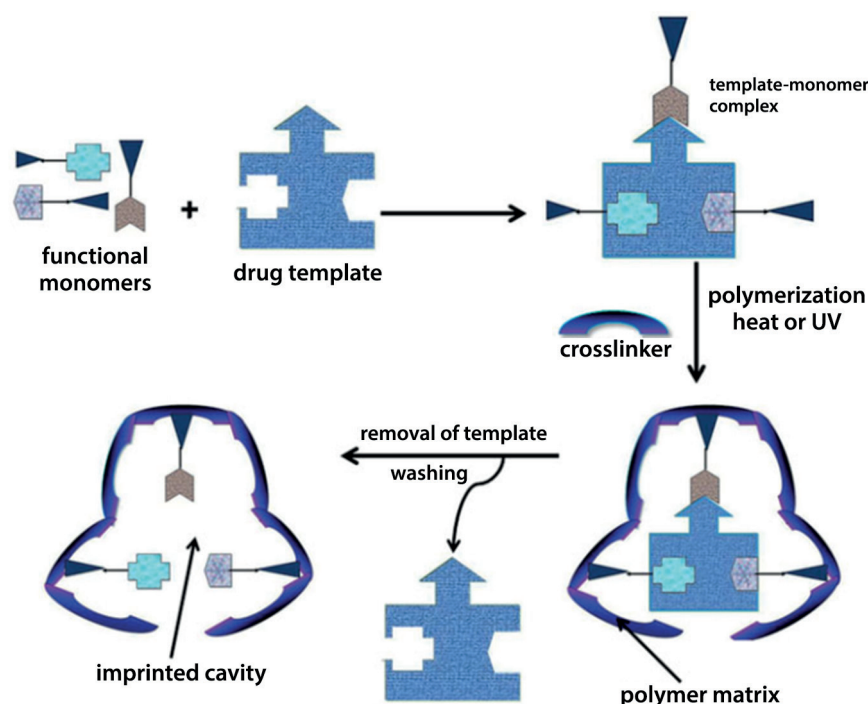


Fig. 5. Schematic representation of the molecular printing process³⁵

UV – ultraviolet.

that are designed to interact with standard molecules, usually drugs.³² After the polymerization process, the areas designed for interaction form a kind of molecular scale template that allows the diffusion to be significantly slowed down.³³ By conducting numerous experiments on the release of the drug substance, it was possible to determine the duration of release, as well as synthetic parameters such as drug concentration or type of polymeric crosslinker.³⁴ This technique has evolved thanks to the knowledge about interactions occurring between human receptors and individual drugs. Such knowledge became the basis for designing the structure of monomers, which allowed the creation of polymer matrices imitating natural receptors with whom the drug interacts in the patient's body. There is a limit on the amount of substance that can be printed if the polymer is to still function as a contact lens.³⁵

In their review article, Tashakori-Sabzevar and Mohajeri described soft contact lenses with molecular printing (Fig. 5), which is shown to be a comprehensive and effective method of optimizing drug release. Such systems show unprecedented control over prolonged loading and release of the drug. In recent years, only a few *in vivo* studies have been published on the release of the drug into the eye from printed lenses. Soft contact lenses are comfortable and biocompatible. However, the ability to print the drug in a conventional lens is quite low, and therefore, the therapeutic concentration is difficult to achieve.³⁵

In studies conducted by Tieppo et al., the Hy with molecular printing was prepared as an innovative method of drug administration. The concentration profile of the drug-printed lens was compared with unprinted matrices and conventional eye drops in the eyes of New Zealand white

rabbits. The results indicated a sustained release of keto-tifen fumarate from printed lenses, a constant concentration of 170 $\mu\text{g}/\text{mL}$ in tear fluid, and significantly higher bioavailability for 26 h. Maximum drug concentrations with molecularly imprinted polymer (MIP), non-imprinted polymer (NIP) and eye drops for tear fluid were 214 $\mu\text{g}/\text{mL}$, 140 $\mu\text{g}/\text{mL}$ and 143 $\mu\text{g}/\text{mL}$, respectively. The maximum concentration times were 240 min, 60 min and 0 min for MIP, NIP and eye drops. In addition, the ability of MIP lenses to accumulate drugs was almost 3 times higher than in NIP. The future of contact lens printing is very promising and requires further clinical and preclinical research. Further advances in polymer engineering and the design of intelligent binding sites in Hys can lead to remarkable advances in the preparation of new drug delivery systems for the eye.³⁶

Dry eye syndrome is caused by a disruption in the tear film, which leads to abnormal hydration of the eye. This may be due to its incorrect composition or excessive evaporation, which results in the drying out of cornea and conjunctiva.³⁷ Soft contact lenses can relieve the symptoms of dry eye by slowly releasing the agent that keeps the eyeball moist. Sil-Hy lenses with sustained, controlled release of hydroxypropyl methylcellulose using a molecular printing strategy were manufactured. The commercial Sil-Hy lens was adapted to release approx. 1000 μg of the drug for up to 60 days continuously at a rate of 16 $\mu\text{g}/\text{day}$ at physiological flows, releasing an equal portion of the drug throughout the use of the matrix. Release rates can be significantly affected by the print effect and the functional weight ratio of the monomer to the template (M/T). The M/T values of 0, 0.2, 2.8, and 3.4 correspond

to the release times of 10, 13, 23, and 53 days, respectively. The Sil-Hy lenses had high optical quality and adequate mechanical properties for patient use. This work highlights the potential of printing in the design and engineering of Sil-Hy lenses to release macromolecules during wear, which can reduce the symptoms of dry eye.³⁸

The goal of the next work was to develop an innovative, supercritical fluid-assisted molecular printing method to give commercial soft contact lenses the ability to absorb specific drugs and control their release. This approach aims to overcome the limitation of the widespread use of pre-formed soft contact lenses by the following: immersion in concentrated drug solutions (only possible for drugs with high water solubility), the use of molecular printing methods that require drug selection before polymerization, and the introduction of a drug adapted to the network. Supercritical carbon dioxide (scCO₂) impregnation tests were performed at 12.0 MPa and 40°C, while scCO₂ extractions were carried out at 20.0 MPa and 40°C. For comparative purposes, conventional experiments of flurbiprofen sorption and drug removal in aqueous solutions were carried out. Soft contact lenses processed with supercritical fluid showed recognition ability and greater affinity for flurbiprofen in an aqueous solution than for structurally related ibuprofen and dexamethasone, suggesting that the formation of a molecular impressed cavities arising through both physical (swelling/plasticizing) and chemical (carbonyl groups in the network with the substituent C-F in medicine) interactions. Processing with scCO₂ resulted in no changes in some of the critical functional properties of soft contact lenses (glass transition temperature, transmittance, oxygen permeability, contact angle), enabled the control of the amount of loaded/released drug molecules (by using several successive processing cycles), and allowed the preparation of hydrophobic therapeutic drug-based soft contact lenses in a much shorter process time than using conventional aqueous molecular printing methods.³⁹

In the another study, a series of Sil-Hy with MIP and NIP was prepared using HEMA as a skeletal monomer, ethylene glycol dimethacrylate (EGDMA) as a crosslinking monomer, methacrylic acid (MAA) as a functional monomer, and dorzolamide (DZD) as a standard molecule. Two molar ratios of DZD:MAA (1:8 and 1:4) and 400 mM MAA were also used in the printing process. The Hys (0.4 mm thick) were synthesized by thermal polymerization at 50°C for 24 h in a polypropylene form. Then, the swelling and binding properties of Hys in water were evaluated. Their sorption and release properties were also tested in 0.9% NaCl and artificial tear fluid. The results showed that the use of MAA as a comonomer and the use of molecular printing techniques increased the capacity of Hys. The optimized printed Hy (MIP1:4), prepared with 400 mM MAA and having a molar ratio of DZD:MAA 1:4, had the highest affinity for DZD and the greatest ability to control the release process in an aqueous environment.⁴⁰

Delivery of drugs from materials prepared in PLGA technology

Lactic and glycolic acid copolymers (PLGA) are one of the most widely studied materials used to deliver drugs to the human body. They are characterized by good biocompatibility and biodegradability, and have been approved by the FDA. These polymers are tested not only for applications in the eyeball but also as tissue scaffolds and implants throughout the body.⁴¹ They exhibit high mechanical strength and release rate, which can be controlled by the relative ratio of lactic acid to glycolic acid in the final material.⁴² The incorporation of several ophthalmic medications in a PLGA matrix on the contact lenses allows the simultaneous delivery of several substances to the patient's eyeball. In vivo research suggests that this solution may maintain controlled drug release effects for up to a month and longer. However, the use of PLGA technology has disadvantages: even the very thin layers of the components interfere with the translucency of the lens and, in consequence, it does not transmit visible light as effectively as a commercial Hy lens. In addition, an adverse effect is an increase in the total thickness of the lens.^{43–46}

Ciolino et al. coated PLGA films with the poly(2-hydroxyethyl methacrylate) (HEMA) through UV polymerization. The HEMA and EGDMA crosslinkers were used as monomers. The solution was photopolymerized to form the bottom layer of a composite contact lens constructed using PHEMA. The PLGA film with a model drug (fluorescein) was manually pressed on a dried PHEMA gel. The drug placed between layers of PHEMA without PLGA film caused a slower release than that of the drug on the PLGA film but faster than that of the drug on the PLGA film coated with PHEMA.⁴⁷

Subsequent studies investigated experimental parameters such as the composition of polymer mixtures, the type of stabilizer and the amount of active pharmaceutical ingredient in the production of polymer drug delivery systems for topical administration of prednisolone to the eye. To achieve this goal, PLGA nanoparticles with prednisolone were prepared by solvent evaporation. Prednisolone was quantified using a validated high-performance liquid chromatography (HPLC) method. The amount of PLGA copolymer had the greatest impact on the size of the nanoparticles, while the amount of used prednisolone had the greatest impact on the drug loading. Longer homogenization time with more prednisolone resulted in the smallest size nanoparticles. The produced nanoparticles had an average particle size of 347.1 ± 11.9 nm with a polydispersity index of 0.081. The nanoparticles were then introduced into the solution before polymerization. Bright and transparent matrices with high drug encapsulation efficiency (EE) in a range between 60% and 92% were successfully prepared. When nanoparticles (NP) with contact materials were compared with control contact lenses

(NP-unloaded), there was a 2% decrease in hydration and an 8% decrease in light transmission. The contact lens wettability remained within the desired range of values (<90°C) even after the introduction of NP. Both NP and NP-unloaded lenses showed a slow release of the drug in vitro over 24 h.⁴⁸

Supply of medicines from charged materials

Many ophthalmic drugs have an ionic charge that can be used to increase absorption and release. The FDA classification of contact lenses is based on the presence or absence of surface charge. This helped predict the deposition of tear components and the antiseptic characteristics of these materials when used with different cleaning solutions.⁴⁹ The surface charge of these materials also had an impact on the uptake and release of pharmaceutical products.^{50,51} The number of anionic molecules such as methyl methacrylate (MMA) was increased to improve the sorption properties of these materials, which allowed a change in charge and increased attraction of charged drug molecules.⁵² However, there are concerns about the surface charge of these molecules as this may increase the tendency for deposition of tear film components (such as proteins) on the lens surface, especially concerning long-term ones.⁵³

Christopher and Chauhan tested the effect of placing electrodes on contact lenses to obtain an electric field gradient for transporting ionic drugs to the cornea. Commercial lenses, loaded with Nile blue and fluorescein as hydrophobic and hydrophilic drug analogs, respectively, were placed on eyeballs of rabbits. The electric field gradient was generated by placing the cathode and anode on the lens diametrically opposite each other. Electric power showed an increase in uptake of Nile blue, and quantity was a function of duration and current intensity. Similar increases in flow were observed for fluorescein. Images recorded with confocal microscopy also showed an increase in dye penetration in the presence of current. Connecting electrical current to the lens can be a minimally invasive and effective approach to obtaining a therapeutic dose of the drug delivered. The results of *ex vivo* experiments suggest that a contact lens containing both cathode and anode may be useful for delivering drugs to the eye using iontophoresis techniques. Since the distribution of the electric field can be accurately predicted, it is possible to obtain a smaller, easy-to-use device, which may result in higher bioavailability and allow for predicting the delivered dose of the drug. In addition, a compact device would be much more convenient for patients than other devices due to the smaller and more localized electric field, and could be worn like a normal contact lens without seriously obstructing the field of view.⁵⁴

Takamatsu et al. proposed a powering system for an electrical contact lens that is capable of iontophoretically delivering drugs to the eye.⁵⁵ A hybrid power generation device is comprised of a wireless power transfer system and a bioabsorbable metal–air primary battery. No hydrogen evolution or pH change was observed in the tear electrolyte, hence it was proposed that the shown power source could power wearable electronics in body fluids.⁵⁶

Zhu et al. presented a new lens embedded in the inner layer of the matrix, which was capable of pH-triggered prolonged drug delivery to the eye with good storage stability. Eudragit S100 and ethyl cellulose film were used as the inner layer, while PHEMA Hy was used as the outer layer. Using diclofenac sodium as a model drug, the obtained matrices were examined and optimized in terms of the ratio of polymer in film, viscosity, the ratio of drug to polymer, the thickness of the inner layer, and the thickness of the PHEMA layer. Drug release was triggered by a change in ambient pH which allowed the storage of the contact lens to embed in the inner layer in a phosphate-buffered solution (PBS) at pH 6.8 with an imperceptible loss of drug and slight changes to the drug release pattern. An *in vivo* pharmacokinetic study in rabbits showed a sustained release of the drug for more than 24 h in the tear fluid, indicating a significant improvement in residence time in the cornea. Correlation between *in vivo* and *in vitro* studies (IVIVC) was established between *in vitro* drug release and *in vivo* drug concentration in tear fluid. In summary, this design of the embedded contact lens within the inner layer can be used as a platform for sustained delivery of drugs to the eye with translational potential in the treatment of ocular diseases.⁵⁷

Faccia et al. used pH-sensitive copolymers containing HEMA with different proportions of 2-(diisopropylamino) ethyl methacrylate (DPA) and different amounts of the crosslinker (i.e., EGDMA). These were rated as pH-sensitive drug delivery systems for potential use in ophthalmic therapies. The characterization of the pH response was carried out using swelling studies and scanning electron microscopy (SEM) analysis. Drug loading and release at different pHs were evaluated using Rhodamine 6G (Rh6G) as a model drug. The obtained results showed that the presence of DPA in copolymers confers pH sensitivity properties.⁵⁸

Contact lenses releasing medicinal substances can be very effective carriers for the delivery of ophthalmic drugs, but usually they are not able to release the drug for more than a few hours. Bengani and Chauhan optimized the interaction of the polymer matrix of the contact lens with hydrophobic fragments of ionic surfactants to adsorb surfactant molecules on a highly packed polymer, and thus created a high surface charge. The ionic drugs then adsorbed onto charged surfaces coated with surfactants with high affinity to reduce the transport speed, which led to a sustained release. In particular, they showed the controlled release of the anionic drug dexamethasone 21-disodium phosphate

from PHEMA contact lenses using the cationic surfactant – cetalkonium chloride (CAC). The drug partition coefficient increases exponentially with the gel surfactant charge according to the Debye–Hückel theory.⁵⁹ In the studied case, the drug was adsorbed on a surfactant-coated polymer and could also diffuse along the surface with a lower diffusivity than that of a free drug. This led to a reduction in effective diffusivity, which was a weighted combination of free and surface diffusion. The addition of the surfactant did not affect the transparency of the lenses, and it had the additional advantages of increasing wettability and significantly reducing protein absorption. A 10% addition of CAC provided a significant reduction in protein uptake for lysozyme serving as the model protein in the *in vitro* studies of protein interactions with Hys. At approx. 10% surfactant exposure, the release time was increased from approx. 2 h to 50 h in 1-day Acuvue® contact lenses.⁶⁰

Odrobinska and Neugebauer synthesized amphiphilic copolymers containing HEMA and MMA by controlled radical transfer polymerization (ATRP) using bromoester modified retinol (RETBr) as a new initiator. An analogous series of copolymers with regulated hydrophilic–hydrophobic balance was obtained using a standard initiator, i.e., ethyl α -bromoisobutyrate (EBriB). The hydrophilic/hydrophobic ratio in the copolymer has been indicated as a key factor regulating the efficiency of encapsulation processes calculated at a range of 5–98%. Polymer systems with satisfactory encapsulation properties were obtained. The release profiles indicated that they are attractive micellar carriers of antioxidants. Due to their activity, they can be used in popular approaches in cosmetology, such as masks, eye patches or compresses.⁶¹

Supply of drugs for patients suffering from diabetes

Most treatments for diabetes-related eye diseases are systemic (oral) or intravitreal. The goal of Alvarez-Rivera et al. was to design contact lenses suitable for the local prevention/treatment of diabetes-related eye pathologies. The main idea was to incorporate the functional groups into the polymer matrix that can reversibly interact with epalrestat, an aldose reductase inhibitor. Several sets of Sil-Hy were synthesized and the content of chemicals such as HEMA, monomethacryloxypropyl-sym-polydimethylsiloxane hydroxypropyl terminated (MCS-MC12) and aminopropyl methacrylamide (APMA) has been changed. Epalrestat was included before or after polymerization, and the load and release profiles were compared. All samples were evaluated in terms of optical properties, oxygen permeability, swelling, cytological compatibility, eye irritation, and corneal penetration (using drug solution as reference). At the 1st release stage, efficacy strongly depended on the APMA content, which allowed for the prolonged release of the drug in 0.9% NaCl for 1 week, both after

synthesis and after loading. Epalrestat-laden Hys also showed anti-cataract activity in an *in vitro* diabetic eye model. In general, biologically inspired Sil-Hy contact lenses are the first attempt at designing contact lenses adapted to the needs of diabetic eyes. These act as platforms for the controlled release of epalrestat, promote drug accumulation in the eyeball and stimulate corneal diffusion.⁶²

Methods for contact lenses modification through the use of lipid layers

The use of deposited layers of liposomes or nanoparticles with the absorbed drug affects the delayed release of drugs from contact lenses. The drug is then released from the liposomes or nanoparticles as a result of the interaction with the tear film. The special feature of this method is that the release of drugs from the deeper layers of the lens goes through the previously used layers. In this way, drug release from these materials usually occurs in several phases with different release kinetics: the initial rapid release phase and the stable, slower diffusion of the drug from the inner layers.^{63,64}

Wang et al. assessed the effect of a 2-week regular application of phospholipid liposomal spray on the thickness of the lipid layer, tear film stability, subjective wearing comfort, visual acuity, and lipid deposition in those wearing Sil-Hy lenses. The phospholipid liposomal spray was applied to the lens of 1 eyeball. On the 14th day of the study, the thickness of the lipid layer and the stability of the tear film increased in the eyes of the treated patients. A larger percentage of participants reported an improvement in sight comfort in the treated eye.⁶⁵

Danion et al. used *in vitro* antibacterial evaluation methods for contact lenses containing LVF-laden liposomes, which were designed to prevent and treat bacterial eye infections such as keratitis. The LVF was incorporated into the liposomes before immobilizing intact liposomes on the surface of soft contact lenses using a multilayer immobilization strategy. The release of LVF from contact lenses containing 2, 5 and 10 layers of liposomes into a saline buffer at 37°C was monitored through measuring fluorescence. The release profile of LVF has been described as a mechanism involving 2 independent first-order kinetic models. The total release of LVF from contact lenses was completed within 6 days. The release of LVF from contact lenses containing 10 layers of liposomes and then soaked overnight in LVF solution was also studied and compared with the reference sample. It consisted of pristine contact lenses with no chemical modification that were previously dried and subsequently hydrated in a drug solution. The antimicrobial activity of the liposome-coated contact lenses was assessed by measuring the diameter of the agar

zone on the agar plate and optical density (OD). Liposome-coated lenses showed antibacterial activity on both the agar and the OD test after 24 h. When the initial bacterial inoculum was equal to or lower than 10^6 CFU/mL, all bacteria were inhibited within 2 h. When using an initial bacterial inoculum of 10^8 CFU/mL, the initial release provided by immersion of liposomal lenses was required for the first hours to inhibit bacterial growth.⁶⁶


Another research group immobilized multilayer liposomes on soft contact lenses. The liposome skeleton was prepared by exposing NeutrAvidin™-coated contact lenses to liposome aggregates produced by the addition of free biotin to the solution. The X-ray photoelectron spectroscopy (XPS) confirmed immobilization of liposomes, while enzyme-linked immunosorbent assay (ELISA) test showed that neutravidin docking was dependent on biotin-neutravidin affinity binding. The kinetics of fluorescent dye release showed that intact liposomes were immobilized on contact lens surfaces. The stability of the surface-immobilized liposomes on contact lens surfaces was temperature-dependent. Surface-associated liposomes can be stored for up to 1 month at 4°C with little release.⁶⁷

In another work, liposome-based coatings were analyzed to control the release of the drug from soft contact lens materials. A LVF-loaded PHEMA Hy material was used as a model system for these studies. The coatings consisted of polyelectrolyte layers containing 1,2-dimristoyl-sn-glycerol-3-phosphocholine (DMPC) and DMPC+cholesterol (DMPC+CHOL) liposomes. The effect of friction and temperature on drug release was studied. The purpose of friction tests was to simulate eyelid blinking to investigate whether soft contact lens materials coated with liposomes can retain their properties, in particular the drug release capacity. It was observed that under the test conditions, the friction did not significantly affect the release of the drug from the liposome-coated PHEMA material. In contrast, an increase in the release temperature led to an increase in the diffusion rate of the drug through the Hy. This phenomenon was recorded in both control and coated samples.⁶⁸

ORCID iDs

Sylwia Stiler-Wyszyńska  <https://orcid.org/0000-0001-5814-0688>

Sylwia Golba  <https://orcid.org/0000-0003-4550-0490>

Justyna Jurek-Suliga  <https://orcid.org/0000-0001-7919-9398>

Sławomir Kuczkowski  <https://orcid.org/0000-0003-1705-178X>

References

- Holgado MA, Anguiano-Domínguez A, Martín-Banderas L. Contact lenses as drug-delivery systems: A promising therapeutic tool. *Arch Soc Esp Oftalmol (Engl Ed)*. 2020;95(1):24–33. doi:10.1016/j.oftale.2019.07.007
- Peral A, Martínez-Aguila A, Pastrana C, Huete-Toral F, Carpena-Torres C, Carracedo G. Contact lenses as drug delivery system for glaucoma: A review. *Appl Sci*. 2020;10(15):5151. doi:10.3390/app10155151
- Franco P, De Marco I. Contact lenses as ophthalmic drug delivery systems: A review. *Polymers*. 2021;13(7):1102. doi:10.3390/polym13071102
- Childs A, Li H, Lewittes DM, et al. Fabricating customized hydrogel contact lens. *Sci Rep*. 2016;6(1):34905. doi:10.1038/srep34905
- Richbourg NR, Peppas NA. The swollen polymer network hypothesis: Quantitative models of hydrogel swelling, stiffness, and solute transport. *Prog Polym Sci*. 2020;105:101243. doi:10.1016/j.progpolymsci.2020.101243
- Gasson A, Morris J. *The Contact Lens Manual: A Practical Guide to Fitting*. 4th ed. Edinburgh, UK: Butterworth-Heinemann; 2010. ISBN:978-0-7506-7590-1.
- White CJ, Byrne ME. Molecularly imprinted therapeutic contact lenses. *Expert Opin Drug Deliv*. 2010;7(6):765–780. doi:10.1517/174252410.03770098
- Efron N, Morgan PB, Woods CA, et al. An international survey of daily disposable contact lens prescribing. *Clin Exp Optom*. 2013;96(1):58–64. doi:10.1111/j.1444-0938.2012.00773.x
- Awwad S, Mohamed Ahmed AHA, Sharma G, et al. Principles of pharmacology in the eye: Principles of pharmacology in the eye. *Br J Pharmacol*. 2017;174(23):4205–4223. doi:10.1111/bph.14024
- Farkouh A, Frigo P, Czejka M. Systemic side effects of eye drops: A pharmacokinetic perspective. *Clin Ophthalmol*. 2016;10:2433–2441. doi:10.2147/OPHT.1118409
- Wichterle O, Lim D, inventors. Process for producing shaped articles from three-dimensional hydrophilic polymers. US patent application 29765761961. Registered on March 28, 1961.
- Yadgarov A. In glaucoma management, less is more. *Ophthalmology Advisor*. <https://www.opthalmologyadvisor.com/topics/glaucoma/in-glaucoma-management-less-is-more>. Published April 23, 2021. Accessed August 12, 2020.
- Carvalho IM, Marques CS, Oliveira RS, Coelho PB, Costa PC, Ferreira DC. Sustained drug release by contact lenses for glaucoma treatment: A review. *J Control Release*. 2015;202:76–82. doi:10.1016/j.jconrel.2015.01.023
- Qin G, Zhu Z, Li S, McDermott AM, Cai C. Development of ciprofloxacin-loaded contact lenses using fluorine chemistry. *Biomaterials*. 2017;124:55–64. doi:10.1016/j.biomaterials.2017.01.046
- Soluri A, Hui A, Jones L. Delivery of ketotifen fumarate by commercial contact lens materials. *Optom Vis Sci*. 2012;89(8):1140–1149. doi:10.1097/OPX.0b013e3182639dc8
- Kamaly N, Yameen B, Wu J, Farokhzad OC. Degradable controlled-release polymers and polymeric nanoparticles: Mechanisms of controlling drug release. *Chem Rev*. 2016;116(4):2602–2663. doi:10.1021/acs.chemrev.5b00346
- Rykowska I, Nowak I, Nowak R. Soft contact lenses as drug delivery systems: A review. *Molecules*. 2021;26(18):5577. doi:10.3390/molecules26185577
- Peng CC, Kim J, Chauhan A. Extended delivery of hydrophilic drugs from silicone-hydrogel contact lenses containing vitamin E diffusion barriers. *Biomaterials*. 2010;31(14):4032–4047. doi:10.1016/j.biomaterials.2010.01.113
- Kim J, Peng CC, Chauhan A. Extended release of dexamethasone from silicone-hydrogel contact lenses containing vitamin E. *J Control Release*. 2010;148(1):110–116. doi:10.1016/j.jconrel.2010.07.119
- Karlgard CCS, Jones LW, Moresoli C. Ciprofloxacin interaction with silicon-based and conventional hydrogel contact lenses. *Eye Contact Lens*. 2003;29(2):83–89. doi:10.1097/01.ICL.00000061756.66151.1C
- Gudnason K, Solodova S, Vilardell A, Masson M, Sigurdsson S, Jonsdottir F. Numerical simulation of Franz diffusion experiment: Application to drug loaded soft contact lenses. *J Drug Deliv Sci Technol*. 2017;38:18–27. doi:10.1016/j.jddst.2016.12.011
- Bikbova G, Oshitari T, Baba T, et al. Diabetic corneal neuropathy: Clinical perspectives. *Clin Ophthalmol*. 2018;12:981–987. doi:10.2147/OPHT.145266
- Kim G, Kim HJ, Noh H. pH sensitive soft contact lens for selective drug-delivery. *Macromol Res*. 2018;26(3):278–283. doi:10.1007/s13233-018-6029-9
- Pimenta AFR, Serro AP, Paradiso P, Saramago B, Colaço R. Diffusion-based design of multi-layered ophthalmic lenses for controlled drug release. *PLoS One*. 2016;11(12):e0167728. doi:10.1371/journal.pone.0167728
- Maulvi FA, Lakdawala DH, Shaikh AA, et al. In vitro and in vivo evaluation of novel implantation technology in hydrogel contact lenses for controlled drug delivery. *J Control Release*. 2016;226:47–56. doi:10.1016/j.jconrel.2016.02.012

26. Paradiso P, Serro AP, Saramago B, Colaço R, Chauhan A. Controlled release of antibiotics from vitamin E-loaded silicone-hydrogel contact lenses. *J Pharm Sci*. 2016;105(3):1164–1172. doi:10.1016/S0022-3549(15)00193-8
27. Hsu KH, Fentzke RC, Chauhan A. Feasibility of corneal drug delivery of cysteamine using vitamin E modified silicone hydrogel contact lenses. *Eur J Pharm Biopharm*. 2013;85(3):531–540. doi:10.1016/j.ejpb.2013.04.017
28. Cheng Chun P, Burke MT, Chauhan A. Transport of topical anesthetics in vitamin E-loaded silicone hydrogel contact lenses. *Langmuir*. 2012;28(2):1478–1487. doi:10.1021/la203606z
29. Cheng Chun P, Burke MT, Carbia BE, Plummer C, Chauhan A. Extended drug delivery by contact lenses for glaucoma therapy. *J Control Release*. 2012;162(1):152–158. doi:10.1016/j.jconrel.2012.06.017
30. Rad MS, Mohajeri SA. Simultaneously load and extended release of beta-methasone and ciprofloxacin from vitamin E-loaded silicone-based soft contact lenses. *Curr Eye Res*. 2016;41(9):1185–1191. doi:10.3109/02713683.2015.1107591
31. Jarosz M. *Normy żywienia dla populacji polskiej*. Warszawa, Poland: Instytut Żywności i Żywienia; 2017. ISBN:978-83-86060-89-4.
32. Hsu KH, Lazon de la Jara P, Ariyavidana A. Release of betaine and dexpantenol from vitamin E modified silicone-hydrogel contact lenses. *Curr Eye Res*. 2015;40(3):267–273. doi:10.3109/02713683.2014.917192
33. Hsu KH, Carbia BE, Plummer C, Chauhan A. Dual drug delivery from vitamin E loaded contact lenses for glaucoma therapy. *Eur J Pharm Biopharm*. 2015;94:312–321. doi:10.1016/j.ejpb.2015.06.001
34. Lee D, Cho S, Park HS, Kwon I. Ocular drug delivery through pHEMA-hydrogel contact lenses co-loaded with lipophilic vitamins. *Sci Rep*. 2016;6(1):34194. doi:10.1038/srep34194
35. Tashakori-Sabzevar F, Mohajeri SA. Development of ocular drug delivery systems using molecularly imprinted soft contact lenses. *Drug Dev Ind Pharm*. 2015;41(5):703–713. doi:10.3109/03639045.2014.948451
36. Tieppo A, White CJ, Paine AC, Voyles ML, McBride MK, Byrne ME. Sustained in vivo release from imprinted therapeutic contact lenses. *J Control Release*. 2012;157(3):391–397. doi:10.1016/j.jconrel.2011.09.087
37. BelBruno JJ. Molecularly imprinted polymers. *Chem Rev*. 2019;119(1):94–119. doi:10.1021/acs.chemrev.8b00171
38. Alvarez-Lorenzo C, Yañez F, Barreiro-Iglesias R, Concheiro A. Imprinted soft contact lenses as norfloxacin delivery systems. *J Control Release*. 2006;113(3):236–244. doi:10.1016/j.jconrel.2006.05.003
39. González-Chomón C, Silva M, Concheiro A, Alvarez-Lorenzo C. Biomimetic contact lenses eluting olopatadine for allergic conjunctivitis. *Acta Biomater*. 2016;41:302–311. doi:10.1016/j.actbio.2016.05.032
40. Yañez F, Martikainen L, Braga MEM, et al. Supercritical fluid-assisted preparation of imprinted contact lenses for drug delivery. *Acta Biomater*. 2011;7(3):1019–1030. doi:10.1016/j.actbio.2010.10.003
41. Kojima T. Contact lens-associated dry eye disease: Recent advances worldwide and in Japan. *Invest Ophthalmol Vis Sci*. 2018;59(14):DES102. doi:10.1167/iovs.17-23685
42. White CJ, McBride MK, Pate KM, Tieppo A, Byrne ME. Extended release of high molecular weight hydroxypropyl methylcellulose from molecularly imprinted, extended wear silicone hydrogel contact lenses. *Biomaterials*. 2011;32(24):5698–5705. doi:10.1016/j.biomaterials.2011.04.044
43. Nikouei BM, Vahabzadeh SA, Mohajeri SA. Preparation of a molecularly imprinted soft contact lens as a new ocular drug delivery system for dorzolamide. *Curr Drug Deliv*. 2013;10(3):279–285. doi:10.2174/1567201811310030004
44. Kruk A, Gadowska-Gajadur A, Sebai A, Ruśkowski P. Rusztowania komórkowe w inżynierii tkankowej. *Wyroby Medyczne*. 2017;4:31–35.
45. Makadia HK, Siegel SJ. Poly lactic-co-glycolic acid (PLGA) as biodegradable controlled drug delivery carrier. *Polymers*. 2011;3(3):1377–1397. doi:10.3390/polym3031377
46. Choi S, Kim J. Therapeutic contact lenses with polymeric vehicles for ocular drug delivery: A review. *Materials (Basel)*. 2018;11(7):1125. doi:10.3390/ma11071125
47. Ciolino JB, Hudson SP, Mobbs AN, et al. A prototype antifungal contact lens. *Invest Ophthalmol Vis Sci*. 2011;52(9):6286. doi:10.1167/iovs.10-6935
48. Ciolino JB, Stefanescu CF, Ross AE, et al. In vivo performance of a drug-eluting contact lens to treat glaucoma for a month. *Biomaterials*. 2014;35(1):432–439. doi:10.1016/j.biomaterials.2013.09.032
49. Ciolino JB, Hoare TR, Iwata NG, et al. A drug-eluting contact lens. *Invest Ophthalmol Vis Sci*. 2009;50(7):3346. doi:10.1167/iovs.08-2826
50. ElShaer A, Mustafa S, Kasar M, Thapa S, Ghatora B, Alany R. Nanoparticle-laden contact lens for controlled ocular delivery of prednisolone: Formulation optimization using statistical experimental design. *Pharmaceutics*. 2016;8(2):14. doi:10.3390/pharmaceutics8020014
51. Green JA, Phillips KS, Hitchins VM, et al. Material properties that predict preservative uptake for silicone hydrogel contact lenses. *Eye Contact Lens*. 2012;38(6):350–357. doi:10.1097/ICL.0b013e318272c470
52. Hutter JC, Green JA, Eydelman MB. Proposed silicone hydrogel contact lens grouping system for lens care product compatibility testing. *Eye Contact Lens*. 2012;38(6):358–362. doi:10.1097/ICL.0b013e318260c959
53. Hui A, Boone A, Jones L. Uptake and release of ciprofloxacin-HCl from conventional and silicone hydrogel contact lens materials. *Eye Contact Lens*. 2008;34(5):266–271. doi:10.1097/ICL.0b013e3181812ba2
54. Musgrave CSA, Fang F. Contact lens materials: A materials science perspective. *Materials (Basel)*. 2019;12(2):261. doi:10.3390/ma12020261
55. Takamatsu T, Sijie Y, Shujie F, Xiaohan L, Miyake T. Multifunctional high-power sources for smart contact lenses. *Adv Funct Mater*. 2020;30(29):1906225. doi:10.1002/adfm.201906225
56. Kakisu K, Matsunaga T, Kobayakawa S, Sato T, Tochikubo T. Development and efficacy of a drug-releasing soft contact lens. *Invest Ophthalmol Vis Sci*. 2013;54(4):2551. doi:10.1167/iovs.12-10614
57. Zhu Q, Liu C, Sun Z, Zhang X, Liang N, Mao S. Inner layer-embedded contact lenses for pH-triggered controlled ocular drug delivery. *Eur J Pharm Biopharm*. 2018;128:220–229. doi:10.1016/j.ejpb.2018.04.017
58. Faccia PA, Pardini FM, Amalvy JI. Evaluation of pH-sensitive poly(2-hydroxyethyl methacrylate-co-2-(diisopropylamino)ethyl methacrylate) copolymers as drug delivery systems for potential applications in ophthalmic therapies/ocular delivery of drugs. *Express Polym Lett*. 2015;9(6):554–566. doi:10.3144/expresspolymlett.2015.52
59. Bengani LC, Chauhan A. Extended delivery of an anionic drug by contact lens loaded with a cationic surfactant. *Biomaterials*. 2013;34(11):2814–2821. doi:10.1016/j.biomaterials.2012.12.027
60. Bengani L. Fundamentals and applications of macromolecular transport in hydrogel contact lenses [doctoral thesis]. Gainesville, USA: University of Florida; 2013. https://ufdcimages.uflib.ufl.edu/UF/E0/04/57/81/00001/BEGANI_L.pdf.
61. Odrobinska J, Neugebauer D. Retinol derivative as bioinitiator in the synthesis of hydroxyl-functionalized polymethacrylates for micellar delivery systems. *Express Polym Lett*. 2019;13(9):806–817. doi:10.3144/expresspolymlett.2019.69
62. Alvarez-Rivera F, Concheiro A, Alvarez-Lorenzo C. Epalrestat-loaded silicone hydrogels as contact lenses to address diabetic-eye complications. *Eur J Pharm Biopharm*. 2018;122:126–136. doi:10.1016/j.ejpb.2017.10.016
63. Christopher K, Chauhan A. Delivery of ionic molecules to anterior chamber by iontophoretic contact lenses. *Eur J Pharm Biopharm*. 2019;140:40–49. doi:10.1016/j.ejpb.2019.04.016
64. Rohit A, Willcox M, Stapleton F. Tear lipid layer and contact lens comfort: A review. *Eye Contact Lens*. 2013;39(3):247–253. doi:10.1097/ICL.0b013e31828af164
65. Wang MTM, Ganesalingam K, Loh CS, et al. Compatibility of phospholipid liposomal spray with silicone hydrogel contact lens wear. *Cont Lens Anterior Eye*. 2017;40(1):53–58. doi:10.1016/j.clae.2016.11.002
66. Danion A, Arsenault I, Vermette P. Antibacterial activity of contact lenses bearing surface-immobilized layers of intact liposomes loaded with levofloxacin. *J Pharm Sci*. 2007;96(9):2350–2363. doi:10.1002/jps.20871
67. Phan CM, Subbaraman L, Liu S, Gu F, Jones L. In vitro uptake and release of natamycin Dex -b- PLA nanoparticles from model contact lens materials. *J Biomater Sci Polym Ed*. 2014;25(1):18–31. doi:10.1080/09205063.2013.830914
68. Paradiso P, Colaço R, Mata JLG, Krastev R, Saramago B, Serro AP. Drug release from liposome coated hydrogels for soft contact lenses: The blinking and temperature effect. *J Biomed Mater Res*. 2017;105(7):1799–1807. doi:10.1002/jbm.b.33715

Application of co-processed excipients for developing fast disintegrating tablets: A review

Sajal Jain^{1,A–D}, Simrandeep Kaur^{1,B,C}, Ritu Rathi^{1,B,D,E}, Upendra Nagaich^{2,C,E,F}, Inderbir Singh^{1,C,E,F}

¹ Chitkara College of Pharmacy, Chitkara University, Rajpura, India

² Amity Institute of Pharmacy, Amity University, Noida, India

A – research concept and design; B – collection and/or assembly of data; C – data analysis and interpretation;

D – writing the article; E – critical revision of the article; F – final approval of the article

Polymers in Medicine, ISSN 0370-0747 (print), ISSN 2451-2699 (online)

Polim Med. 2023;53(1):59–68

Address for correspondence

Inderbir Singh

E-mail: inderbir.singh@chitkara.edu.in

Funding sources

None declared

Conflict of interest

None declared

Received on September 24, 2022

Reviewed on November 30, 2022

Accepted on December 20, 2022

Published online on March 16, 2023

Abstract

The introduction of tablet dosage forms has brought a revolution in the pharmaceutical drug delivery system. Different forms of tablets have been developed based on the target site, the onset of action, and therapeutic drug delivery methods. Fast-disintegrating tablets (FDTs) are the most promising pharmaceutical dosage form, especially for pediatric and geriatric patients having difficulty swallowing. The key feature of FDTs is quick drug release soon after their administration through the oral cavity. With innovations in the formulation of FDTs, the demand for excipients with better functionalities, particularly in terms of flow and compression characteristics, has increased. Co-processed excipients are a mixture of 2 or more conventional excipients that provides significant benefits over the individual excipients while minimizing their shortcomings. Such multifunctional co-processed excipients minimize the number of excipients that are to be incorporated into tablets during the manufacturing process. The present review discusses FDTs formulated from co-processed excipients, their manufacturing techniques, and the latest research, patents and commercially available co-processed FDTs.

Key words: flowability, fast disintegrating tablet, co-processed excipient, compressibility

Cite as

Jain S, Kaur S, Rathi R, Nagaich U, Singh I. Application of co-processed excipients for developing fast disintegrating tablets: A review. *Polim Med.* 2023;53(1):59–68.

doi:10.17219/pim/158009

DOI

10.17219/pim/158009

Copyright

Copyright by Author(s)

This is an article distributed under the terms of the Creative Commons Attribution 3.0 Unported (CC BY 3.0) (<https://creativecommons.org/licenses/by/3.0/>)

Introduction

– fast-disintegrating tablets

Tablets are a widely accepted oral solid pharmaceutical dosage form around the world.¹ Among these dosage forms, fast-disintegrating tablets (FDTs) have gained interest due to their rapid disintegration time.² They were first developed in the late 1970s and have been of key interest to the pharmaceutical industry because of their enhanced bioavailability and rapid onset of action.^{3,4} Dysphagia is the medical term for swallowing difficulties and is most frequent in geriatric and pediatric patients. To overcome such complications, FDTs are designed to exhibit quick breakdown within the oral cavity, hence eliminating the need for chewing and conjoint water consumption.⁵ They are also known as fast dispersing, rapidly dissolving, rapidly melting, and quick disintegrating tablets. Some commonly used disintegrants for the preparation of FDTs are starch, modified starch, sucrose, mannitol, microcrystalline cellulose (MCC), alginic acid, cross-linked polyvinyl pyrrolidone (PVP), and many more.⁶ As per the Food and Drug Administration (FDA), all FDTs are categorized under the Oral Disintegrating Tablets category.^{7–9} Orodispersible tablets are those that disperse in less than 3 min in the buccal cavity before swallowing. In the oral cavity, such tablets disintegrate into small granules or melt from a hard solid configuration into a gel-like structure that allows effortless swallowing of a drug. These tablets form a soft paste or liquid suspension in the oral cavity, providing a pleasant mouthfeel and effortless swallowing. Following their disintegration, there is minimal or no residue in the oral cavity.^{8–10}

The FDTs have uniform advantages such as exceptional stability, ease of manufacturing and handling, good patient compliance, enhanced bioavailability and palatability, and accurate dosing.¹¹ They are susceptible to humidity and temperature, and are suitable for patients that suffer from dry mouth and are on anticholinergic therapy. Moreover, FDTs disintegrate quickly and exhibit speedy absorption in the oral cavity. Such tablets lead to an increase in drug bioavailability, avoid first-pass metabolism and result in reduced dosing.^{9,12} Some of the key advantages of FDTs are depicted in Fig. 1.

There are different patented and conventional manufacturing techniques for the preparation and development of FDTs, and several of them are listed in Fig. 2.¹³ Table 1



Fig. 1. Advantages of fast-disintegrating tablets (FDTs)

summarizes the patented techniques used for the preparation of FDTs alongside their active ingredients and patent owner details.^{13–18}

Excipients

Excipients are non-therapeutic components that are part of any pharmaceutical formulation. These substances act as bulking agents and stability enhancers, and support the therapeutic efficacy of the active pharmaceutical ingredient.^{19–21} The most commonly used excipients in the tablet dosage form are diluents, binders, disintegrants, glidants, lubricants, surfactants, pH-adjusting agents, sugar (as sweetening agent), mucoadhesive polymers, and coating and coloring agents.²² Table 2 briefly presents the functionality of each excipient with examples.^{23–30}

For the development of FDTs, superdisintegrants are widely used in the pharmaceutical industry to minimize the disintegration time. Agar powder and amino acids are examples of naturally available disintegrants that are

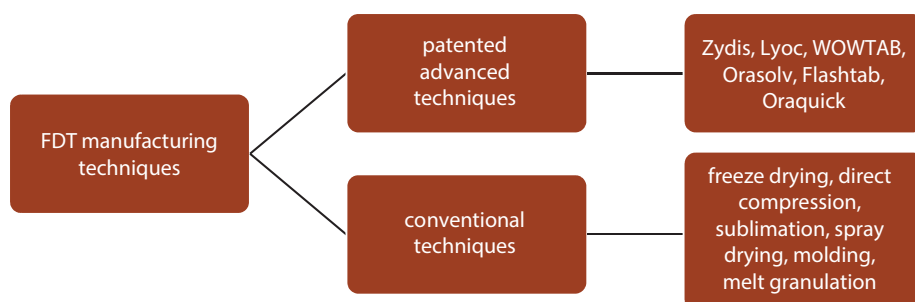


Fig. 2. Fast-disintegrating techniques

Table 1. Patented technologies for fast-disintegrating tables (FDTs)

Technology name	Basis of technology	Active ingredient	Name-patent owner	Reference
WOWTAB	direct compression	famotidine	Yamanouchi Pharma Tech Inc	[13]
Orasolv	direct compression	paracetamol, zolmitriptan	Cima Labs Inc	[14] and [15]
Zydis	lyophilization	loratidine	R.P Scherer inc.	[13] and [16]
Lyoc	lyophilization	phloroglucinol hydrate	Farmlyoc	[13] and [17]
Oraquick	micromask taste masking	hyoscyamine sulphate	K.V Pharm. Co., Inc	[14] and [17]
Flashtab	direct compression	ibuprofen	Ethypharm	[14] and [18]

Table 2. Excipients commonly used in the pharmaceutical industry

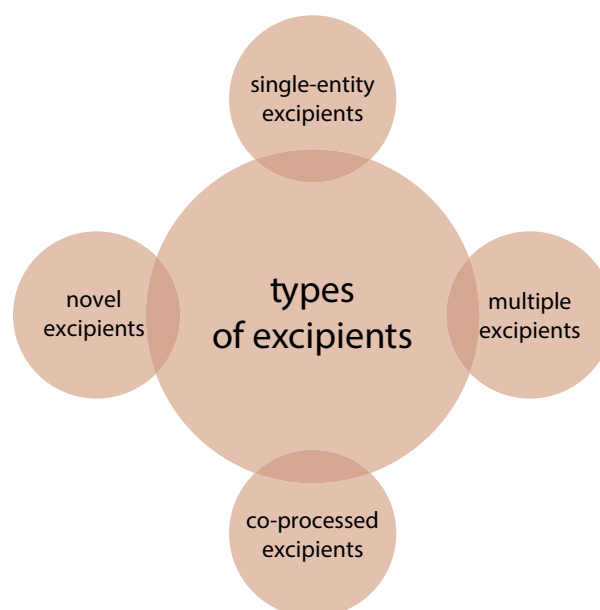
Excipient	Function	Example	Reference
Binders	provides plasticity and boosts the interparticulate bonding strength in tablet	starch, gelatin, acacia	[23] and [24]
Disintegrants/ superdisintegrants	rapidly absorbs water and results in a quick breakdown of tablet	crosscarmellose sodium, crosspovidone	[25] and [26]
Diluents	produces desired/required bulk of the tablet	microcrystalline cellulose, lactose monohydrate, calcium phosphate dehydrate	[27]
Lubricants	minimizes tablet adhesion with the surface of dies and punches	magnesium stearate, talc, silica	[28]
Glidants	improves flowability characteristics	colloidal silicon dioxide, talc	[28]
Coloring agent	improves tablet appearance and patient acceptance	dyes and pigments	[29]
Flavoring agent	employed in orodispersible tablets, assures a better mouth feel	peppermint oil, spearmint oil	[30]

used in the preparation of FDTs.³¹ Agar powder, due to its large porous size and overall volume, promotes rapid water permeation into the tablet, consequently resulting in fast tablet disintegration.³² Incorporation of amino acids such as proline and serine promotes rapid tablet disintegration due to enhanced wettability.³³

non-compensia excipients intended to physically alter their characteristics without any significant alteration in their chemical properties. Co-processing is achieved with standard techniques such as granulation, milling, spray drying, etc.^{36,37}

Types of pharmaceutical excipients

Figure 3 illustrates different types of pharmaceutical excipients used in the preparation of solid dosage forms. Each of these excipients is defined as a single-entity excipient consisting of 1 characteristic component that acts as a primary principal component for the excipients, for example cellulose. Multiple excipients are a blend of 2 or more excipients developed using low to moderate shear force. Under applied pressure, individual constituents are combined without any considerable changes in chemical characteristics, and the individual excipients remain distinct at a particulate level, for example MCC + lactose.³⁴ Novel excipients are excipients that undergo chemical modifications to establish a new excipient. Modifications lead to improvement in solubility and permeability, and result in overall performance enhancement.³⁵ Co-processed excipients are a blend of 2 or more compendia/

**Fig. 3.** Types of pharmaceutical excipients

Co-processed excipients

Co-processed excipients are a mixture of 2 or more compendia/non-compendial excipients that improves physical characteristics without any significant chemical transformations or displaying multifunctional activity.³⁸ Diverse co-processing methods are used in pharmaceutical industries, such as spray drying, solvent evaporation, crystallization, melt extrusion, and many more.^{39–41} Co-processed excipients are developed through inclusion of one excipient into the particle framework of another (second) excipient by employing techniques such as co-drying.⁴² These excipients are designed to address the divergent pitfalls in flowability, compressibility, disintegration potential, lubricant sensitivity, solubility, and permeability, and boost the desired properties of excipients as well as promote production procedure at low expenditure.^{40,43}

Steps of co-processing

1. Excipient recognition – on the basis of excipient characteristics, attributes, properties, and functionality parameters.
2. Screening of the appropriate proportions of excipients.⁴⁰
3. Examination of the particle size requisite for co-processing. This step is of utmost importance as when excipient is processed in the dispersed phase, post-processing the particle size of the excipient depends on its initial size.⁴⁰
4. Electing of an appropriate drying process – for example, spray drying or flash drying.⁴³

Excipients elected of co-processing should complement each other; for example, mannitol is poorly compressible and a low hygroscopic polyol, and therefore is co-processed with sorbitol that displays good compressibility characteristics as well as high hygroscopicity. Appropriate compression behavior is also required in an ideal tablet excipient, thereby requiring harmony between plasticity and brittleness.⁴⁴ Figure 4 shows a diagrammatic representation of the co-processing approach.

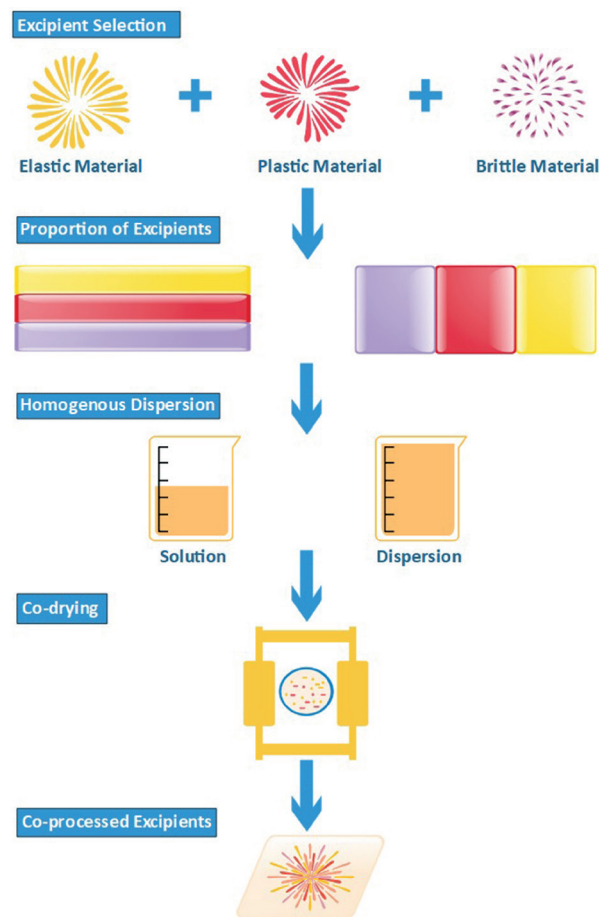


Fig. 4. Steps for co-processing

Co-processing is performed using various other techniques. Table 3 presents the advantages and limitations of each co-processing technique.^{42,45–48}

Function of co-processed excipients in FDT formulations

Co-processed excipients play a vital role in FDT formulations as they improve the flow and wetting properties,

Table 3. Methods of co-processing commonly used in the pharmaceutical industry

Methods	Advantages and limitations	Reference
Granulation/agglomeration	Enhancement in physical properties including flowability, wettability and product appearance. It is a swift processing technique, and can be accomplished with conventional equipment as well.	[42]
Spray drying	Reduced disintegration time, improved tablet hardness and compressibility behavior promotes simultaneous blending as well as drying of both soluble and insoluble compounds. This amends the speed of tableting machine. Limitations: rapid drug release increases the risk of burst effect, not a suitable method for particles with complex morphological structure.	[45]
Melt extrusion	Less time-consuming, high reproducibility, appropriate for establishing intricate shapes, uniform dispersion can be achieved. Limitations: high equipment cost and increased threat of thermal degradation due to high temperature.	[46]
Fluid bed spray granulation (FBSG)	Tablets display faster disintegration and dissolution characteristics and abated friability; technique suitable for high-speed tableting machines.	[47]
Wet granulation	Cost-effective method, can be executed with conventional tableting equipment and less process variables.	[48]

modify the compression characteristics, improve the superdisintegration characteristics, and provide superior tableability. They also enhance thixotropic characteristics by adjusting viscosity, promoting rapid tablet breakdown and contributing to quick therapeutic action (therefore making the tablets appropriate for emergency circumstances).^{27,49–51} Employing co-processed excipients in FDT formulations eliminates the need for any additional excipients or lubricant, and reduces the time and cost associated with FDT production.^{52–54}

Sunil et al. employed a spray drying technique for the co-processing of MCC, mannitol and aerosil in varying ratios. The prepared excipients were evaluated for different parameters, such as Carr index, Hausner ratio and angle of repose to determine the flow characteristics of the material. The developed co-processed excipients displayed better flow properties compared to a physical admixture of such excipients.⁵⁵ Pituanan et al. prepared the co-processed pre-gelatinized cassava starch (PCS) with acacia gum (AG) in different proportions using a direct compression method. The developed co-processed excipients were examined regarding their morphology, flow characteristics and moisture content. The result revealed that FDTs prepared using these co-processed excipients exhibit reduced wetting and disintegration time, and altered friability and hardness.⁵⁶ The FDTs of montelukast were formulated by co-processing mannitol and sodium starch glycolate with the incorporation of a solvent evaporation process by Kumar et al. The prepared formulation was evaluated for hardness, thickness, drug content uniformity, and drug release properties. The results reported that the developed formulation displayed reduced wetting and disintegration time.⁵⁷ Rao et al. prepared atorvastatin FDTs using novel co-processed excipients crosscarmellose sodium (CCS) and sodium starch glycolate (SSG) in different proportions by employing a direct compression technique. The developed formulation displayed shorter disintegration time in comparison to individual excipients.⁵⁸ Chlorpromazine HCl orodispersible tablets were designed by Deshmukh et al. using an admixture of excipients, SSG and crospovidone (CP) in varying ratios with a direct compression technique. The developed co-processed excipients were examined regarding their flow characteristics, Carr index and Hausner ratio. The developed FDTs of chlorpromazine exhibit reduced wetting and disintegration time, and enhanced patient acceptance.⁵⁹

Omeprazole FDTs were formulated by More et al. using co-processed CCS and CP. Carr index, angle of repose and Hausner ratio of developed co-processed excipients were evaluated. The formulated orodispersible tablets exhibited improved drug release characteristics.⁶⁰ The spray drying method was used by Shirsand et al. for co-processing mannitol and microcrystalline cellulose in various proportions for developing glibenclamide FDTs. The co-processed excipients were then evaluated; the FDTs formulated using

an admixture of excipients showed better stability and improved drug release properties.⁶¹ Pusapati et al. formulated atorvastatin calcium tablets by employing a direct compression technique using co-processed acacia-calcium carbonate (CaCO_3). The hardness, dissolution profile and friability of those tablets were examined. Results revealed that the formulation containing 3% acacia showed less dissolution time and proved to be the overall best formulation.⁶² Irbesartan FDTs were formulated using co-processed excipients by Madhvi et al. employing a melt agglomeration technique; the bitter taste of a drug was masked using aspartame or by complexing with β -cyclodextrin. The developed tablets were examined for friability, hardness, strength, and dissolution profile. The results reported that melt agglomeration was a better choice for designing FDTs using novel co-processed excipients.⁶³

Table 4 presents a brief outline of the studies conducted on FDTs manufactured using co-processed excipients.^{50,55–76} In continuation of the studies concerning co-processed FDT, several patents are discussed below.

A co-processed mixture of sugar alcohol (such as mannitol) and MCC was patented in 2015. This composition displayed reduced lubricant sensitivity and a better compaction profile, and is widely employed in the preparation of pharmaceutical dosage forms.⁷⁷ Admixture of pharmaceutical co-processed excipients MCC, polacrilin sodium and partially pregelatinized starch were patented and utilized in the formulation of ibuprofen tablets using a direct compression technique, as the admixture of excipients displayed better flowability and improved compressibility.⁷⁸ A co-processed admixture of xanthan gum and guar gum excipients was used in the preparation of venlafaxine tablets. Such a combination of pharmaceutical excipients was patented and serves as a bulking, disintegrating, swelling, and gelling agent.⁷⁹

There are various patents filed for FDTs which utilize co-processed excipients – Table 5 presents a selection of those patents and patent applications. Many co-processed excipients have been introduced into the market and are commercially available.^{77–89} Table 6 lists commercially available FDTs prepared using co-processed excipients.^{40,90–94}

Conclusions

The FDTs are extensively used because of their quick disintegration time and rapid onset of action. Excipients play a vital role in the formulation of tablets and their therapeutic action. A variety of excipients are used to produce FDTs, so there is always a need to search for an excipient with improved functionality that can cater to the high demand for excipients in the pharmaceutical industry. A co-processed excipient is a solution that reduces the use of excessive excipients in the formulation and results in a cost-effective manufacturing process. Co-processed

Table 4. Studies on fast-disintegrating tablets (FDTs) using co-processed excipients

Co-processed excipients	Method	Remarks	Reference
Chitosan + aerosil	co-precipitation	Enhanced flow properties and compression behavior.	[50]
MCC + mannitol + aerosil	spray drying	Co-processed excipient causes quick dispersion of tablet in oral cavity and reduced disintegration time, and is cost-effective.	[55]
PCS + AG	direct compression	PCS + AG co-processed excipient exhibits improved flow characteristics and swelling index, with shorter wetting and disintegration time.	[56]
SSG + mannitol	solvent evaporation	Reduced disintegration time and wetting time, improvement in flow properties.	[57]
Crosscarmellose + SSG	lyophilization	Formulation had lesser disintegration time in contrast to individual excipients.	[58]
CP + SSG	direct compression	Reduced disintegration time, improved flowability, better compression characteristics.	[59] and [64]
CP + CCS	solvent evaporation	Enhanced mechanical resistance, uniform weight, lessened disintegration as well as wetting time.	[60]
MCC + manitol	spray drying	Better flowability, improved drug disintegration, enhanced stability and dissolution rates.	[61]
Acacia + calcium carbonate	direct compression	Reduced dissolution time, improved disintegration as well as dissolution rates, good flow properties.	[62]
Lactose monohydrate + mannitol + PEG + CP	melt granulation	Enhanced functionality, rapid drug dissolution, increased loading, potential taste masking.	[63]
CP + SSG + CCS	dry granulation	Enhanced formulation stability and reproducibility, better flow characteristics, increased dissolution rate.	[65]
CP + CCS	direct compression	Better flow and compression characteristics, expeditious disintegration and ameliorated drug dissolution.	[66]
CP + SSG	solvent evaporation	Reduced disintegration time, improved wetting properties, drug content and stability.	[67]
Mannitol + MCC + CP + SSG + aerosil + CCS	direct compression	High degree of stability, better flowability, appropriate hardness and reduced disintegration time.	[68]
CP + Kyron T-314	solvent evaporation	Better flow properties and compression behavior, and decreased disintegration time.	[69]
Mannitol + MCC	spray drying	Improvement in dissolution of FDTs, better wetting properties, reduced disintegration time.	[70]
Lactose + mannitol	melt granulation	Improved flow properties and reduced disintegration time.	[71]
DCP + starch	direct compression	Fast disintegration and better compression characteristics.	[72]
MCC + CP + SiO ₂	spray drying	Better flowability, compressibility and decreased disintegration time.	[73]
Sucrose + sorbitol	direct compression	Faster disintegration, better palatability and pleasant taste.	[74]
MCC + DCP	wet granulation	Better disintegration, friability, compression, weight uniformity and crushing force.	[75]
MCC + lactose + PVP + PEG	melt granulation	Reduced disintegration time, better flow characteristics, appropriate dilution potential, shorter processing time.	[76]

DCP – dicalcium phosphate; AG – acacia gum; MCC – microcrystalline cellulose; CP – crospovidone; PCS – pre-gelatinized cassava starch; PVP – polyvinyl pyrrolidone; PEG – polyethylene glycol; SSG – sodium starch glycolate; CCS – crosscarmellose sodium.

excipients display improved properties in comparison to individual excipients. They reduce the use of excipients in the formulation, thus reducing the overall concentration of the dosage form. Despite having these benefits, co-processed excipients entail certain challenges in terms of their recognition in pharmacopoeia. Hence, extensive research is ongoing in this field and several patents have been filed for co-processed excipients, but there is still no standard characterization for these in the pharmacopoeia. Considering the benefits that co-processed excipients

provide, the future for such excipients is very promising. A new combination of excipients and improved techniques of co-processing would gain more attention from researchers and the pharmaceutical industry.

ORCID iDs

Sajal Jain  <https://orcid.org/0000-0002-5932-2210>
 Simrandeep Kaur  <https://orcid.org/0000-0002-3623-2116>
 Ritu Rathi  <https://orcid.org/0000-0002-9367-1975>
 Upendra Nagaich  <https://orcid.org/0000-0003-0076-6885>
 Inderbir Singh  <https://orcid.org/0000-0002-1860-4246>

Table 5. Patents for fast-disintegrating tablets (FDTs) using co-processed excipients

Patent No.	Co-processed excipients	Properties	Reference
US 8,932, 692 B2 JAN 13.2015	MCC + sugar alcohol	Improved compactibility characteristics, less lubricant sensitivity, ameliorated ejection properties.	[77]
WO/2016/046693	polacrillin potassium + partially pregelatinized starch + MCC	Improved flowability and compressibility characteristics.	[78]
WO/2017/013682A1	xanthum gum + guar gum	Bulking agent, emulsifying agent, binder, disintegrant, viscosity enhancer, swelling agent and gelling agent.	[79]
WO/2013/052114A1	MCC + sodium CMC	Enhanced stabilizer.	[80]
WO/2003/051338	mannitol + sorbitol	Excipient shows non-filamentous microstructure.	[81]
US 4744987A	MCC + CaCO ₃	Economical and exhibits lower lubricant sensitivity. ⁸⁰	[82]
US/2010/0266682	sodium carbonate + PEG	pH-modifying agent, decreases NaCO ₃ caking.	[83]
EP/1886671	colloidal silica + corn starch	Employed as diluents and disintegrant in fast-release formulations.	[84]
WO/2014/165246A1	vinyl lactum derived polymer + silicon dioxide	Enhances flow characteristics and compaction behavior.	[85]
EP 3 682 901 A1 22.07.2020 BULLETIN 2020/30	mannitol + PVP	Uniform size and size distribution along with less relative variations.	[86]
US202200 47511A1	MCC + CaCO ₃	Improved performance of drug and less lubricant sensitivity.	[87]
US20100286164A1	MCC + SiO ₂ + polyol/sugar blend	Exhibits better processing and fast disintegration.	[88]
WO/95/17831	galactommanan (locust bean gum) + glucommanan	Extensively used as viscosity enhancer and gelling agent.	[89]

MCC – microcrystalline cellulose; CP – crospovidone; PCS – pre-gelatinized cassava starch; PVP – polyvinyl pyrrolidone; PEG – polyethylene glycol; SSG – sodium starch glycolate

Table 6. Commercially available fast-disintegrating tablests (FDTs) developed using co-processed excipients

Brand name	Adjuvants	Advantages and applications	Reference
Prosolv	MCC + SiO ₂	Rapid disintegration, enhancement in flow properties.	[40]
Avicel	MCC + guar gum	Decreased grittiness, smoother and creamy mouthfeel, better tablet palatability and patient acceptance.	[90]
Ludiflash	mannitol + CP + PVA	Rapid disintegration and dissolution, ameliorated mechanical strength, better flow properties, smooth and pleasant mouthfeel. Exclusively designed for mouth-dissolving tablets.	[40] and [91]
Pharma burst	mannitol + CP + SiO ₂	Superior organoleptic characteristics, rapid disintegration.	[92]
F Melt	mannitol + xylitol + CP + MCC	Rapid disintegration, better flow characteristics, improves tablet quality.	[93]
PanExcea MC 200G	MCC + CP + HPMC	Rapid disintegration and dissolution, enhanced blending, ensures direct compression with high-speed tableting.	[94]

PVA – polyvinyl acetate; MCC – microcrystalline cellulose; CP – crospovidone; HPMC – hydroxypropyl methylcellulose.

References

- Aly S. Study of the tableting properties of MCR, a newly coprocessed cellulose-based direct compression excipient. *Arch Pharmacol Ther.* 2021;3(2):37–38. doi:10.33696/Pharmacol.3.026
- Heer S, Jindal S, Mishra G, et al. Formulation and characterization of oral rapid disintegrating tablets of levocetirizine. *Polim Med.* 2019; 48(1):31–40. doi:10.17219/pim/99951
- Garg N, Dureja H, Kaushik D. Co-processed excipients: A patent review. *Recent Pat Drug Deliv Formul.* 2013;7(1):73–83. doi:10.2174 /187221113804805847
- Goyal R, Nagpal M, Arora S, Dhingra GA. Development and optimization of fast dissolving tablets of losartan potassium using natural gum mucilage. *J Pharm Technol Res Manag.* 2013;1(2):153–169. doi:10.15415 /jptrm.2013.12009
- Nagpal M, Goyal A, Kumar S, Singh I. Starch-silicon dioxide coprecipitate as superdisintegrant: Formulation and evaluation of fast disintegrating tablets. *Int J Drug Deliv.* 2012;4(2):164–174. https://www.researchgate.net/publication/256303503_Starch-silicon_dioxide_coprecipitate_as_superdisintegrant_formulation_and_evaluation_of_fast_disintegrating_tablets. Accessed September 10, 2022.
- Odeniyi M, Omotoso O, Adepoju A, Jaiyeoba K. Starch nanoparticles in drug delivery: A review. *Polim Med.* 2019;48(1):41–45. doi:10.17219/pim/99993
- Fu Y, Yang S, Jeong SH, Kimura S, Park K. Orally fast disintegrating tablets: Developments, technologies, taste-masking and clinical studies. *Crit Rev Ther Drug Carrier Syst.* 2004;21(6):433–476. doi:10.1615/CritRevTherDrugCarrierSyst.v21.i6.10
- Parkash V, Maan S, Deepika, Yadav S, Hemlata, Jogpal V. Fast disintegrating tablets: Opportunity in drug delivery system. *J Adv Pharm Tech Res.* 2011;2(4):223. doi:10.4103/2231-4040.90877
- Sharma B, Arora G, Singh I. Application of SeDeM expert system in formulation and development of fast disintegrating tablets using starch-glycine conjugates as superdisintegrant. *J Res Pharm.* 2019; 23(5):839–850. doi:10.35333/jrp.2019.32
- Ghourichay MP, Kiaie SH, Nokhodchi A, Javazadeh Y. Formulation and quality control of orally disintegrating tablets (ODTs): Recent advances and perspectives. *Biomed Res Int.* 2021;2021:6618934. doi:10.1155/2021/6618934

11. Panraksa P, Zhang B, Rachtanapun P, Jantanasakulwong K, Qi S, Jantrawut P. 'Tablet-in-syringe': A novel dosing mechanism for dysphagic patients containing fast-disintegrating tablets fabricated using semisolid extrusion 3D printing. *Pharmaceutics*. 2022;14(2):443. doi:10.3390/pharmaceutics14020443
12. Malaak FA, Zeid KA, Fouad SA, El-Nabarawi MA. Orodispersible tablets: Novel strategies and future challenges in drug delivery. *Res J Pharm Technol*. 2019;12(11):5575. doi:10.5958/0974-360X.2019.00966.1
13. Kapse N, Bharti V, Birajdar A, Munde A, Panchal P. Co-processed superdisintegrants: Novel technique for design orodispersible tablets. *J Innov Pharm*. 2015;2(4):541–555. <https://innovareacademics.in/journals/index.php/ajpcr/article/view/23010/13950>. Accessed September 10, 2022.
14. Shukla D. Mouth dissolving tablets I: An overview of formulation technology. *Sci Pharm*. 2009;77(2):309–326. doi:10.3797/scipharm.0811-09-01
15. Gupta M, Sharma S, Gupta M, Sen P. Formulation and evaluation of fast dissolving tablets. *Int J Curr Pharm*. 2021;13(3):13–19. <http://impactfactor.org/PDF/IJCPR/13/IJCPR,Vol13,Issue3,Article2.pdf>. Accessed September 10, 2022.
16. Costa JSR, de Oliveira Cruvinel K, Oliveira-Nascimento L. A mini-review on drug delivery through wafer technology: Formulation and manufacturing of buccal and oral lyophilizates. *J Adv Res*. 2019;20:33–41. doi:10.1016/j.jare.2019.04.010
17. Agiba AM, Eldin AB. Insights into formulation technologies and novel strategies for the design of orally disintegrating dosage forms: A comprehensive industrial review. *Int J Pharm Pharm Sci*. 2019;11(9):8–20. doi:10.22159/ijpps.2019v11i9.34828
18. Gupta H, Bhandari D, Sharma A. Recent trends in oral drug delivery: A review. *Recent Pat Drug Deliv Formul*. 2009;3(2):162–173. doi:10.2174/187221109788452267
19. Elder DP, Kuentz M, Holm R. Pharmaceutical excipients: Quality, regulatory and biopharmaceutical considerations. *Eur J Pharm Sci*. 2016;87:88–99. doi:10.1016/j.ejps.2015.12.018
20. Sam T, Ernest TB, Walsh J, Williams JL. A benefit/risk approach towards selecting appropriate pharmaceutical dosage forms: An application for paediatric dosage form selection. *Int J Pharm*. 2012;435(2):115–123. doi:10.1016/j.ijpharm.2012.05.024
21. Main A, Bhairav BA, Saudager RB. Coprocessed excipients for tableting: Review article. *Res J Pharm Technol*. 2017;10(7):2427. doi:10.5958/0974-360X.2017.00429.2
22. van der Merwe J, Steenekamp J, Steyn D, Hamman J. The role of functional excipients in solid oral dosage forms to overcome poor drug dissolution and bioavailability. *Pharmaceutics*. 2020;12(5):393. doi:10.3390/pharmaceutics12050393
23. Uhumwangho M, Okor R, Eichie F, Abbah C. Influence of some starch binders on the brittle fracture tendency of paracetamol tablets. *Afr J Biotechnol*. 2006;5(20):1950–1953. <https://www.ajol.info/index.php/ajb/article/view/55919>. Accessed September 10, 2022.
24. Davies WL, Gloor WT. Batch production of pharmaceutical granulations in a fluidized bed II: Effects of various binders and their concentrations on granulations and compressed tablets. *J Pharm Sci*. 1972;61(4):618–622. doi:10.1002/jps.2600610428
25. Meruva S, Thool P, Gong Y, Karki S, Bowen W, Kumar S. Role of wetting agents and disintegrants in development of danazol nanocrystalline tablets. *Int J Pharm*. 2020;577:119026. doi:10.1016/j.ijpharm.2020.119026
26. Bisharat L, AlKhatib HS, Muhaissen S, et al. The influence of ethanol on superdisintegrants and on tablets disintegration. *Eur J Pharm Sci*. 2019;129:140–147. doi:10.1016/j.ejps.2019.01.004
27. Khobragade D, Parshuramkar P, Anusha V, Potbhare M, Patil A. Pharmaceutical evaluation of effects of hydrophilicity and hydrophobicity of three commonly used diluents on tablet formulation. Part II: SR tablets. *Int J Pharm Chem*. 2015;5(3):93–103. https://www.researchgate.net/publication/275029385_Pharmaceutical_evaluation_of_effects_of_hydrophilicity_and_hydrophobicity_of_three_commonly_used_diluents_on_tablet_formulation-Part_II_IR_tablets. Accessed September 10, 2022.
28. Kanher PR. Lubricants in pharmaceutical solid dosage forms with special emphasis on magnesium stearate. *World J Pharm Res*. 2017;6(9):131–146. doi:10.20959/wjpr20179-9170
29. Šuleková M, Smrčová M, Hudák A, Heželová M, Fedorová M. Organic colouring agents in the pharmaceutical industry. *Fol Vet*. 2017;61(3):32–46. doi:10.1515/fv-2017-0025
30. Joshua J, Jyothish F, Surendran S. Fast dissolving oral thin films: An effective dosage form for quick release. *Int J Pharm Sci Rev Res*. 2016;38(1):282–289. https://www.researchgate.net/publication/303106242_Fast_Dissolving_Oral_Thin_Films_An_Effective_Dosage_Form_for_Quick_Releases. Accessed September 10, 2022.
31. Al-Khattawi A, Mohammed AR. Compressed orally disintegrating tablets: Excipients evolution and formulation strategies. *Exp Opin Drug Deliv*. 2013;10(5):651–663. doi:10.1517/17425247.2013.769955
32. Ito A, Sugihara M. Development of oral dosage form for elderly patients: Use of agar as base of rapidly disintegrating oral tablets. *Chem Pharm Bull*. 1996;44(11):2132–2136. doi:10.1248/cpb.44.2132
33. AlHusban F, ElShaer A, Kansara J, et al. Investigation of formulation and process of lyophilised orally disintegrating tablet (ODT) using novel amino acid combination. *Pharmaceutics*. 2010;2(1):1–17. doi:10.3390/pharmaceutics2010001
34. Swami A, Chavan P, Chakankar S, Tagalpallear A. A review on multifunctional excipients with regulatory considerations. *J Pharm Res Int*. 2021;33(45B):189–201. doi:10.9734/jpri/2021/v33i45B32796
35. Kanojia N, Kaur L, Nagpal M, Bala R. Modified excipients in novel drug delivery: Need of the day. *J Pharm Technol Res Manag*. 2013;1(1):81–107. doi:10.15415/jptrm.2013.11006
36. Kozarewicz P, Loftsson T. Novel excipients: Regulatory challenges and perspectives. The EU insight. *Int J Pharm*. 2018;546(1–2):176–179. doi:10.1016/j.ijpharm.2018.05.048
37. Patil S, Pandit A, Godbole A, Dandekar P, Jain R. Chitosan based co-processed excipient for improved tableting. *Carbohydr Polym Technol Appl*. 2021;2:100071. doi:10.1016/j.carpta.2021.100071
38. Kaur L, Singh I. Microwave grafted, composite and coprocessed materials: Drug delivery applications. *Ther Deliv*. 2016;7(12):827–842. doi:10.4155/tde-2016-0055
39. Dominik M, Vraníková B, Svačinová P, et al. Comparison of flow and compression properties of four lactose-based co-processed excipients: Cellactose® 80, CombiLac®, MicroceLac® 100, and StarLac®. *Pharmaceutics*. 2021;13(9):1486. doi:10.3390/pharmaceutics13091486
40. Bhatia V, Dhingra A, Chopra B, Guarve K. Co-processed excipients: Recent advances and future perspective. *J Drug Deliv Sci Technol*. 2022;71:103316. doi:10.1016/j.jddst.2022.103316
41. Bowles BJ, Dziemidowicz K, Lopez FL, et al. Co-processed excipients for dispersible tablets. Part 1: Manufacturability. *AAPS PharmSciTech*. 2018;19(6):2598–2609. doi:10.1208/s12249-018-1090-4
42. Chaudhari P, Phatak A, Dessai U. A review: Co processed excipients-an alternative to novel chemical entities. *Int J Pharm Chem*. 2012;1(4):1480–1498. <https://asset-pdf.scinapse.io/prod/2182347153/2182347153.pdf>. Accessed September 10, 2022.
43. Saha S, Shahiwala AF. Multifunctional coprocessed excipients for improved tableting performance. *Exp Opin Drug Deliv*. 2009;6(2):197–208. doi:10.1517/17425240802708978
44. Lawal MV. Modified starches as direct compression excipients: Effect of physical and chemical modifications on tablet properties. A review. *Starch – Stärke*. 2019;71(1–2):1800040. doi:10.1002/star.201800040
45. Al-Zoubi N, Gharaibeh S, Aljaberi A, Nikolakakis I. Spray drying for direct compression of pharmaceuticals. *Processes*. 2021;9(2):267. doi:10.3390/pr9020267
46. Liu J. Properties of lipophilic matrix tablets containing phenylpropanolamine hydrochloride prepared by hot-melt extrusion. *Eur J Pharm Biopharm*. 2001;52(2):181–190. doi:10.1016/S0939-6411(01)00162-X
47. Medarević D, Djuriš J, Krkobabić M, Ibrić S. Improving tableting performance of lactose monohydrate by fluid-bed melt granulation co-processing. *Pharmaceutics*. 2021;13(12):2165. doi:10.3390/pharmaceutics13122165
48. Suresh P, Sreedhar I, Vaidhiswaran R, Venugopal A. A comprehensive review on process and engineering aspects of pharmaceutical wet granulation. *Chem Eng J*. 2017;328:785–815. doi:10.1016/j.cej.2017.07.091
49. Lekshmi P, Pramod K, Ajithkumar KC. Co-processed excipients for tableting. *Res J Pharm Dosage Form Technol*. 2016;8(1):46. doi:10.5958/0975-4377.2016.00007.0
50. Jain S, Rathil R, Nagaich U, et al. Co-processed tablet excipient composition, its preparation and use. US10071059 B2: Patent spotlight [published online as ahead of print on November 16, 2022]. *Pharm Pat Anal*. 2022. doi:10.4155/ppa-2022-0036

51. Sohail Arshad M, Zafar S, Yousef B, et al. A review of emerging technologies enabling improved solid oral dosage form manufacturing and processing. *Adv Drug Deliv Rev.* 2021;178:113840. doi:10.1016/j.addr.2021.113840
52. Daraghme N, Chowdhry B, Leharne S, Al Omari M, Badwan A. Co-processed chitin-mannitol as a new excipient for oro-dispersible tablets. *Marine Drugs.* 2015;13(4):1739–1764. doi:10.3390/md13041739
53. Zade A, Wani M, Limaye D, et al. A systematic review on co-processed formulation and development. *Ann Romanian Soc Cell Biol.* 2021;25(4):17140–17147.
54. Chauhan SI, Nathwani SV, Soniwala MM, Chavda JR. Development and characterization of multifunctional directly compressible co-processed excipient by spray drying method. *AAPS PharmSciTech.* 2017;18(4):1293–1301. doi:10.1208/s12249-016-0598-8
55. Sunil A, Shirsand SB, Baig SA. Development of novel coprocessed excipients for the design of fast dissolving tablet. *Indo Am J Pharm.* 2019;9(5):457–462. <https://iajpr.com/archive/volume-9/september-2019#>. Accessed September 10, 2022.
56. Pituanan BS, Surini S. Fast-disintegrating tablet formulation of ginger (*Zingiber Officinale Rosc.*) extract using coprocessed excipient of pregelatinized cassava starch-acacia gum. *Int J Appl Pharm.* 2017;9:154. doi:10.22159/ijap.2017.v9s1.77_84
57. Kumar K, Chopra H, Sharma GK. Formulation and evaluation of fast dissolving tablet of montelukast by using co-processed excipients. *Res J Pharm Technol.* 2019;12(11):5543. doi:10.5958/0974-360X.2019.00961.2
58. Rao S, Sravya K, Padmalatha K. Formulation and evaluation of fast dissolving tablets of atorvastatin using novel co-processed excipients. *J Pharm Sci Res.* 2021;13(8):474–480. <https://www.jpsr.pharmainfo.in/Documents/Volumes/vol13issue08/jpsr13082109.pdf>. Accessed September 10, 2022.
59. Deshmukh S, Quazi A, Sharaf A. Formulation and evaluation of fast dissolving tablets of chlorpromazine hydrochloride using novel co-processed superdisintegrants. *Res J Pharm Tech.* 2012;5(9):1235–1240. <https://www.indianjournals.com/ijor.aspx?target=ijor&volume=5&issue=9&article=018>. Accessed September 10, 2022.
60. More S, Mohite S, Kumar A, Thakran A. Formulation development and evaluation of orodispersible tablet of omeprazole by using co-processed superdisintegrant. *Res J Pharm Dosage Form Technol.* 2012;4(4):216–220. <https://rjpdft.com/HTMLPaper.aspx?Journal=Research%20Journal%20of%20Pharmaceutical%20Dosage%20Forms%20and%20Technology;PID=2012-4-4-5>. Accessed September 10, 2022.
61. Shirsand S, Gumate R, Jonathan V. Novel co-processed spray dried super disintegrants designing of fast dissolving tablets. *Dhaka Univ J Pharm Sci.* 2016;15(2):167–172. <https://www.banglajol.info/index.php/JPharma/article/view/30933>. Accessed September 10, 2022.
62. Pusapati R, Rapeti S, Kumar K, Murthy T. Development of co-processed excipients in the design and evaluation of atorvastatin calcium tablets by direct compression method. *Int J Pharm Investig.* 2014;4(2):102. doi:10.4103/2230-973X.133059
63. Madhvi K, Mehta K, Vadalala KR, Jay C, Sandip K. Design and development of co-processed excipients for fast dissolving tablets of irbesartan by melt agglomeration technique. *J Pharm Investig.* 2015;45(2):163–186. doi:10.1007/s40005-014-0163-y
64. Nagendrakumar D, Raju S, Shirsand S, Para M. Design of fast dissolving granisetron HCL tablets using novel coprocessed superdisintegrants. *Int J Pharm Sci Rev Res.* 2010;1(1):58–62. <https://www.globalresearchonline.net/volume1issue1/Article%20012.pdf>. Accessed September 10, 2022.
65. Suthar R, Chotai N, Shah D. Formulation and evaluation of fast dissolving tablets of ondansetron by solid dispersion in superdisintegrants. *Indian J Pharm Educ Res.* 2013;47(3):49–55. doi:10.5530/ijper.47.3.8
66. Patel H, Gohel M. A review on development of multifunctional co-processed excipient. *J Crit Rev.* 2016;3(2):48–54. <https://www.jcreview.com/admin/Uploads/Files/61c71ada76a5c4.13238358.pdf>. Accessed September 10, 2022.
67. Naikwade J, Patil V, Katkade M. Formulation & evaluation of fast dissolving tablets of amlodipine besylate by using co-processed superdisintegrants. *Br J Pharm Res.* 2013;3(4):865–879. <https://www.banglajol.info/index.php/ICPJ/article/view/11614/8496>. Accessed September 10, 2022.
68. Ashoor J, Rajab N, Ghareeb M, Abdulrasool A. Preparation and evaluation of orodispersible tablets of finasteride using co-processed excipients. *Int J Pharmacy Pharm Sci.* 2013;5(2):64–69. <https://innovareacademics.in/journal/ijpps/Vol5Issue2/6648.pdf>. Accessed September 10, 2022.
69. Ladola MK, Gangurde AB. Development and evaluation of melt-in-mouth tablets of metoclopramide hydrochloride using novel co-processed superdisintegrants. *Indian J Pharm Sci.* 2014;76(5):423–429. PMID:25425756. PMID:PMC4243259.
70. Shirwaikar A, Joseph A, Srinivasan K, Jacob S. Novel co-processed excipients of mannitol and microcrystalline cellulose for preparing fast dissolving tablets of glipizide. *Indian J Pharm Sci.* 2007;69(5):633. doi:10.4103/0250-474X.38467
71. Awasthi R, Deepak G, Pawar V, Sharma G, Kulkarni G. Development of directly compressible co-processed excipients for solid dosage forms. *Sch Res J.* 2010;2(6):151–165. <https://www.scholarsresearchlibrary.com/articles/development-of-directly-compressible-coprocessed-excipients-for-solid-dosage-forms.pdf>. Accessed September 10, 2022.
72. Mourya A, Prajapati S, Jain S, Alok S. Formulation and evaluation of fast dissolving tablets of acetaminophen. *Int J Pharm Sci.* 2012;3(2):610–614. <https://ijpsr.com/bft-article/formulation-and-evaluation-of-fast-dissolving-tablets-of-acetaminophen/>. Accessed September 10, 2022.
73. Avachat A, Ahire V. Characterization and evaluation of spray dried co-processed excipients and their application in solid dosage forms. *Indian J Pharm Sci.* 2007;69(1):85. doi:10.4103/0250-474X.32114
74. Bowe KE. Recent advances in sugar-based excipients. *Pharm Sci Technol Today.* 1998;1(4):166–173. doi:10.1016/S1461-5347(98)00043-1
75. Viscasillas Clerch A, Fernandez Campos F, del Pozo A, Calpena Campmany AC. Pharmaceutical design of a new lactose-free coprocessed excipient: Application of hydrochlorothiazide as a low solubility drug model. *Drug Dev Ind Pharm.* 2013;39(7):961–969. doi:10.3109/03639045.2012.686507
76. Gohel MC, Jogani PD. Exploration of melt granulation technique for the development of coprocessed directly compressible adjuvant containing lactose and microcrystalline cellulose. *Pharm Dev Technol.* 2003;8(2):175–185. doi:10.1081/PDT-120018487
77. Li JX, Carlin B, Ruszkay T, inventors; FMC Corp, assignee. Co-processed microcrystalline cellulose and sugar alcohol as an excipient for tablet formulations. United States patent US 8,932,629.2015. URL: <https://patents.google.com/patent/US8932629B2/en>.
78. Nathwani S, Vasoya J, Nathwani R. A coprocessed pharmaceutical excipient. International patent WO/2016/046693A1.2016. March 31, 2016. <https://patents.google.com/patent/WO2016046693A1/en?oq=WO%2f2016%2f046693A1>.
79. Pawar H, Kama S, Choudhary P, Gavasane A, Gide P. Process of preparation of coprocessed polymer and its pharmaceutical application. International patent WO 2017/013682 A1.2017. January 26, 2017. <https://patents.google.com/patent/WO2017013682A1/en?oq=WO+2017%2f013682+A1.2017>.
80. Tan Z, Lynch M, Sestrick M, Yaranossian N. Stabilizer composition of microcrystalline cellulose and carboxymethylcellulose, method for making and uses. International patent WO 2013/052114A1.2013. April 11, 2013. <https://patents.google.com/patent/WO2013052114A1/en?oq=WO+2013%2f052114A1.2013>.
81. Norman G, Nuguru K, Amin A, Chandar S. Coprocessed carbohydrate system as a quick dissolve matrix system for solid dosage forms. US patent 7,118,765 B2.2006. October 10, 2006. <https://patents.google.com/patent/US7118765B2/en?oq=US+7%2c118%2c765+B2.2006>.
82. Mehra D, West K, Wiggins J. Coprocessed microcrystalline cellulose and calcium carbonate composition and its preparation. US patent 4,744,987. May 17, 1988. <https://patents.google.com/patent/US4744987A/en?oq=US+4%2c744%2c987A.1988>.
83. Davar N, Kavalakatt P, Pather I, Ghosh S. Polyethylene glycol-coated sodium carbonate as a pharmaceutical excipient and compositions produced from the same. US patent application 2010/0266682 A1. 2010. October 21, 2010. <https://patents.google.com/patent/US20100266682A1/en?oq=US+2010%2f0266682+A1.2010>.
84. Badwan A, Al-Remawi M, Rashid I. Starch silica co-precipitate, method for preparing the same and use thereof. European patent application 1886671A1.2008. February 13, 2008. <https://patents.google.com/patent/EP1886671A1/en?oq=EP+1886671A1.2008>.

85. Tewari D, Titova Y, Beissner B, Durig D. Coprocessed silica coated polymeric composition. US patent US 10,172,944 B2. January 8, 2019. <https://patents.google.com/patent/US10172944B2/en?q=US10172944+B2.2019>.
86. Rigo M, Garcia M, Pina J, Palma S, Allemandi D, Bucala V. Co-processed excipient, obtained by spray-drying, usable as a pharmaceutical excipient or food additive. International patent WO2013175405 A1.2013. November 28, 2013. <https://patents.google.com/patent/WO2013175405A1/en?q=WO2013175405+A1.2013>.
87. de Miguel L, Lander S. High performance excipient comprising co-processed microcrystalline cellulose and surface-reacted calcium carbonate. US patent 20220047511A1. 2022. February 17, 2022. <https://patents.google.com/patent/US20220047511A1/en>.
88. Schaible D, Meijas L. Orally disintegrating excipients. US patent application US 20100285164 A1. November 10, 2010. <https://patents.google.com/patent/US20100285164A1/en?q=US+20100285164+A1.2010>.
89. Modliszewski J, Ballard A. Coprocessed galactomannan-glucomannan. US patent 5,498,436. March 12, 1996. <https://patents.google.com/patent/US5498436A/en?q=US+5498436+A.+1996>.
90. Rojas J, Kumar V. Comparative evaluation of silicified microcrystalline cellulose II as a direct compression vehicle. *Int J Pharm*. 2011;416(1): 120–128. doi:10.1016/j.ijpharm.2011.06.017
91. Gohel MC, Jogani PD. A review of co-processed directly compressible excipients. *J Pharm Pharm Sci*. 2005;8(1):76–93. doi:10.1016/j.ijpharm.2011.06.017
92. Pawar S, Ahirrao S, Kshirsagar S. Review on novel pharmaceutical coprocessed excipients. *Pharm Reson*. 2019;2:14–20. <https://www.pharmaexcipients.com/wp-content/uploads/2019/11/Review-on-novel-pharmaceutical-co-processed-excipients.pdf>. Accessed September 10, 2022.
93. Patel RP. Spray drying technology: An overview. *Indian J Sci Technol*. 2009;2(10):44–47. doi:10.17485/ijst/2009/v2i10.3
94. Deorkar N, Farina J, Miinea L, Randive S. Directly compressible high functionality granular microcrystalline cellulose based excipient, manufacturing process and use thereof. US patent application US 20110092598 A1.2011. April 11, 2011. <https://patents.google.com/patent/US20110092598A1/en?q=US+20110092598+A1.2011>.

Identification of botanicals using molecular biotechnology

Mohd Imran^{1,A–F}, Haya Majid^{2,D,E}, Tasha Riaz^{1,D}, Shayan Maqsood^{1,B}

¹ Department of Pharmacognosy and Phytochemistry, School of Pharmaceutical Education and Research, Jamia Hamdard University, New Delhi, India

² Centre for Translational and Clinical Research, School of Chemical and Life Sciences, Jamia Hamdard University, New Delhi, India

A – research concept and design; B – collection and/or assembly of data; C – data analysis and interpretation;

D – writing the article; E – critical revision of the article; F – final approval of the article

Polymers in Medicine, ISSN 0370-0747 (print), ISSN 2451-2699 (online)

Polim Med. 2023;53(1):69–79

Address for correspondence

Mohd Imran

E-mail: imranidrisi00786@gmail.com

Funding sources

None declared

Conflict of interest

None declared

Received on March 5, 2023

Reviewed on April 5, 2023

Accepted on April 7, 2023

Published online on June 20, 2023

Abstract

The available information on the abundance of restorative plants on earth is incomplete, and the data regarding botanicals from various countries differ significantly. The substantial development of the worldwide natural botanical market is attributable to the expanding revenue of global drug companies trading herbal medicines. This essential type of traditional medical care is depended on by approx. 72–80% of individuals. Even though numerous restorative plants are readily used, they have never been subject to the same strict quality guidelines as conventional drugs. Nonetheless, it is vital to have specific organic, phytochemical, and molecular tools and methods for identifying restorative plant species so that traditional and novel plant products can be safely used in modern medicine. Molecular biotechnology approaches provide a reliable and accurate way to identify botanicals and can be used to ensure the safety and efficacy of plant-based products. This review explores various molecular biotechnology approaches and methods for identifying botanicals.

Key words: genomic DNA, herbal drugs, phytotechnology

Cite as

Imran M, Majid H, Riaz T, Maqsood S. Identification of botanicals using molecular biotechnology.

Polim Med. 2023;53(1):69–79. doi:10.17219/pim/163119

DOI

10.17219/pim/163119

Copyright

Copyright by Author(s)

This is an article distributed under the terms of the Creative Commons Attribution 3.0 Unported (CC BY 3.0)

(<https://creativecommons.org/licenses/by/3.0/>)

Introduction

Evidence on character and safety is of primary importance among different essential factors in the quality verification of plant-based medications. Character refers to botanical identity, authenticity and quality of the plant material used, which requires the avoidance of quality reduction and misrepresentation of herbal medications. Such factors include the presence of harmful constituents, low efficacy or anything else that is related to the fundamental claim that the plant has health-promoting properties.¹

In the context of herbal medications, misrepresentation refers to any deceptive or misleading practices that can occur during the production, labeling, or marketing of herbal products. This can include various forms of misrepresentation, such as:

Substitution: The intentional or unintentional substitution of one plant species with another that may have different therapeutic properties or potential safety concerns. For example, using a cheaper or more readily available plant as a substitute for the desired plant species.

Adulteration: The addition of undeclared substances or contaminants to the herbal product, which can affect its quality, efficacy, or safety. Adulteration can occur by adding lower quality plant material, synthetic compounds, or other substances that are not disclosed on the product label.

False labeling: Providing incorrect or misleading information on the product label, such as inaccurate botanical names, misleading claims about the product's composition or therapeutic effects, or incorrect information about the geographical origin or processing methods.

The morphology (visible with a naked eye) and appearance of plant-based medications have been demonstrated in the literature, yet it should be considered that the validity of a medication cannot be ensured with certainty by identification of plants alone. Indeed, significant experience in pharmacognosics and the utilization of legitimate standardized drugs are also required.²

Scientists can distinguish the complicated ingredients of all basic molecular elements of a natural supplement using imaging modalities and automated high-performance liquid chromatography (HPLC) analysis. Indeed, well-defined HPLC methods using specific markers meet the prerequisites of legitimate science-based verification of natural medications, and fulfilling strict requirements of the International Council for Harmonization Rejection (ICH) regarding potential misrepresentations and corruption of herbal medications for wellbeing reasons should likewise be possible employing such procedures.³

All plants in the world are assigned a genus and species name for portrayal and references in herbaria since the founding of binomial terminology by Carl von Linné in 1753, such as *Chamomilla* (genus), and *recutita* and *inodora* (species). Based on genetic, morphological and structural attributes, subspecies and substance races should also be discerned so that an alternate subjective

and quantitative synthetic structure of constituents can be created.⁴

Consequently, we should reason that surveying the natural properties of herbal medications is a fundamental necessity and should be the primary aim before a plant can be formally included into an authoritative Pharmacopeia.⁵

DNA-based confirmation of natural plants

Recently, therapeutic plants have become popular in Western nations, where the desire to use natural remedies has developed and such use is now considered an option by doctors and patients. There has been evidence of increasing interest in herbal drugs (natural preparations) as they are easily available and can be generally utilized as medicines with possibly lesser side effects in comparison to synthetically derived drugs. As such, they are protective and do not cause any antagonistic effects. Nonetheless, the natural origin of herbs does not guarantee their safety. Some herbs may have intrinsic toxicity, and there is a risk of substitution, contamination, and adulteration of herbal products. Additionally, misidentification of plant species can occur, especially considering the wide variety of species used in herbal medicine. These factors can have potential adverse effects on the quality and safety of botanical products.⁶

It has been demonstrated that contamination or substitution of herbs has caused illness and even deaths. A case of neuropathy and encephalopathy was recorded after the administration of a preparation derived from the herb *Gentiana rigescens radix*. Further examination revealed that poisoning had occurred due to contamination by *Podophyllum emodi* or *Podophyllum hexandrum*, which contain the neurotoxin podophyllotoxin and were found growing underneath the original preparation. A few instances of renal injury related to *Stephania tetrandra* in a weight reduction formulation were caused by *Aristolochia fangchi*, which contains the highly poisonous aristolochic acid, a nephrotoxin that causes urethral cancer, among others. In this case, the confusion arose from the similarity of the 2 plants in Chinese nomenclature.⁷

Consequently, to guarantee the quality and efficacy of natural medications, and ensure the wellbeing of the patients, identifying the plant species is essential. However, distinguishing natural components, which regularly comprise dried or prepared parts, is by and large troublesome due to the change of characteristics through drying, particularly when a herb has more than 1 name or when a common name is used for more than 1 herb.⁸

Validation of natural material on the DNA level

Genetics are thought to provide unwavering quality in the verification of natural materials at the DNA level due

to the advances in molecular biotechnology and plant genetics. Moreover, the use of DNA-based molecular marker methods for understanding species of therapeutic plants is still expanding. Such improvements are particularly helpful for identifying species that are regularly confused or adulterated with other plants, and for species that are morphologically or phytochemically indistinguishable.⁹

The DNA is a remarkably stable macromolecule that is not influenced by external factors, meaning that it can be recovered from fresh, dried and prepared natural materials. In contrast, substance fingerprinting is unequivocally influenced by the sample age, physiological conditions, environmental impact development region, reaping period, drying, and storage conditions. Moreover, the DNA marker particles are not tissue-specific and, in this way, can be distinguished at all phases of organic growth. Also, a modest quantity of a sample is adequate for examination.¹⁰ Table 1 presents a comparison of DNA profiling techniques for herbal authentication and quality control.

Types of DNA markers utilized in plant genome analysis

The DNA-based molecular strategies that have been utilized to assess DNA polymorphisms for plant taxa verification include hybridization polymerase chain reaction (PCR) and sequencing techniques. Currently, multi-locus sequence analysis (MLSA) is frequently used in phylogenetic investigations and has demonstrated its discriminatory ability. In addition, recent improvements in the sensitivity

of high-throughput DNA microarrays have allowed for the definitive identification of taxon on a larger scale.¹¹

Random amplified polymorphic DNA

Random amplified polymorphic DNA (RAPD) method employs arbitrarily arranged short-engineered oligonucleotides (10 bp long) as primers to produce countless random DNA fragments using PCR. The enhanced DNA segments are separated with the use of agarose gel electrophoresis and visualized using ethidium bromide dye or SyBRgreen. The polymorphisms in the enhanced fragments are brought about by:

- 1) base replacement or excision at the preparation sites,¹²
- 2) primer insertions at loci too far apart to result in amplification or¹³
- 3) insertions or deletions that change the size of the amplified fragment.¹⁴

Due to its ease of use (no prior DNA sequence information is required), low expense, ability to produce a high volume of DNA markers within a brief time frame, and the use of non-complex equipment, RAPD has a wide scope of applications.¹⁵

Arbitrarily primed PCR

Arbitrarily primed PCR (AP-PCR) is a distinct form of RAPD that uses single primers of 10–50 bps in length during a 3-stage amplification process. The initial 2 annealing cycles are completed in a low-stringent environment, with the main cycle employing high-stringency conditions and primers of various length. Polyamide gel

Table 1. Comparison of DNA profiling techniques for herbal authentication and quality control.¹ The table is based on the most frequent molecular tools and does not represent all DNA-based molecular techniques²⁷

Molecular technique	Importance of authenticity	Reproducibility	Quantity of DNA required	Level of polymorphism	Locus specificity	Technical demand	Sequence information required	Automation	Development cost	Running cost
ISSR	++	medium	low	medium	no	low	no	yes	low	low
AFLP	++	high	medium	medium	no	medium	no	yes	medium	low
ARMS	++	high	high	low	yes	low	yes	yes	low	medium
RAPD	+	low	low	medium	no	low	no	yes	low	low
RFLP	+	high	high	medium	yes	high	yes	no	high	medium
SSR	+	high	low	high	no	low	yes	yes	medium	high
RAMPO	+	medium	low	medium	yes	high	no	yes	medium	medium
CAPS	++	high	low	low	yes	low	yes	yes	low	medium
SCAR	++	high	low	low	yes	low	yes	yes	low	medium
CAPS	++	high	low	low	yes	low	no	difficult	medium	medium
LAMP	+	high	low	low	yes	medium	yes	yes	low	medium
SNP	+	high	low	high	yes	medium	yes	yes	low	high
Microarray	+++	high	low	high	yes	high	yes	yes	high	high
Barcoding	+++	high	low	low	yes	medium	yes	yes	medium	medium

ISSR – inter simple sequence repeat; AFLP – amplified fragment length polymorphism; ARMS – amplification-refractory mutation system; RAPD – random amplified polymorphic DNA; RFLP – restriction fragment length polymorphism; SSR – simple sequence repeats; RAMPO – random amplified microsatellite polymorphism; CAPS – cleaved amplified polymorphic sequences; SCAR – sequence-characterized amplified regions; LAMP – loop-mediated isothermal amplification; SNP – single nucleotide polymorphism.

electrophoresis is chiefly used to examine the obtained products. This method is utilized in a variety of genetic investigations and for species identification. However, similar to RAPDs, fingerprints produced using single primers can cause reproducibility issues since slight changes in cycling conditions can affect the appearance of the bands.¹⁶

DNA amplification fingerprinting

As an adaptation of the RAPD strategy, the technique of DNA amplification fingerprinting (DAF) in thermostable conditions allows primers to efficiently enhance amplification at multiple random sites on each DNA strand and to produce fingerprints with novel DNA patterns. Polyacrylamide gels and silver staining are used to resolve the amplicons.¹⁷

Inter simple sequence repeats

Inter simple sequence repeats (ISSRs), or single primer amplification reaction (SPAR) markers, are exceptionally adequate, replicable, profoundly polymorphic, and advantageous to use in higher plants. They are utilized in genetic fingerprinting, quality labeling, phylogenetic investigation, species and cultivator identification, and the evaluation of hybridization. The ISSRs resemble RAPDs, though ISSR primers are located in microsatellite (SSR) regions and are longer in length (around 14 bp) than RAPD primers. The procedure uses basic sequence repeats (the ISSRs) with mono-, di- or trinucleotide repeats of 4–10 repeating units. The SSRs are abundant and highly polymorphic, and are distributed throughout the genome. Moreover, this method is efficient and more conservative. Also, the technique does not require sequencing data and does not use radioactive material.¹⁸

Amplified fragment length polymorphism

An amplified fragment length polymorphism (AFLP) is a powerful tool that combines RFLM and PCR for DNA fingerprinting of the organismal genome and can screen countless loci (ca. 50–100 parts for each response) for polymorphisms. Similar to ISSR, AFLP does not require prior sequencing data for the targeted genome and is exceptionally reproducible. It is utilized for DNA fingerprinting, usually when very little data is available on the plant genome under study. Some advantages of AFLP include the rapid procedure, high genomic bounty, low labor requirements, abundant data, high reproducibility, and the ability to detect a high number of loci in a single reaction. Furthermore, no information about the target genome is required for preliminary development.¹⁹

Random amplified microsatellite polymorphism

Random amplified microsatellites (RAMS), or random amplified hybridization microsatellite (RAHM), is a mix

of arbitrarily prepared PCR microsatellites (RAPDs) used for hybridization and production of polymorphic hereditary fingerprints, and does not require prior genomic information. As in RAPDs, the genomic DNA is initially amplified with a single random 10-mer primer or microsatellite-complimentary 15- to 16-mer PCR primer. This method produces highly reproducible banding patterns, which allow for clear identification of species-specific groups. Furthermore, random amplified microsatellite polymorphism (RAMPO) fragments are less sensitive to error than RAPD fragments due to their homology and the strong signal produced from the hybridization of distinct polymorphisms (i.e., the existence of repeat sequences in a particular microsatellite). The RAMPO is, for the most part, utilized for the identification and separation of genotypes within germplasms and populaces, such as *Ficus* and *Phoenix dactylifera*.²⁰

Restriction fragment length polymorphism

Restriction fragment length polymorphism (RFLP) is widely utilized for recognizing changes at the DNA level and depends on the correlation of banding patterns from DNA sequences digested by specific restriction enzymes (e.g., HaeIII, EcoRI, BamHI). These enzymes are a class of endonucleases produced by microorganisms that can digest specific DNA sequences, with each protein recognizing a particular palindromic sequence. They detect and digest the DNA in a predictable manner, which generates restriction fragments of defined lengths. The length of these fragments varies between species if there are differences between the cleavage loci of a specific restriction endonuclease. Restriction sites are detected and then altered by point mutation, insertion, deletion, or translocation to produce distinct fragments that are separated and detected using gel electrophoresis. A few drawbacks of this method are that it is time-consuming, expensive, requires extensive labor, and needs large amounts of DNA.²¹

Microsatellites or single sequence repeats

Microsatellites, short tandem repeats (STRs), or simple sequence length polymorphisms (SSLPs), are the smallest class of monotonous DNA sequences and have 2–6 bps. They are dispersed throughout most eukaryotic genomes, meaning there is a wide variety in the quantity of repeating units that are profoundly polymorphic. Microsatellites have a broad assortment of uses, such as marker-guided reproduction, population genetics and genome mapping. Indeed, the marker sequence and the extensive number of alleles allow for the detection of significant degrees of similarities and differences between closely related species or strains. A few downsides of microsatellites are that their use is time-consuming, and when the target DNA is unknown, there are high costs associated with the isolation and separation of each locus.²²

Selectively amplified microsatellite polymorphic loci

The selectively amplified microsatellite polymorphic loci (SAMPL) strategy encompasses the high multiplexing ratio of the AFLP method and the high degree of microsatellite polymorphisms. The method uses AFLP-type primers matched to a complementary microsatellite primer to detect polymorphisms using restriction digestion and selective amplification. The microsatellite primer restriction fragments that have linked adapter sequences are then amplified through primers complementary to the adapter sequences. A restriction of multi-locus SSR profiling is that it only detects a portion of the microsatellite polymorphisms due to the prevalence of predominant markers, which makes it difficult to distinguish allelic sections in complex DNA fingerprints.²³

Directed amplification of minisatellite-region DNA

The directed amplification of minisatellite-region DNA (DAMD) strategy is essentially a DNA fingerprinting technique in which the loci of variable number tandem repeats (VNTR) of hypervariable repeats are enhanced at moderately high stringencies. The double repeat DNA sequences in minisatellites and VNTR are longer (around 10–60 bp themes) than microsatellites, though microsatellites display extensive polymorphisms due to their duplicate number of double repeat loci. The VNTR central sequence is utilized as a primer to coordinate the amplification of minisatellite loci DNA using PCR and can provide data similar to RAPD for species identification.⁹ However, with the utilization of longer primers in DAMD, enhanced DNA fingerprinting is produced, and consequently, DAMD is more reproducible than RAPD.²⁴

Single nucleotide polymorphisms

Single-base pairing locations in the genotypes of a minimum of 2 persons are termed single nucleotide polymorphisms (SNPs), at which various alleles are available. Single-base pair contrasts are created between DNA sequences through polymorphisms caused by point transformation. The SNPs are used for identifying people, ecotypes and species, and are proficient molecular markers for genetic examination and rearing projects. Environmental and transformative investigations also use SNPs. Furthermore, some molecular markers depend on SNPs, such as RFLPs, cleaved amplified polymorphic sequences (CAPS), amplification-refractory mutation system (ARMS), and single-strand conformation polymorphism (SSCP). Many great SNP sequences in exemplar DNA have been demonstrated in DNA microarrays (biotechnology organizations). Furthermore, SNPs are applied to the verification of *Perilla*, *Dendrobium officinale*, *Panax* cultivars, and *Boehmeria* species.²⁵

Amplification-refractory mutation system

Amplification-refractory mutation system, or allele-specific polymerase chain response (AS-PCR), is a method for separating alleles. It is a simple, versatile and powerful technique for the detection of minor deletions or transformations, including SNPs. It uses a dynamic screening test that does not require any type of marking, because agarose gel electrophoresis and ethidium bromide staining are utilized for basic visualization of the amplified product. However, oligonucleotides with a random 30-mer sequence will not function as a PCR primer in the ARMS. Another disadvantage of the ARMS method is that it only amplifies the test DNA at the objective allele and does not enhance the non-target allele. In this procedure, the enhancement and approval steps are joined to such an extent that the presence or absence of the objective allele is analyzed by the presence or absence of a PCR product. Nonetheless, this procedure has been applied to the validation of *Alisma*, *Panax*, *Rheum*, *Dendrobium*, and *Curcuma*.²⁶

Cleaved amplified polymorphic sequence

Cleaved amplified polymorphic sequence (CAPS) detects polymorphisms using a combination of target DNA amplification and restriction enzyme digestion in a 2-stage process. In the initial step, amplification of a characterized sequence uses specific 22–25-bp primers and is followed by restriction of the PCR product using suitable enzymes. Agarose gels and ethidium bromide are then used to isolate the separated restriction fragments. The capacity to distinguish DNA polymorphisms is higher for SSRs and AFLPs than for CAPS due to the limited size of the restriction fragments and the nucleotide changes that are fundamental for CAPS identification. For validation of *Astragalus*, *Alisma*, *Duboisia*, *Sinopodophyllum*, *Dysosma*, *Fritillaria*, *Ephedra*, *Artemisia*, *Panax*, *Actinidia*, *Attractylodes*, *Glehnia*, *Dendrobium*, and *Codonopsis*, PCR-RFLP has been used.²⁷

Sequence-characterized amplified regions

Sequence-characterized amplified regions (SCAR) are another type of RAPD-determined molecular that avoids many of the shortcomings of RAPDs. Cloned polymorphic RAPD or ISSR fragments with specific oligonucleotide primers are utilized alongside SCAR markers to rapidly enhance nucleic acids indicative of natural materials. Polymorphic regions from the cloned RAPDs or ISSRs are selected from known sequences and used as primers to amplify and map SCAR markers. The SCAR recognize just a single locus, their amplification is less sensitive to reaction conditions, and they tend to exhibit dominance due to a partial overlap with the primers, so they are invaluable over RAPD markers. This strategy has been used for validation of *Panax* and separation of types of *Artemisia*,

Phyllanthus, *Pueraria*, *Sinocalycanthus*, *Embelia*, and *Lycium*.²⁸

Single-strand conformational polymorphism

Single-strand conformational polymorphism is a transformation procedure. Under denaturing conditions, this method results in single-stranded DNA (ssDNA) folding into a tertiary conformation. The ssDNA is changed into the tertiary structure through the interaction of nucleotides in the DNA sequences, which also influence the mobility of the ssDNA during gel separation, with differences in bands indicating SNPs. The F-SSCP is a modified form of SSCP that includes the enhancement of the target sequence using fluorescent probes, and although this technique is not often applied for verification, it has been used for validating *Boesenbergia*.²⁹

Methylation-sensitive amplified polymorphism

Methylation-sensitive amplified polymorphism (MSAP) is a modified AFLP method developed to screen genomic DNA methylation. The methylation-sensitive chemicals HpaII and MspI are used twice to digest genomic DNA, followed by the methylation-insensitive EcoRI. The digested samples are ligated using double-stranded DNA (dsDNA) adapters, pre-amplified using pre-selective or non-selective primers, and then amplified using a pair of selective primers. The MSAP was first developed to identify DNA methylation processes in dimorphic parasites and later adjusted for the recognition of cytosine methylation in the rice genome, pepper, apples, and Siberian ginseng.⁷

Loop-mediated isothermal amplification

Loop-mediated isothermal amplification (LAMP) is used to enhance target nucleic acids with high specificity and efficacy and is done under isothermal conditions. The method uses an auto-cycling process to segment and displace DNA, followed by hybridization carried out by a DNA enzyme with high helix displacement activity. It was applied to identify *Panax ginseng* and to distinguish the plant from *Panax japonicus* using *Ginseng radix*. It was subsequently utilized to pinpoint sites of *Lophophora williamsii* and *Curcuma longa*.³⁰

Strand displacement amplification

Constraints of PCR-based methods for differentiating plants come from their low latency, though hybridization-based microarrays offer a rapid, high-throughput tool for genotype identification. In this regard, strand displacement amplification (SDA) is a technique created using combined genomics. The DNA library consists of 49 angiosperm

plants in which all non-angiosperm genomic DNA was extracted using the Clontech® PCR-Select™ complementary DNA (cDNA) Deduction unit (Takara, Shiga, Japan). The SDA is superior to regular molecular identification techniques in terms of exactness, versatility and efficacy, as well as being high-throughput with expansive applications. Moreover, the technique exhibits substantial potential for genotyping, as demonstrated by the extraction of the non-angiosperm DNA. This review demonstrates the capability of setting up a high-throughput microarray-based autonomous genotyping procedure of significant angiosperm clades. The SDA procedure was suitable for 2 separate ginseng species, *P. ginseng* and *Panax quinquefolius*, which are often blended and contaminated. Furthermore, SDA was sufficiently sensitive to identify contamination debasement of 10% *P. quinquefolius* in *P. ginseng*.³¹

Multiplex ligation-dependent probe amplification

Multiplex ligation-dependent probe amplification (MLPA) is a semi-quantitative PCR-based method suitable for identifying clinical plants, and is a popular research tool because of its minimal expense and versatility. It utilizes the versatility of the PCR, though it broadens the specificity by including an important ligation step which ensures only DNA sequences that have been hybridized are detected. A typical PCR primer is used for the amplification of all target sequences, which is a critical element that ensures the general evaluation of each focus against a control sample.³²

Ongoing polymerase chain reaction

Continuous quantitative PCR is a widely used method for measuring nucleic acids in molecular diagnostics. It offers advantages such as sensitivity, specificity and reproducibility. However, like any diagnostic method, it has its limitations. These limitations may include issues related to primer design, sample quality, amplification efficiency, and the potential for false-positive or false-negative results. It is important to carefully consider these limitations and optimize the experimental conditions in order to ensure accurate and reliable results when using continuous quantitative PCR in molecular diagnostics. It has become the principal specialized stage for nucleic acid discovery both in research and routine diagnostics. By estimating the buildup of amplified products during the PCR using fluorescent technology, it can identify a specific DNA sequence in a sample. The process has been used for the routine validation of the Chinese medicinal plant *Cimicifuga foetida* and its 4 substitutes: *C. simplex*, *C. dahurica*, *C. heracleifolia*, and *C. acerina*, through examination of recombinant DNA (rDNA) using an inner translated spacer (ITS) and fluorescence liquefying bend

investigation. In addition, continuous PCR has been used to investigate debasements of the genera *Euphorbia*, *Gentiana* and *Drynaria*.³³

DNA sequencing analysis

The Sanger dideoxy-sequencing method was designed in the 1970s and is used for DNA sequencing. It is the most common way of generating reads of the bases or nucleotides, such as A, T, G, and C, of a specific molecule of DNA. The DNA is duplicated through chromosomal replication and can be carried out using capillary electrophoresis, in a cylinder, or on a microtiter plate with very small samples. The sequence read length is 50–1000 bps. If the loci to be sequenced outperforms the length of a standard sequencing read, internal reactions must be utilized to reproduce the total sequence of a more drawn-out DNA region.³⁴ Most DNA sequencing methods utilize slim electrophoresis to isolate DNA particles dependent on their size and fluorescent probes for labeling and identifying the 4 bases. Currently, Sanger dideoxy-sequencing is a widely used method in molecular biology with various applications. It is particularly valuable in studying phylogenetic relationships, population genetics, systematics, and advancing our understanding of genetic diversity. By sequencing DNA samples using the Sanger method, researchers can compare sequences and analyze genetic variations within and between populations. This information helps in elucidating evolutionary relationships, determining genetic markers, and studying the genetic basis of various traits or diseases. The versatility of Sanger dideoxy-sequencing allows researchers to explore a wide range of genetic questions and make significant contributions to the fields of phylogenetics, population genetics, systematics, and molecular biology as a whole. The sequencing examinations dependent on molecular ITS have been applied to *Panax*, *Yamaji*, *Fritillaria*, *Asarum*, *Astragalus*, *Dendrobium*, *Leonurus*, *Perilla*, *Phyllanthus*, *Rehmannia*, *Salvia*, *Swertia*, *Plantago*, *Bupleurum*, and *Euphorbia*. For validation of *Adenophora*, *Aconitum*, *Angelica*, *Astragalus*, *Curcuma*, *Epimedium*, *Fritillaria*, *Crocus*, *Ligularia*, *Pueraria*, and *Saussurea*, a 5S rDNA intergenic spacer marker has been utilized. Also, 18S rDNA has been evaluated in *Dioscorea*, *Pinellia* and *Panax* from atomic DNA.³

DNA barcoding

DNA barcoding is a novel molecular and bioinformatics tool with enormous scope. It is intended to provide fast, precise, automatable, and accurate species identification with high validity. This innovation requires a novel nucleotide sequence of small DNA fragments (400–800 bps), which are then used with specific reference sequences to distinguish samples and find unknown taxa. Also, it utilizes a shorter hereditary indicator from a regular locus (similar to a creature's plastidial DNA, atom or mitochondria).

The ideal DNA marker should be useful for a wide scope of taxa (expansiveness of order application), readily retrievable with an all-inclusive preliminary duo, be sufficiently brief to be open to bidirectional sequencing, and provide exceptional grouping and maximal separation among species. The key example is the genus *Dendrobium* (Orchidaceae), which is represented by 78 varieties within Chinese botanical system, with 14 endemics. However, wide surface areas coupled with great morphological variability render species identification challenging.¹⁶

In light of preparation techniques, *Herba dendrobii* is characterized as a new *Dendrobium* as well as “Fengdou Shihu”, along with “Huangcao Shihu”, as it is the dominant type of *Herba dendrobii* in traditional Chinese medicine (TCM). A further noteworthy model where different varieties are utilized in TCM is the genus *Fritillaria* (Liliaceae), which incorporates 24 varieties and 15 species and is endemic in China. *Bulbus fritillariae* is the most famous homegrown prescription in China and is being utilized as an antitussive and expectorant herb.³⁵ The *Fritillaria* genus encompasses several species that are utilized in TCM, including *F. thunbergii*, *F. cirrhosa*, *F. unibracteata*, *F. przewalskii*, *F. delavayi*, *F. ussuriensis*, *F. walujewii*, *F. pallidiflora*, *F. hupehensis*, *F. anhuiensis*, and *F. puqiensis*. These species may have similar names, making it challenging for buyers to distinguish between them. Additionally, there may be a lack of specific and distinct attributes or characteristics associated with each species, further adding to the confusion. It is important to ensure accurate identification and quality control of these substances (the plant components) used in TCM to maintain their safety and efficacy. Therefore, for quality control and normalization of *Fritillaria* as a natural medication, DNA barcoding is the main reliable technique for the identification of accurate species.³⁶

DNA microarrays (DNA chip technology)

The innovative “biochip” technology is intended to recognize fluorescently marked DNA or ribonucleic acid (RNA) fragments through their hybridization to oligonucleotides. The DNA microarray innovation offers a high pace of creation for the simultaneous assessment of numerous qualities in many taxa. This innovation is utilized for the identification and confirmation of natural medications, though we need to distinguish particular DNA sequences of interest in every species to design a standard test on a chip to use for comparisons. The DNA fragments of a normal sample are immobilized and organized on a microarray and attached with glass slides, silicon or nylon layers.³⁷

Presently, DNA chip technology has been applied for the identification of different types of *Fritillaria*, *Dendrobium* and *Bupleurum*. Species-specific oligonucleotide assays were obtained through the 5S ribosomal RNA quality of *Euphorbia kansui*, *Pinellia ternata*, *Teucrium*

divaricatum, *Pinellia cordata*, *Aconiti kusnezoffii*, *Typhonium giganteum*, *Croton tiglium*, *Dysosma tatula*, *Dysosma pleiantha*, *Dysosma versipellis*, *Hyoscyamus niger*, *Pinellia pedatisecta*, *Datura innoxia*, *Rhododendron molle*, *Strychnos nux-vomica*, *Alocasia macrorrhiza*, *Datura metel*, and *Aconitum carmichaeli*.³⁸

Examples of DNA-based validation of natural plants

Olive oil is sold with 20% or more fake oils, and as artificial and unsaturated fats are similar, it is difficult to separate them using standard methods. However, the complete genomic DNA was isolated using olive oil mixed with sunflower oil and canola, and was investigated for SNPs in non-coding loci of *psbA-trnH* and the incomplete coding area of the *matK* plastid. The amplification of these DNA loci was completed with specific primers using PCR, and the obtained DNA sequences were aligned to standardized tag sequences of the canola and sunflower oil DNA. This combination of molecular science methodology and bioinformatics technology is a practical strategy for guaranteeing the purity of olive oil by aligning contaminated DNA fragments with their standardized DNA after blending canola and sunflower oil into olive oil. Adulteration of up to 5% in olive oil can be quickly detected using this plastid-based sub-atomic DNA innovation.³⁹

The genome sequence of *Parthenium argentatum* plastid was shown to have 152,803 bps. In addition, it was demonstrated that the genomic configuration of the *P. argentatum* chloroplast is similar to that of *Helianthus annuus*, based on the general connection of specific protein expression patterns. Unlike *Guizotia abyssinica*, *H. annuus* and *Lactuca sativa*, *P. argentatum* (guayule) is a latex-producing woody shrub and was marketed to individuals with type I latex hypersensitivity as a hypoallergenic protectant. The total chloroplast genomes of *L. sativa*, *H. annuus* and *G. abyssinica*, along with the plastid genome of *P. argentatum*, have more modest 3.4 kb reversals compared to the larger 23 kb *matK* and *psbA-trnH* spacer chloroplast DNA used for the standard identification of other *Parthenium* species: *P. schottii*, *P. argentatum*, *P. hysterophorus*, and *P. tomentosum*. When contrasted with the sequences of plastid genomes, namely *L. sativa*, *G. abyssinica*, *H. annuus*, and *Asteraceae*, the DNA-based validation method revealed distinction through the development of the 4 genomes. The improvement in chloroplast-specific DNA standardized probes was then used to identify *Parthenium* varieties.⁴⁰

The RAPD has been widely used for the detection of genetic inconsistencies within plants. This approach was initially utilized to genetically identify 11 arid species of plants, including *Bassia eriophora*, *Caylusea hexagyna*, *Sonchus oleraceus*, *Zilla spinosa*, *Lycium shawii*, *Rumex vesicarius*, *Zygophyllum propinquum* ssp. *migahidii*, *Andrachne telephioides*, *Achillea fragrantissima*,

Withania somnifera, and *Moricandia sinaica*, gathered in various areas of Saudi Arabia. Five primers were used to amplify the plant species DNA, and the RAPD profiles increased from 307 to 1772 bps. Pairwise comparisons between promotions, given the extent of shared homology created by the primers used, were determined with the assistance of the StatistixL program v. 1.7 (<https://www.statistixl.com/download/>) using Jaccard's similarity coefficient. A significant value of 0.32 was shown between *L. shawii* and *A. fragrantissima*, and a least pairwise likeness of 0 was seen between *A. telephioides*, *Z. spinosa*, *B. eriophora*, *B. eriophora*, and *Z. propinquum* when the 5 primers were consolidated.⁴¹

Boerhavia diffusa, also called Punarnava, is a herb native to India and is frequently used in traditional Indian medicine. Precise identification and clustering of *B. diffusa* are critical for improving the adequacy and biosafety of the medications prepared with the use of this herb. The DNA barcoding strategies are used to identify and isolate *B. diffusa* through closely related species. The phylogenetic examination of the 4 types of *Boerhavia* with potential for tagging included ribosomal DNA locales ITS, ITS2, ITS1, and the chloroplast plastid *psbA-trnH*. Grouping arrangement uncovered 26% polymorphic regions in ITS, 30% in ITS1, 16% in ITS2, and 6% in *psbA-trnH*, separately. A phylogenetic tree was built for 15 varieties using the ITS sequences that differentiated *B. diffusa* from different species. The ITS1 had a higher change/transversion proportion, level of variety and pairwise distance, which separate *B. diffusa* from different types of *Boerhavia*. The concentrate uncovered that the potential candidate regions that could be utilized for distinguishing *B. diffusa* and verifying its natural products were ITS and ITS1.⁴²

Valerian (*Valeriana officinalis*) is a therapeutic herb generally utilized as a gentle sedative and anxiolytic. Among the vast number of synthetic constituents (such as flavonoids, alkaloids, terpenoids, and iridoids) found in valerian root, the active ingredients that are liable to have a soothing effect are valerenic acid (C15 sesquiterpenoid) and valerena-4,7(11)-diene. The NGS (Roche 454 pyrosequencing; Roche Diagnostics, Basel, Switzerland) was used to generate 1 million record reads of valerian roots to identify an active terpene synthase. Two sesquiterpene synthases were identified (VoTPS1 and VoTPS2) from the collected records, both of which demonstrated dominating articulation designs in the root. Transgenic yeasts VoTPS2 and VoTPS1 delivered germacrene C/germacrene D and valerena-4,7(11)-diene, separately, as significant terpene products. Purified VoTPS1 and VoTPS2 recombinant proteins affirmed these actions in vitro with pharmacokinetics (K_m of $\sim 10 \mu\text{M}$ and k_{cat} of 0.01 s^{-1}) shown for the 2 chemicals. The design of the valerena-4,7(11)-diene created from the VoTPS2 signals was additionally validated through ^{13}C -nuclear magnetic resonance (NMR) along with gas chromatography-mass spectrometry (GC-MS) in correlation with an engineered standard. Kumar et al.

described a methodology that includes cutting-edge sequencing and the use of metabolically designed organisms to understand terpenoid variety in restorative plants.⁴³

Phyllanthus (Euphorbiaceae) varieties, well known due to their hepatic defensive action, are used in a few traditional medicines in native medical services in India. They are traded as crude homegrown medications. Samples of *Phyllanthus* that are used in crude drugs were acquired from 25 shops in south India and consisted of 6 unique varieties, such as *Phyllanthus amarus*, which were identified by examining their morpho-taxonomical properties and through molecular investigations. Testing revealed that 76% of the pharmaceutical assays consisted of *P. amarus* at a purity >95%, without admixtures. The remaining 24% of shops had 5 distinct species of *Phyllanthus*, including *P. maderaspatensis*, *P. fraternus*, *P. debilis*, *P. kozhikodiana*, and *P. urinaria*. The chloroplast DNA region, psbA-trnH, was used to generate species-specific DNA standardized tag marks for *Phyllanthus* species. The DNA scanner tag psbA-trnH locus of the chloroplast can successfully isolate *Phyllanthus* species and can be subsequently utilized to determine species admixtures in the raw drugs made from *Phyllanthus*.⁴⁴

In this specific case, *Ruta graveolens*, which is sold as a dried restorative herb, was found to be contaminated with *Euphorbia dracunculoides*. The contamination of *Ruta graveolens* with *Euphorbia dracunculoides* represents an instance where the intended herb was adulterated or substituted with another species. This contamination highlights the importance of quality control and proper identification of herbs to ensure their safety and efficacy for consumers. The genomic DNA was extracted from leaves (100 mg each) using a modified cetyltrimethylammonium bromide (CTAB) protocol. The ITS sequences of ribosomal DNA (nrDNA-ITS) and chloroplast spacer sequences (rpoB and rpoC1) have favorable plant DNA barcoding qualities. These spacer groupings were amplified, sequenced and confirmed with a Basic Local Alignment Search Tool (BLAST) search. The sequence arrangements were made using ClustalX (<http://www.clustal.org/clustal2/>) to search for contrasts in the groupings. A DNA marker was then created dependent on rpoB and rpoC1 of the nrDNA-ITS to detect the *E. dracunculoides* contaminants in the *R. graveolens* samples. *Ruta graveolens* (289 and 264 bps) and *E. dracunculoides* (424 bps) sequences were created through different groupings of the nrDNA-ITS and amplified to accelerate the verification cycle. This marker effectively recognized the species in extricated assays using just 5 ng DNA/ μ L.⁴⁵

Future developments

The development of new computerized methods and specific instruments for DNA examination, such as smaller-than-expected sequencing, nanoscale DNA

sequencing, microsphere-based suspension cluster, and cutting-edge sequencing, will bring about further innovations. Other promising advancements include nanopore technology for the highly precise identification of DNA bases, and Zenith, an enzymatic genotyping tool for investigating tens to thousands of genomic variations in a single multiplexed response. Another emerging technique is the oligonucleotide ligation assay (OLA), which has a broad scope in the multiplex examination of nucleic acid sequences, and can discover known single SNPs and separate alleles in polymorphic genes. These novel ways to deal with DNA sequencing guarantee deep genomic investigation, exhibit a high multiplexing limit, and open up many new ways for genotyping and future taxon identification.⁴⁶

The new high-throughput sequencing (HTS) advances allow for the development of new molecular methodologies. An equal sequencing innovation, delivering a large number of DNA sequences (altogether 0.5–60 giga base sets) in a solitary run, has transformed genomic research in science and medicine. These cutting-edge sequencing stages, such as the Roche 454, Illumina, Solexa, Helicos, and Applied Biosystems framework, can arrange DNA quicker and at much lower costs than the standard 96-well setup of Sanger sequencing.⁴⁷


Cutting-edge sequencing strategies such as NGS can help answer new and long-standing questions. Even though no “third generation” methods have been made monetarily accessible yet, a few organizations have advanced models that propose dynamic concepts.⁴⁸

Conclusions


The effort to identify specific types of medicinal plants and produce both conventional and novel natural compounds suitable for use in medical science requires accurate botanical, phytochemical and biochemical recognition methods.

ORCID iDs

Mohd Imran  <https://orcid.org/0000-0001-7349-3019>

Haya Majid  <https://orcid.org/0000-0003-1439-1172>

Tasha Riaz  <https://orcid.org/0000-0002-4785-9715>

Shayan Maqsood  <https://orcid.org/0000-0003-1985-6581>

References

1. Wagner H, Ulrich-Merzenich G, eds. *Evidence and Rational Based Research on Chinese Drugs*. Vienna, Austria: Springer Vienna; 2013. doi:10.1007/978-3-7091-0442-2
2. Skalli S, Bencheikh RS. Safety monitoring of herb-drug interactions: A component of pharmacovigilance. *Drug Saf*. 2012;35(10):785–791. doi:10.1007/BF03261975
3. Li S, Han Q, Qiao C, Song J, Lung Cheng C, Xu H. Chemical markers for the quality control of herbal medicines: An overview. *Chin Med*. 2008;3(1):7. doi:10.1186/1749-8546-3-7
4. Altukhov Y, Salmenkova E. DNA polymorphism in population genetics [in Russian]. *Russian J Genet*. 2002;38(9):989–1008. doi:10.1023/A:1020288812170

5. Chawla H. *Introduction to Plant Biotechnology*. 3rd ed. Boca Raton, USA: CRC Press; 2011. doi:10.1201/9781315275369
6. Zhao Z, Hu Y, Liang Z, Yuen J, Jiang Z, Leung K. Authentication is fundamental for standardization of Chinese medicines. *Planta Med*. 2006;72(10):865–874. doi:10.1055/s-2006-947209
7. Lian CL, Wadud MdA, Geng Q, Shimatani K, Hogetsu T. An improved technique for isolating codominant compound microsatellite markers. *J Plant Res*. 2006;119(4):415–417. doi:10.1007/s10265-006-0274-2
8. Kumar P, Gupta V, Misra A, Modi D, Pandey B. Potential of molecular markers in plant biotechnology. *Plant Omics*. 2009;2(4):141–162. https://www.pomics.com/Pradeep_2_4_2009_141_162.pdf. Accessed February 15, 2023.
9. Silva LM, Montes De Oca H, Diniz CR, Fortes-Dias CL. Fingerprinting of cell lines by directed amplification of minisatellite-region DNA (DAMD). *Braz J Med Biol Res*. 2001;34(11):1405–1410. doi:10.1590/S0100-879X2001001100005
10. Heath DD, Lwama GK, Devlin RH. PCR primed with VNTR core sequences yields species specific patterns and hypervariable probes. *Nucl Acids Res*. 1993;21(24):5782–5785. doi:10.1093/nar/21.24.5782
11. Hamilton AC. Medicinal plants, conservation and livelihoods. *Biodivers Conserv*. 2004;13(8):1477–1517. doi:10.1023/B:BIOC.0000021333.23413.42
12. Luo YM, Zhang WM, Ding XY, et al. SNP marker and allele-specific diagnostic PCR for authenticating herbs of Perilla [in Chinese]. *Yao Xue Xue Bao*. 2006;41(9):840–845. PMID:17111830.
13. Ding G, Zhang D, Feng Z, Fan W, Ding X, Li X. SNP, ARMS and SSH authentication of medicinal *Dendrobium officinale* KIMURA et MIGO and application for identification of Fengdou drugs. *Biol Pharm Bull*. 2008;31(4):553–557. doi:10.1248/bpb.31.553
14. Warriar RR, Joshi G, Arunkumar AN. DNA fingerprinting in industrially important medicinal trees. *Ann Phytomed*. 2019;8(1):19–35. doi:10.21276/ap.2019.8.1.3
15. Wang G, Sun B, Zhu H, et al. Protective effects of emodin combined with danshensu on experimental severe acute pancreatitis. *Inflamm Res*. 2010;59(6):479–488. doi:10.1007/s00011-009-0152-1
16. Hollingsworth M. Book review: *DNA Fingerprinting in Plants: Principles, Methods and Applications*, 2nd ed. Weising K, Nybom H, Wolff K, Kahl G. 2005. Boca Raton: CRC Press. \$99.95 (paperback). 472 pp. *Ann Botany*. 2006;97(3):476–477. doi:10.1093/aob/mcj057
17. Li C, Liu Z, Tian J, et al. Protective roles of Asperosaponin VI, a triterpene saponin isolated from *Dipsacus asper* Wall on acute myocardial infarction in rats. *Eur J Pharmacol*. 2010;627(1–3):235–241. doi:10.1016/j.ejphar.2009.11.004
18. Liang Z, He M, Fong W, Jiang Z, Zhao Z. A comparable, chemical and pharmacological analysis of the traditional Chinese medicinal herbs *Oldenlandia diffusa* and *O. corymbosa* and a new valuation of their biological potential. *Phytomedicine*. 2008;15(4):259–267. doi:10.1016/j.phymed.2008.01.003
19. Zhu S, Fushimi H, Cai S, Komatsu K. Species identification from ginseng drugs by Multiplex Amplification Refractory Mutation System (MARMS). *Planta Med*. 2004;70(2):189–192. doi:10.1055/s-2004-815502
20. Chatti K, Saddoud O, Salhi-Hannachi A, Mars M, Marrakchi M, Trifi M. Analysis of genetic diversity and relationships in a Tunisian fig (*Ficus carica*) germplasm collection by random amplified microsatellite polymorphisms. *J Integr Plant Biol*. 2007;49(3):386–391. doi:10.1111/j.1744-7909.2007.00396.x
21. Yang DY, Fushimi H, Cai SQ, Komatsu K. Polymerase chain reaction-restriction fragment length polymorphism (PCR-RFLP) and Amplification Refractory Mutation System (ARMS) analyses of medicinally used *Rheum* species and their application for identification of *Rheum rhizoma*. *Biol Pharm Bull*. 2004;27(5):661–669. doi:10.1248/bpb.27.661
22. Fugh-Berman A. Herb-drug interactions. *Lancet*. 2000;355(9198):134–138. doi:10.1016/S0140-6736(99)06457-0
23. Sasaki Y, Fushimi H, Cao H, Cai SQ, Komatsu K. Sequence analysis of Chinese and Japanese curcuma drugs on the 18S rRNA gene and *trnK* gene and the application of amplification-refractory mutation system analysis for their authentication. *Biol Pharm Bull*. 2002;25(12):1593–1599. doi:10.1248/bpb.25.1593
24. Seyedimoradi H, Talebi R. Detecting DNA polymorphism and genetic diversity in Lentil (*Lens culinaris* Medik.) germplasm: Comparison of ISSR and DAMD marker. *Physiol Mol Biol Plants*. 2014;20(4):495–500. doi:10.1007/s12298-014-0253-3
25. Maeda M, Nishimura Y, Kumagai N, et al. Dysregulation of the immune system caused by silica and asbestos. *J Immunotoxicol*. 2010;7(4):268–278. doi:10.3109/1547691X.2010.512579
26. Semagn K, Bjørnstad Å, Ndjiondjop M. An overview of molecular marker methods for plants. *Afr J Biotechnol*. 2006;25(5):2540–2568. <https://www.ajol.info/index.php/ajb/article/view/56080>. Accessed February 15, 2023.
27. Heubl G. DNA-based authentication of TCM-plants: Current progress and future perspectives. In: Wagner H, Ulrich-Merzenich G, eds. *Evidence and Rational-Based Research on Chinese Drugs*. Vienna, Austria: Springer Vienna; 2012:27–85. doi:10.1007/978-3-7091-0442-2_2
28. Rhouma S, Dakhloui-Dkhil S, Ould Mohamed Salem A, et al. Genetic diversity and phylogenetic relationships in date-palms (*Phoenix dactylifera* L.) as assessed by random amplified microsatellite polymorphism markers (RAMPOs). *Sci Hortic*. 2008;117(1):53–57. doi:10.1016/j.scienta.2008.03.013
29. Albani MC, Battey NH, Wilkinson MJ. The development of ISSR-derived SCAR markers around the seasonal flowering locus (SFL) in *Fragaria vesca*. *Theor Appl Genet*. 2004;109(3):571–579. doi:10.1007/s00122-004-1654-4
30. Orita M, Iwahana H, Kanazawa H, Hayashi K, Sekiya T. Detection of polymorphisms of human DNA by gel electrophoresis as single-strand conformation polymorphisms. *Proc Natl Acad Sci U S A*. 1989;86(8):2766–2770. doi:10.1073/pnas.86.8.2766
31. Munthali M, Ford-Lloyd BV, Newbury HJ. The random amplification of polymorphic DNA for fingerprinting plants. *Genome Res*. 1992;1(4):274–276. doi:10.1101/gr.1.4.274
32. Kurane J, Shinde V, Harsulka A. Application of ISSR marker in pharmacognosy: Current update. *Phcog Rev*. 2009;3(6):216–228. <https://www.phcogrev.com/article/2009/3/6>. Accessed February 17, 2023.
33. Makino R, Yazyu H, Kishimoto Y, Sekiya T, Hayashi K. F-SSCP: Fluorescence-based polymerase chain reaction-single-strand conformation polymorphism (PCR-SSCP) analysis. *Genome Res*. 1992;2(1):10–13. doi:10.1101/gr.2.1.10
34. Techaprasan J, Klinbunga S, Jenjittikul T. Genetic relationships and species authentication of Boesenbergia (*Zingiberaceae*) in Thailand based on AFLP and SSCP analyses. *Biochem Syst Ecol*. 2008;36(5–6):408–416. doi:10.1016/j.bse.2007.10.006
35. Jayasinghe R, Kong S, Coram TE, et al. Construction and validation of a prototype microarray for efficient and high-throughput genotyping of angiosperms. *Plant Biotechnol J*. 2007;5(2):282–289. doi:10.1111/j.1467-7652.2007.00240.x
36. Holme IB, Dionisio G, Brinch-Pedersen H, et al. Cisgenic barley with improved phytase activity: Cisgenic barley. *Plant Biotechnol J*. 2012;10(2):237–247. doi:10.1111/j.1467-7652.2011.00660.x
37. Bartelson KJ, Singh RP, Foxman BM, Deng L. Catalytic asymmetric [4 + 2] additions with aliphatic nitroalkenes. *Chem Sci*. 2011;2(10):1940. doi:10.1039/c1sc00326g
38. Park HG, Yang Song J, Hwan Park K, Hwan Kim M. Fluorescence-based assay formats and signal amplification strategies for DNA microarray analysis. *Chem Eng Sci*. 2006;61(3):954–965. doi:10.1016/j.ces.2005.05.054
39. Murhadi WR. Good corporate governance and earning management practices: An Indonesian case. *SSRN Journal*. 2010. doi:10.2139/ssrn.1680186
40. Baldwin BG, Sanderson MJ, Porter JM, Wojciechowski MF, Campbell CS, Donoghue MJ. The ITS region of nuclear ribosomal DNA: A valuable source of evidence on angiosperm phylogeny. *Ann Missouri Bot Gard*. 1995;82(2):247. doi:10.2307/2399880
41. Jewell M. Clinical application of VASER-assisted lipoplasty: A pilot clinical study. *Aesthet Surg J*. 2002;22(2):131–146. doi:10.1067/maj.2002.123377
42. Selvaraj D, Shanmughanandhan D, Sarma RK, Joseph JC, Srinivasan RV, Ramalingam S. DNA barcode ITS effectively distinguishes the medicinal plant *Boerhavia diffusa* from its adulterants. *Genomics Proteomics Bioinformatics*. 2012;10(6):364–367. doi:10.1016/j.gpb.2012.03.002
43. Kumar S, Kahlon T, Chaudhary S. A rapid screening for adulterants in olive oil using DNA barcodes. *Food Chem*. 2011;127(3):1335–1341. doi:10.1016/j.foodchem.2011.01.094
44. Arif IA, Bakir MA, Khan HA, et al. Application of RAPD for molecular characterization of plant species of medicinal value from an arid environment. *Genet Mol Res*. 2010;9(4):2191–2198. doi:10.4238/vol9-4gmr848

45. Selvaraj D, Shanmughanandhan D, Sarma RK, Joseph JC, Srinivasan RV, Ramalingam S. DNA barcode ITS effectively distinguishes the medicinal plant *Boerhavia diffusa* from its adulterants. *Genomics Proteomics Bioinformatics*. 2012;10(6):364–367. doi:10.1016/j.gpb.2012.03.002
46. Pyle BW, Tran HT, Pickel B, et al. Enzymatic synthesis of valeren-4,7(11)-diene by a unique sesquiterpene synthase from the valerian plant (*Valeriana officinalis*). *FEBS J*. 2012;279(17):3136–3146. doi:10.1111/j.1742-4658.2012.08692.x
47. Srirama R, Senthilkumar U, Sreejayan N, et al. Assessing species admixtures in raw drug trade of *Phyllanthus*, a hepato-protective plant using molecular tools. *J Ethnopharmacol*. 2010;130(2):208–215. doi:10.1016/j.jep.2010.04.042
48. Al-Qurainy F, Khan S, Tarroum M, Al-Hemaid FM, Ali MA. Molecular authentication of the medicinal herb *Ruta graveolens* (*Rutaceae*) and an adulterant using nuclear and chloroplast DNA markers. *Genet Mol Res*. 2011;10(4):2806–2816. doi:10.4238/2011.November.10.3

Global uses of traditional herbs for hepatic diseases and other pharmacological actions: A comprehensive review

Akram Choudhary^{1,A,D}, Mohammad Noman^{1,B}, Uzma Bano^{2,E}, Jamal Akhtar^{3,E}, Yahya Shaikh^{1,C}, Mohammad Shahar Yar^{1,E,F}

¹ Department of Pharmaceutical Chemistry, School of Pharmaceutical Education and Research (SPER), Jamia Hamdard University, New Delhi, India

² School of Unani Medical Education and Research (SUMER), Jamia Hamdard University, New Delhi, India

³ Central Council for Research in Unani Medicine, Ministry of Ayurveda, Yoga & Naturopathy, Unani, Siddha, Sowa Rigpa, and Homeopathy (AYUSH), Government of India, New Delhi, India

A – research concept and design; B – collection and/or assembly of data; C – data analysis and interpretation;

D – writing the article; E – critical revision of the article; F – final approval of the article

Polymers in Medicine, ISSN 0370-0747 (print), ISSN 2451-2699 (online)

Polim Med. 2023;53(1):81–89

Address for correspondence

Akram Choudhary

E-mail: Akramchoudhary1593@gmail.com

Funding sources

Financial support and scholarships were granted by the Central Council for Research in Unani Medicine (CCRUM) (grant/award No. 16-116/2021).

Conflict of interest

None declared

Received on March 23, 2023

Reviewed on May 1, 2023

Accepted on May 8, 2023

Published online on June 1, 2023

Abstract

Hepatocellular carcinoma (HCC) is the 7th most common cancer and the 3rd leading cause of cancer-related death worldwide. It is resistant to the majority of chemotherapeutics and has a dismal prognosis. Hepatocellular carcinoma is a prevalent complication of chronic liver disease (CLD) in India. Primary liver cancer is the 6th most common cancer worldwide and the 4th most prevalent cause of cancer-related death. In 2018, it affected 841,000 people and caused 782,000 deaths around the world. Thus, research into the tumor cycle and its prevention through suitable herbal (Unani/Ayurvedic) medication is critical for reducing the impact of primary liver cancer. Treatment options for end-stage liver cancer are limited, necessitating costly liver transplantation, which is unavailable in most countries. Here, we present the results of a comprehensive literature survey to determine the benefits of using various herbs with liver protective and antioxidant properties. This information will be useful to researchers working on liver carcinoma and free radical scavenging, both of which are important in curbing potential carcinogens.

Key words: HCC, anti-oxidant, *Bauhinia variegata*, *Picrorhiza kurroa*, traditional Unani medicine

Cite as

Choudhary A, Noman M, Bano U, Akhtar J, Shaikh Y, Shahar Yar M. Global uses of traditional herbs for hepatic diseases and other pharmacological actions: A comprehensive review.

Polim Med. 2023;53(1):81–89. doi:10.17219/pim/165977

DOI

10.17219/pim/165977

Copyright

Copyright by Author(s)

This is an article distributed under the terms of the Creative Commons Attribution 3.0 Unported (CC BY 3.0) (<https://creativecommons.org/licenses/by/3.0/>)

Introduction

Hepatocellular carcinoma (HCC) is one of the most common types of solid tumor. Currently, more than 800,000 HCC cases are diagnosed annually around the world.¹ This tumor is highly aggressive, as currently evidenced by the annual mortality rate of approx. 700,000 worldwide.² Primary liver cancer is the 3rd leading cause of cancer-related death and the 7th most prevalent cancer worldwide. About 782,000 people died as a result of it in 2018, and it affected 841,000 people around the world. Malignant hepatocytes are the origin of the cancer known as HCC.^{3,4} Currently, only a few therapeutic alternatives are available for HCC patients. Thus, the first step in developing new therapeutic techniques entails gaining a thorough understanding of the biochemical underpinnings of HCC.⁵ Pathological mechanisms that lead to various chronic liver disorders include the progressive destruction and regeneration of liver parenchyma. Some of the most prevalent chronic liver illnesses are viral hepatitis, alcoholic or non-alcoholic fatty liver disease, autoimmune hepatitis, cirrhosis, and HCC.⁶ Their main causes are excessive alcohol use, viral infection, obesity, diabetes, and drug-induced liver injury. Chronic liver illnesses cause approx. 3.9–6.9 deaths per 100,000 people in various parts of the world.⁷ Hepatocellular carcinoma is an especially prevalent complication of chronic liver disease (CLD) in India, with over 22,000 new cases of primary liver cancer recorded annually. Secondary liver cancer is 20 times more common than primary liver cancer.

When compared to other cancers, HCC is extremely complex. It is most commonly linked to chronic liver illnesses like hepatitis or cirrhosis, which can be caused by a variety of factors. Cirrhosis is a precursor to most HCC cases, while developing HCC deteriorates liver function; thereby, HCC and cirrhosis both are impacting each other. Furthermore, HCC is resistant to a wide range of toxins as well as the majority of chemotherapeutics. Several clinical trials have used high dosages of chemotherapeutic drugs to overcome the resistance of HCC. However, such efforts have failed to provide any significant benefits for HCC patients. Another distinguishing feature of HCC is the inherent tendency of HCC cells to penetrate the portal vein and develop in its lumen; the HCC cells might then be transported away via the bloodstream, thereby resulting in distant metastasis.

Hepatocellular cancer therapy choices are severely limited due to such difficulties. Surgical resection, ablation and chemoembolization are effective only in a small number of individuals. Protein kinase inhibitors, such as sorafenib, improve survival for a limited period. Hepatocellular carcinoma has an exceptionally low overall survival rate of 4%, underscoring therapeutic limitations and posing a serious health burden. For individuals with cirrhosis and end-stage liver disorders, liver transplantation is currently the only curative option.⁸

The Unani system of medicine is one of the oldest traditional medical systems, with centuries of experience in treating CLD and cirrhosis. A wide range of single and compound medication formulations have been shown to help people with CLD. Antifibrotic and liver regeneration properties are the most common uses for these formulations.⁹

Antioxidants

In recent years, numerous studies have emerged regarding the potential role of nutrition in illness prevention. Antioxidants, particularly those produced from natural sources (e.g., herbal medications), such as Indian medicinal plants, are particularly important in this context. Consequently, antioxidants have numerous potential applications, especially in human health, such as illness prevention and treatment.^{10,11} Radiation exposure, environmental contaminants and metabolized medication by-products all produce free radicals. Antioxidants are compounds that prevent oxidation. They are also known as “powerful antioxidants” since they use radicals to produce minor reactive species. Exogenous and endogenous antioxidants are divided in 2 categories based on their source. Antioxidants help to prevent diseases such as cancer, diabetes, inflammation (e.g., liver inflammation, i.e. cirrhosis, CLD, cardiovascular disease (CVD), cataract, nephrotoxicity, and neurological diseases.¹²

Hepatocellular carcinoma

Hepatocellular carcinoma is a rapidly growing clinical concern that mostly affects people with cirrhosis and CLD. It is most common in Africa and Asia, where the endemic frequency of hepatitis C virus (HCV) and hepatitis B virus (HBV) greatly promotes the development of CLD and, as a result, HCC. Hepatocellular carcinoma is generally identified at an advanced stage after observing weight loss, indications of decompensated liver disease, and right-upper-quadrant pain; however, it can now be detected at an earlier stage through cirrhosis screening, serum alpha-fetoprotein (AFP) measurements and cross-sectional imaging tests. Understanding and characterizing hepatic cancer stem cells (HCSs) is crucial for understanding HCC origins.¹³ If the nature of HCSs can be thoroughly defined, patients with end-stage liver disease will receive effective and well-organized care more often.¹⁴ Organ shortages remain a key limiting factor even in developed countries, with only a small percentage of all patients having access to transplantation. Local ablative therapy, such as chemoembolization, potentially innovative chemotherapeutic drugs and radiofrequency ablation (RFA), may bring relief to and prolong the life of these patients. With the introduction of very effective direct-acting

antivirals (DAAs) for hepatitis,¹⁵ the incidence of hepatitis-related HCC is prognosed to decrease.¹⁶ The progression and management of HCC will most likely be determined by a mix of virus-specific, environmental, immune-related, and host genetic factors.¹⁸

Pharmacological applications of Unani herbs

Kachnar (*Bauhinia variegata* Linn.)

Bauhinia variegata L. is a medium-sized ornamental plant that grows up to 10–15 m tall and belongs to the Fabaceae family and Caesalpinioideae subfamily. Its common name in English is mountain ebony, while Kachnar is its Urdu name. It is a deciduous tree that loses its leaves in November and December, and remains leafless between January and April. When trees are young, they have a smooth, dark brownish bark with grey puberulent branches. The species is native to Asia (specifically India, Pakistan, China, and Nepal) (Fig. 1 and Table 1).

Hepatoprotective activity

The hepatoprotective activity of Kachnar in Sprague Dawley rats examined utilizing oral doses of 100 mg/kg and 200 mg/kg stem bark extracts exhibited hepatotoxic action against carbon tetrachloride-induced hepatotoxicity. These extracts specifically increase total protein levels and decrease the levels of alanine transaminase (ALT), aspartate aminotransferase (AST), gamma-glutamyl transferase (GGT), alkaline phosphatase (ALP), and total lipids.¹⁸ Leaf infusions are used to treat piles, worms, tumors, diarrhea and dysentery, and also exhibit laxative properties.¹⁹

Manoj et al. reported that ethanolic extracts of *Bauhinia variegata* protect rats against carbon tetrachloride-induced liver damage. A solution of carbon tetrachloride (1 mL/kg) diluted in olive oil (1:1) was administered orally to cause liver injury. The standard medicine was silymarin

(100 mg/kg). The potencies of *Bauhinia variegata* ethanolic extract (BVEE) at 400 mg/kg and 600 mg/kg were higher compared to BVEE at 200 mg/kg and 100 mg/kg.²⁰

Yadava and Reddy reported that the trypsin inhibitory activity of *Bauhinia variegata* anti-inflammatory activity was due to flavanone glycoside, which is found in the roots.²¹

Anti-tumor activity

Azevedo et al. investigated Kachnar anti-tumor activity because an insulin-like protein was detected in its leaves, and since it has also been widely utilized as an anti-diabetic treatment.²² Anti-tumor potential of Kachnar was investigated and it was discovered that an ethanolic and aqueous extract of its stem had an anti-tumor impact on Swiss albino mice with Dalton's ascetic lymphoma (DAL).²³ Experiments on induced DEN liver tumors and human cancer lines showed chemopreventive and cytotoxic effects.²⁴

Antioxidant activity

The antioxidant activity of Kachnar, which contains a potent flavonoid called quercetin, influences several enzymatic activities via interactions between biomolecules and quercetin's chemical component.²⁵ An antioxidant activity evaluation of aqueous and ethanolic extracts of Kachnar root was performed in vitro by scavenging free radicals with 1,2-diphenyl-1-2 picrylhydrazyl (DPPH).²⁶ The antioxidant and DNA-protecting activities of a methanolic extract of Kachnar bark MEB (methanol extract *Bauhinia variegata*) were observed in vitro against H₂O₂-induced oxidative damage to pBR322 plasmid DNA. The MEB and its polar sub-fractions EAB (ethyl acetate fraction *Bauhinia variegata*), NBB (n-butanol *Bauhinia variegata*) and REB (remaining extract *Bauhinia variegata*) showed high antioxidant activity and are reported to have the potential to prevent H₂O₂-induced oxidative damage to pBR322 DNA. The phenolic/flavonoid chemical richness of Kachnar bark extract/fractions may account for their H₂O₂ high antioxidant activity and DNA protective capabilities.²⁷



Active constituents

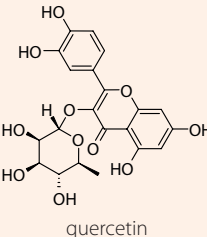
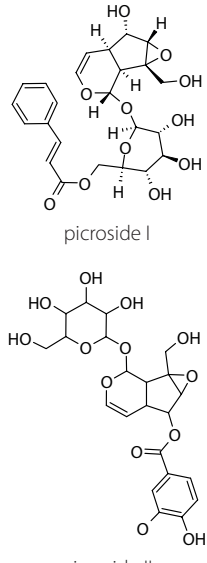
Kaempferol -3-glucoside, β -sitosterol, lupeol, tannins, carbohydrates, crude protein, fibers, calcium, amides, reducing sugars, vitamin C, quercitrin, apigenin, phosphorus, quercetin, rutin, apigenin -7-O-glucoside, dotetracont-15-en-9-ol and heptatriacontan-12,13-dioleic.

Botanical name: *Bauhenia Veriagata* Linn.

Family: Leguminosae Caesalpinioideae

Fig. 1. Kachnar and its active constituent

Table 1. Summary of Unani drugs

Name of the plant	Common names	Details about the plant	Active constituents	Structure	Uses	References
Kachnar (<i>Bauhinia variagata</i> Linn), (Leguminosae Caesalpinioideae)	mountain ebony (English), Rakta kanchan (Marathi), Kachnar (Hindi) Kempu mandara (Kannada), Shemmandarai (Tamil), Daevakanchanamu (Telgu)	It may be found all across India, particularly in Punjab and central and south India, up to an altitude of 1300 m in the sub-Himalayan and outer Himalayan regions	kaempferol-3-glucoside, β -Sitosterol, lupeol, tannins, carbohydrates, crude protein, fibers, calcium, amides, reducing sugars, vitamin C, quercitrin, apigenin, phosphorus, quercetin, rutin, apigenin-7-O-glucoside, dotetracont-15-en-9-ol and heptatriacontan-12, 13-diol etc.	 quercetin	bronchitis, leprosy, inflammation, bacterial infection, liver diseases, diarrhea, dysentery, skin illnesses, leprosy, intestinal worms, wounds, ulcers, fungal infection, ulcers, and tumors	19–26, 32–35
Kutki (<i>Picrorhiza kurroa</i>) (Plantaginaceae)	Kardi, Karoi, Karwi (Hindi), Kutki (Urdu), Kurki (Nepali), Katukhurohani (Malayam), Anjani (Arishta, Katumbhara (Sanskrit), Katuka-rogani, Katukarogani, Katukurohini (Telugu), Acokarokini, Akutam, Amakkini (Tamil)	It is found primarily in the Himalayan regions, which includes from Garhwal to Bhutan, north Burma, west China, and southeast Tibet. The species can be found in huge numbers at elevations of 3000–5000 m.	Picoside I, picoside II, and cucurbitacins, iridoid glycoside d-mannitol, kutkiol, kutki sterol, and apocynin. This species has only been assessed for a few biological functions, including antimicrobial, antidiabetic, anti-asthmatic, hepatoprotective, antioxidant, immunomodulatory, anticancer, anti-inflammatory, nephroprotective, analgesic, and cardioprotective.	 picoside I picoside II	anemia, stomach ache, asthma, obesity, malaria, fever, skin illnesses, bronchial asthma, immunological disorders, and viral hepatitis	44–46, 50–54

Antimicrobial activity

Parekh et al. discovered that Kachnar has antimicrobial properties and is effective against Gram-negative bacteria, which were suppressed using Kachnar leaf extract. However, the antibacterial range of Kachnar is somewhat limited. The polar extracts were effective against *Escherichia coli*, *Pseudomonas* spp. and *Klebsiella pneumoniae*. The antibacterial, bio-enhancement and anti-inflammatory capabilities of *Staphylococcus aureus* are inhibited by the Kachnar bark powder.²⁸

The antibacterial activities of methanolic Kachnar flower extracts were assessed by studying Gram-positive *Staphylococcus epidermis*, *Bacillus subtilus* and *S. aureus*, and Gram-negative *E. coli*, *S. flexineria* and *P. aeruginosa*. Microorganism development was suppressed depending on specific dosages of these methanolic extracts.²⁹

Antiulcer activity

Kachnar's antiulcer activities were reported in rats, and an ethanolic extract of Kachnar stems showed an antiulcer efficacy against stomach ulcers caused by pyloric ligation and aspirin-induced ulcers. The volume of gastric acid

secretion was also reduced by the ethanolic extract from stem of Kachnar and the total acidity, free acidity and ulcer index control became lower as the ulcer healed.^{30,31}

Arain et al. reported that pain, diabetes, infections, ulcers, jaundice, and leprosy can all be treated using Kachnar stems, roots and leaves.³²

Antibacterial activity

When Kachnar extracts were used against *S. aureus*, *Bacillus cereus*, *Pseudomonas pseudoalcaligenes*, *K. pneumoniae*, and *E. coli*, they exhibited antibacterial activity against all these species. Specifically, methanolic extracts have a higher antibacterial activity than aqueous extracts.³³

In another study, it has been reported that when the cup plate method was used, Kachnar demonstrated antibacterial and antifungal activities in 50 mg/mL, 100 mg/mL and 200 mg/mL petroleum ether, chloroform, acetone-water, and water extracts. Gram-positive bacteria, *S. aureus* and *E. coli*, were used to test the antibacterial activity, while *Candida albicans* and *Aspergillus niger* were utilized to test antifungal activity. Kachnar displayed an intensive antibacterial and antifungal action.³⁴

Anti-inflammatory activity

Mohamed et al. identified anti-inflammatory and analgesic activities of Kachnar, and reported that leaves of Kachnar contain novel triterpene saponins that reduce edema, while also lowering PGE2 (prostaglandin E2) levels in serum, liver homogenate and granuloma. Triterpene saponin treatment reduced the diameters of hepatic and pulmonary granulomas, which is thought to be related to its anti-inflammatory properties. Furthermore, in both visceral and cerebral nociceptive mice models, the chemical constituents present in the Kachnar showed analgesic effects.³⁵

In another investigation, it was shown that Kachnar reduced the anti-inflammatory actions of several flavanol glycosides found in *Bauhinia* spp. Flower buds can be used to treat cough, piles, liver disorders, and eye problems, as well as act as an astringent in hematuria and catamenia.³⁶

A study of the anti-inflammatory properties of mountain ebony found that extracts contain a sufficient amount of anti-inflammatory properties.³⁷ Gunalan et al. reported strong anti-inflammatory actions, as determined with gas chromatography–mass spectrometry (GC-MS) analysis.³⁸

Antidiabetic activity

Azevedo et al. reported that leaf and stem bark of Kachnar contain insulin-like proteins, which are widely employed as an anti-diabetic ingredient in a variety of popular treatments.²²

Dewangan et al. reported the discovery of D-pinitol, a bioactive chemical, in Kachnar leaves. This substance is a natural product of the cyclic polyol group and has hypoglycemic properties.³⁹ Shahana et al. reported antidiabetic activities of Kachnar since this plant contains a domain structure with the same amino acid sequence as insulin. In a strepto-zotocin-induced diabetes model, they found that insulin can successfully lower blood glucose levels in hyperglycemia. The high blood glucose levels in streptozotocin-induced and alloxan-induced diabetic rats were lowered when alcoholic and hydroalcoholic extracts of Kachnar leaves were administered orally at a dosage of 200 mg/kg.⁴⁰

Wound-healing activity

A study by Gyawali et al. showed that Kachnar in combination of other plants has satisfactory wound healing properties compared to standard drugs. Kachnar, *Rhododendron arboreum* and *Myrica esculenta* can be combined in various ratios to create a polyherbal liniment. They investigated antioxidant and wound-healing properties of polyherbal ointments containing methanolic extracts of Kachnar, *Myrica esculenta*, *Rhododendron arboretum*, and *Rhododendron esculenta*. The DPPH assay was used to examine the antioxidant activities of Kachnar, *Myrica esculenta*, *Rhododendron arboreum*, *Pyrus pashia*, and *Psidium guajava*. They combined Kachnar, *Rhododendron*

arboreum and *Myrica esculenta* in a 1:1:2 ratio to prepare a 10% w/w ointment. In the excision wound model, the herbal ointment-treated rats were completely healed, but the framycetin-treated, blank and control groups still had 2.72%, 4.5% and 5.73% wound areas, respectively.⁴¹

In another study, Sharma et al. evaluated the wound-healing activity of Kachnar using the percentage of wound closure, time of epithelialization, hydroxyproline estimation, and histological examinations of the granulation tissue for the excision wound model, and tensile strength measurement for the incision wound model. Both aqueous and ethanolic extracts of the root of *Bauhinia variegata* Linn. demonstrated considerable wound healing efficacy. In both wound types, ethanolic extract demonstrated wound healing activity comparable to the control. The histological assessment confirmed the outcome of wound healing activity. The phenolic content of ethanolic and aqueous extracts was determined to be 14.88 g/mg of pyrocatechol equivalents and 22.62 g/mg of pyrocatechol equivalents, respectively. The high level of flavonoids in the ethanolic and aqueous extracts resulted in substantial wound healing activity.⁴²

Kutki (*Picrorhiza kurroa* Royle ex Benth.)

“Picros” means bitter in Greek, whereas “rhiza” denotes root. *Picrorrhiza kurroa* is thus referred to as bitter root. In Ayurveda and Unani medicine, a plant genus in the Plantaginaceae family is known as “Kutki”, “Kurro” or “Indian gentian”. Due to potent iridoid glycosides present in the plant, a large body of pharmacological research has demonstrated its anti-cancer activity. The medication Kutki is made up of dried rhizome and root of *Picrorhiza kurroa*. It is a low-growing perennial herb, more or less hairy, that grows up to 20 cm tall. *Picrorhiza kurroa* is among India’s best-known medications, widely used from Sikkim to Kashmir in the northwestern Himalayas (Fig. 2, Table 1).

Antidiabetic activity

Picrorhiza kurroa inhibits hypoglycemic activity and the major phytoconstituents present in these plants show potent antidiabetic activity.^{43,44} He et al. reported that in rats with alloxan-induced diabetes, *Picrorhiza kurroa* plant extracts lowered blood glucose levels. Streptozotocin-induced diabetic rats were administered a herbal formulation that reduced the expression of malondialdehyde (MDA) and nicotinamide adenine dinucleotide phosphate (NADPH)-oxidase-dependent superoxide production in the diabetic kidney, demonstrating that *Picrorhiza kurroa* affects diabetic nephropathy by inhibiting redox active inflammation.⁴⁵ Husain et al. investigated the significant antidiabetic potential of this plant’s alcoholic extract in type 2 diabetes mellitus caused by streptozotocin-nicotinamide in rats and obtained similar results.⁴⁶



Active constituents

Glycosides, 1-(4-hydroxy-3-methoxyphenyl)ethanone, 1-(4-hydroxy-3-methoxyphenyl)ethanone, 3-phenylprop-2-enoic acid, veronicoside

Botanical name: *Picrorhiza kurroa*

Family: Plantaginaceae

Fig. 2. Kutki and its active constituent

In another study, Husain et al. investigated the mechanism of antidiabetic effects in diabetic (streptozotocin-induced) experimental mice, in which *Picrorhiza kurroa* extracts boosted insulin-mediated GLUT-4 expression, thereby increasing glucose absorption by skeletal muscles.⁴⁷

Husain et al. in yet another study examined *Picrorhiza kurroa* for its potential role in cell induction in insulin production, with the hypothesis that it improved cell regeneration and thereby provided relief from type 1 diabetes.⁴⁷

Hepatoprotective activity

Hepatocytes are cells that make up the major parenchymal tissue in the liver. Roughly 70–85% of the liver's mass consists of fat. Hepatic damage is caused by the death of hepatocytes when the levels of normal serum transaminase enzymes are elevated.⁴⁸ Jia et al. reported that by enhancing intestinal absorption, the herbal extract provided advanced nutraceutical activity for superior hepatoprotection.⁴⁹

The ethanol resistance of picroliv isolated from *Picrorhiza kurroa* has been noted in toxicity investigations in comparison to typical hepatoprotective drugs, such as Catapol, silymarin and andrographolide. The animal model exhibited good response to these medications. The ALP levels have dropped, while enzymatic assays such as glutamic-oxaloacetic transaminase (GOT), ALT and aldehyde have shown greater inhibitions compared with ALP. Therefore, it was suggested that *Picrorhiza kurroa* causes potent hepatoprotective effect.⁵⁰

Hepatoprotective efficacy of picrocliv against ethanol-induced toxicity in rats is dosage-dependent.⁵¹ In rats, ethanolic extract of *Picrorhiza kurroa* rhizomes and roots showed hepatoprotective activity against rifampicin- and isoniazid-induced hepatitis. The plant minimized drug-induced changes.^{52,53} Floersheim et al. reported that in mice poisoned with lethal quantities of Amanita mushrooms, the therapeutic efficiency of Kutki was higher than that of normal silybinin.⁵⁴

Anticancer activity

The anticancer properties of *Picrorhiza kurroa* are due to its constituents, such as picroside I, picroside II, cucurbitacins, apocynin, and others.⁵⁵ Mallick et al. discovered anticancer activity of *Picrorhiza kurroa* and reported that a failure of the apoptosis system could result in endless cell division and proliferation. The dichloromethane fraction of *Picrorhiza kurroa* demonstrated effective anticancer activity and may be worth investigating for cancer therapy.⁵⁶ Picroliv inhibited chemically caused cancer in rats in a dosage-dependent manner, thereby increasing the survival rate to roughly 65%,⁵⁷ while N-nitrosodiethylamine-induced hepatocarcinogenesis was greatly reduced by *Picrorhiza kurroa* extract.⁵⁸

Antioxidant activity

Kalaivani and Mathew found that antioxidant agents present in this plant act as radical scavengers, thereby protecting the human body from a variety of ailments. Activity of liver enzymes was lower in patients with liver cirrhosis after therapy with *Picrorrhiza kurroa plant extract*.⁵⁹ Deshpande et al. showed that liver enzyme activity was lowered in liver cirrhosis patients after therapy with the *Picrorhiza kurroa plant extract*.⁶⁰ Such extracts have been shown to be efficient antioxidants for evaluating lipid peroxidation inhibition; it was demonstrated by Rajkumar et al. who used radical scavenging tests, ferric reducing antioxidant property assay and thiobarbituric acid assays.⁶¹

Picrorrhiza kurroa rhizome ethanol extract at 20 mg/kg b.w. healed the stomach wall of indomethacin-induced gastric ulcerated rats through an in vivo free radical scavenging action. Krupashree et al. used a variety of antioxidant testing methods to confirm the antioxidant efficacy of *Picrorrhiza kurroa* leaf fractions. The extract shown considerable reducing capability along with antioxidant properties, with IC₅₀ values of 75.16 3.2 g/mL for DPPH radical scavenging and 55.5 4.8 g/mL for metal chelating, respectively. The *Picrorrhiza kurroa* extract's antioxidant and radical scavenging properties suggest

that it may be useful as a food supplement and source of natural antioxidants for a variety of oxidative stress-related disorders.⁶²

Anti-inflammatory activity

Picrorrhiza kurroa rhizome is a traditional medicine used to treat inflammatory conditions.⁶³ The active phytoconstituent apocynin, found in root extracts, has been shown to have anti-inflammatory activities. The fact that *Picrorrhiza kurroa* inhibits edema at a rate of 29.8% indicates that it is an effective anti-inflammatory medication.⁶⁴

The rhizome extract of *Picrorrhiza kurroa* considerably reduces joint inflammation. It also has anti-inflammatory properties against chemically generated inflammation and might be considered a high-quality natural analgesic.⁶⁵

The anti-inflammatory effects and production of thromboxane A₂ was suppressed by apocynin in a dosage-dependent manner, but the release of prostaglandins E₂ and F_{2α} increased. Arachidonic acid-induced aggregation of bovine platelets was reduced by apocynin, potentially by the reduction of thromboxane production.

Immunomodulatory activity

The immunomodulatory activity of *Picrorrhiza kurroa* was investigated, as well as the immunostimulatory activity of biopolymeric fractions. Biopolymeric fractions have been isolated from medicinal plants and used as a source of therapeutic agents. The most promising biopharmacological activities of these biopolymers are their immunomodulatory effects. The biopolymeric fraction RLJ-NE-205 was isolated and purified from the rhizomes of *Picrorrhiza kurroa*. An immunomodulatory agent is a type of medicine that, depending on its effect on the immune system, can either stimulate or suppress the immune system.⁶⁶ In mice, ethanolic extract of *Picrorrhiza kurroa* leaves was able to stimulate humoral and cell-mediated immune system components, as well as phagocytosis.⁶⁷

In another study, Hussain et al. reported that antigen non-specific defense was aided by 2 potent anticomplementary polymeric fractions. Those findings support the hypothesis that preparations from *Picrorrhiza kurroa* roots may have an impact on immunological processes, as the alcoholic extract of the root is more effective than the aqueous extract in causing a delayed hypersensitivity reaction. In mice, the effects of an ethanolic extract of each medication on delayed hypersensitivity, humoral responses to sheep red blood cells, skin allograft rejection, and reticuloendothelial system phagocytic activity were investigated. *Picrorrhiza kurroa* has been found to be an immunostimulant with both cell mediated and humoral actions.⁶⁸

Cardioprotective activity

Nandave et al. reported that rats given 200 mg/kg *Picrorrhiza kurroa* root extract alone showed no significant alterations; however, no changes were observed

in a pre-processed in vivo model when given isoproterenol, which induced hemodynamic and left ventricular dysfunction, lipid peroxidation, and oxidative stress.

In cases of coronary artery disease, the plant's root extract provided excellent prevention. Pre-treatment with root extract significantly reduced isoproterenol-induced oxidative stress. The numerous enzymes involved in lipid peroxidation, such as myocardial superoxide dismutase (SOD), catalase, and glutathione, block the outflow of myocyte creatine kinase-MB (CK-MB) and lactate dehydrogenase (LDH) enzymes. Those findings imply that the root extract has potent cardioprotective qualities.⁶⁹

Conclusions

The findings presented here improve our understanding of herbal active chemicals and herbal composite formulae for the treatment and prevention of HCC. *Bauhinia variegata* Linn. and *Picrorrhiza kurroa* have been identified as sources of active compounds with a wide spectrum of pharmacological activities, and have a high potential for driving the development of new remedies. They are widely used in the traditional healthcare system in India. They provide significant protection against a wide range of cancers, as well as other diseases.

Despite the fact that several studies have examined the anticancer effects and other qualities of these natural remedies, no cure for cancer has yet been discovered. Because of their anti-HCC and antioxidant properties, the plants presented in this review have anticancer potential. Finally, this article includes information on anticancer medicinal plants utilized across the globe. It is crucial that novel anticancer drugs produced from medicinal plants receive more research attention.

ORCID iDs

Akram Choudhary  <https://orcid.org/0000-0001-5242-2529>
 Mohammad Noman  <https://orcid.org/0000-0002-5496-7378>
 Uzma Bano  <https://orcid.org/0000-0002-3011-1524>
 Jamal Akhtar  <https://orcid.org/0000-0001-8400-4778>
 Yahya Shaikh  <https://orcid.org/0000-0002-7939-0851>
 Mohammad Shahar Yar  <https://orcid.org/0000-0001-9298-0154>

References

- Ribes J, Clèries R, Esteban L, Moreno V, Bosch FX. The influence of alcohol consumption and hepatitis B and C infections on the risk of liver cancer in Europe. *J Hepatol.* 2008;49(2):233–242. doi:10.1016/j.jhep.2008.04.016
- Parkin DM, Bray F, Ferlay J, Pisani P. Estimating the world cancer burden: GLOBOCAN 2000. *Int J Cancer.* 2001;94(2):153–156. doi:10.1002/ijc.1440
- Bray F, Ferlay J, Soerjomataram I, Siegel RL, Torre LA, Jemal A. Global cancer statistics 2018: GLOBOCAN estimates of incidence and mortality worldwide for 36 cancers in 185 countries. *CA Cancer J Clin.* 2018;68(6):394–424. doi:10.3322/caac.21492
- Mokdad AA, Singal AG, Yopp AC. Liver cancer. *JAMA.* 2015;314(24):2701. doi:10.1001/jama.2015.15425
- D'Alessandro N. Multifactorial nature of hepatocellular carcinoma drug resistance: Could plant polyphenols be helpful? *World J Gastroenterol.* 2007;13(14):2037. doi:10.3748/wjg.v13.i14.2037

6. Hong M, Li S, Tan H, Wang N, Tsao SW, Feng Y. Current status of herbal medicines in chronic liver disease therapy: The biological effects, molecular targets and future prospects. *Int J Mol Sci.* 2015;16(12):28705–28745. doi:10.3390/ijms161226126
7. Setiawan VW, Stram DO, Porcel J, Lu SC, Le Marchand L, Nouredin M. Prevalence of chronic liver disease and cirrhosis by underlying cause in understudied ethnic groups: The multiethnic cohort. *Hepatology.* 2016;64(6):1969–1977. doi:10.1002/hep.28677
8. Carr BI. *Understanding Liver Cancer: A Tale of Two Diseases.* Tarporley, UK: Springer Healthcare Ltd.; 2014. doi:10.1007/978-1-910315-02-6
9. Rashid B. Oral health in perspective of Unani literature: A review. *Int J Unani Integr Med.* 2018;2(2):10–13. <https://www.unanijournal.com/articles/26/2-1-5-886.pdf>. Accessed September 22, 2022.
10. Sies H, Packer L, August J, Murad F, Anders M, Coyle J, eds. *Antioxidants in Disease Mechanisms and Therapy.* San Diego, USA: Academic Press; 1996. ISBN:978-0-08-058130-9.
11. Halliwell B, Gutteridge JMC. *Free Radicals in Biology and Medicine.* 5th ed. Oxford, UK: Oxford University Press; 2015. ISBN:978-0-19-871747-8.
12. Neha K, Haider MR, Pathak A, Yar MS. Medicinal prospects of antioxidants: A review. *Eur J Med Chem.* 2019;178:687–704. doi:10.1016/j.ejmech.2019.06.010
13. Xu LB. Role of liver stem cells in hepatocarcinogenesis. *World J Stem Cells.* 2014;6(5):579. doi:10.4252/wjsc.v6.i5.579
14. Gonzalez SA, Keeffe EB. Risk assessment for hepatocellular carcinoma in chronic hepatitis B: Scores and surveillance. Perspective. *Int J Clin Pract.* 2012;66(1):7–10. doi:10.1111/j.1742-1241.2011.02808.x
15. Mathew S, Faheem M, Archunan G, et al. In silico studies of medicinal compounds against hepatitis C capsid protein from north India. *Bioinform Biol Insights.* 2014;8:159–168. doi:10.4137/BBI.S15211
16. Mathew S, Ali A, Abdel-Hafiz H, et al. Biomarkers for virus-induced hepatocellular carcinoma (HCC). *Infect Genet Evol.* 2014;26:327–339. doi:10.1016/j.meegid.2014.06.014
17. Maily L, Robinet E, Meuleman P, Baumert TF, Zeisel MB. Hepatitis C virus infection and related liver disease: The quest for the best animal model. *Front Microbiol.* 2013;4:213. doi:10.3389/fmicb.2013.00212
18. Kumar S, Baniwal P, Kaur J, Kumar H. Kachnar (*Bauhinia variegata*). In: Nayik GA, Gull A, eds. *Antioxidants in Fruits: Properties and Health Benefits.* Singapore: Springer Singapore; 2020:365–377. doi:10.1007/978-981-15-7285-2_18
19. Chatterjee A, Pakrashi SC; Council Of Scientific And Industrial Research–National Institute Of Science Communication and Policy Research (CSIR–NISCP) (New Delhi, India); eds. *The Treatise on Indian Medicinal Plants.* New Delhi, India: Publications & Information Directorate; 1991. ISBN:978-81-7236-011-5, 978-81-7236-010-8.
20. Manoj A, Kumar A, Yunus S. Screening of hepatoprotective activity of ethanolic extract of stem bark of *Bauhinia variegata* in rats. *Int J Pharm Pharm Sci.* 2013;5(2):624–628. <https://innovareacademics.in/journal/ijpps/Vol5Suppl2/6808.pdf>. Accessed March 23, 2023.
21. Yadava RN, Reddy VMS. Anti-inflammatory activity of a novel flavonol glycoside from the *Bauhinia variegata* Linn. *Nat Prod Res.* 2003;17(3):165–169. doi:10.1080/1478641031000104127
22. Azevedo CR, Maciel FM, Silva LB, et al. Isolation and intracellular localization of insulin-like proteins from leaves of *Bauhinia variegata*. *Braz J Med Biol Res.* 2006;39(11):1435–1444. doi:10.1590/S0100-879X2006001100007
23. Raj Kapoor B, Jayakar B, Anandan R, Kavimani S. Anti-ulcer effect of *Bauhinia variegata* Linn. in rats. *J Nat Remedies.* 2003;3(2):215–217. <https://www.informaticsjournals.com/index.php/jnr/article/view/170>. Accessed February 17, 2023.
24. Raj Kapoor B, Jayakar B, Muruges N, Sakthisekaran D. Chemoprevention and cytotoxic effect of *Bauhinia variegata* against N-nitrosodiethylamine induced liver tumors and human cancer cell lines. *J Ethnopharmacol.* 2006;104(3):407–409. doi:10.1016/j.jep.2005.08.074
25. Maldonado PD, Barrera D, Rivero I, et al. Antioxidant S-allylcysteine prevents gentamicin-induced oxidative stress and renal damage. *Free Radic Biol Med.* 2003;35(3):317–324. doi:10.1016/S0891-5849(03)00312-5
26. Rajani G, Ashok P. In vitro antioxidant and antihyperlipidemic activities of *Bauhinia variegata* Linn. *Indian J Pharmacol.* 2009;41(5):227. doi:10.4103/0253-7613.58513
27. Sharma N. Evaluation of *Bauhinia variegata* L. bark fractions for in vitro antioxidant potential and protective effect against H₂O₂-induced oxidative damage to pBR322 DNA. *Afr J Pharm Pharmacol.* 2011;5(12):1494–1500. doi:10.5897/AJPP11.457
28. Parekh J, Karathia N, Chanda S. Evaluation of antibacterial activity and phytochemical analysis of *Bauhinia variegata* L. bark. *Afr J Biomed Res.* 2009;9(1):53–56. doi:10.4314/ajbr.v9i1.48773
29. Kulshrestha P, Kumar P, Mishra A, et al. The antimicrobial activity of *Bauhinia variegata* Linn. flower extract (methanolic). *Asian J Pharm Clin Res.* 2011;4(1):46–47. <https://innovareacademics.in/journal/ajpcr/Vol4Suppl1/382.pdf>. Accessed February 11, 2023.
30. Raj Kapoor B, Jayakar B, Muruges N. Antitumour activity of *Bauhinia variegata* on Dalton's ascitic lymphoma. *J Ethnopharmacol.* 2003;89(1):107–109. doi:10.1016/S0378-8741(03)00264-2
31. Prusty B, Kiran B, Bhargavi V, Subudhi S. Anti-ulcer investigation of the different extract of bark of *Bauhinia variegata* Linn (*Caesalpinaceae*) by pyloric ligation & aspirin plus pyloric ligation model. *Int J Pharm Biol Sci.* 2012;2(1):248–262. https://ijpbs.com/ijpbsadmin/upload/ijpbs_50c866113ef30.pdf. Accessed December 13, 2022.
32. Arain S, Memon N, Rajput M, Sherazi S, Bhanger M, Mahesar S. Physico-chemical characteristics of oil and seed residues of *Bauhinia variegata* and *Bauhinia linnæi*. *Pakistan J Anal Environ Chem.* 2012;13(1):6. <http://pjaec.pk/index.php/pjaec/article/view/199>. Accessed January 22, 2023.
33. Pokhrel NR, Adhikari RP, Baral MP. In-vitro evaluation of the antimicrobial activity of *Bauhinia variegata*, locally known as koiralo. *World J Microbiol Biotechnol.* 2002;18(1):69–71. doi:10.1023/A:1013969628634
34. Patil JK, Jalalpure SS, Sayyed HYH, Hiremath RD, Chouhan MK. Evaluation of antibacterial and antifungal potential of (linn.) stem *Bauhinia variegata* bark. *Indian J Nat Prod.* 2015;29(1):44–55.
35. Mohamed MA, Mammoud MR, Hayen H. Evaluation of antinociceptive and anti-inflammatory activities of a new triterpene saponin from *Bauhinia variegata* leaves. *Z Naturforsch C J Biosci.* 2009;64(11–12):798–808. doi:10.1515/znc-2009-11-1208
36. Mali RG, Dhake AS. *Bauhinia variegata* Linn. (mountain ebony): A review on ethnobotany, phytochemistry and pharmacology. *Orient Pharm Exp Med.* 2009;9(3):207–216. doi:10.3742/OPEM.2009.9.3.207
37. Bansal V, Malviya R, Deeksha P, Malviya T, Sharma P. Phytochemical, pharmacological profile and commercial utility of tropically distributed plant. *Global J Pharmacol.* 2014;8(2):196–205. [https://idosi.org/gjpp/8\(2\)14/12.pdf](https://idosi.org/gjpp/8(2)14/12.pdf). Accessed November 5, 2022.
38. Gunalan G, Vijayalakshmi K, Saraswathy A, Hoper W, Tamilvannan T. Anti-inflammatory activities of phytochemicals from *Bauhinia variegata* Linn. leaf: An in silico approach. *J Chem Pharm Res.* 2014;6(9):334–348. <https://www.jocpr.com/articles/antiinflammatory-activities-of-phytochemicals-from-bauhinia-variegata-linn.pdf>. Accessed March 21, 2023.
39. Dewangan P, Verma A, Kesharwani D. Isolation of D-pinitol: A bioactive carbohydrate from the leaves of *Bauhinia variegata* L. *Int J Pharm Sci Rev Res.* 2014;24(1):43–45. <https://globalresearchonline.net/journalcontents/v24-1/08.pdf>. Accessed February 10, 2023.
40. Shahana S, Nikalje A, Nikalje G. A brief review on *Bauhinia variegata*: Phytochemistry, antidiabetic and antioxidant potential. *Am J Pharmtech Res.* 2017;7:186–197. https://www.researchgate.net/publication/313674462_A_Brief_Review_on_Bauhinia_variegata_Phytochemistry_Antidiabetic_and_Antioxidant_potential. Accessed December 23, 2022.
41. Gyawali R, Hengaju A, Thapa P, et al. Antioxidant and wound healing property of polyherbal ointment of Nepalese medicinal plants. *Int J Allied Med Sci Clin Res.* 2016;4(2):275–283. https://www.academia.edu/34156708/Antioxidant_and_Wound_Healing_Property_of_Polyherbal_Ointment_of_Nepalese_Medicinal_Plants. Accessed January 19, 2023.
42. Sharma RK, Rajni GP, Nathiya D, Sharma AK. Assessment of wound healing activity of roots of *Bauhinia variegata* Linn. by excision and incision model in albino rats. *Asian J Res Pharm Sci.* 2015;5(3):145–152. doi:10.5958/2231-5659.2015.00023.5
43. Kumar A, Kavimani S, Jayaveera K. A review on medicinal plants with potential antidiabetic activity. *Int J Phytopharmacol.* 2011;2(2):53–60. https://www.researchgate.net/publication/270814387_International_Journal_of_Phytopharmacology_A_REVIEW_ON_MEDICINAL_PLANTS_WITH_POTENTIAL_ANTIDIABETIC_ACTIVITY. Accessed February 12, 2023.
44. Goel R, Bhatia D, Gilani S, Katiyar D. Medicinal plants as antidiabetics: A review. *Int Bull Drug Res.* 2012;1(2):100–107. https://www.researchgate.net/publication/292349915_MEDICINAL_PLANTS_AS_ANTI-DIABETICS_A_REVIEW. Accessed February 5, 2023.

45. He LJ, Liang M, Hou FF, Guo ZJ, Xie D, Zhang X. Ethanol extraction of *Picrorhiza scrophulariiflora* prevents renal injury in experimental diabetes via anti-inflammation action. *J Endocrinol*. 2009;200(3):347–355. doi:10.1677/JOE-08-0481
46. Husain GM, Singh PN, Kumar V. Antidiabetic activity of standardized extract of *Picrorhiza kurroa* in rat model of NIDDM. *Drug Discov Ther*. 2009;3(3):88–92. PMID:22495535.
47. Husain GM, Rai R, Rai G, Singh HB, Thakur AK, Kumar V. Potential mechanism of anti-diabetic activity of *Picrorhiza kurroa*. *Tang (Humanitas Medicine)*. 2014;4(4):27.1–27.5. doi:10.5667/TANG.2014.0013
48. Navarro VJ, Senior JR. Drug-related hepatotoxicity. *N Engl J Med*. 2006;354(7):731–739. doi:10.1056/NEJMra052270
49. Jia D, Barwal I, Thakur S, Yadav SC. Methodology to nanoencapsulate hepatoprotective components from *Picrorhiza kurroa* as food supplement. *Food Biosci*. 2015;9:28–35. doi:10.1016/j.fbio.2014.10.005
50. Visen P, Binduja S, Patnaik G, Dhawan B, Agarwal D. Protective activity of picroliv isolated from *Picrorhiza kurroa* against ethanol toxicity in isolated rat hepatocytes. *Indian J Pharmacol*. 1996;28(2):98–101. <https://www.ijp-online.com/article.asp?issn=0253-7613;year=1996;volume=28;issue=2;spage=98;epage=101;aulast=Visen;type=0>. Accessed September 22, 2022.
51. Saraswat B, Visen PKS, Patnaik GK, Dhawan BN. Ex vivo and in vivo investigations of picroliv from *Picrorhiza kurroa* in an alcohol intoxication model in rats. *J Ethnopharmacol*. 1999;66(3):263–269. doi:10.1016/S0378-8741(99)00007-0
52. Jeyakumar R, Rajesh R, Meena B, et al. Antihepatotoxic effect of *Picrorhiza kurroa* on mitochondrial defense system in antitubercular drugs (isoniazid and rifampicin)-induced hepatitis in rats. *J Med Plants Res*. 2008;2(1):17–19. <https://www.internationalscholarsjournals.com/articles/antihepatotoxic-effect-of-picrorhiza-kurroa-on-mitochondrial-defense-system-in-antitubercular-drugs-isoniazid-and-rifamp.pdf>. Accessed December 7, 2022.
53. Shukla S, Kumar K. Hepatoprotective efficacy of *Picrorhiza kurroa* in experimentally induced hepatotoxicity in cockerels. *Int J Curr Microbiol Appl Sci*. 2017;6(4):2614–2622. doi:10.20546/ijcmas.2017.604.304
54. Floersheim GL, Bieri A, Koenig R, Pletscher A. Protection against *Amanita phalloides* by the iridoid glycoside mixture of *Picrorhiza kurroa* (kutkin). *Agents Actions*. 1990;29(3–4):386–387. doi:10.1007/BF01966472
55. Sindhu N, Pratima T, Ashwini W. Isolation of a cucurbitacin from *Picrorhiza kurroa* by column chromatography and its characterization. *Res J Pharm Biol Chem Sci*. 2011;2(3):149–156. [https://www.rjpbcs.com/pdf/2011_2\(3\)/19.pdf](https://www.rjpbcs.com/pdf/2011_2(3)/19.pdf). Accessed August 13, 2022.
56. Mallick MdN, Singh M, Parveen R, et al. HPTLC analysis of bioactivity guided anticancer enriched fraction of hydroalcoholic extract of *Picrorhiza kurroa*. *Biomed Res Int*. 2015;2015:513875. doi:10.1155/2015/513875
57. Jeena KJ, Joy KL, Kuttan R. Effect of *Embilica officinalis*, *Phyllanthus amarus* and *Picrorrhiza kurroa* on N-nitrosodiethylamine induced hepatocarcinogenesis. *Cancer Lett*. 1999;136(1):11–16. doi:10.1016/S0304-3835(98)00294-8
58. Joy KL, Rajeshkumar NV, Kuttan G, Kuttan R. Effect of *Picrorrhiza kurroa* extract on transplanted tumours and chemical carcinogenesis in mice. *J Ethnopharmacol*. 2000;71(1–2):261–266. doi:10.1016/S0378-8741(00)00168-9
59. Kalaivani T, Mathew L. Free radical scavenging activity from leaves of *Acacia nilotica* (L.) Wild. ex Delile, an Indian medicinal tree. *Food Chem Toxicol*. 2010;48(1):298–305. doi:10.1016/j.fct.2009.10.013
60. Deshpande N, Das R, Manohar M, Das V, Kandi S, Ramana K. Antioxidant effects of *Picrorhiza kurroa* rhizome extracts in alcoholic cirrhosis of liver. *Am J Pharmacol Sci*. 2015;3(2):49–51. <http://pubs.sciepub.com/ajps/3/2/4/index.html>. Accessed January 27, 2023.
61. Rajkumar V, Guha G, Ashok Kumar R. Antioxidant and anti-neoplastic activities of *Picrorhiza kurroa* extracts. *Food Chem Toxicol*. 2011;49(2):363–369. doi:10.1016/j.fct.2010.11.009
62. Krupashree K, Hemanth Kumar K, Rachitha P, Jayashree GV, Khanum F. Chemical composition, antioxidant and macromolecule damage protective effects of *Picrorhiza kurroa* Royle ex Benth. *S Afr J Botany*. 2014;94:249–254. doi:10.1016/j.sajb.2014.07.001
63. Singh GB, Bani S, Singh S, et al. Antiinflammatory activity of the iridoids kutkin, picroside-1 and kutkoside from *Picrorhiza kurroa*. *Phytother Res*. 1993;7(6):402–407. doi:10.1002/ptr.2650070604
64. Kantibiswas T, Marjit B, Maity LN. Effect of *Picrorhiza kurroa* Benth. in acute inflammation. *Anc Sci Life*. 1996;16(1):11–14. PMID:22556764. PMID:PMCID:3331136.
65. Kumar R, Gupta YK, Singh S, Arunraja S. *Picrorhiza kurroa* inhibits experimental arthritis through inhibition of pro-inflammatory cytokines, angiogenesis and MMPs. *Phytother Res*. 2016;30(1):112–119. doi:10.1002/ptr.5509
66. Gupta A, Khajuria A, Singh J, et al. Immunomodulatory activity of biopolymeric fraction RLJ-NE-205 from *Picrorhiza kurroa*. *Int Immunopharmacol*. 2006;6(10):1543–1549. doi:10.1016/j.intimp.2006.05.002
67. Sharma ML, Rao CS, Duda PL. Immunostimulatory activity of *Picrorhiza kurroa* leaf extract. *J Ethnopharmacol*. 1994;41(3):185–192. doi:10.1016/0378-8741(94)90031-0
68. Hussain A, Shadma W, Maksood A, Ansari S. Protective effects of *Picrorhiza kurroa* on cyclophosphamide-induced immunosuppression in mice. *Phcog Res*. 2013;5(1):30. doi:10.4103/0974-8490.105646
69. Nandave M, Ojha SK, Kumari S, et al. Cardioprotective effect of root extract of *Picrorhiza kurroa* (Royle Ex Benth) against isoproterenol-induced cardiotoxicity in rats. *Indian J Exp Biol*. 2013;51(9):694–701. PMID:24377128.

